WEC PROPRIETARY CLASS 3

[redacted]

[redacted]

Westinghouse Energy Systems

WCAP-12986 SG-91-12-007

Kewaunee Steam Generator

Tube Plugging Criteria for

ODSCC at Tube Support Plates

November, 1991

Approved by: _____

M. J. Wootten, Manager
Steam Generator Technology & Engineering

Table of Contents

Table of Contents (Continued)

List of Tables

List of Tables (Continued)

List of Figures

List of Figures (Continued)

List of Figures (Continued)

List of Figures (Continued)

List of Figures (Continued)

1.0 INTRODUCTION

This report provides the technical basis for tube plugging criteria for outside diameter stress corrosion cracking (ODSCC) at tube support plate (TSP) intersections in the Kewaunee steam generators (S/G). The recommended plugging criteria are based upon bobbin coil inspection voltage amplitude which is correlated with tube burst capability and leakage potential. The recommended criteria are demonstrated to meet the guidelines of Regulatory Guide (R.G.) 1.121.

The tube plugging criteria are based upon the conservative assumptions that the tube to TSP crevices are open (negligible crevice deposits or TSP corrosion) and that the TSPs are displaced under accident conditions. The ODSCC existing within the TSPs is thus assumed to be free span degradation under accident conditions and the principal requirement for tube plugging considerations is to provide margins against tube burst per R.G. 1.121. The open crevice assumption leads to maximum leak rates compared to packed crevices and also maximizes the potential for TSP displacements under accident conditions. Laboratory tests performed with incipient denting or dented tube intersection show no leakage or very small leakage such that leakage even under steam line break (SLB) conditions would be negligible.

It is demonstrated, using Plant A-1 as an example, that if the crevices are packed as a consequence of TSP corrosion or if small tube to TSP gaps are present, TSP displacements under accident conditions are minimal such that tube burst would be prevented by the presence of the TSPs. TSP displacement analyses under SLB loads were also performed for the open crevice assumption with the further conservative assumption of zero friction at the tube to TSP intersections and at the TSP wedge to wrapper interaction. The wedges are installed in the TSP to wrapper gaps to align the TSPs for tubing of the S.G.s. While the TSP wedges are pressed into the gap during manufacturing, the forces are not known and thus the preload or friction force at the TSP to wrapper interface is not known. It is reasonable to expect that the friction forces at the TSP to wrapper interface would significantly reduce TSP displacements under accident conditions. However, the analytical results based upon the open crevice/zero friction assumptions indicate the potential for TSP displacements under SLB conditions such that prevention of tube rupture cannot be assured for the 51 Series S/Gs with the applied analytical assumptions. Therefore the requirements for tube burst margins assuming free span degradation have been applied to develop the tube plugging criteria for Kewaunee S/Gs.

The plugging criteria were developed from testing of laboratory induced ODSCC specimens, extensive examination of pulled tubes from operating S/Gs and field experience for leakage due to indications at TSPs. The recommended criteria represent conservative criteria based upon Electric Power Research Institute (EPRI) and industry supported development programs that are continuing toward further refinement of the plugging criteria. The currently available data base permits use of burst pressures at the lower 95% confidence bound as the basis for the tube plugging limits.

Implementation of the tube plugging criteria is supplemented by 100% bobbin coil inspection requirements at TSP elevations having ODSCC indications, reduced operating leakage requirements, inspection guidelines to provide consistency in the voltage normalization and rotating pancake coil (RPC) inspection requirements for the larger indications left in service to characterize the principal degradation mechanism as ODSCC. In addition, it is required that potential SLB leakage be calculated for tubes left in service to demonstrate that the cumulative leakage is less than allowable limits.

Two tubes were pulled from Plant A-2 in November, 1990 to provide direct support for these criteria. Testing on these pulled tubes included leak rate tests, burst pressure tests and destructive examinations to establish crack morphology. In addition, results of prior pulled tube examinations from Plant A-1 and 2 and other plants have been used to support the tube pluggir g criteria.

To provide the technical bases for tube plugging due to ODSCC at TSPs, the following activities have been performed as documented in this report:

- o Summary of Regulatory Requirements against which the recommended plugging criteria are evaluated - Section 3
- o Review of Plant A-1,A-2 and other plant pulled tube examinations - Section 4
- o Review of Kewaunee eddy current inspection results including historical growth rate data - Section 5
- o Review of field experience from pulled tube data and plant leakage occurrences to define the field data base which is supplemented by laboratory tests to develop the plugging criteria - Section 6
- o Preparation of cracked test specimens for non-destructive examination (NDE) and leak testing in a model boiler or doped steam environment for inducing ODSCC cracks, or by cyclic fatigue to produce cracks in the test samples - Section 7
- o NDE analysis guidelines,measurement uncertainties, and NDE inspection results for the test specimens based upon defined procedure and data analysis guidelines and including sensitivity to: probe manufacturer, open or packed crevices, tube wear, etc. -Section 8
- o Burst and leak testing to relate the NDE parameters to burst pressure and SLB leak rates - Section 9
- o Results of test specimen destructive examinations to assess prototypicality of sample tube crack morphology and to characterize test specimen crack sizes and depths - Section 10
- o SLB evaluations to assess TSP displacements under SLB loads, plant requirements on SLB leakage limits and a description of the SLB leakage model - Section 11
- o Integration of the inspection and burst test results to develop the tube plugging criteria - Section 12

The overall summary and conclusions for this report are described in Section 2.

2.0 SUMMARY AND CONCLUSIONS

The report describes the technical support for tube plugging criteria for ODSCC at TSPs applicable to the Kewaunee S/Gs. The plugging criteria are based upon use of bobbin coil (BC) inspection voltage amplitudes. These eddy current measurements are directly correlated to tube integrity issues including tube burst margins and the potential for tube leakage under postulated accident conditions. Eddy current and leak rate measurements from pulled tubes and laboratory cracked specimens as well as field data have been used to correlate voltage plugging limits to leakage potential and tube burst margins. Regulatory Guide 1.121 for tube integrity guidelines as well as the General Design Criteria are shown to be satisfied by the tube plugging criteria of this report.

This section summarizes the tube plugging criteria under Overall Conclusions (Section 2.1) and the key results of the development program under Summary (Section 2.2).

2.1 Overall Conclusions

The general approach taken to develop the tube plugging criteria for ODSCC at TSPs includes:

1) Specifying conservative burst correlations based on free span ODSCC under design basis accident conditions to demonstrate structural integrity.

2) Conservatively assuming open crevice conditions to maximize leakage potential.

3) Satisfying the R.G. 1.121 structural guidelines for tube burst margins by establishing a conservative structural limit on voltage amplitude that assures 3 times normal operating pressure differential for tube burst capability.

4) Satisfying the updated safety analysis report (USAR) requirements for allowable leakage under accident conditions by demonstrating that the dose rate associated with potential leakage from tubes remaining in service is a small fraction of 10 CFR 100 limits.

5) Including considerations for crack growth and NDE uncertainties in both the structural assessment and SLB leakage analysis.

6) Specifying a requirement to perform 100% BC inspection for all hot leg TSP intersections and all cold leg intersections down to the lowest cold leg TSP where ODSCC indications have been identified.

The resulting tube plugging criteria for ODSCC at TSPs in Kewaunee S/Gs can be summarized as follows:

Tube Plugging Criterion

Tubes with bobbin coil indications within the TSPs exceeding 3.5 volts will be plugged or repaired.

SLB Leakage Criterion

Predicted SLB leak rates from ODSCC at TSPs for the tubes left in service must be less than 260 gpm for each S/G, including considerations for NDE uncertainties and ODSCC growth rates.

Inspection Requirements

A 100% bobbin coil inspection shall be performed for all hot leg TSP intersections and all cold leg intersections down to the lowest cold leg TSP with ODSCC indications.

All tubes with bobbin coil indications >1.5 volts at TSP intersections shall be inspected using RPC probes. The RPC results shall be evaluated to support ODSCC as the dominant degradation mechanism. Indications at TSPs confirmed to be ODSCC shall be reinspected by RPC during alternate refueling outages for reconfirmation as ODSCC.

Operating Leakage Limits

Plant shutdown will be implemented if normal operating leakage exceeds 150 gpd per S/G.

Exclusions from Tube Plugging Criterion

Tubes with RPC indications not attributable to ODSCC or with circumferential indications shall be evaluated for tube plugging based on a 50% eddy current indicated depth limit.

Although the tube plugging guidelines of R.G. 1.121 are used to establish tube plugging limits, the potential for tube burst at SLB conditions is shown to be negligible based on both deterministic crack length considerations and probability estimates. The burst pressure versus crack length correlation utilizing the Belgian burst data (EPRI NP-6864-L) developed under prototypic flow conditions show that a through wall crack length of 0.84 inch is required for tube burst at SLB pressure differentials. This crack length exceeds the 0.75 inch TSP thickness which bounds the potential crack lengths for ODSCC at TSPs. Consequently, tube burst for ODSCC is essentially precluded by the crack length limit. More over, an alternate assessment was performed by considering the probabilities associated with a limiting EOC (end of cycle) voltage including growth and comparing with the probability of tube burst at the limiting EOC voltage amplitudes. This analysis shows that an indication left in service at the tube plugging limit would have a probability of burst at SLB conditions of $\sim 5 \times 10^{-7}$ per cycle. This value does not include the probability of an SLB event occuring; hence the actual burst probability (combined probability of SLB and burst) would be further reduced. Thus tube burst is not a significant concern for application of the plugging limits for ODSCC at TSPs. The use of free span burst pressure criteria to establish tube plugging limits thus leads to very conservative plugging limits.

2.2 Summary

A summary of the results of this report is provided below:

Regulatory Requirements

- Tube integrity acceptance criteria for S/G tubes are defined in Regulatory Guide 1.121 and

General Design Criteria. For tubes with through wall cracks, these criteria establish guidelines for tube burst margins and operating leakage limits. The tube plugging limits of this report are developed to demonstrate that these guidelines are met.

- USAR accident analyses include tube leak rates utilized to show acceptable radiological consequences. A limiting accident condition leak rate of 260 gpm per S/G in an SLB event was developed to meet site boundary dosage limits. At each outage, projected potential SLB leak is determined for tubes left in service to demonstrate satisfaction of the 260 gpm leakage limit.

Pulled Tubes from Plant A S/Gs

- Two tubes pulled from Plant A-2 in 1990 and one tube pulled in 1986 (examined in 1991) have been leak and burst tested to support the tube plugging criteria. Prior Plant A pulled tubes with significant cracks include one additional tube from Unit 2 and one from Unit 1. These tubes had crack depths exceeding 60% and voltages ranging from 0.3 to 9.9 volts. Three tubes having voltages ranging from 2.8 to 9.9 volts had short through wall indications. None of these tubes were identifiable as leakers in service. Nine additional Plant A-2 TSP intersections from 3 tubes were destructively examined and found to have insignificant (<22% depth) degradation.

- Two of the five Plant A tubes with significant indications had bobbin coil amplitudes of 2.8 and 9.9 volts, indicated depths of 82% and 86% and through wall crack lengths of 0.18 and 0.15 inch, respectively. Laboratory tests showed no significant leakage (a few drops indistinguishable from test system leakage) at normal operating conditions. These tubes had very low SLB leak rates of <0.2 l/hr (~1 gpd).

- Two of the five Plant A tubes at 1.44 and 7.2 volts with bobbin coil indicated depths of 68% and 83% had actual crack depths of 78% and 100% (0.02" through wall crack length), respectively. The tube with the 1.44 volt indication was leak tested with no leakage at normal operating and SLB conditions. It can be inferred from the crack morphology that the tube with the 7.2 volt indication would not have measurable leakage even at SLB conditions.

- Free span burst pressures for the Plant A pulled tubes exceeded 5900 psi and thus exceed Reg. Guide 1.121 guidelines for 3 times normal operating pressure differentials (4590 psi) on a temperature and minimum property adjusted basis.

- A total of 14 TSP intersections from 8 tubes have been examined for TSP degradation. The tube pulls occurred between 1985 and 1990. ODSCC was the dominant degradation mechanism in all cases. Only one of the tube exam results showed significant inter-granular attack (IGA) involvement.

Pulled Tubes from Other S/Gs

- In addition to the 8 tubes pulled from Plant A, the overall pulled tube data base includes 15 pulled tubes with 40 tube to TSP intersections that have both NDE and destructive examination results. The bobbin coil indications for these tubes range from 0.1 to 2.3 volts with indicated depths up to 88%. One tube with a 1.9 volt indication had a through wall crack, 0.01" long. None of these tubes would be expected to leak even at SLB conditions and all would have free span burst pressures that satisfy Reg. Guide 1.121 acceptance criteria.

- These pulled tubes support no leakage at normal operating or SLB conditions at voltages up to 1.5 volts, independent of depth, while the Plant A tubes indicate no measurable operating leakage up to about 10 volts and very low leakage at SLB conditions above 2.8 volts.

- Overall, the pulled tube data show multiple, segmented axial cracks with short lengths for the deepest penetrations. Through wall cracks have been identified in 4 tubes but the associated crack lengths are short (<0.18") and have no measurable leakage at normal operating conditions.

- Pulled tube examination results have been reviewed from 4 plants with more significant IGA involvement than found at the Plant A S/Gs. These results indicate that the degradation develops as IGA + SCC particularly when maximum IGA depths greater than about 25% are found. A large number (>100) of axial cracks around the tube circumference are commonly found in these tubes. The maximum depth of IGA is typically 1/3 to 1/2 of the SCC depth.

- Comparisons of corrosion morphology between tubes have been made semi-quantitavely using comparisons of cracking density, extent of IGA associated with the major cracks and extent (depth, width) of IGA involvement.

Operating Plant Experience

- To date, only 3 tubes in operating S/Gs have been identified as probable tube leakers attributable to ODSCC at TSPs. The occurrences were in two European plants (no leakers for ODSCC at TSPs have been identified in domestic plants). These leaking tubes had bobbin coil indicated depths exceeding 75% and voltage amplitudes of 7.7, 13 and 39 volts. Plant leak rates associated with these tubes cannot be quantified as other tubes with PWSCC contributed to the total primary coolant leak rates of 63 and 140 gpd at the two plants.

- Bobbin coil inspection results from domestic and European units for tubes with no identifiable leakage have been collected to support selection of plugging limits for no expected operating leakage. These data include indications exceeding 10 volts amplitude and generally support negligible leakage for ODSCC at TSPs.

- Based on voltage versus actual depth trends from pulled tubes, indications with IGA and IGA/SCC show comparable or higher voltage levels than obtained for SCC with minor IGA. These data support adequate detectability for IGA and IGA/SCC degradation using bobbin coil inspections.

- Inspection results from French units provide growth trends at BOC (beginning of cycle) amplitudes higher than those obtained from domestic units. The French data indicate that percent voltage growth is essentially independent of BOC voltage amplitude. Kewaunee data, which are at lower BOC amplitudes, show a trend toward decreasing percent voltage growth with increasing amplitude. For conservatism, percent voltage growth is assumed to be independent of amplitude to develop the tube plugging limits.

Kewaunee Operating Experience for ODSCC at TSPs

- Results from prior inspections at Kewaunee were evaluated to develop growth rates for both voltage amplitudes and indicated depths. This assessment indicates that the ODSCC growth rates are very low.

- Average growth rates of indications at TSP locations over the last operating cycle were 0.09 volt and 0.01 volt respectively in Kewaunee S/Gs A and B. These average values were calculated by treating negative voltage growths as zero growth. Conservative voltage growth rate over the last operating cycle was 5% (both S/Gs combined).

- A number of tube/TSP intersections were tested using RPC during the 1991 Kewaunee inspection. Review of the overall RPC data suggests that the support plate indications are axial ODSCC signals. This conclusion is valid for the hot leg indications and the relatively large number of cold leg indications observed at Kewaunee.

- A review the Kewaunee eddy current data shows evidence of general corrosion of the support plate holes. However, the data does not support the presence of large amounts of magnetite in the crevices. This is also supported by the lack of dent indications at TSP intersections.

TSP Displacement Under SLB Loads

- Under SLB loading conditions, axial displacement of the TSPs with respect to the tube can occur thereby exposing the ODSCC from within the crevice. Incipient denting and dented conditions at TSP intersections, if present, would prevent TSP displacement under SLB conditions. Conservative analysis assumptions, such as no friction which also ignores the TSP to wedge to wrapper contact forces, lead to overestimates of the TSP displacements. Given these assumptions, it could not be assured that the TSPs would envelope the ODSCC at the times of increasing primary to secondary pressure differentials in an SLB event. Therefore, the Kewaunee plugging criterion described in this report is based upon conservatively treating ODSCC within TSP crevices as free span degradation.

Preparation of Cracked Specimens

- Samples cracked due to ODSCC in model boilers with simulated TSP intersections have been found to produce crack morphologies and leak rates typical of field experience. This method of sample preparation is used for development of the tube plugging limits.

- Samples prepared in doped steam were found to yield relatively open cracks, with less prototypic crack morphology and voltage amplitudes as well as non-prototypically high leak rates due to the high hoop stresses applied to crack these specimens within reasonable test periods. These samples have only been applied for tests with dented TSP intersections to demonstrate the influence of dented crevices on leak rates.

- Fatigue induced crack specimens have also been used to evaluate the influence of dented crevices on leak rates. Fatigue cracks were used based upon the capability to closely control through wall crack lengths and the reasonably predictable and relatively high leak rates associated with fatigue cracks.

Non-Destructive Examinations (NDE)

- Bobbin coil measurements on laboratory prepared uniform IGA specimens show voltage amplitudes exceeding 1-2 volts for ~30% IGA depth. These results support the field data trends indicating IGA and IGA/SCC detectability at comparable voltage levels to that found for SCC.

- The NDE program applied to laboratory specimens included sensitivity comparisons for probes manufactured by two vendors. The probe vendor has been found to have no impact on the NDE results based on using 400 kHz for voltage calibration and a 400/100 kHz mix for analysis. However, each of the probes can have different frequency response characteristics. This effect can be minimized by calibrating each of the frequencies individually or calibrating the planned mix channel. The latter has been recommended for implementation in the Kewaunee S/G inspections. Probe centering uncertainty has been found to be <5% for "new", unworn probes based on results of EC tests performed in a horizontal position (orientation) of a specimen with EDM notches (notches at the top or bottom).

- The bobbin coil voltage response for magnetite packed crevices is essentially the same as found for open crevices. The results show a 5% increase in response with the magnetite present and a scatter of about 10%. Thus the presence of magnetite does not significantly influence the bobbin coil voltage measurements.

- An example typical of field experience for which the environment (residual TSP, small dent responses) can mask or distort the indication response was found in one test specimen. When the amplitude response grew from 0.3 to 0.7 volts after leak testing and handling, the indication could be readily detected. These small responses, which are masked by environmental factors in operating S/Gs (as shown by pulled tube results) do not impact the serviceability of the S/G, as the indications are small compared to the plugging limits of this report.

- Voltage calibrations for different ASME standards were compared against the laboratory standard used in this program. Variations up to 18% were identified. Pending incorporation of a voltage verification requirement in ASME standard certifications, an ASME standard calibrated against the laboratory standard will be utilized in Kewaunee S/G inspections for consistent voltage normalization.

- Bobbin coil probe wear sensitivity tests were performed by varying the diameter of the probe centering devices to determine changes in voltage and depth responses against a 4 hole standard. The test results indicate that probe wear typical of field inspections leads to voltage variations of [ ]^{a} between the 4 holes staggered around the tube circumference. To limit uncertainties associated with probe wear, a four staggered hole standard will be implemented in Kewaunee S/G inspections. If voltage amplitudes between the 4 holes differ by more than [ ]^{a}, the probe will be replaced. Pending additional field experience with the probe wear standard, the NDE uncertainty for probe wear has been increased to 20%.

- The variables affecting the voltage/burst correlation can be split into NDE uncertainties and burst correlation uncertainties. The NDE uncertainty represents the repeatability of a voltage measurement and is dominated by probe centering variations as a result of probe wear. Minimizing the uncertainty on repeatability of voltage measurements reduces the spread or uncertainty in the burst correlation. The remaining voltage measurement uncertainties contribute to the burst pressure correlation uncertainty and influence plugging limits through use of the lower 95% confidence level on the voltage/burst correlation to establish the voltage plugging limits.

Leak Rate and Tube Burst Testing

- Leak rates at normal operating and SLB conditions have been measured for 29 model boiler specimens with voltage levels as high as 137 volts. Overall, the model boiler data indicate that [ ]^{9} volt indications are required for significant (>10 gpd) operating leakage.

- Burst pressure tests were performed for 27 model boiler specimens and 13 intersections from 8 pulled tubes. The model boiler and pulled tube burst pressure measurements were combined to develop a correlation of burst pressure versus bobbin coil voltage. This correlation was reduced for operating temperatures and minimum material properties to determine the voltage amplitude that satisfies the R.G. 1.121 structural guidelines for burst capability of 3 times normal operating pressure differentials. The results evaluated at the lower 95% prediction interval define a [ ]^{a} volt amplitude for the structural limit on tube burst margins. Although the high voltage data base is small, the burst correlations indicate that a [ ]^{9} volt ODSCC crack would meet the SLB burst pressure requirement of 2650 psi at the lower 95% confidence level.

- Available burst data for laboratory uniform IGA specimens and pulled tubes with IGA/SCC are enveloped by the voltage/burst correlation dominated by ODSCC data.

- The model boiler and pulled tube leak rate measurements have been applied to define a correlation of SLB leak rate to bobbin coil voltage. This correlation, including defined uncertainty levels, is used to calculate potential SLB leakage for tubes returned to service following an outage.

- Leak rates for the 3 model boiler tubes tested with magnetite packed crevices that showed some leakage, had increased leak rates after the magnetite was removed from the crevice.

- Leak rates were also measured for 11 tubes with incipient denting and dented conditions, average dent sizes less than 1 mil and including through wall fatigue cracks up to 0.7 inch long. Only [ ]^{9} of these dented tubes leaked at normal operating or SLB conditions even though open crevice leakage for the 0.7 inch fatigue cracks would exceed 1000 gpd. The [ ]^{9} at normal operating and SLB conditions, respectively, had a 0.5 inch long fatigue crack and an average dent size of <0.2 mils.

Specimen Destructive Examinations

- Destructive examinations of the model boiler specimens show crack morphologies typical of the pulled tube experience. Destructive examinations were performed on model boiler specimens following burst testing to characterize the cracks associated with typical voltage levels and leak rates.

- Destructive examination of a laboratory induced dent specimen has shown corrosion product layers that are relatively dense and leakage paths that are highly tortuous which is consistent with the negligible leakage found for dented tube conditions.

Tube Plugging Criteria

- The pulled tube and model boiler leak rate and burst data together with field leakage

experience and field inspection results have been used to relate bobbin coil voltage to tube integrity to define tube plugging limits.

- The burst pressure versus voltage correlation defines a voltage of [ ]^{a} volts for the structural limit to meet R.G. 1.121 burst margins. The voltage structural limit is reduced by conservative allowances of 20% for NDE uncertainties and 40% for crack growth to obtain a tube plugging limit of 3.5 volts.

- An SLB leakage model is defined for demonstrating that projected SLB leakage from tubes left in service is less than the allowable 260 gpm per steam generator. The SLB leakage model is a probabilistic model that combines an inspection determined distribution for voltage indications, voltage growth rate distributions, eddy current uncertainties and a leak rate versus voltage formulation to obtain the projected cumulative EOC SLB leak rate for all indications left in service. If the plugging criteria and SLB leakage model are applied to the last Kewaunee inspection results, the projected SLB leakage for the end of the next cycle would be 0.1 gpm.

- RPC inspection for indications above 1.5 volts is required to establish that the more significant indications are ODSCC. The 1.5 volt threshold for RPC inspection provides a threshold value below which non-ODSCC indications would be acceptable for continued operation and SLB leakage is expected to be negligible.

- An operating leakage limit of 150 gpd has been established to provide for detection of a rogue crack which could leak at much higher SLB leak rates than used in the criteria limits. The 150 gpd limit permits detection of a through wall crack of about [ ]^{a} inch for nominal leak rates and about [ ]^{a} inch for lower 2 σ (standard deviation) leak rates.

- To enhance consistency of the field EC inspection guidelines with the data base used to develop the plugging limits, the Kewaunee inspections will include: use of an ASME standard calibrated against the laboratory standard; use of a staggered 4-hole standard to assess probe wear effects and normalization of voltages to 3.4 volts for 400/100 kHz (support plate -- Mix.1) on the four 100% ASME holes.

3.0 REGULATORY REQUIREMENTS

3.1 General Design Criteria

The eddy current voltage based plugging criteria, which establishes a basis for removing tubes from service experiencing outside diameter stress corrosion cracking (SCC) occurring at tube support plate intersections in the Kewaunee steam generators, have been developed to ensure compliance with the applicable General Design Criteria of Appendix A of Part 50 of Title 10 of the Code of Federal Regulations (10CFR50). The GDCs considered are: 2, 4, 14, 15, 31, and 32 and are summarized below.

GDC 2, Design Basis for Protection Against Natural Phenomena, requires that structures, systems and components important to safety be designed to withstand the effects of earthquakes in combinations with the effects of design basis loadings without loss of safety function.

GDC 4, Environmental and Missile Design Bases, requires that structures, systems, and components important to safety are designed to accommodate the effects of and to be compatible with the environmental conditions associated with normal operation, maintenance, testing, and postulated accident condition loadings, including loss-of-coolant accidents.

GDC 14, Reactor Coolant Pressure Boundary, requires the reactor coolant pressure boundary to be designed, fabricated, erected, and tested so as to have an extremely low probability of abnormal leakage, of rapidly propagating to failure, and of gross rupture.

GDC 15, Reactor Coolant System Design, requires the reactor coolant system and associated auxiliary, control, and protection systems to be designed with sufficient margin to assure the design margins of the reactor coolant pressure boundary are not exceeded during any condition of normal operation, including anticipated operating occurrences.

GDC 31, Fracture Prevention of the Reactor Coolant Pressure Boundary, requires that the reactor coolant pressure boundary shall be designed with sufficient margin to ensure that when stressed under operating, maintenance, testing, and postulated accident condition loadings, the boundary behaves in a nonbrittle manner and the probability of a rapidly propagating fracture is minimized.

GDC 32, Inspection of the Reactor Coolant Pressure Boundary, requires that components that are part of the reactor coolant pressure boundary be designed to permit periodic inspection and testing of critical areas to assess their structural and leaktight integrity.

General Design Criteria 2 and 4 are considered in Section 3.3 below where the potential for steam generator tube collapse during the combined effects of LOCA + SSE loadings are addressed for the Kewaunee steam generators.

3.2 Regulatory Guide 1.121

Background

R.G. 1.121, "Bases for Plugging Degraded PWR Steam Generator Tubes" issued for comment in August of 1976, describes a method acceptable to the NRC staff for meeting GDCs 14, 15, 31, and 32 by reducing the probability and consequences of steam generator tube rupture through determining the limiting safe conditions of degradation of steam generator tubing, beyond which tubes with unacceptable cracking, as established by inservice inspection, should be removed from service by plugging. The recommended plugging criteria for the tube support plate elevation OD SCC occurring in the Kewaunee steam generators may result in tubes with both partial through-wall and through-wall (non-leaking) cracks being returned to service. In the limiting case, the presence of a through-wall crack alone is not reason enough to remove a tube from service. The regulatory basis for leaving through-wall cracks in service in the Kewaunee steam generators is provided below.

Steam generator "tube failure" is defined by the NRC within RG 1.83 as the full penetration of the primary pressure boundary with subsequent leakage. Consistent with this definition, upon the implementation of the tube plugging criteria of this report, known leaking tubes will be removed from service from the Kewaunee steam generators. Steam generator tube bundle leak tightness will be re-established by conducting 100% bobbin coil inspection of the S/G tubes. The tube plugging criteria of this report are established such that operational leakage is not anticipated.

The NRC defines steam generator tube rupture within RG 1.121 as any perforation of the tube pressure boundary accompanied by a flow of fluid either from the primary to secondary side of the steam generator or vice versa, depending on the differential pressure condition. As stated within the regulatory guide, the rupture of a number of single tube wall barriers between primary and secondary fluid has safety consequences only if the resulting fluid flow exceeds an acceptable amount and rate.

Consistent with the philosophy of the NRC's definition of tube rupture, during testimony by the NRC staff (on March 24, 1976) to provide information to the Atomic Safety and Licensing Board (ASLB) on the plans for measures to reasonably assure steam generator tube integrity under operating conditions including off-nominal and accident condition loadings at Kewaunee, the following definition of loss of steam generator tube integrity was provided. Loss of steam generator tube integrity means loss of "leakage integrity". Loss of "leakage integrity" is defined as the degree of degradation by a through-wall crack penetration of a tube wall membrane that can adversely affect the margin of safety leading to "tube failure", burst, or collapse during normal operation and in the event of postulated accidents. Acceptable service in terms of tube integrity limits the allowable primary to secondary leakage rate during normal operating conditions, and assures that the consequences of postulated accidents would be well within the guidelines of 10CFR100. In order to assure steam generator tube integrity is not reduced below a level acceptable for adequate margins of safety, the NRC staff position focused on specific criteria for limiting conditions of operation. These include:

1. Secondary Water Monitoring
2. Primary-to-Secondary tube leakage
3. Steam Generator Tube Surveillance
4. Steam Generator Tube Plugging Criteria

Tubes with through-wall cracks will maintain "leakage integrity" and are acceptable for continued operation if the extent of cracking can be shown to meet the following RG 1.121 criteria:

1. Tubes are demonstrated to maintain a factor of safety of 3 against failure for bursting under normal operating pressure differential.

2. Tubes are demonstrated to maintain adequate margin against tube failure under postulated accident condition loadings (combined with the effects of SSE loadings) and the loadings required to initiate propagation of the largest longitudinal crack resulting in tube rupture. All hydrodynamic and flow induced forces are to be considered in the analysis to determine acceptable tube wall penetration of cracking.

3. A primary-to-secondary leakage limit under normal operating conditions is set in the plant technical specifications which is less than the leakage rate determined theoretically or experimentally from the largest single permissible longitudinal crack. This action would ensure orderly plant shutdown and allow sufficient time for remedial action(s) if the crack size increases beyond the permissible limit during service.

The voltage based plugging criteria for indications at tube support plate elevations discussed in this report are shown to meet all of the necessary acceptance criteria.

3.3 Steam Generator Tube Deformation Discussion

In addressing the combined effects of the LOCA and SSE loadings (as required by GDC 2) on the steam generator component, [

]^{a}.

This issue has been addressed for the Kewaunee steam generators through the application of leak-before-break principles to the primary loop piping. A detailed leak before break analysis has been performed for Kewaunee. Based on the results, it is concluded that the leak-before-break methodology (as permitted by GDC 4) is applicable to the Kewaunee reactor coolant system primary loops and, thus, the probability of breaks in the primary loop piping is sufficiently low that they need not be considered in the structural design basis of the plant. Excluding breaks in the RCS primary loops, the LOCA loads from the large branch lines breaks were also assessed and found to be of insufficient magnitude to result in steam generator tube collapse. Using results from recent tests and analysis programs (discussed more fully in section

11.2), it has also been shown that no tubes will undergo permanent deformation where the change in diameter exceeds 0.025 inch. Although specific leakage data is not available, it is judged that deformations of this magnitude will not lead to significant tube leakage. On this basis no tubes need to be excluded from the APC for reasons of deformation resulting from combined LOCA + SSE loading.

4.0 PULLED TUBE EXAMINATIONS

4.1 General Tube Pull Results at Support Plate Locations

The type of intergranular corrosion with regard to crack morphology and density (number, length, depth) of cracks can influence the structural integrity of the tube and the eddy current response of the indications. For support of tube plugging criteria, the emphasis for destructive examination is placed upon characterizing the morphology (SCC, IGA involvement), the number of cracks, and characterization of the largest crack networks with regard to length, depth and remaining ligaments between cracks. These crack details support interpretation of structural parameters such as leak rates and burst pressure, and of eddy current parameters such as measured voltage, depth and crack lengths with the goal of improving structural and eddy current evaluations of tube degradation. In selective cases, such as the 1990 Plant A-2 pulled tubes, the pulled tube evaluations included leak rate and burst pressure measurements for further support of the integrity and plugging limit evaluations.

4.1.1 Types of OD Corrosion Degradation Observed at Support Plate Crevice Locations

Intergranular corrosion morphology can vary from IGA to SCC to combinations of the two. IGA (Inter Granular Attack) is defined as a three dimensional corrosion degradation of grain boundaries. The radial dimension has a relatively constant value when viewed from different axial and circumferential coordinates. IGA can occur in isolated patches or as extensive networks which may encompass the entire circumferential dimension within the concentrating crevice. The growth of IGA is relatively stress independent. IGSCC (Intergranular Stress Corrosion Cracking) is defined as a two dimensional corrosion degradation of grain boundaries that is more stress dependent than IGA. (Transgranular SCC in Alloy 600, caused by exposures to lead (Pb) environments, has only been rarely observed in the field at support plate crevice locations.) IGSCC is typically observed in the axial-radial plane in steam generator tubing, but can occur in the circumferential-radial plane or in combinations of the two planes. The IGSCC can occur as a single two dimensional crack, or it can occur with branches coming off the main plane. Both of the IGSCC variations can occur with minor to major components of IGA. The IGA component can occur simply as an IGA base on the tube OD with SCC protruding through the IGA base or the SCC plane may have a IGA degradation along the crack plane, independent of any surface IGA. Based on laboratory corrosion tests, it is believed that the latter, SCC protrusions with IGA components along the crack plane grow at rates similar to that of SCC, as opposed to the slower rates usually associated with only IGA. When IGSCC and IGA are both present, the IGSCC will penetrate through wall first and provide the leak path. The density of cracking can vary from one single large crack (usually a macrocrack composed of many microcracks which nucleated along a line that has only a very small width and which then grew together by intergranular corrosion) to hundreds of very short microcracks that may have partially linked together to form dozens of larger macrocracks. Note that in cases where a very high density of cracks are present (usually axial cracks) that also have significant IGA components, then the outer surface of the tube (crack origin surface) can form regions with effective three dimensional IGA. Axial deformations of the tube may then cause circumferential appearing openings on the outer surface of the tube within the three dimensional network of IGA; the networks are sometimes mistakenly referred to as circumferential cracks. The axial cracks will still be the deeper and the dominant degradation, as compared to the IGA.

As described in Sections 4.2 and 4.3, the Plant A tubes examined show dominantly SCC crack networks with IGA components that vary from minor to, in one case, significant.* The larger eddy current indications for the 1990 pulled tubes are principally related to the single, large macrocrack found for these tubes.

4.1.2 Through Wall SCC at Support Plate Crevice Locations

The following presents OD intergranular corrosion data at support plate intersection locations on steam generator tubes which have experienced through wall corrosion. The latest results for the 1990 examination of through wall cracks at the support plate locations at Plant A-2, however, are presented in Section 4.2.

Plant A-2, Steam Generator C, Hot Leg Tube R31-C46, Support Plate 1

OD origin, axially oriented, intergranular stress corrosion cracks were observed confined entirely within the first support crevice region on hot leg tube R31-C46, removed in 1986 from Steam Generator C of Plant A-2. Destructive examination was confined to half of the tube circumference (the half with a single axial NDE indication). The main crack, composed of at least four microcracks which grew together, was 0.52 inch long and was through wall for approximately 0.02 inch. The morphology of the individual microcracks was branched SCC with moderate IGA components to the SCC. Figure 4-1 shows a sketch of SEM (scanning electron microscope) fractographic results of the main crack (only the mid to upper poriton of the crack was examined) and a sketch of the overall crack distribution observed within the support plate crevice region. Figure 4-2 shows a sketch of the crack distribution (a composite of two transverse metallographic sections) and depth as viewed by metallography as well as a micrograph of a crack showing the crack morphology. In addition to the main macrocrack, (which included a 46% deep axial crack next to the main crack), two smaller axial cracks were observed at other circumferential positions on the half-circumference section examined.

Field eddy current probe inspection (in April 1986, just prior to the tube pull) of the first support plate crevice region produced a 6.2 volt, 81% deep indication in the 400/100 kHz differential mix channel. Voltage renormalization (see Section 6.6) to the calibration standards of this report yields 7.2 volts for this indication.

Plant B-1, Steam Generator C, Hot Leg Tube R4-C61, Support Plate 5

OD origin, axially orientated, intergranular stress corrosion cracks were observed confined entirely within the fifth support plate crevice region on the hot leg side of tube R4-C61 from Steam Generator C of Plant B-1. Six axial macrocracks were observed around the circumference. The largest of these was examined by SEM fractography without any

---

* To provide some quantification of the terms minor, moderate and significant with respect to the degree that IGA is found in association with SCC that has IGA components along the crack plane, the SCC crack depth and IGA widths are used as follows. The depth (D) of the crack and the width (W) of the IGA at the mid-depth of the crack are measured and the ratio (D/W) of these values determined. "Minor" IGA components is defined as having a D/W ratio of greater than 20, "moderate" as having a D/W ratio between 3 and 20, and "significant" as having a D/W ratio of less than 3.

metallography. The macrocrack was 0.4 inch long and through wall for 0.01 inch. However, the crack was nearly (effectively) through wall for 0.1 inch. The macrocrack was composed of seven individual microcracks that had mostly grown together by intergranular corrosion (the separating ledges had intergranular features that ranged from 40 to 90% of the length of the ledges). Since no metallography was performed on the axial cracks, it is not possible to definitively describe the axial crack morphology at this location. At the eighth support plate region of the same tube, metallography showed that the morphology was that of SCC with a crack depth to IGA width ratio (D/W) of 15. Figure 4-3 summarizes the crack distribution and morphology data for the fifth support plate crevice region.

In addition to the OD origin axial macrocracks observed at the fifth support plate region, five local areas had circumferential intergranular corrosion. The maximum penetration observed for the circumferential cracking was 46% through wall. The morphology of the circumferential cracking was more that of IGA patches than of SCC. Figure 4-4 provides micrographs of relevant cracks showing the morphology of axial and circumferential cracks. As stated above, the axial cracks had a morphology of IGSCC with a moderate D/W ratio of 15 while the circumferential cracking had a morphology more like that of IGA, with a D/W ratio of 1.

Field eddy current bobbin probe inspection (in June 1989, just prior to the tube pull) of the fifth support plate crevice region produced a 1.9 volt, 74% deep indication in the 550/100 kHz differential mix.

4.2 Plant A-2 1990 Tube Pull Results at TSP Locations

Hot leg tubes R4-C73 and R21-C22 were pulled from Steam Generator B and hot leg tube R38-C46 was pulled from Steam Generator C. The sections pulled included the first support plate region from each tube. Laboratory NDE, leak and burst testing, and destructive examinations were performed. The following summarizes the data obtained at the first support plate region of each tube.

NDE Testing

Laboratory eddy current testing was performed using 0.720 inch diameter bobbin and RPC probes. RPC results showed a main axial indication within the support plate crevice region of tube R4-C73. The length of the signal was 0.44 inch and the depth was estimated as 77 to 82% deep based on an ASME drilled hole standard. In addition to the main signal, a less intense RPC signal was observed parallel to the main axial signal approximately 20 to 30° away. Tube R21-C22 produced a single axial indication within its first support plate crevice region. The 0.5 inch long RPC signal was estimated to be 76 to 81% deep. Tube R38-C46 had a 90% deep RPC signal that was 0.4 inches long. Note that this tube was elongated during the tube pull. As consequence of the reduced OD dimension, a 0.69 inch diameter RPC probe was used.

Laboratory bobbin probe examination of tubes R4-C73 and R21-C22 was performed using two 0.720 inch diameter bobbin probes. One was a brand new Echoram probe with very stiff spacers (it was difficult to insert the probe into the tube). The other was a slightly used (in terms of length of tubing previously examined) SFRM Zetec probe in which the spacers were less stiff (probe insertion into the tubes was easy). The probes were pulled mechanically through the tubes at speeds similar to those used in the field; however, unlike the field situation, the tubes were examined with the tubes positioned horizontally. In addition, multiple passes were made

with each probe with the specimen being rotated between each pass to vary the position of the crack indication. Table 4.1 presents the results. An indication was observed within both support plate crevice locations. Depth estimates were similar for both of the support plate crevice regions and for both of the probes. A range of 86 to 91% deep covered all depth estimates. The voltage varied noticeably depending on the probe used and the orientation of the specimen, with the stiffer Echoram probe producing the smaller voltage variation. For tube R4-C73, the Echoram probe voltage variation ranged from 3.6 to 4.3 volts. For tube R21-C22, the Echoram probe voltage variation ranged from 9.6 to 11.6 volts.

While tube R38-C46 was reduced in diameter during the tube pull, the Zetec 0.72 inch diameter bobbin probe could still be used for the laboratory examination. However, it passed through the deformed tube with difficulty. Consequently, the estimates of depth and voltage are not judged to be reliable. The field bobbin test produced a 1.4 volt signal with an indicated depth of 68%. This is considered more reliable than the laboratory result of 4.8 volts and 90% depth. Since the tube pull opened crack networks which were readily visible, the larger laboratory voltage is not surprising.

Double wall radiography was performed using four rotations. No crack indications were observed on tube R21-C22 but a single axial crack-like indication was observed within the first support plate region of tube R4-C73. The faint indication, located near 0°, was 0.3 inch long and was located entirely within the support plate crevice region. These results imply that any deep corrosion cracks present on the two pulled tubes from S/G-B are very tight. OD measurements of the pulled tubes from S/G-B showed that the average diameter of both tubes was 0.8755 inch with a 0.001 inch ovality. No noticeable tube deformation occurred during tube pulling to open any corrosion cracks. Tube R38-C46 from S/G-C was noticeably reduced in diameter. The tube had an average OD of 0.830 inch within the TSP crevice region. Radiography of tube R38-C46 showed three main locations of crack networks within the TSP crevice region. The crack networks contain both axial and circumferential indications. The circumferential cracks were wide, as would be expected for a tube which experienced elongation during the tube pull.

Ultrasonic testing was also performed on the support plate specimens. A 0.4 inch long axial indication was observed near 330° on tube R21-C22 within the support plate crevice region. On tube R4-C73 a 0.25 inch axial indication was observed near 30° within the support plate crevice region. A shorter and fainter axial indication was also observed near 70°. On tube R38-C46 three patches of indications were noted, one near 20°, one near 230°, and one near 340°. All were located within the TSP crevice region.

Leak and Burst Testing

Following NDE characterization, the three tube sections from the first support plate region were leak and burst tested. The leak tests were performed in two parts. The specimens were first tested under simulated normal operating conditions. At a test temperature of 616 °F, the primary side of the specimen was connected by insulated pressure tubing to an autoclave maintained at a pressure of 2250 psi by bottled nitrogen gas. The specimen was located in a second autoclave maintained at 616 °F and a pressure of 750 psi, resulting in a differential pressure of 1500 psi. The 750 psi pressure in the second autoclave was maintained by a back pressure regulator (BPR) connected to the autoclave by pressure tubing. Any water vapor passing through the BPR was then passed through cooling coils immersed in ice water. The amount of condensed water was measured as a function of time. Following the initial leak testing,

a simulated steam line break (SLB) leak test was performed using the same system. For the SLB test, the primary pressure was increased to 3050 psi and the secondary side pressure was decreased to 400 psi resulting in a pressure differential of 2650 psi.

Leak test data are presented in Table 4.2. Results from the SLB test are considered reliable. The measured SLB leak rates were [
]^{9} and no leakage for tube R38-C46. These values are considerably below the maximum leak rate capability of the system, estimated to be approximately 2 l/hr based on a test with the test specimen removed. Results for the normal operating conditions are considered to be less accurate. The observed leak rate for tube R4-C73 was [
]^{9} for tube R21-C22. No leakage was observed for tube R38-C46. These rates include any overflows from the back pressure regulator (BPR). Leakage through the BPR was encountered, especially with the testing of tube R21-C22. The BPR may have contributed to the entire amount of leakage observed* for the normal operating condition test. While this amount of overflow from the BPR is small in comparison to the SLB test leak rates, it is very large in comparison to potential leak rates from the normal operating conditions test. Consequently, the normal operating condition leak rate at the lower end of potential leak rates for these specimens should be considered zero. The upper value presented, at least for tube R21-C22, probably includes significant contributions from the BPR.

Room temperature burst tests were performed on the two specimens following leak testing. The specimens were pressurized with water at a pressurization rate of approximately 1000 psi/sec. Tygon tubing internal bladders were inserted into the specimens to permit testing with their through wall corrosion cracks. No support plate restraints were placed on the specimens. Consequently, the burst pressures measured may be lower than would be observed in the presence of a support plate.

The first support plate region of tube R4-C73 burst at [ ]^{9} psi, the first support plate region of tube R21-C22 burst at [ ]^{9} psi, and the first support plate region of tube R38-C46 burst at [ ]^{9} psi. Table 4.2 presents this data as well as other burst data characterizing the specimens.

Characterization of the Corrosion Cracks

Figure 4-5 shows a sketch of the SEM fractographic observations on the burst fracture face of the first support plate region of tube R4-C73. Within the center of the burst opening, a 0.42 inch long OD origin macrocrack was observed. The macrocrack was located at an orientation**

---

* Prior to initiation of the leak tests, the specimen fittings were tested to verify that they were leak tight. The fittings were tested by pressurizing the specimens with 500 to 600 psi air and holding the specimens and their fittings under water. No fitting leaks were observed. The R4-C73 specimen was observed to leak air bubbles at the location of the support plate at a pressure of 500 psi air. The R21-C22 specimen did not leak air bubbles at a pressure of 600 psi. Consequently, it is believed reasonable that the normal operating leak rate for tube R21-C22 should be lower than that for tube R4-C73. This would also be consistent with the SLB leak results.

** In the orientation system used, 0° faces the steam generator divider plate and 90° is clockwise of 0° when looking in the primary flow (up) direction.

of 20° and was entirely confined to within the support plate crevice region. It had only intergranular corrosion features. The macrocrack was composed of four microcracks, all of which had joined together by intergranular corrosion. The crack was through wall for 0.18 inch. A parallel axial macrocrack was observed near 40°. It was 0.46 inch long and up to 69% through wall. In addition, numerous short axial cracks were observed at various locations within the crevice region. The depth of these short cracks ranged from minor penetrations to 34%. Figure 4-5 also provides a sketch estimating the crack distribution within the support plate crevice region as well as a description of the crack morphology of the main macrocrack. Figure 4-6 provides a sketch of the crack distribution and depth within the center of the support plate crevice region as determined by metallography. The main crack morphology was that of SCC with moderate IGA components (D/W = 4). The width of IGA surrounding the SCC is estimated to be approximately 0.012 inch, except at the OD surface where the width was larger. Other cracks tended to have less IGA components. Figure 4-7 provides micrographs showing both the main crack morphology as well as the crack morphology of one of the lesser cracks. The morphology of the latter crack, which has been opened wide by tube deformation, is more that of IGSCC (D/W = 12).

Figure 4-8 shows a sketch of the SEM fractographic observations on the burst fracture face of the first support plate region of tube R21-C22. Within the center of the burst opening, a 0.50 inch long OD origin macrocrack was observed. The macrocrack was located at an orientation of 330° and was entirely confined to within the support plate crevice region. The corrosion crack had only intergranular features. The macrocrack was composed of four microcracks. Three of the microcracks were joined by intergranular corrosion, while the top most microcrack was still separated from the others by metal. The macrocrack was through wall for approximately 0.15 inch. Figure 4-8 also provides a description of the crack morphology. The crack morphology was that of SCC with significant IGA components. The width of IGA surrounding the SCC is estimated to be approximately 0.030 inch (D/W = 1.7). One additional crack was later observed on the specimen by metallographic examination. Figure 4-9 provides a sketch of the crack distribution and depth observed by metallography. Figure 4-10 provides micrographs of the cracks. As can be observed, the secondary crack morphology had lesser IGA components (D/W = 19 to 37).

Figure 4-11 shows a sketch of the SEM fractographic observations on the burst fracture face of the first support plate region of tube R38-C46. A 0.37 inch long, OD origin, axial macrocrack was observed. The intergranular crack was up to 78% through wall and was contained within the support plate crevice region. The macrocrack was composed of numerous microcracks which had an unusual spatial distribution. They had orientations which ranged from axial to circumferential generating a spider-like crack distribution. Three other crevice locations had less deep but significant intergranular crack distributions. Their locations are also shown in Figure 4-11. Figure 4-12 shows the crack distribution and depth as determined by transverse metallographic examinations. Figure 4-13 shows photomicrographs of cracks in transverse sections obtained from within the crevice region. The cracks are opened wide by tube deformation. The morphology of the cracks is that of IGSCC with minor to moderate IGA components (D/W = 14 to 28).

4.3 Prior Pulled Tube Examinations from Plant A at TSP Locations

Prior to 1990, a total of 10 hot leg support plate intersection locations on steam generator tubing removed from Plant A-2 were examined. In 1985 the first three hot leg support plate

regions of tube R34-C44 from Steam Generator A were destructively examined. In 1986 the first support plate region of tube R31-C46 from the hot leg side of Steam Generator C was destructively examined as described in Section 4.1. In 1989 the first three support plate regions of tubes R16-C50 and R16-C53 from the hot leg side of Steam Generator C were destructively examined. Of these 10 support plate locations, 6 were found to have OD origin intergranular corrosion. In addition, a support plate region of a tube removed in 1989 from Plant A-1 was examined. The support plate region of this tube also had OD origin intergranular corrosion. The following describes the extent and morphology of the degradation found.

Plant A-2, 1985 Examination

The first three support plate regions of hot leg tube R34-C44 from Steam Generator A were destructively examined to determine the origin of residual eddy current signals left at the location of the support plates after frequency mixing to eliminate the support plate signal. No corrosion degradation was found by destructive examination at the three support plate locations.

Plant A-2, 1986 Examination

The first support plate region of hot leg tube R31-C46 from Steam Generator C was destructively examined. A 6.16 volt, 81% deep eddy current signal was detected in the field bobbin probe examination using a 400/100 kHz frequency mix. Renormalization to the standard used in this report yielded 7.2 volts. Destructive examination found a 0.5 inch long macrocrack that extended from 0.1 inch above the support plate bottom edge location to 0.2 inch below the top edge location. The crack averaged 80 to 90% through wall with a local area penetrating 100% through wall for a length of 0.02 inch. The macrocrack was composed of a number of axially orientated microcracks which had grown together by corrosion. The intergranular cracking was of OD origin and a number of shallow cracks existed parallel and nearby to the major macrocrack. The morphology of the cracking was predominately SCC, but moderate IGA components (D/W = 3.2) were also present.

Plant A-2, 1989 Examination

Two hot leg steam generator tubes from Plant A-2, Steam Generator C were examined to determine the origin of residual eddy current signals at support plate locations. The destructive examination included the crevice region at support plates 1-3 of tubes R16-C50 and R16-C53.

All six support plate intersections had residual type eddy current signals. The second support plate region of both tubes was chosen for more detailed examination. Following removal of both ID and OD deposits by honing, abrasion, and later by chemical cleaning, the eddy current examination was repeated. No significant change was observed in the eddy current signals indicating that the residuals were not related to surface deposits.

Destructive examination of tube R16-C50 found OD origin intergranular corrosion within the first and second support plate regions. No corrosion degradation was found within the third support plate crevice region. The first support plate region had only an isolated region of minor OD origin, intergranular, axial SCC. The maximum depth of SCC was 0.007 inch. The second support plate region from tube R16-C50 had experienced some negligible (no wall thickness change measurable) OD general corrosion with some intergranular penetrations. While most of the tube OD cracking within the TSP crevice regions had these features, at one location the intergranular corrosion was somewhat deeper though still regarded as minor. At this location,

0.2 inch below the support plate top edge, the penetrations formed two short parallel axial cracks, 0.06 inch long and up to 0.0015 inch deep. Consequently, all three support plate regions of tube R16-C50 had no, or only very minor, IGSCC degradation. Figure 4-14 shows a micrograph of the largest crack found, that within the first support plate crevice region. The morphology is that of IGSCC with only minor to moderate IGA components.

Destructive examination of tube R16-C53 found OD origin intergranular corrosion within all three support plate regions. The first support plate region of tube R16-C53 had numerous OD origin, intergranular, axial stress corrosion cracks, but the depth of cracking was shallow (0.0055 inch maximum depth). At the second support plate of tube R16-C53, axial intergranular stress corrosion cracking was found on the tube OD concentrated near the support plate top edge and to a lesser extent near the support plate bottom edge. There were dozens of very tight stress corrosion cracks located discontinuously around the circumference, but located within all four quadrants of the tube. The maximum depth of penetration was 0.011 inch (22%). The third support plate region also had numerous but relatively shallow OD origin, intergranular, axial SCC. The maximum depth of degradation was 0.0065 inch. Consequently, the only support plate region of tube R16-C53 with corrosion degradation of any potentially noticeable (by eddy current) depth was the second support plate region where the maximum depth was 0.011 inch (22% through wall). The morphology of these cracks ranged from that of IGSCC (Figure 4-15) to that of IGSCC with significant IGA components (Figure 4-16).

In summary, the 1989 pulled tubes were removed primarily to determine the cause of eddy current support plate residual signals. Laboratory eddy current testing showed that the residual eddy current signals were not caused by surface deposits. Destructive examination also showed that the residual signals were not caused by corrosion degradation, even though minor OD origin SCC was present at five of the six support plate locations. For tube R16-C50 the deepest support plate region SCC was 0.007 inch while for tube R16-C53 the deepest crack was 0.011 inch. For the other support plate locations with cracks, the deepest cracks were 0.0015, 0.0055, and 0.0065 inch.

Plant A-1, 1989 Pulled Tube Examination

The first support plate crevice region of hot leg tube R20-C26 from Steam Generator C of Plant A-1 was destructively examined. Dozens of short, OD origin, intergranular, axial stress corrosion cracks existed within the crevice region and just above the crevice region. Most of these cracks were found within two 30° wide axial bands on opposite sides of the tube. The band located at 255 to 285° extended from the support plate bottom edge to just above the support plate top edge. The deepest crack in this band penetrated 62% through wall and was located approximately 0.2 inch below the top edge. The second band occurred between 75 and 105° with the cracking extending from the bottom edge to approximately 0.275 inch above the support plate top edge. Within the crevice region, the deepest crack in the second band of cracks occurred near the support plate top edge. This crack was 42% through wall. Above the top edge, the depth of cracking decreased rapidly. At 0.13 inch above the top edge, the deepest crack was 10% through wall. With respect to the length of individual cracks, they were typically much less than 0.1 inch long. Where individual cracks had grown together, cracks up to 0.13 inch long were found. Figure 4-17 sketches the crack distribution found within the first support plate crevice region and also provides crack depth data. Figures 4-18 and 4-19 provide photomicrographs of typical cracks as observed in transverse metallographic sections that have been deformed to open cracks. The morphology is that of IGSCC with minor to moderate IGA components (D/W = 17 to 28). Figure 4-20 shows similar transverse micrographs, but ones

in which not all cracks were opened during the tube deformation.

Field eddy current inspection (bobbin probe) of the first support plate region revealed (by initial interpretation) no corrosion degradation. Later analysis suggested a very low voltage (0.2 volts) indication signal, partially hidden between larger voltage dent signals. Laboratory bobbin probe inspection produced similar results, with an indication voltage of 0.4 volts within the overall 7 volt dent signal. The phase angle of the indication component, within the overall dent signal, suggested a 61% deep indication. RPC testing revealed many indications confined to within the crevice region.

4.4 IGA and Corrosion Morphology at Support Plate Crevice Locations

A review of available Westinghouse tube pull data was made for the purpose of comparing corrosion morphology in various plants and for determining the extent of IGA (in contrast to the IGSCC previously discussed in Sections 4.1.1, 4.1.2, 4.2, and 4.3) present at support plate crevice locations on steam generator tubing. This review also included recent data from Plant L tube R12-C8 from Steam Generator D. Due to its special interest, the Plant L tube will be discussed first in detail.

4.4.1 IGA and Corrosion Morpholgy at Support Plate Crevice Locations at Plant L

Corrosion Degradation at the First Support Plate Region of Tube R12-C8

A summary of corrosion observations at the first support plate region of plugged tube R12-C8 is as follows. Within the first support plate crevice region of tube R12-C8, very high densities of axially oriented IGSCC microcracks were observed. Corrosion was not observed outside of the crevice region. The microcracks had moderate IGA components associated with them. A good description of the microcracks would be that of IGA fingers, with the depth of the cracks typically being 6 to 18 times the width of the IGA associated with the crack. The microcracks were less than 0.05 inch long, in axial extent. The density of support plate region cracking was significantly higher than that observed for most other domestic power plants. For a given elevation, crack densities of three to five hundred individual microcracks could be extrapolated to exist around the circumference based on metallographic and SEM fractographic data if the maximum local crack density observed extended completely around the circumference. (For tubes examined by Westinghouse at support plate regions, crack densities of 1 to 10 are most typically observed. The highest, support plate region, crack density previously observed in tube examinations by Westinghouse was 20 to 100 at Plant D-2. It has been reported that high crack densities of approximately 300 cracks over the circumference of a support plate region have also been observed in some EdF steam generators.) Because of the very high densities of cracks and the IGA associated with the cracks, local regions sometimes formed effective patches of IGA. (Alternatively, the IGA patches may have formed independently of the IGSCC.) The depth of these IGA patches was typically half that of the the maximum depth of cracking penetrating through the IGA patch. The largest circumferential length of continuous IGA observed by metallography was 0.05 inch, or approximately 7 degrees, with a maximum depth of 33%. The maximum depth of IGSCC in the same general region was approximately 85%. Figure 4-21 provides supporting metallographic data.

Another aspect of the very high density of axially orientated microcracks, was the formation of larger axial macrocracks. (Before this aspect can be considered, further details regarding the

destructive examination need to be mentioned. The first support plate region was initially separated circumferentially near the center of the crevice region by applying a tensile force axially to the tube. The fracture would have occurred where the volumetric corrosion degradation was deepest. SEM fractography of the separation showed intergranular corrosion greater than 10% deep over 310 degrees of the circumference. Table 4.3 presents complete depth data for the corrosion front. It is believed that the corrosion front was composed of a large number of axially orientated cracks that frequently had interconnecting IGA components. The deepest region of corrosion was 80 to 92% deep, via IGSCC, over approximately 20 degrees of the circumference.) Above this local region with the deepest corrosion, the tubing was deformed to open any axial crack networks. Many were revealed. One of the deeper looking ones was broken apart and SEM fractography was performed. A fairly uniform crack front was observed from the support plate crevice center to the support plate crevice top. The front ranged from 41 to 55% through wall, with an average depth of 48%. Several ledges were observed in the fractograph where it is believed that individual, axially oriented, microcracks had joined together to form the macrocrack. Below the support plate center, only metallography was performed. Transverse metallography (Figure 4-21) revealed the morphology of the axial cracking and IGA in the form of IGSCC with moderate IGA components and IGA patches at the bases of the IGSCC. Axial metallography was performed from the bottom edge of the crevice to the center of the crevice region, through a region with corrosion. A fairly uniform corrosion front, approximately 50% through wall, was observed that is similar to that revealed by SEM fractography above the center of the crevice. From this data it is concluded that axial macrocrack networks existed from the bottom edge of the support plate crevice region to the top edge, with the crack fronts having a fairly uniform depth.

Corrosion Degradation at the Second Support Plate Region of Tube R12-C8

Metallographic data available from the second support plate crevice region of tube R12-C8 indicated approximately 50 axial penetrations around the circumference. The morphology of the penetrations was typically that of narrow IGA fingers. The maximum depth of cracking observed was approximately 48% through wall. ABB (CE) has reported that the maximum depth of the intermittently distributed, effective surface IGA was 27% through wall. Note that the ABB (CE) definitions of IGA may have produced larger values than would have been produced by a Westinghouse definition of IGA.

Corrosion Degradation at the Third Support Plate Region of Tube R12-C8

After burst testing of the third support plate crevice region (room temperature burst occurred at 10,500 psi), visual examination revealed numerous, axially oriented, corrosion openings adjacent to the main burst opening. Most of the corrosion appeared to be shallow. SEM fractography performed on the burst opening showed intergranular corrosion existing from the bottom to the top edge of the crevice region. Large ledges (with dimple rupture features) were frequently observed between axially orientated microcracks. Transverse metallography showed approximately 106 cracks around the circumference with a morphology of axial IGSCC with moderate IGA components. The maximum depth of cracking was 55%. ABB (CE) calculated that the maximum depth of effective surface IGA approached 33% through wall. Again, the ABB (CE) definition of IGA may have produced larger values than may have been produced by a Westinghouse definition of IGA.

Corrosion Degradation of Other Tubes From Plant L

Preliminary destructive examination of the first, second, and third support plate regions of tube R29-C70 has produced the following results. All three regions had similar corrosion degradation. Axially oriented IGSCC with only minor to moderate IGA components was present without effective surface IGA (intermittent minor surface IGA, 1 to 2 grains deep, was occasionally present). The absence of the effective surface IGA is in contrast to the results for tube R12-C8. At a mid-support plate elevation, 2 to 3, 5, and 4 cracks were found distributed around the circumference for the first, second and third support plate regions, respectively. The presence of such a small number of cracks is typical of support plate cracking at many power plants and is in great contrast to the results for tube R12-C8 from Plant L. The burst strengths for the three regions were 10,400 psi, 9000 psi, and 10,400 psi, respectively. SEM fractography of the burst faces showed IGSCC macrocracks, confined to the crevice regions, that were 0.29, 0.62 and 0.45 inch long, respectively. These macrocracks were composed of microcracks that were separated by ligaments with dimple rupture fractures. The numbers of such microcracks were 3, 6 and 7, respectively, for the first, second and third support plate crevice regions.* The maximum spacing between microcrack ledges with tensile overload features was 0.17, 0.23 and 0.16 inch, respectively. The maximum depth of IGSCC observed was 56%, 76%, and 50 to 74%, respectively.

Preliminary destructive examination of the first, second, and third support plate regions of tube R30-C64 has produced the following results. All three regions had similar corrosion degradation. Axially oriented IGSCC with only minor to moderate IGA components was present without effective surface IGA (intermittent minor surface IGA, 1 to 2 grains deep, was occasionally present). The absence of the effective surface IGA is again in contrast to the results for tube R12-C8 and is similar to the results for tube R29-C70. At a mid-support plate elevation, 35, ~78, and ~93 cracks were found distributed around the circumference for the first, second and third support plate regions, respectively. The presence of this moderate number of cracks is also typical of support plate cracking at many power plants and is in contrast to the results for tube R12-C8 from Plant L, at least for the first support plate region. The burst strengths for the three regions were 10,500 psi, 8800 psi, and 10,200 psi, respectively. SEM fractography of the burst faces showed IGSCC macrocracks, confined to the crevice regions, that were 0.25, 0.61 and 0.45 inch long, respectively. These macrocracks were composed of microcracks that were separated by ligaments with dimple rupture fractures. The numbers of such microcracks were ~20, 6 to 7, and 9 respectively, for the first, second and third support plate crevice regions.* The maximum spacing between microcrack ledges with tensile overload features was 0.12, 0.23 and 0.11 inch, respectively. The maximum depth of IGSCC observed was ~60%, ~64%, and 50%, respectively.

Summary

All three support plate regions of Plant L plugged tube R12-C8 had multiple axial IGSCC macrocrack networks from the bottom to the top edge of the crevice. The first support plate region had the deepest cracking, 92% through wall. For the second and third support plate regions, the maximum crack depths were 48 and 55%, respectively. In addition, effective IGA patches were observed. In the case of the first support plate crevice location, the IGA patches

---

* Other ligaments or ledges with intergranular features were also present.

occurred in regions with the highest crack densities. The depths of the IGA patches were typically half that of the associated axial cracking. For the second and third support plate regions, limited data was directly available regarding the IGA patches, but it was reported by CE that the maximum depths of IGA for these two support plate regions were 27% and 33%, respectively. The six support plate regions from non-plugged tubes R29-C70 and R30-C64 had corrosion more typical of other plants: a small to moderate number of axial IGSCC, moderate IGA components to the cracking, and no separate IGA (patch IGA). While the IGSCC on tubes R29-C70 and R30-C64 had IGA components, the appearance was more that of stress corrosion cracking than that of IGA fingers as was observed at the first support plate region of tube R12-C8.

4.4.2 Comparison of Plant L Support Plate Corrosion to Support Plate Corrosion at Other Plants

It is difficult to compare corrosion morphology from one plant to another since the visual, metallographic and SEM fractographic data are frequently not comparable and seldom provide a complete description. It is especially difficult if the person doing the comparison has not directly worked with the raw data since it will not be known if the reported data represents typical or the more spectacular and extreme data. With these caveats, the following presents a corrosion comparison in which the raw data, not just the reported data, were all studied by the same person.

To compare support plate corrosion morphology, three ways of data characterization were utilized. All three need to be considered to characterize the corrosion. The first measures cracking density. Since most cracking within support plates is axial in nature, cracking density is usually measured from a transverse metallographic section. If a complete section is available, the cracking density at the given elevation can be directly measured. If only a partial section is available, an estimate by extrapolation can be made. Cracking densities were arbitrarily divided into three density categories: low (1 to 24 cracks); moderate (25 to 100 cracks); and high (greater than 100 cracks). Note that since most axial cracking is composed of short microcracks, usually less than 0.05 inches long, a cracking density of say 25 at a given elevation would correspond to several hundred microcracks within a support plate region. The second way of characterizing the data involved measuring the amount of IGA associated with a given crack. To do this the depth of the crack was divided by the width of the IGA as measured at the mid-depth of the crack, creating a ratio D/W. Again, three arbitrary D/W categories were created: minor (D/W > 20) (all or most PWSCC would be included in this category if it were being considered in this analysis); moderate (D/W 3 to 20); and significant (D/W < 3) where for a given crack with a D/W of 1 or less, the morphology approaches that of patch IGA. The third way of characterizing the data involved considering the extent of IGA present on the the tube, but only the IGA not obviously associated with a single crack was considered. Consequently, IGA independent of cracking is measured and IGA associated with the interaction of more than one crack is measured. The measurement of IGA arbitrarily divided the circumferential extent of IGA into three categories: negligible (IGA < 5% deep); moderate (IGA 5 to 10% deep); and significant (IGA greater than 10% deep).

Table 4.4 presents a corrosion morphology comparison of Plant L support plate region data, similar data from other plants examined by Westinghouse, and data from laboratory corrosion tests conducted in model boilers. With respect to cracking density at support plate locations, it is obvious that the cracking densities at Plant L for the first support plate region of tube R12-C8 are considerably higher than experienced at other plants examined by Westinghouse. However, similar cracking densities of several hundred cracks at a given support plate elevation

are believed to exist in some EdF plants in Europe and in some plants in Japan. The cracking densities for the other support plate regions of tubes R12-C8, R29-C70, and R30-C64 are more typical of other power plants with low to moderate crack densities. With respect to the amount of IGA associated with the axial IGSCC, the Plant L data are similar to those at most other plants; moderate IGA components are found in association with the axial IGSCC. With respect to the extent of IGA, only Plant L (tube R12-C8 only) and Plant M-2, among the plants examined by Westinghouse, were found to have significant IGA (greater than 10% through wall). It is believed in the case of Plant L that the formation of IGA in the form of IGA patches is a result of the high cracking densities and IGA aspects associated with the individual cracks. Where the cracks are particularly close together, IGA patches form at the base of the cracks where the width of the IGA is greatest. In the case of Plant M-2, the typical IGA morphology was that of uniform IGA as is shown in the lower two photomicrographs in Figure 4-22. The top photomicrograph in Figure 4-22 also shows uniform IGA but with some axial IGSCC appearing through the uniform IGA.

While not examined by Westinghouse, the following presents data regarding Plant J-1 and Plant N-1. Figure 4-23 and 4-24 show photomicrographs from the first and second support plate regions of tube R8-C74 of steam generator 2 of European Plant J-1. The intergranular corrosion appears to be very similar to that at Plant L. Table 4.4 presents qualitative morphological data. While there is a slightly lower crack density, the extent of IGA associated with individual cracks is similar (moderate D/W ratios), the extent and depth of IGA is similar and the origin of the IGA also appears to be that of closely spaced axial IGSCC interacting near the surface to form local IGA patches. It is also interesting that the maximum depth of IGA compared to the depth of IGSCC is similar, typically one-third to one-half of the IGSCC depth. The data from the support plate regions at Plant N-1 was not in a form where firm conclusions regarding corrosion morphology could be made. Table 4.4 also presents an attempt to force conclusions from the data available to Westinghouse. Averaging the data from the three support plate regions, it is concluded that a corrosion morphology similar to Plant L (tube R12-C8) and Plant J-1 exists at Plant N-1.

Table 4.1

Laboratory Eddy Current Data for Tubes Removed from Plant A-2

Results at Bottom TSP Location for All Tubes

Examination	Tube R4-C73	Tube R21-C22	Tube R38-C46
RPC Exam	Axial indication with faint parallel indication 20 to 30 degrees away; 0.44 inch long, 77-82% deep.	Axial indication; 0.5 inch long, 76-81% deep.	Axial indication 0.4 inch long, 90% deep.
Bobbin Exam			
Echoram Probe	Indication 86-88% deep; voltage ranged from 3.6 to 4.3 volts depending on specimen orientation.	Indication 86-87% deep; voltage ranged from 9.6 to 11.6 volts depending on specimen orientation.	Use field data only: 1.4 volts, 68% deep.
Zetec Probe	Indication 86-91% deep; voltage ranged from 2.6 to 5.0 volts depending on specimen orientation.	Indication 86-90% deep; voltage ranged from 7.7 to 14.2 volts depending on specimen orientation.	

Table 4.2

Leak and Burst Data for Tubes Removed from Plant A-2

Results at Bottom TSP Location for All Tubes

Test	Tube R4-C73	Tube R21-C22	Tube R38-C46
Leak Test			
Operating Leak Rate (delta P = 1500 psi)	[		]*
Steam Line Break Rate (delta P = 2650 psi)	[		]*
Burst Test			
Burst Pressure (psig)	[		]*
Burst Ductility (% delta D)	5.6	6.8	7.6
Burst Opening Length (inches)	0.439	0.784	0.881
Burst Opening Width (inches)	0.135 (OD), 0.100 (ID)	0.210 (OD), 0.148 (ID)	0.167

---

* Problems with back pressure regulator increased the measured leak rate.

Table 4.3

Depth of Corrosion Observed on Circumferential Fracture Face from Center of the First Support Plate Crevice Region for Plant L Tube R12-C8

Circumferential Location (degrees)	Maximum Depth of Penetration (%)
0	62
10	90
20	92
30	78
40	52
50	60
60	52
70	40
80	18
90	60
100	48
110	48
120	56
130	60
140	58
150	60
160	56
170	44
180	56
190	2
200	14
210	10
220	18
230	8
240	14
250	14
260	16
270	14
280	44
290	40
300	44
310	18
320	18
330	0
340	16
350	0

TABLE 4.4

Comparison of Intergranular Corrosion Morphology at Support Plate Regions on S/G Tubing and Laboratory Specimens

Data Source	Cracking Density (as Measured or Estimated for One Plane)*			Extent of IGA Associated with the Major Cracks			Extent of OD IGA (Not Obviously Associated with a Single Crack)		
	Low (1-24 Cracks)	Moderate (25 - 100 Cracks)	High (Greater than 100)	Minor (D/W** >20)	Moderate (D/W 3 to 20)	Significant (D/W <3)	Negligible (<5% Deep)	Moderate (5 to 10% Deep)	Significant (>10% Deep)
Plant A-2									
R31-C46 SP1	-6				3.2		0		
R4-C73 SP1	-8				4.2		0		
R21-C22 SP1	-2					1.7	0		
R38-C46 SP1	-10			14-28			0		
Plant B-1									
R4-C61 SP1 (2H)	-4			25			0		
R4-C61 SP3 (8H)	-15 (for axial) -5 Circ. Cracks)				15 (for axial), -1 (for Circ. Cracks)		2% Deep Intermittently around circumference		
R4-C61-SP5 (12H)	-8 (Circ. Cracks)					1-2	0		
Plant J-1									
L8-C74 SP1			≤141		14-20				~200°, max. depth ~40%.
L8-C74 SP2			≤176		10-15				~80°, max. depth ~20%.
Plant N-1									
L59-C95 SP1			≤340		4 (misleading ratio for these cracks, should be larger value)				45°, max. depth 20%.
L59-C95 SP2	0 (no cracks just IGA)								45°, max. depth 13%.

* Since most support plate cracking is composed of short axial microcracks, typically 0.02 to 0.05 inch long for a 50% deep crack, a microcracking density of 25 could be associated with more than several hundred individual microcracks within a support plate crevice region.

** D=Depth of SCC as measured from the OD surface exclusive of any surface IGA. W=Width of IGA component to the SCC as measured at the mid-point of the SCC.

TABLE 4.4 (Continuation)

Comparison of Intergranular Corrosion Morphology at Support Plate Regions on S/G Tubing and Laboratory Specimens

Data Source	Cracking Density (as Measured or Estimated for One Plane)*			Extent of IGA Associated with the Major Cracks			Extent of OD IGA (Not Obviously Associated with a Single Crack)		
	Low (1-24 Cracks)	Moderate (25 - 100 Cracks)	High (Greater than 100)	Minor (D/W** >20)	Moderate (D/W 3 to 20)	Significant (D/W <3)	Negligible (<5% Deep)	Moderate (5 to 10% Deep)	Significant (>10% Deep)
Plant N-1 (Cont.)									
L120-C12 SP3	3			34 (not accurate since obtained from unetched specimen)			1% deep intermittently around circumference		
Plant P									
R16-C60 SP1		80		Minor to moderate (no quantitative data available)			0		
Plant D-2									
R7-C38 SP1		90			4-8		0		
R7-C38 SP2		42			15		0		
R7-C38 SP3		23		24			1% deep intermittently around circumference		
R11-C25 SP3		~50			14		0		

* Since most support plate cracking is composed of short axial microcracks, typically 0.02 to 0.05 inch long for a 50% deep crack, a microcracking density of 25 could be associated with more than several hundred individual microcracks within a support plate crevice region.

** D=Depth of SCC as measured from the OD surface exclusive of any surface IGA. W=Width of IGA component to the SCC as measured at the mid-point of the SCC.

TABLE 4.4 (Continuation)

Data Source	Cracking Density (as Measured or Estimated for One Plane)*			Extent of IGA Associated with the Major Cracks			Extent of OD IGA (Not Obviously Associated with a Single Crack)		
	Low (1-24 Cracks)	Moderate (25 - 100 Cracks)	High (Greater than 100	Minor (D/W >20)	Moderate (D/W 3 to 20)	Significant (D/W <3)	Negligible (<5% Deep)	Moderate (5 to 10% Deep)	Significant (>10% Deep)
Plant M-2									
R29-C46CL SP1	0 (-50 if IGA fronts are defined as cracks with L/W ≤ 1)					≤ 1 if crack is defined as being present			≥300° uniform IGA; max. depth 26%
Plant C-2									
R26-C56 SP1 (2H)		36				2-10		2°, max. depth 8%	
Plant B-2									
R6-C67 SP1 (2H)	16				18		0		
R6-C67 SP3 (8H)		28			15		4% deep intermittently around circ.		
R6-C67 SP5 (11H)	6				ND		ND		
Plant L									
R12-C8 SP1			~400 (272-504)		6-18				210° at SP Center, less above and below Center, max. depth 43% by Metallography. Intermittently distributed,
R12-C8 SP2		50			Moderate (no quantitative data available)				max. depth 27%. Intermittently distributed,

* Since most support plate cracking is composed of short axial microcracks, typically 0.02 to 0.05 inch long for a 50% deep crack, a microcracking density of 25 could be associated with more than several hundred individual microcracks within a support plate crevice region.

** D=Depth of SCC as measured from the OD surface exclusive of any surface IGA. W=Width of IGA component to the SCC as measured at the mid-point of the SCC.

TABLE 4.4 (Continuation)

Comperison of Intergranular Corrosion Morphology at Support Plate Regions on S/G Tubing and Laboratory Specimens

Data Source	Cracking Density (Measured or Estimated for One Plane)*			Extent of IGA Associated with the Major Cracks			Extent of OD IGA (Not Obviously Associated with a Single Crack)		
	Low (1-24 Cracks)	Moderate (25 - 100 Cracks)	High (Greater than 100)	Minor (D/W** >20)	Moderate (D/W 3 to 20)	Significant (D/W <3)	Negligible (<5% Deep)	Moderate (5 to 10% Deep)	Significant (>10% Deep)
Plant L (Cont.)									
R12-C8 SP3			106		Moderate (no quantitative data available)				max. depth 33%.
R29-C70 SP1	2-3				Minor to moderate (no quantitative data available)		-0		
R29-C70 SP2	5				Minor to moderate (no quantitative data available)		-0		
R29-C70 SP3	4				Minor to moderate (no quantitative data available)		-0		
R29-C64 SP1		35			Minor to moderate (no quantitative data available)		-0		
R30-C64 SP2		78			Minor to moderate (no quantitative data available)		-0		

* Since most support plate cracking is composed of short axial microcracks, typically 0.02 to 0.05 inch long for a 50% deep crack, a microcracking density of 25 could be associated with more than several hundred individual microcracks within a support plate crevice region.

** D=Depth of SCC as measured from the OD surface exclusive of any surface IGA. W=Width of IGA component to the SCC as measured at the mid-point of the SCC.

TABLE 4.4 (Continuation)

Comparison of Intergranular Corrosion Morphology at Support Plate Regions on S/G Tubing and Laboratory Specimens

Data Source	Cracking Density (as Measured or Estimated for One Plane)*			Extent of IGA Associated with the Major Cracks			Extent of OD IGA (Not Obviously Associated with a Single Crack)		
	Low (1-24 Cracks)	Moderate (25 - 100 Cracks)	High (Greater than 100)	Minor (D/W** >20)	Moderate (D/W 3 to 20)	Significant (D/W <3)	Negligible (<5% Deep)	Moderate (5 to 10% Deep)	Significant (>10% Deep)
Plant L (Cont.)									
R30-C64 SP3		93			Minor to moderate (no quantitative data available)	~0			
Laboratory Tests									
571-1	1			~50			0		
543-4	5			40			0		
536-1	2			60			0		
543-4	13				14		0		
525-1	4				14		0		
533-3	10			11-40			0		
SL-FN-11	10				11		0		

* Since most support plate cracking is composed of short axial microcracks, typically 0.02 to 0.05 inch long for a 50% deep crack, a microcracking density of 25 could be associated with more than several hundred individual microcracks within a support plate crevice region.

** D=Depth of SCC as measured from the OD surface exclusive of any surface IGA. W=Width of IGA component to the SCC as measured at the mid-point of the SCC.

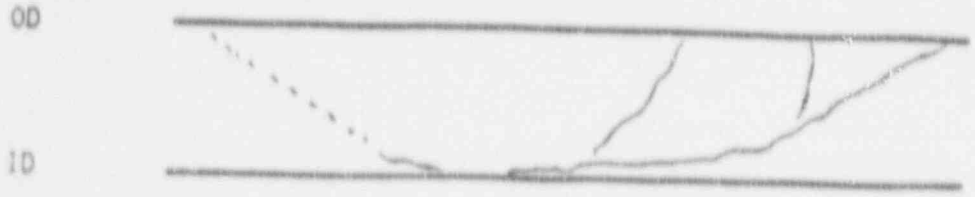

Sketch of Burst Crack

Macrocrack Length = 0.52 inch

Throughwall Length = 0.02 inch

Number of Microcracks = at least 3

Morphology = IGSCC with moderate IGA components

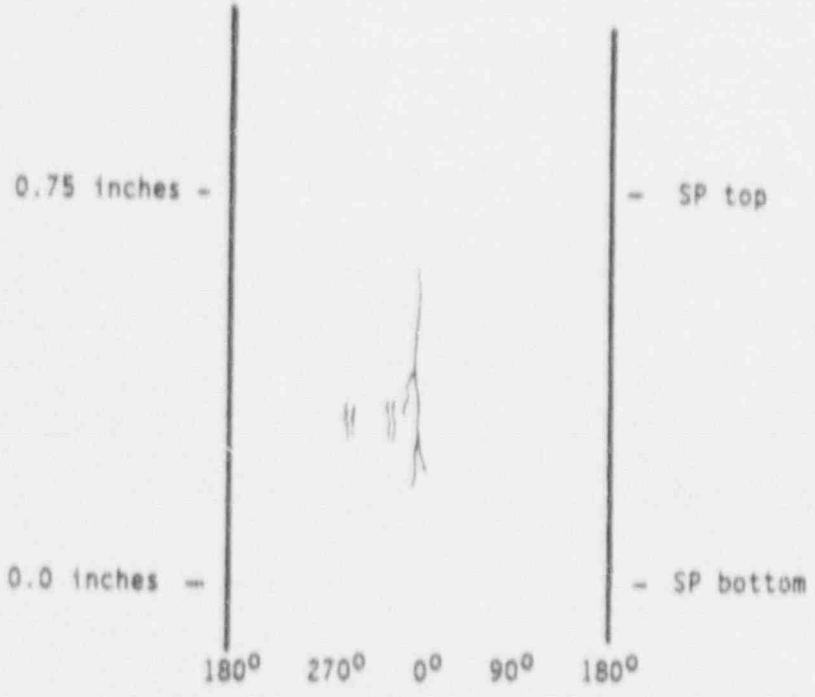

Sketch of Crack Distribution

Figure 4-1. Summary of crack distribution and morphology observed on the first support plate crevice region of tube R31-C46.

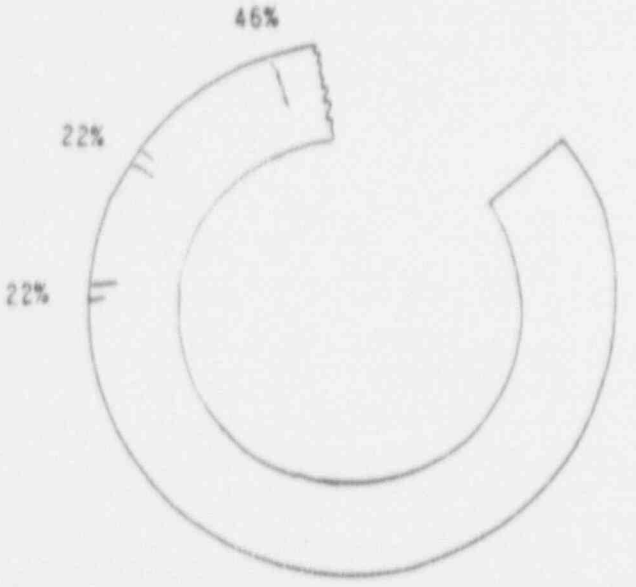

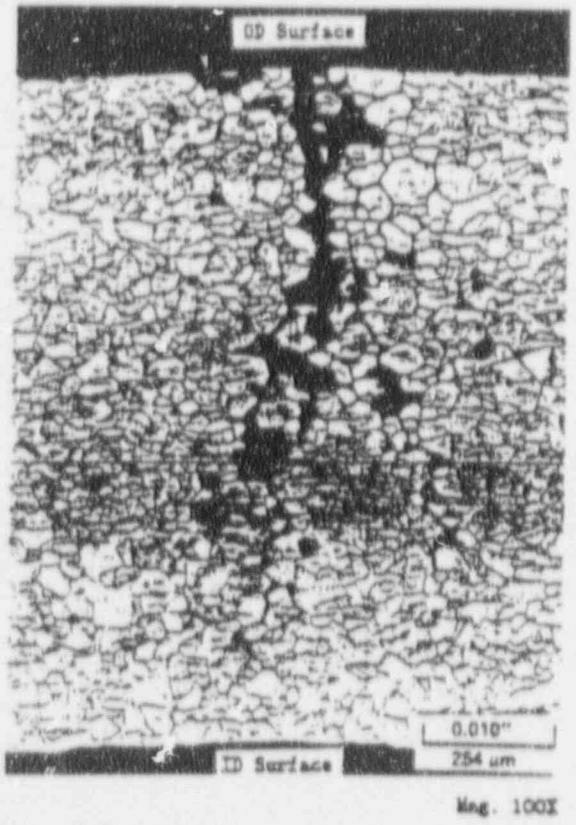

Figure 4-2. Secondary crack distribution and a photomicrograph of one of the cracks in a transverse metallographic section of the first support plate crevice region of tube R31-C46. The crack morphology is that of IGSCC with moderate IGA components.

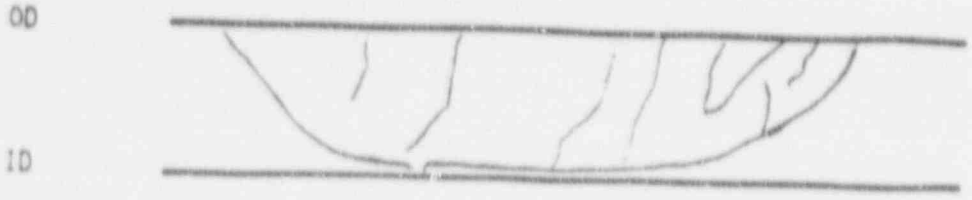

Sketch of Burst Crack

Macrocrack Length = 0.4 inch

Throughwall Length = 0.01 inch

Number of Microcracks = 7 (all ligaments have predominantly intergranular features)

Morphology = IGSCC with some IGA aspects (circumferential cracking has more IGA characteristics)

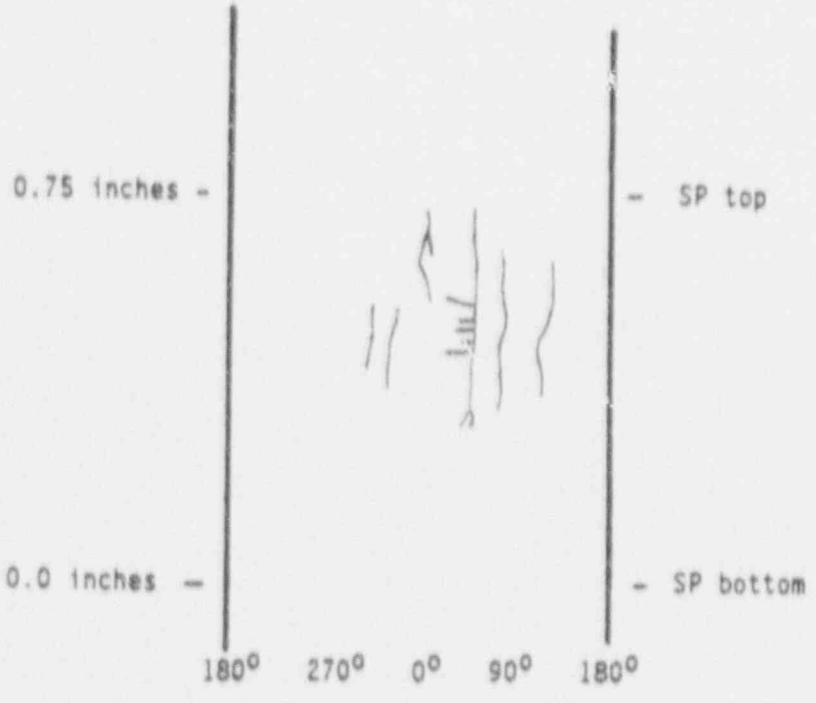

Sketch of Crack Distribution

Figure 4-3. Description of OD origin corrosion at the fifth support plate crevice region of tube R4-C61.

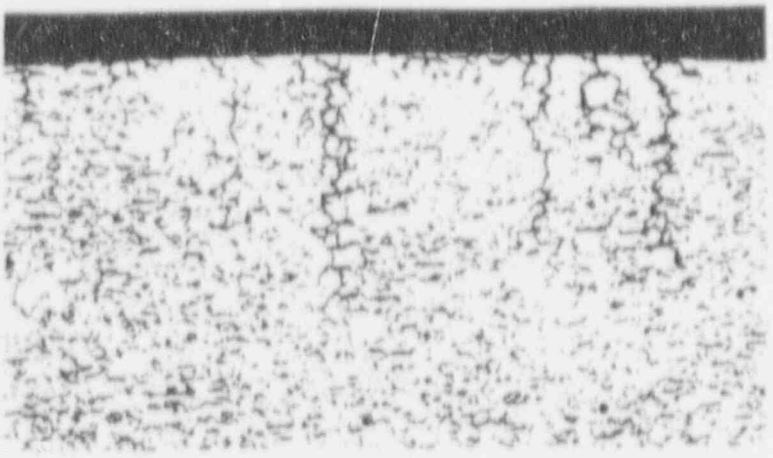

Mag. 100X

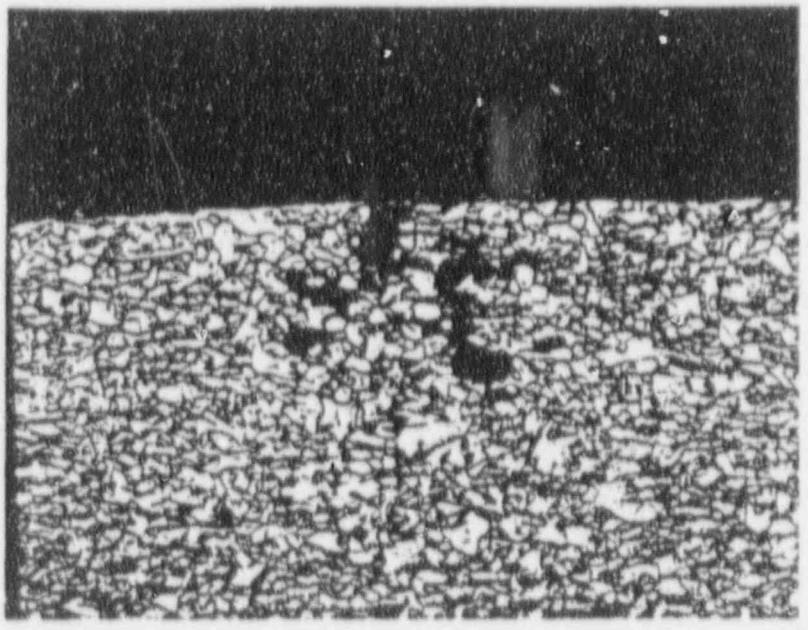

Mag. 100X

Figure 4-4. Photomicrographs of tube R4-C61 corrosion degradation. Top photo shows axial crack morphology (transverse section) at the eighth support plate location (no transverse metallography was performed at the fifth support plate region). Bottom photo shows circumferential crack morphology (axial section) at fifth support plate region.

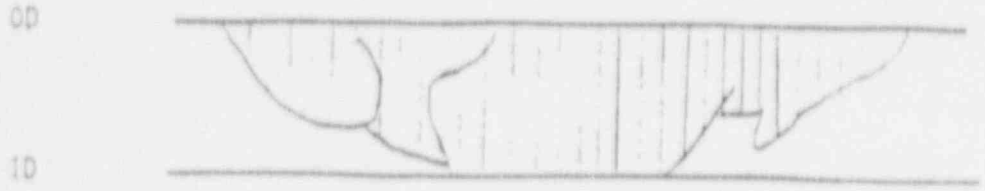

Sketch of Burst Crack

Macrocrack length = 0.42 inches

Throughwall Length = 0.18 inches

Number of Microcracks = 4 (all ligaments with intergranular features)

Morphology = Intergranular SCC with some IGA characteristics (width of IGA 0.012 inches)

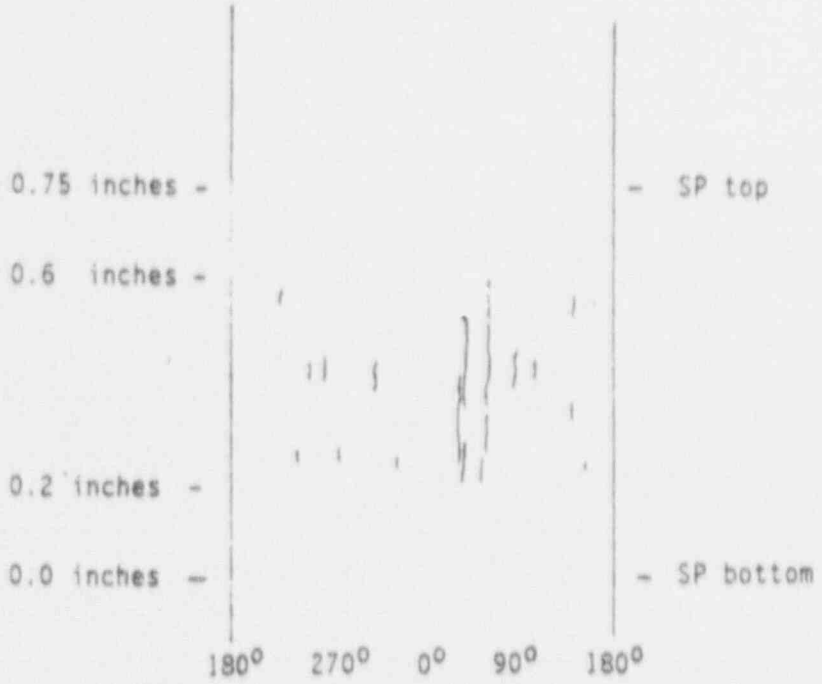

Sketch of Crack Distribution

Figure 4-5. Description of OD origin corrosion at the first support plate crevice region of tube R4-C73.

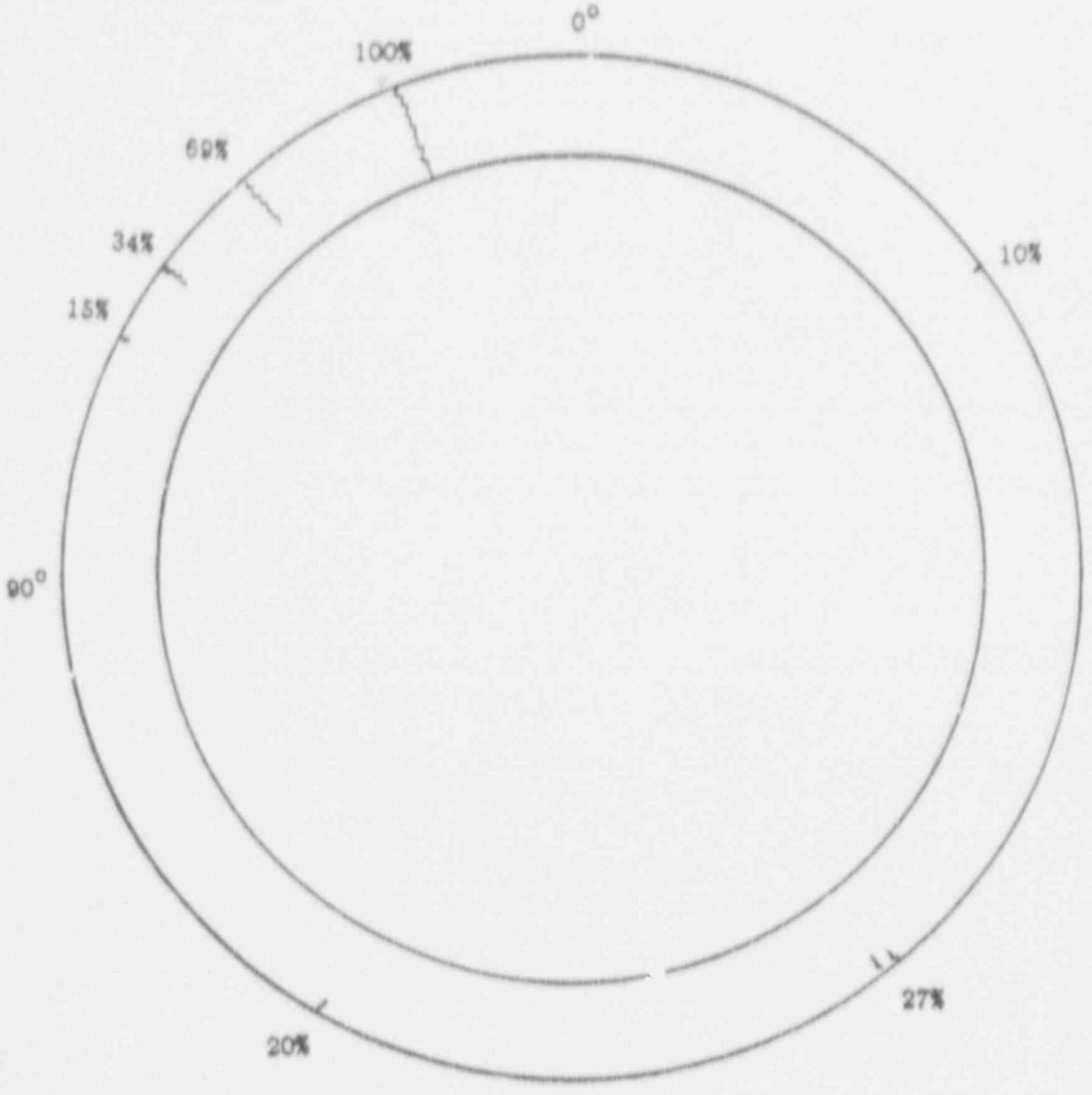

Figure 4-6. Sketch of crack distribution and depth within the center of the first support plate intersection in tube R4-C73.

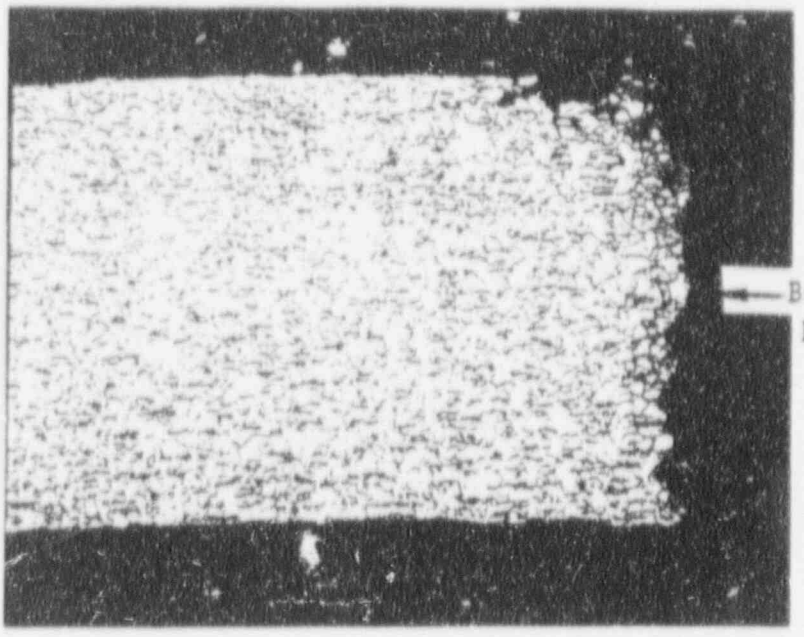

Mag. 50X

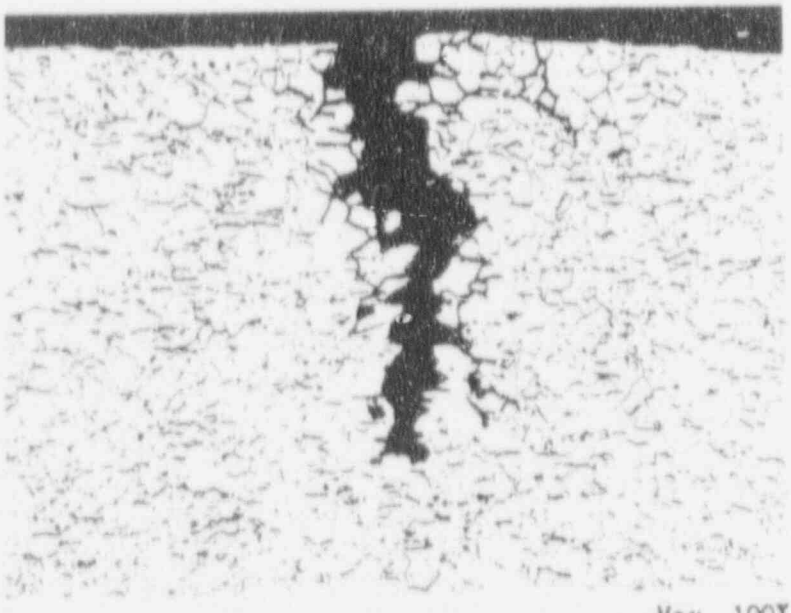

Mag. 100X

Figure 4-7. Top photomicrograph is from a transverse section through one half of the main burst crack. The crack morphology is that of IGSCC with some IGA characteristics (width of IGA is 0.006 inch on one side of the crack). Bottom micrograph is from a transverse section through a typical crack located near the burst crack. The morphology is that of IGSCC with only minor IGA characteristics. (Note: crack is opened wide by tube deformation).

Sketch of Burst Crack

Macrocrack Length = 0.50 inches

Throughwall Length = 0.15 inches

Number of Microcracks = 4 (two ligaments with intergranular features, one with ductile overload features)

Morphology = Intergranular SCC with significant IGA characteristics (width of IGA 0.030 inches)

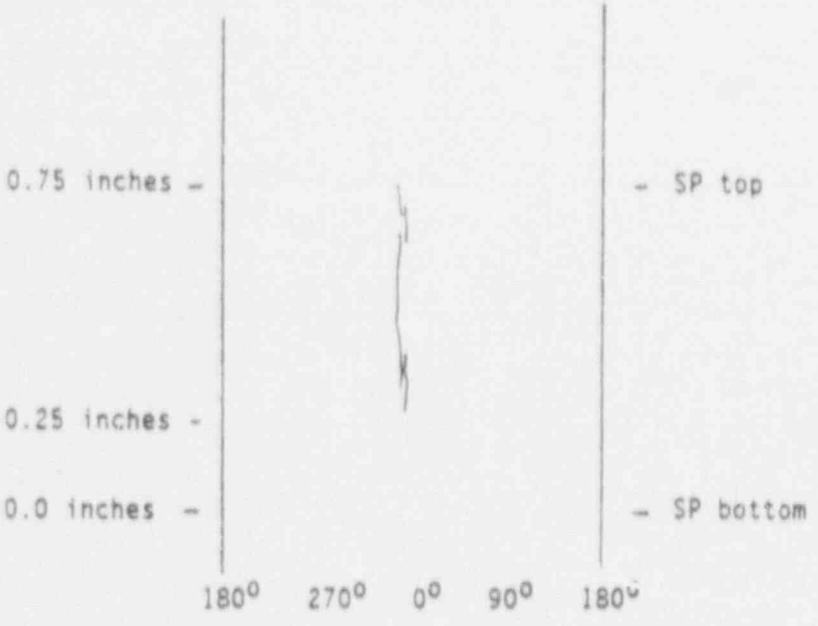

Sketch of Crack Distribution

Figure 4-8. Description of OD origin corrosion at the first support plate crevice region of tube R21-C22.

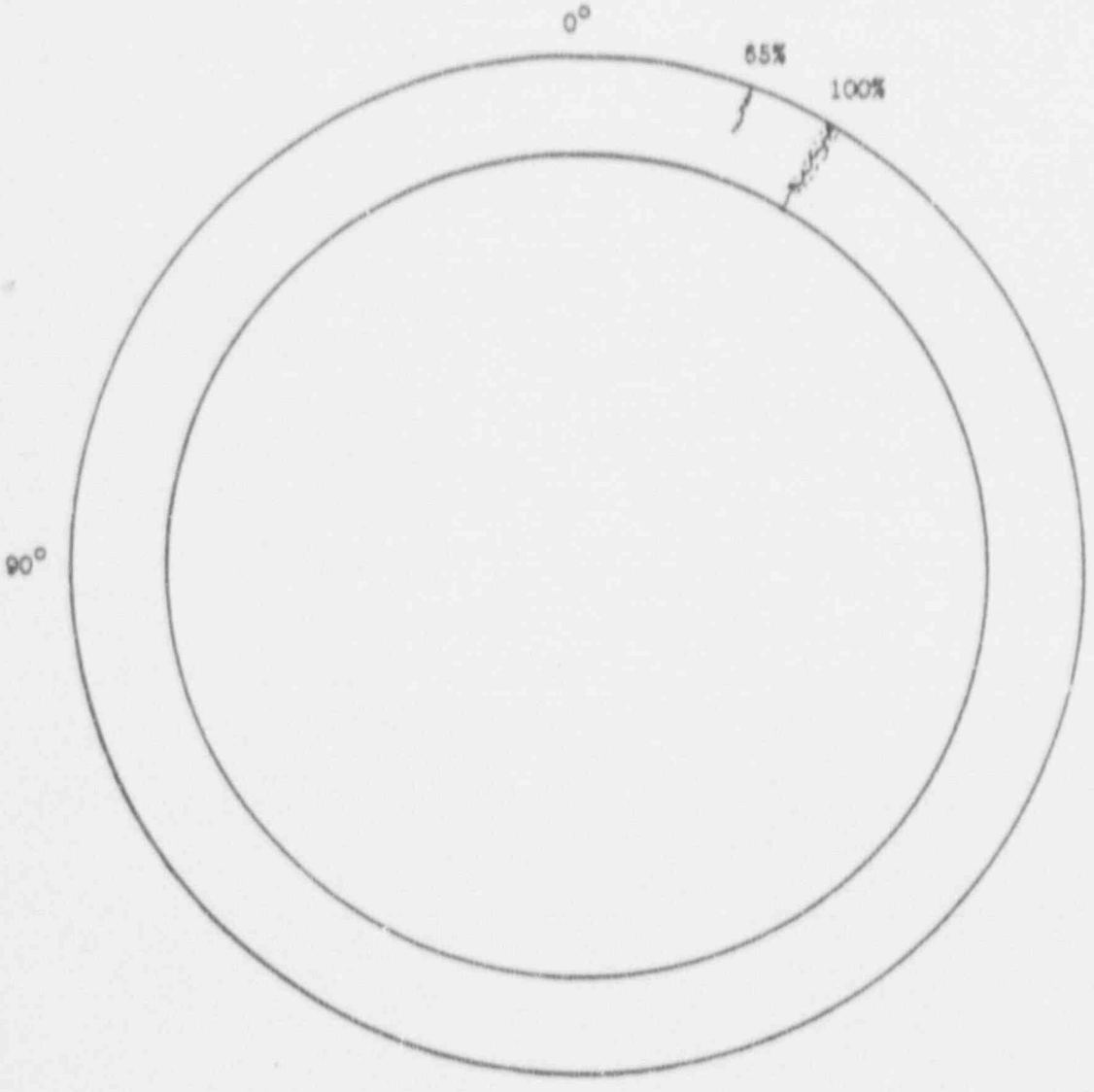

Figure 4-9. Sketch of crack distribution and depth within the first support plate crevice region in tube R21-C22.

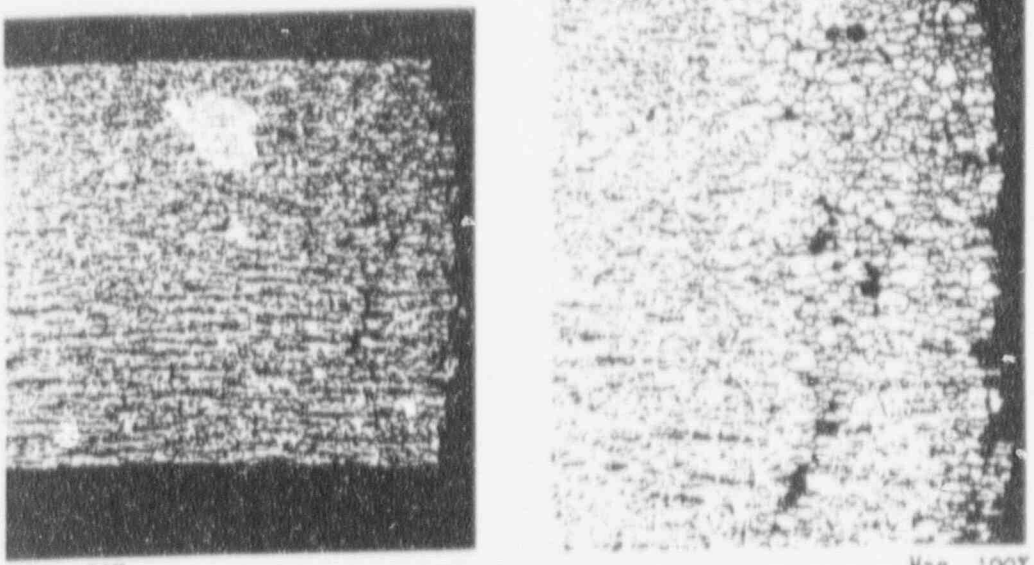

Mag. 50X

Mag. 100X

Mag. 100X

Figure 4-10. Top micrographs are from a transverse section through one half of the main burst crack. The morphology is that of IGSCC with significant IGA characteristics (width of IGA is 0.015 inch on one side of the crack). Bottom micrograph is from a transverse section through the only other crack found in the crevice region. Its morphology is more that of IGSCC. (Note: crack has been opened wide by tube deformation).

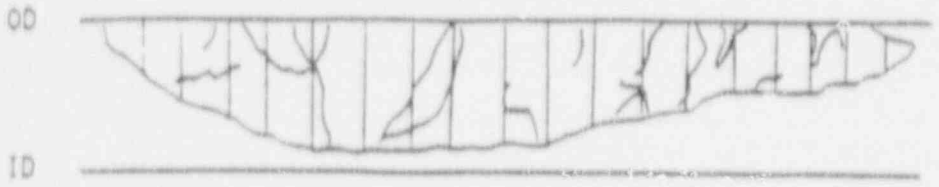

Sketch of Burst Crack

Macrocrack Length = 0.37 inches

Throughwall Length = 0 (78% throughwall)

Number of Microcracks = numerous (ligaments have intergranular features)

Morphology = Intergranular SCC with minor IGA features (Unusual spider-shaped crack distribution)

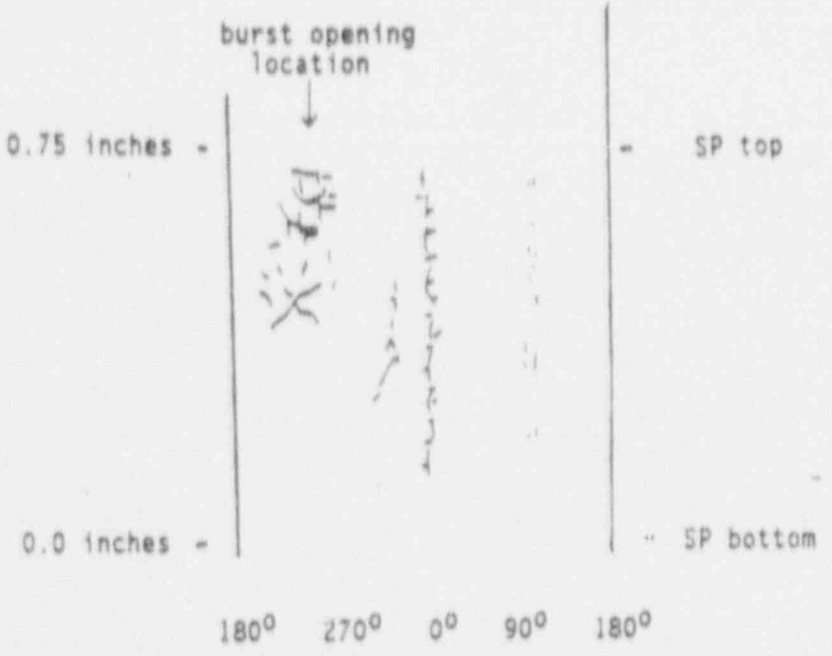

Sketch of Crack Distribution

Figure 4-11. Description of OD origin corrosion at the first support plate crevice region of tube R38-C46.

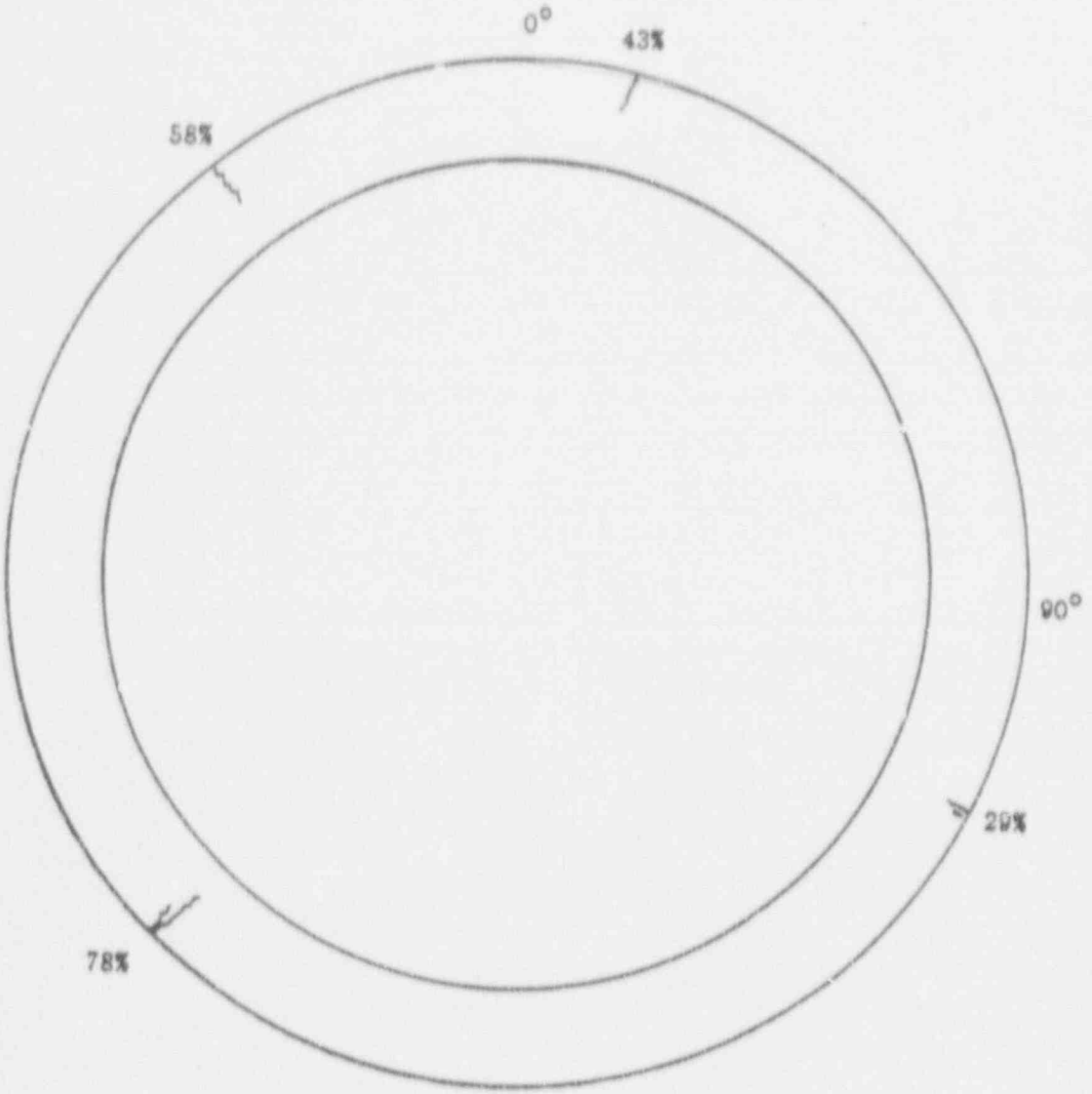

Figure 4-12. Summary of distribution and maximum depth of cracks found within the first support plate crevice region of tube R38-C46.

Area D

Area C

Figure 4-13. Photmicrographs of a transverse metallographic section through the first support plate crevice region of tube R38-C46. The crack morphology is that of IGSCC with minor IGA characteristics. Mag. 100X.

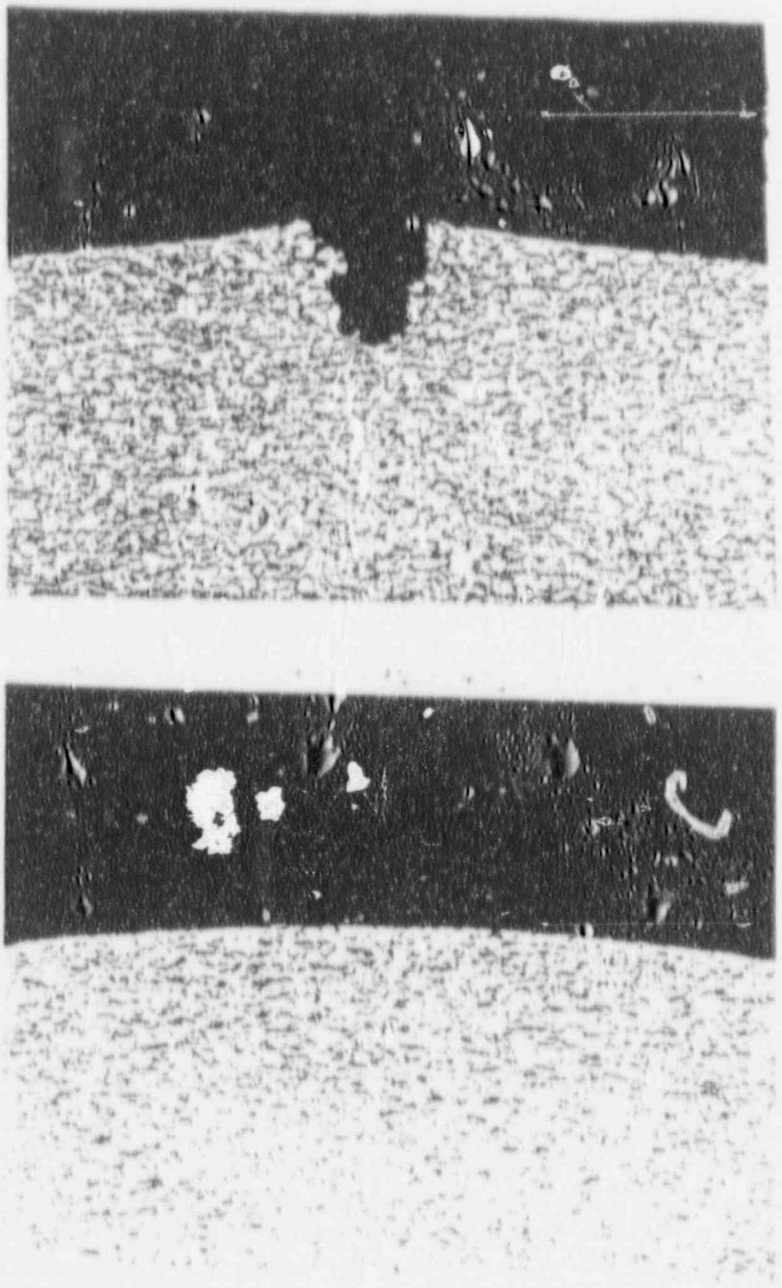

Figure 4-14. Cracks at the OD surface of Plant A tube R16-C50 at the first tube support plate crevice. Mag. 100X.

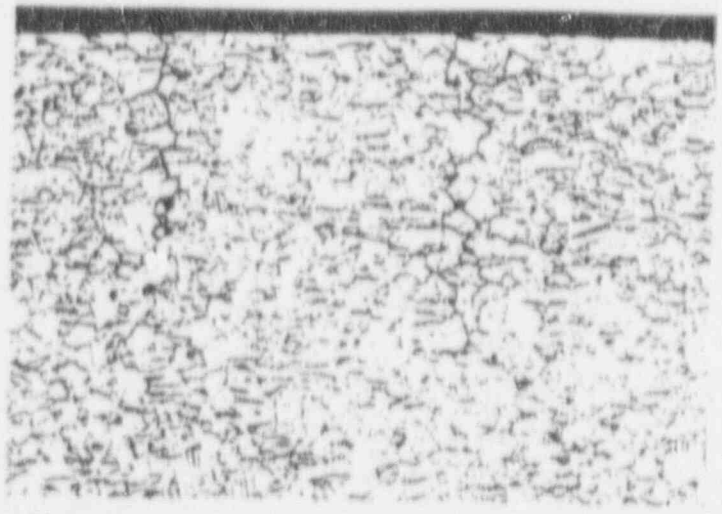

H

I

J

Figure 4-15. Photomicrographs of a transverse section from the first support plate crevice region of tube R16-C53. Mag. 100X.

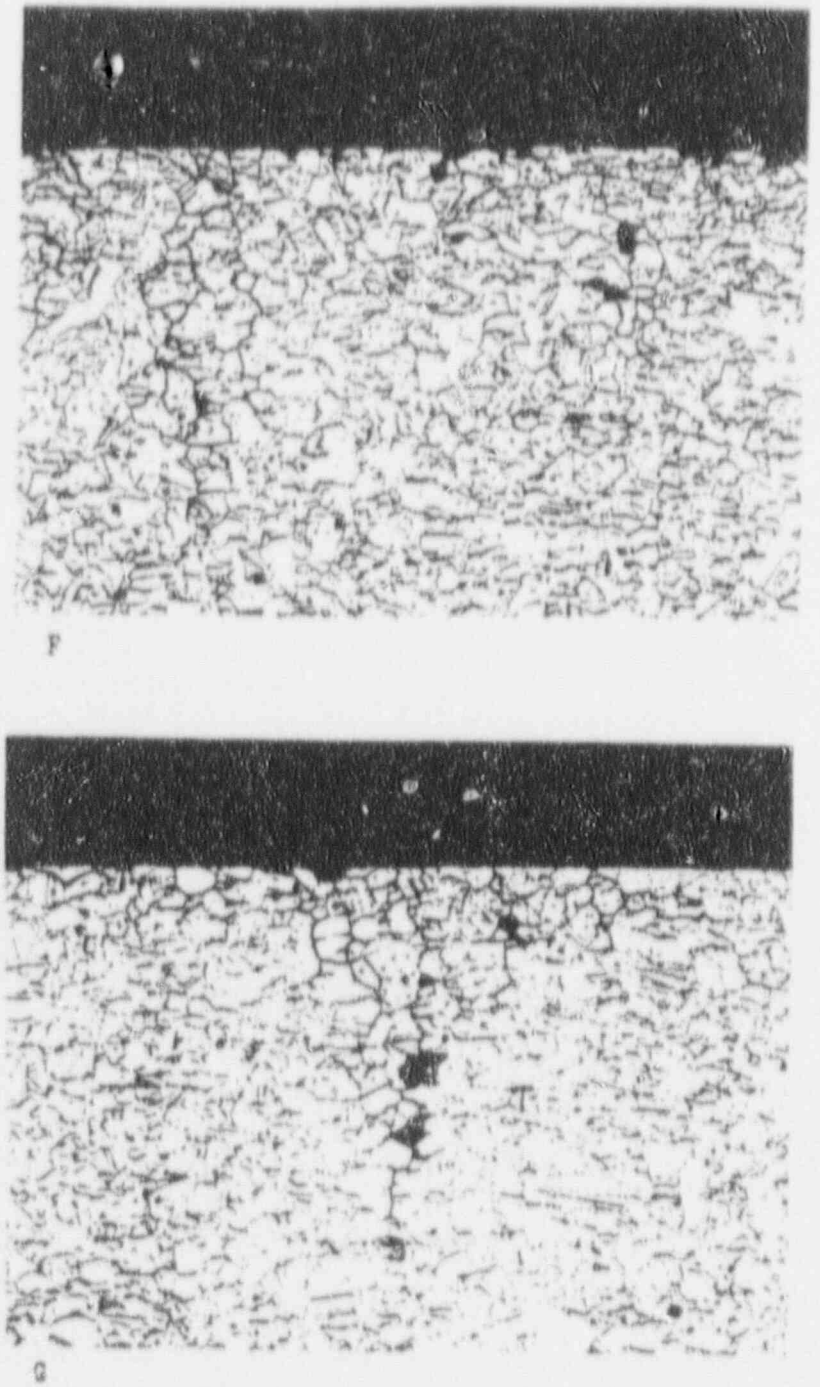

Figure 4-16. Additional micrographs from the same transverse section shown in Figure 4-15, tube R16-C53. Mag. 100X.

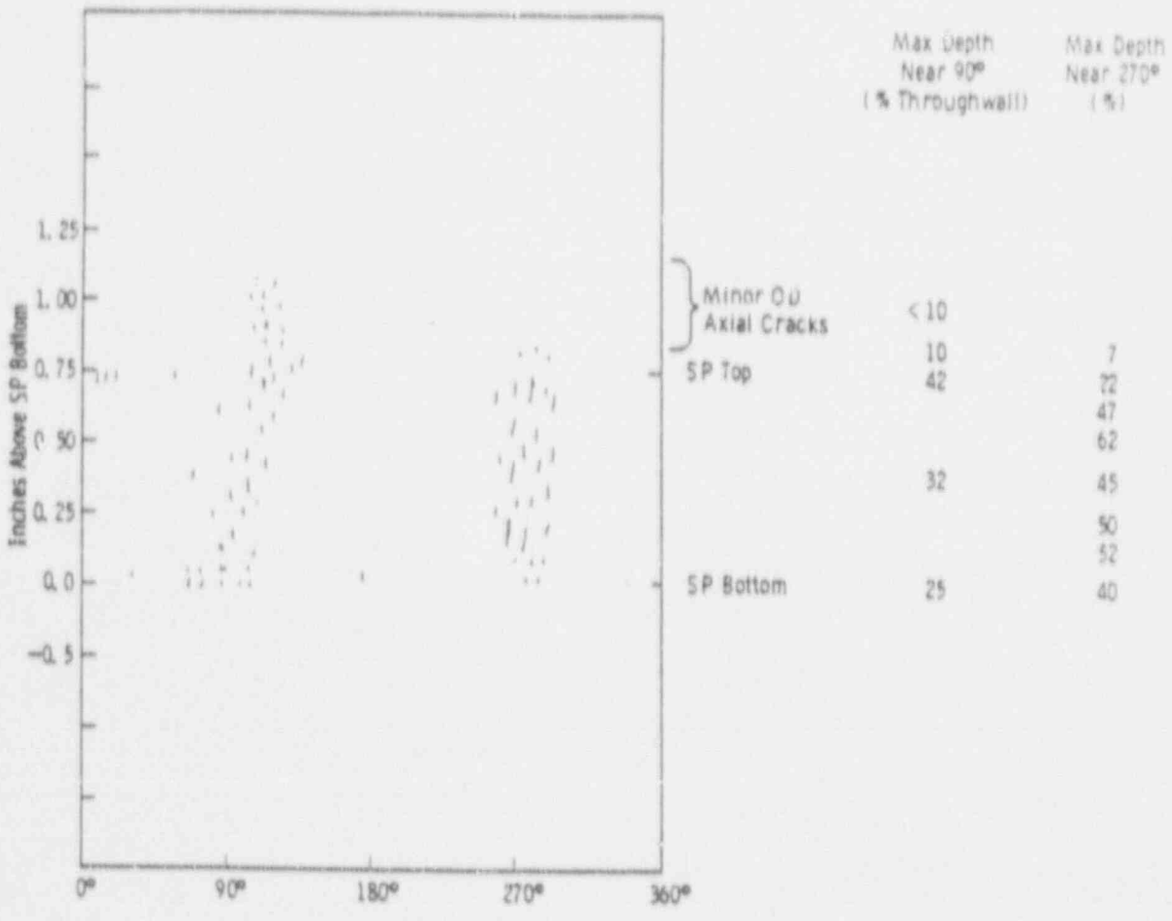

Figure 4-17. Crack network location at first support plate region on tube R20-C26 HL.

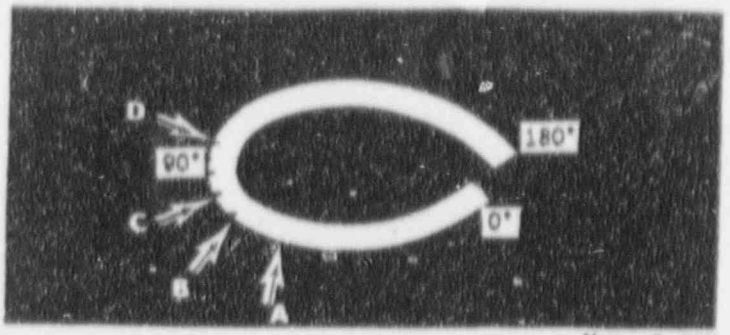

Mag. 3.25X

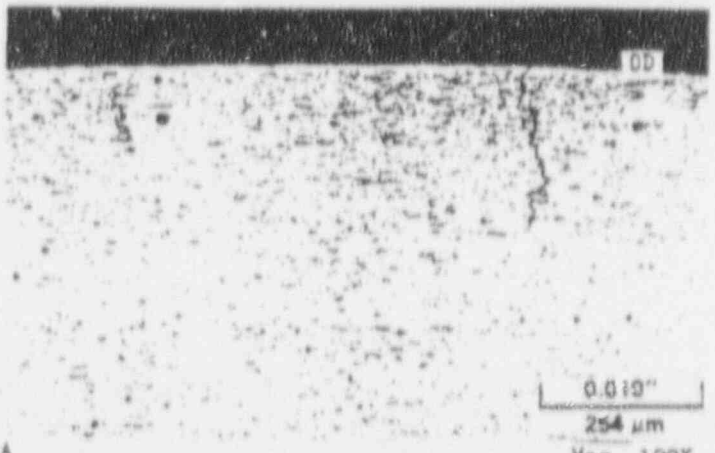

A

Mag. 100X

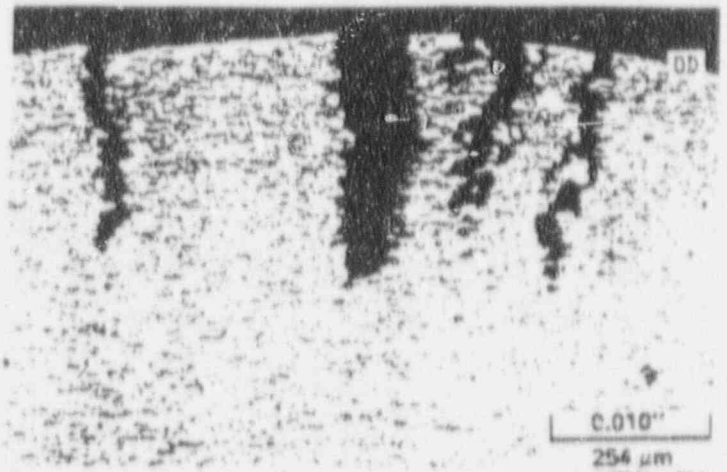

B

Mag. 100X

Figure 4-18. Transverse metallographic section through tube R20-C26 HL at the mid-point of the first support plate crevice region (90° deformed half) with crack details in Areas A and B.

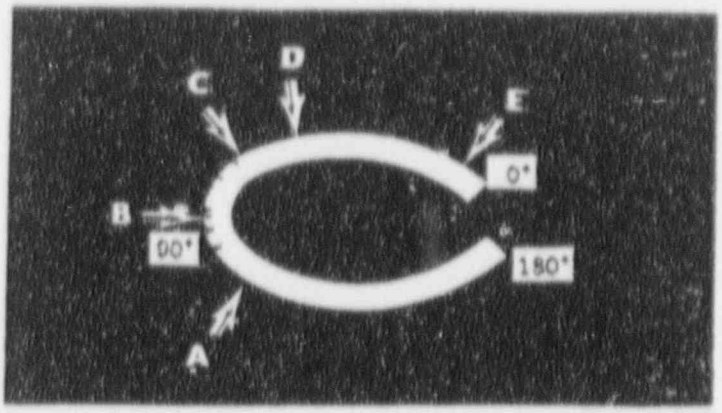

Mag. 3.25X

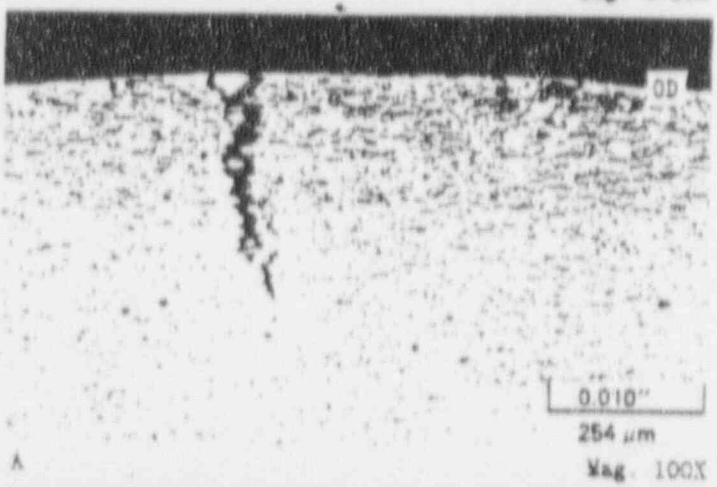

A

Mag. 100X

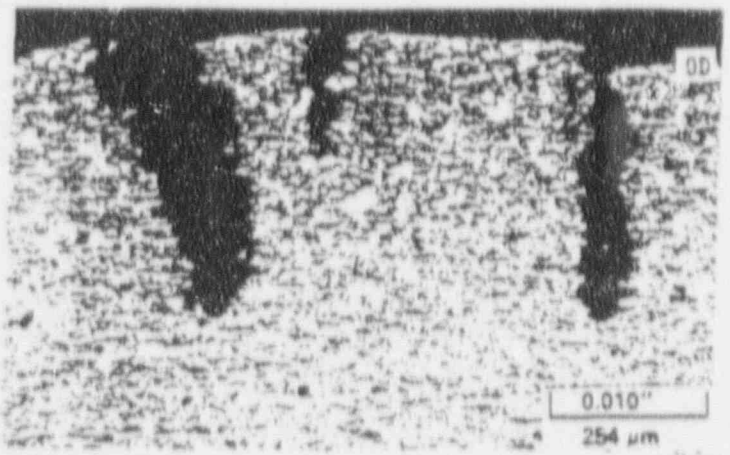

B

Mag. 100X

Figure 4-19. Transverse metallographic section through Plant A tube R20-C26 HL at the first support plate crevice region (90° deformed half) below the support plate crevice top with crack details in Areas A and B.

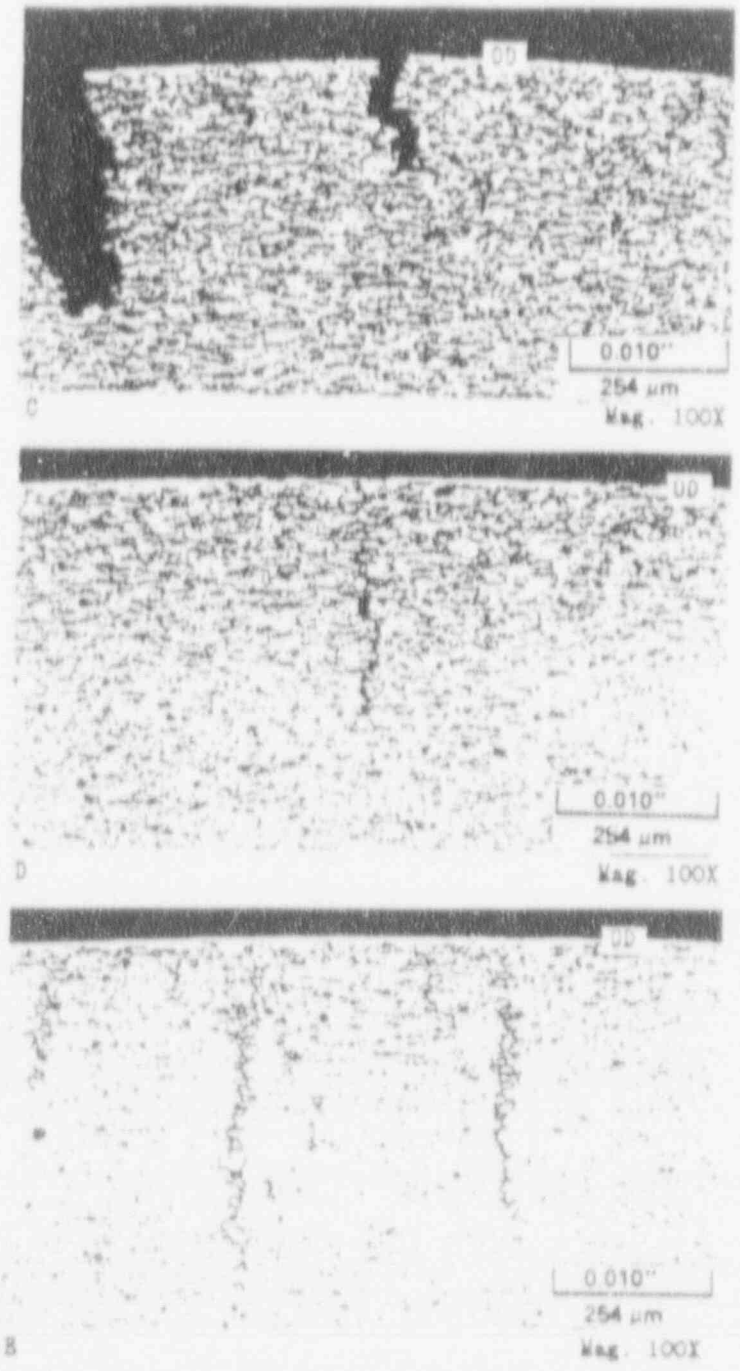

Figure 4-20. Crack details in Areas C, D, and E of metallographic cross section shown in previous figure, tube R20-C26 HL.

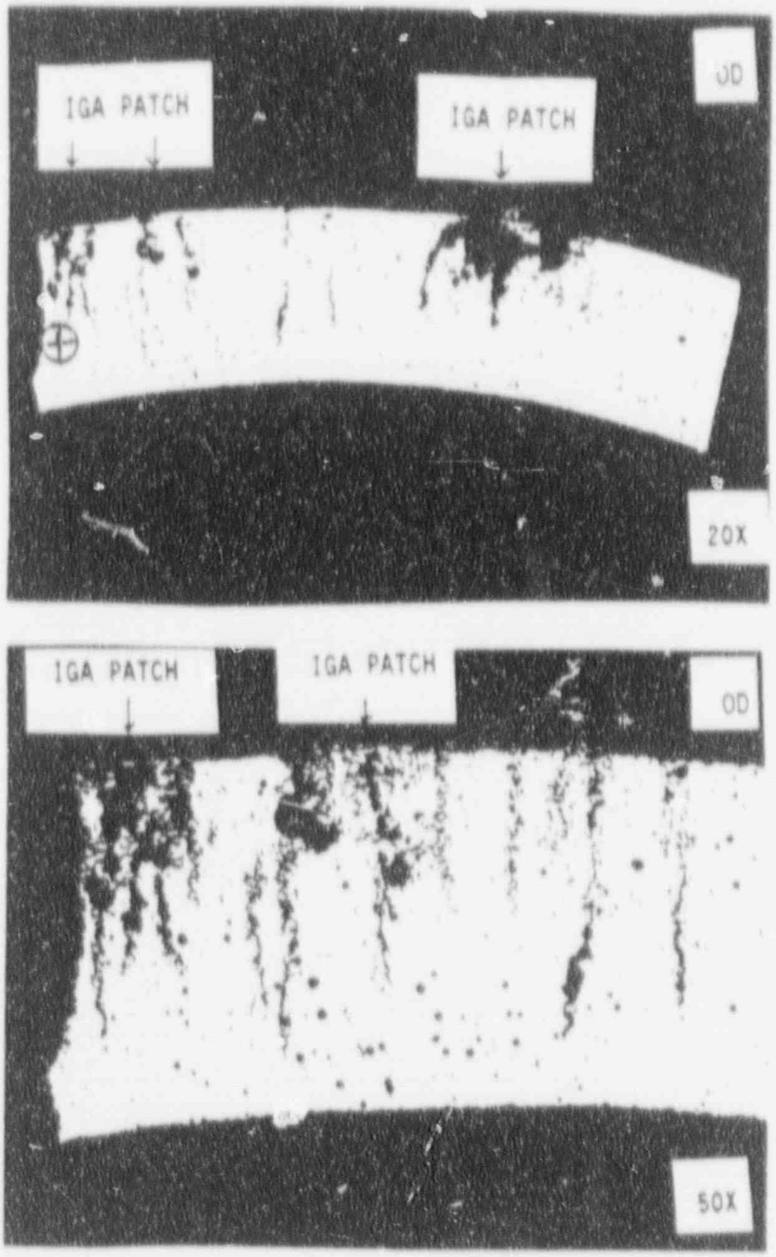

Figure 4-21. Transverse optical micrographs obtained just below the circumferential fracture at the center of the support plate. The circumferential location is that where the deepest corrosion was found. The deepest axial IGSCC is 85% through wall and three IGA patches are observed: one 43% through wall and 0.015 inch long, one 33% through wall and 0.05 inch long, and one 28% through wall and 0.015 inch long. The axial IGSCC had IGA aspects to individual cracks. These aspects can be characterized by ratios comparing the crack length (depth from OD surface) to IGA width at the mid-crack location. L/W ratios vary from 6 to 18. Plant L.

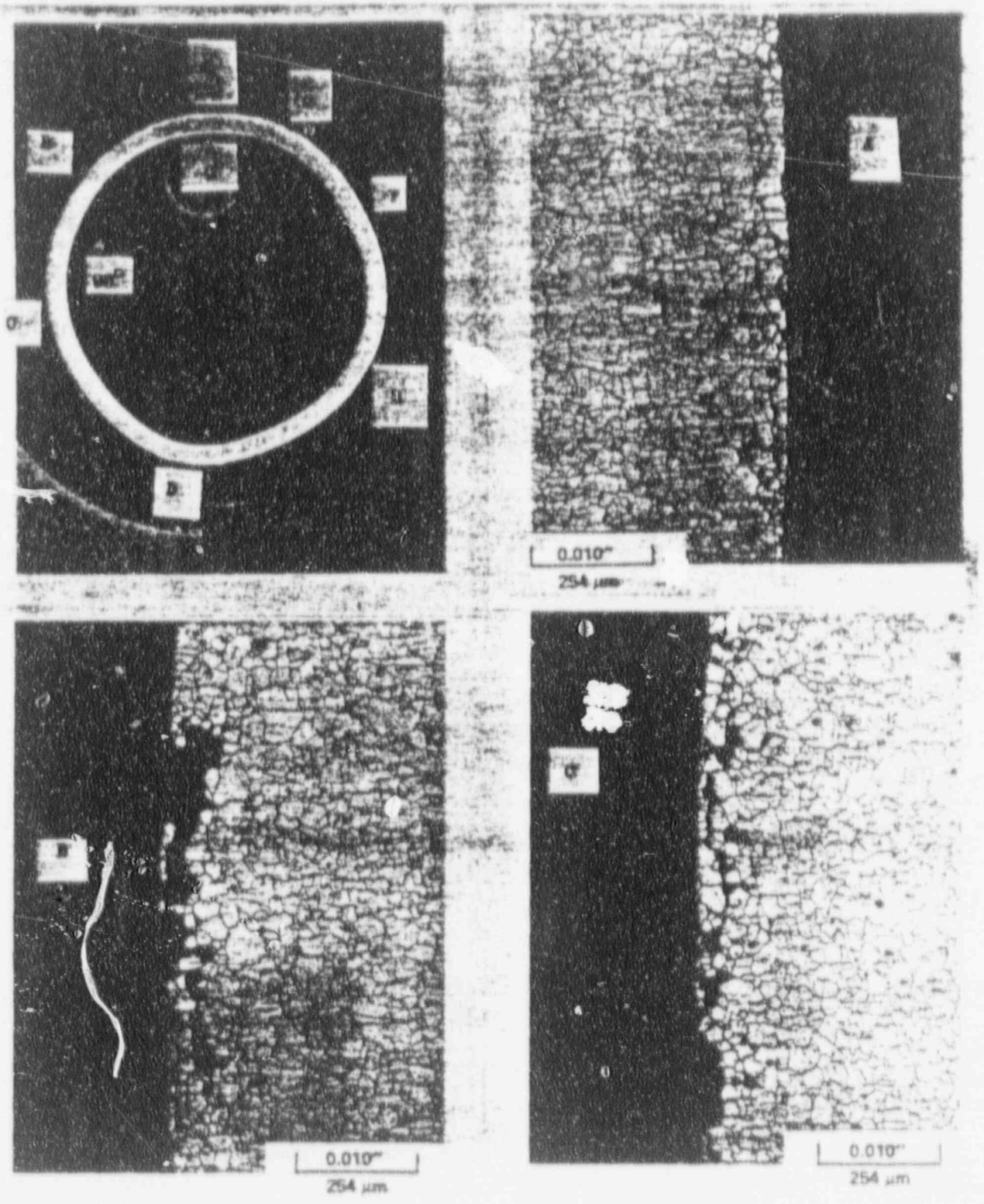

Figure 4-22 Transverse metallography at 0.2 inches above first support plate bottom edge showing almost continuous OD IGA around circumference. Maximum depth is 24%.

Tube R29-C46 CL, Plant M-2

17X

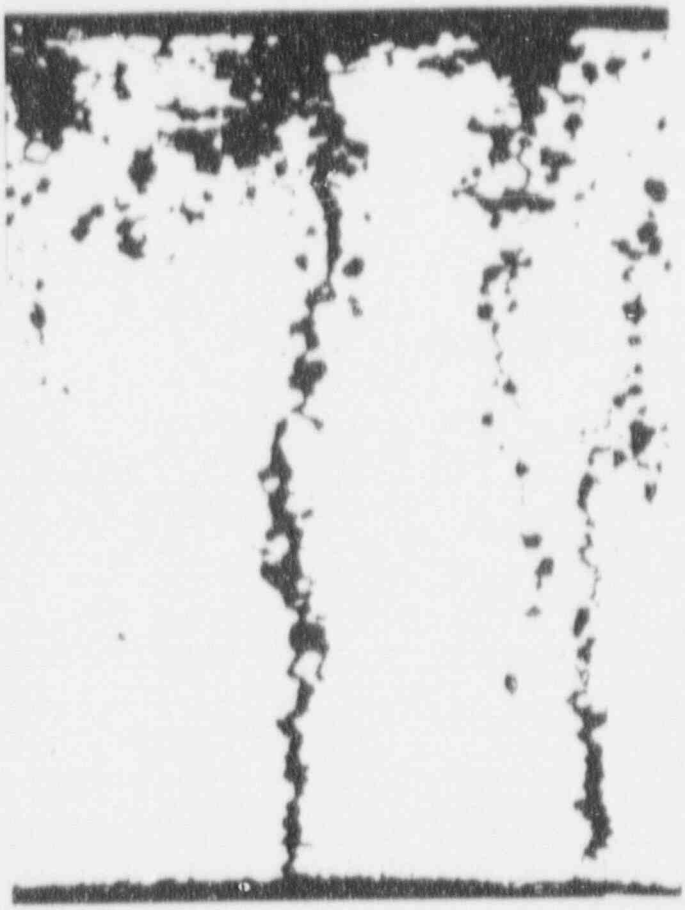

85X

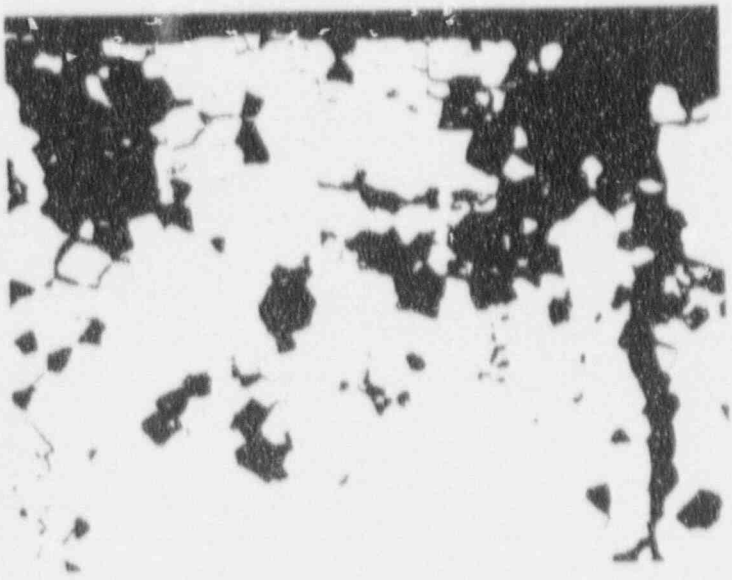

170X

Figure 4-23 Transverse photomicrographs of intergranular corrosion at the first support plate region of tube L8-C74 from Plant J-1

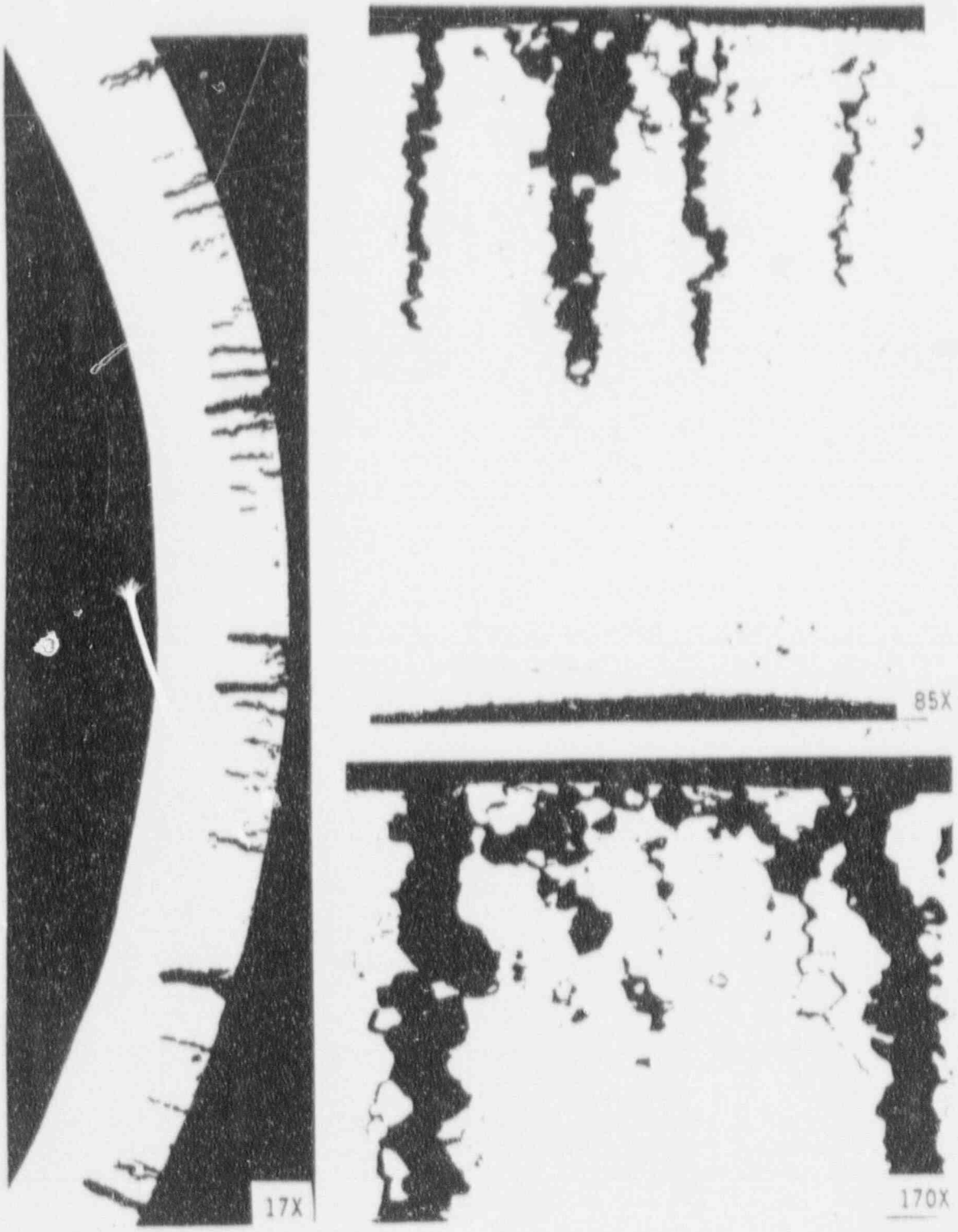

Figure 4-24 Transverse photomicrographs of intergranular corrosion at the second support plate region of tube L8-C74 from Plant J-1

5.0 KEWAUNEE INSPECTION RESULTS

5.1 March 1991 Inspection

A scheduled inspection of the Kewaunee steam generators was conducted during the refueling outage in March, 1991. All tubes in service were inspected by bobbin coil eddy current tests. The following is a summary of the results relating to ODSCC indications at tube support plates (TSP).

Nearly 70% of the tube support plate indications were in S/G-B and the remaining in S/G-A. In S/G-B, more indications were found on the cold leg side than on the hot leg side. Figure 5-1 displays the frequency distribution of TSP indications by support plate locations. Of all plate locations, support plate 6C (sixth plate from the bottom, in the cold leg) in S/G-B had the greatest number of indications. The lowest and highest plates had more indications than the intermediate level TSPs. The number of indications at each TSP location as a percentage of the total in each S/G is shown in Figure 5-2. In S/G-A, the largest percentage of indications were in the lowest hot leg suport plate (Plate 1H), followed by the highest cold leg TSP (Plate 7C). In S/G-B, the largest percent TSP indications were in Plate 6C, followed by Plate 7C.

In general, the TSP indications at Kewaunee had low amplitudes. Over 95% of the indications were of less than 2 volt amplitude (400/100 kHz mix channel). A frequency distribution of the voltage amplitudes from the 1991 inspection is shown in Figure 5-3. The distribution of number of indications is shown in the upper figure while the corresponding percentage distribution is shown in the lower figure. In each S/G, about half of the indications were in the range of 0.5 to 1.0 volt. None of the TSP indications in S/G-A and only a few indications in S/G-B (excluding a few dent signals) were above 2.5 volts in amplitude.

With respect to the depth of the indications (percent tube wall penetration), majority of the signals were attributed to low indicated depths. A frequency distribution of estimated wall penetration of the indications is shown in the upper half of Figure 5-4. It may be noted that in both S/Gs, only a few indications exceeded 50% wall penetration. The percentage distribution of tube wall penetration of TSP indications is shown in the lower portion of Figure 5-4. Tubes plugged during the 1991 outage, in accordance with the existing plugging criteria, are included in these figures.

5.2 Past Inspections

A review of the past eddy current inspection results was conducted to assess the progression of ODSCC in the Kewaunee S/Gs. 34 Tubes from S/G-A and 13 tubes from S/G-B were plugged for support plate indications during the 1990 outage. These plugged tubes formed the sample for this reevaluation which was performed in the lab using data from eddy current tests conducted in the field. For these tubes, the available eddy current test results for outages in 1987 through 1990 were evaluated. There were other tubes with "distorted indications" (DI) at the support plates; however, only the data from the plugged tubes were reevaluated in the current study and hence is likely to be conservative (large growth rates). Some of these tubes had indications at more than one tube support plate (TSP) intersection and hence the number of total indications reviewed exceeds the number of plugged tubes.

The OD indications were present in both the hot leg and the cold leg. It was noted during the evaluation that the growth in amplitudes between 1989 and 1990 in S/G-A were, by and large, negative. This was found to result from using a different calibration standard for the 1989 inspection. A correction to the 1989 voltages was applied by comparing the signal voltages for the 100% ASME holes on the field data tapes for the two years. Accordingly, the recorded amplitudes from the 1989 inspection in S/G-A were reduced by 29% prior to further processing of the data. Such a correction was not needed for the depth estimates for the reasons discussed in the following paragraph

The ASME standard for flaw depths specifies a tolerance of $\pm$ 3 mils or 20% whichever is less, whereas the diametric tolerance is $\pm$ 10 mils. This leads to a possible diametric variation of $\pm$ 15% and $\pm$ 5%, respectively, for the 100% and 20% deep ASME holes assuming that the machined standard is within the specifications. The engineering drawing for the calibration standard used during the inspection provides the exact as-built (measured) depths for the machined flaws; but does not give the as-built diameters of the flaws. Further, the accuracy of the 100% depth hole is absolute. Thus while the standard was well suited for depth estimates with high degree of confidence, the signal amplitude estimates tend to be less reliable due to the variation in hole diameters in the standard.

The eddy current signals found in the field data are generally distorted which contributes to the uncertainty in the depth estimates and signal amplitudes. The uncertainty in the estimates would depend on the extent of the signal distortions. It was sometimes possible to reduce this uncertainty by comparing the inspection signals at a given location from different outages (years). An example of this is illustrated in Figures 5-5 and 5-6. The 1990 inspection results shown in Figure 5-5 has very little distortion and provides depth and amplitude estimates with high level of confidence. The 1989 data for the same tube-TSP intersection (Figure 5-6) is highly distorted. Two different interpretations of this signal are shown in the figure. A reading of 0.58 volt and 51% depth (rather than the other estimate of 0.85 volt and 46% depth) was found to be more consistent with the 1990 estimate of 0.54 volt and 48% depth.

The bobbin voltage indications ranged from 0.16 to 3.5 volts. Growth in amplitude for each year from 1987 through 1990 were calculated where data was available from prior inspections. Growth estimates were calculated only for the cases where data was available for at least two years; i.e., no assumption about the depth or signal voltage for prior years was made if such data was not available.

Figure 5-7 shows a plot of the growth in amplitude from 1989 to 1990 as a function of the 1989 amplitude for the indications in both S/Gs. It may be noted that the amplitude growth ranged from -0.3 to +0.9 volts in S/G-A and from -0.4 to +0.7 volts in S/G-B. The negative growths (and possibly some of the high positive growth values) result from the uncertainties in the eddy current inspection and data evaluation. Overall, the distribution of amplitudes and their growths are similar in the two S/Gs. Figure 5-8 shows the growths in amplitude during the three cycles in both S/Gs as a function of the amplitude in prior inspection. A frequency distribution of the voltage growth between 1989 and 90 in both S/Gs is shown in Figure 5-9. Please note that the mode (interval of highest frequency) is near 0.0 volt.

The average growth in amplitude for all indications was calculated for each of the three cycles for both S/Gs. This is plotted as a trend curve for each S/G in Figure 5-10. The number of indications used in the calculation of the average is also shown in the figure, next to each point.

In S/G-A, the average growth in amplitude from 1989 to 1990 was only 0.17 volt. The growths during the prior two cycles in that generator were 0.13 and 0.09 volt. The average growth rates in S/G-B during the last three cycles were 0.18, 0.13 and 0.08 volt, respectively.

The standard deviation associated with the growths in amplitude during the last cycle was 0.26 volt for each of the two S/Gs. As discussed before, part of the scatter results from the uncertainty in the eddy current tests and the data evaluation and the remaining from the variability in growth between indications. Please note that the average growth from 1987 to 1988 in S/G-B was calculated from only four (4) data points. The accuracy of the data is not high enough to pay attention to the small differences in the averages between cycles and between S/Gs; nor to the slopes of the trend lines. These differences may be attributable to randomness of the data. Overall, it may be noted that the average amplitude growths in each S/G is low, being in the range of 0.1 to 0.2 volt per year.

Figure 5-11 shows a plot of the growth in indicated depth from 1989 to 1990 as a function of the 1989 depth for the indications in both S/Gs. It may be noted that the growth ranged from -8% to +37% through wall. The negative growths (and possibly some of the high positive growth values) result from the uncertainties (10 to 15% depth) in the eddy current inspection and depth estimation. One significant observation from the figure is the very low growths for indications above 60% through wall. Overall, the distribution of indication depths and their growths are similar in the two S/Gs. Figure 5-12 shows the growths in depth during the three cycles in both S/Gs as a function of the indicated depth from prior inspection. The generally low growth rates for indications above 60% appear to be consistent across both S/Gs over the three cycles.

The average growth in indicated depth for all indications was calculated for each of the three cycles for each S/G. This is plotted as a trend curve for each S/G in Figure 5-13. The number of indications used in the calculation of the average is also shown in the figure, next to each point. For both generators, the average growth during each cycle was below 10%. The negative average growth of -7% calculated for S/G-B between 1987 and 1988 results from only 4 data points, and cannot be taken seriously. Further, it is not clear whether the slope of the trend lines has any significance. The only meaningful conclusion is that the average growth in indicated depths is less than 10% and that indications above 60% in depth have small growths.

5.3 Percent Growth in Voltage Amplitude

As discussed in Section 5.2, the growth in amplitude per fuel cycle ranged from -0.4 to +0.9 volts. Experience with the data European plants suggests (however, this is not supported by data from Kewaunee or two other domestic units) that the percent growth in amplitude tends to be stable. This suggests that the small amplitude indications grow by smaller voltages and that large amplitude signals are more likely to grow by a larger amplitude during the subsequent cycle. Percent growth is calculated from the ratio of the amplitude growth during an operating cycle to the amplitude of the signal during the prior inspection. Figure 5-14 shows a plot of the percent growth in amplitude vs the bobbin voltage during the prior inspection. The re-evaluation of the EC results from 1987 to 1990 on tubes plugged in 1990 for TSP indications formed the basis for this data.

The average growth rate of all these indications were calculated for Kewaunee. In the calculation of the average, the negative growth rates were conservatively treated as zero growth rates. This

would a higher average estimate than if the negative values were not modified. The calculated average amplitude growth for Kewaunee from 1987 to 90 is 29% per fuel cycle. This is comparable to the ODSCC growth rates observed at other plants. As noted before, population for this calculation consisted of only the tubes plugged during the 1990 outage. This may have also resulted in conservatively high growth rates than if all TSP indications were included in the population. However, the growth rate calculation during the last fuel cycle was based on all the TSP indications as described below.

Estimation of the amplitude growth in the last fuel cycle showed that between 1990 and 91 the average amplitude growth was only 13% in S/G-A and 2% in S/G-B. Again, negative growth rates were treated as zero growths for this computation. The combined average growth for both S/Gs was 5% during the last cycle. Inclusion of this data in the calculation of average growth during the last four cycles (from 1987 to 91) results in an overall average growth rate of 13.3% for Kewaunee. However, a value of 40% was used conservatively in the determination the plugging limit in Section 12. A summary of the average growth rates and their standard deviations during the last four fuel cycles is listed in Table 5.1. It may be noted from this table that the value of 40% exceeds even the highest average growth rates determined for prior cycles.

Percent growth rates in bobbin amplitude during the last fuel cycle ranged from -63% to +116%. A frequency distribution of the percentage growth rates is displayed in Figure 5-15. This figure also shows the cumulative probability distribution of percentage growth rates in the Kewaunee S/Gs during the latest cycle (1990-91).

5.4 Review of TSP Corrosion and Crevice Packing

Review of the field data shows strong evidence of general corrosion of the support plate holes. This can be observed in the 10 kHz data (top right frame in the following figures). Figure 5-16 shows the standard support plate signal (10 volts in Channel #7) which may be compared to the signals from the field inspection as shown in Figures 5-17 through 5-22. It may be noted that the support plate signals for these example tubes is only about 6 volts. This is strong evidence that the support plate holes in the S/G are larger than the standard support plate hole. Accumulation of magnetite in the crevice could result in some reduction in the signal amplitude. However, the following observations suggest absence of large amounts of magnetite in the crevice. Figure 5-23 shows the influence of magnetite on support plate signal. Please note that the magnetite packing of the crevice results in a rotation of the signal (Channel #7 in the figure). There is hardly any evidence of signal rotation for the example intersections displayed in Figures 17 through 22. Thus the data does not support the presence of large amounts of magnetite in the crevices. This assessment is further supported by the lack of dent indications at TSP intersections in this plant. The 1991 inspection results showed only three dent signals at tube support plates. One of these was in S/G-A and the other two in S/G-B.

5.5 RPC Inspection Results

During the 1991 outage, RPC inspection was performed on several tubes with bobbin coil indications at the TSP locations. These included tubes in both S/Gs at various support plates in both hot and cold legs. In general, RPC testing of a given tube-TSP intersection was performed to resolve distorted bobbin signals (those without depth estimates from bobbin data). The review of the RPC data indicates that the TSP signals are due to ODSCC. Most of them are single axial

indications and some are multiple axial signals. Most of the RPC traces could be easily interpreted. However, interpretation of the signal is difficult in some cases as a result of noise or other complexity in the RPC results.

A sample of the RPC traces are shown in Figures 5-24 and 5-25. The four traces in Figure 5-24 are from the hot leg TSP locations in S/G-A. These traces are clearly attributable to axial indications. The first (5-23a) was in tube R37C75 (S/G-A) at the second TSP in hot leg (2H). The bobbin coil test of this location had a signal amplitude of 0.82 volts (400/100 kHz mix). The other traces in the figure are from the lowest support plate in the hot leg (1H) and had bobbin amplitudes of 1.36 (5-23b: R2C18), 1.01 (5-23c: R33C36), and 1.. / (5-23d: R26C28) volts.

Figure 5-25 shows RPC traces from cold leg support plate locations of S/G-B. The two upper traces, 5-25a and 5-25b are from the upper support plates and show clear multiple axial crack indications. 5-25a signal in R38C48 tube (S/G-B) at the sixth TSP in the cold leg (6C) had a bobbin signal amplitude of 1.67 volts. The 5-25b trace is from R21C43 tube in the same S/G, at the 5C location; the corresponding bobbin indication amplitude was 1.42 volts. The two lower traces in the figure are from the peripheral region of the cold leg in the same S/G. Trace 5-24c is from the 6C location of tube R36C75 and is identified as a single axial indication. It had a bobbin amplitude of 1.07 volts. The trace from the 2C location of tube R15C91 (0.54 volt bobbin amplitude) is shown in Figure 5-25d. It is clear that the flaw is on the OD of the tube. However, unambiguous characterization of this signal is quite difficult; it was called a single axial indication by the field analyst.

These are examples of the RPC traces from the 1991 Kewaunee inspection. Review of the overall RPC data suggests that the support plate indications are axial ODSCC signals. This conclusion is also valid for the large number of cold leg indications observed at Kewaunee.

Bobbin testing had shown ten (10) TSP indications with amplitudes above 2 volts. Of these, nine were in the cold leg. Since each of these ten indications were sized for depth of penetration, they were not tested with RPC. Therefore, characterization of the indications with greater than 2 volts bobbin amplitude using direct RPC data is not available. However, meaningful information can be drawn from the available data. Only two (2) cold leg indications above 1.4 volts bobbin amplitude were tested using RPC. Both of these had multiple axial indications (see Figure 5-25 a and b). Eight (8) cold leg indications at/above 1.2 volts bobbin amplitude were RPC tested. Of these, four (i.e., 50%) had multiple axial flaws. These figures suggest that the cold leg TSP indications with greater than 2 volts bobbin amplitudes and shallow depths of penetration are multiple axial cracks. This can be confirmed by RPC testing of these during the next inspection.

Table 5.1

Voltage Growth Per Cycle for Kewaunee S/Gs (1)

Unit / Cycle	Number of Indications	Average Voltage	% Growth/Cycle Average	% Growth/Cycle Std. Dev.	% ≥ 0 Growth/Cycle Average	% ≥ 0 Growth/Cycle Std. Dev.
1987 to 1988	22	0.86	16%	83%	34%	69%
1988 to 1989	37	0.95	23%	63%	31%	57%
1989 to 1990	55	0.96	19%	37%	24%	32%
1990 to 1991						
Entire voltage range	187	0.88	-15%	26%	5%	16%
V_{BOC} < 0.75 volt	63	0.57	-7%	31%	9%	21%
V_{BOC} ≥ 0.75 volt	124	1.52	-19%	22%	3%	12%
Average over last 4 cycles			-2%	44%	13%	35%

Notes

1. Voltage growth percycle determined as $(V_{EOC} - V_{BOC}) / V_{BOC}$
2. Growth per cycle obtained by conservatively setting voltage change $(V_{EOC} - V_{BOC})$ to zero if measured change is negative.

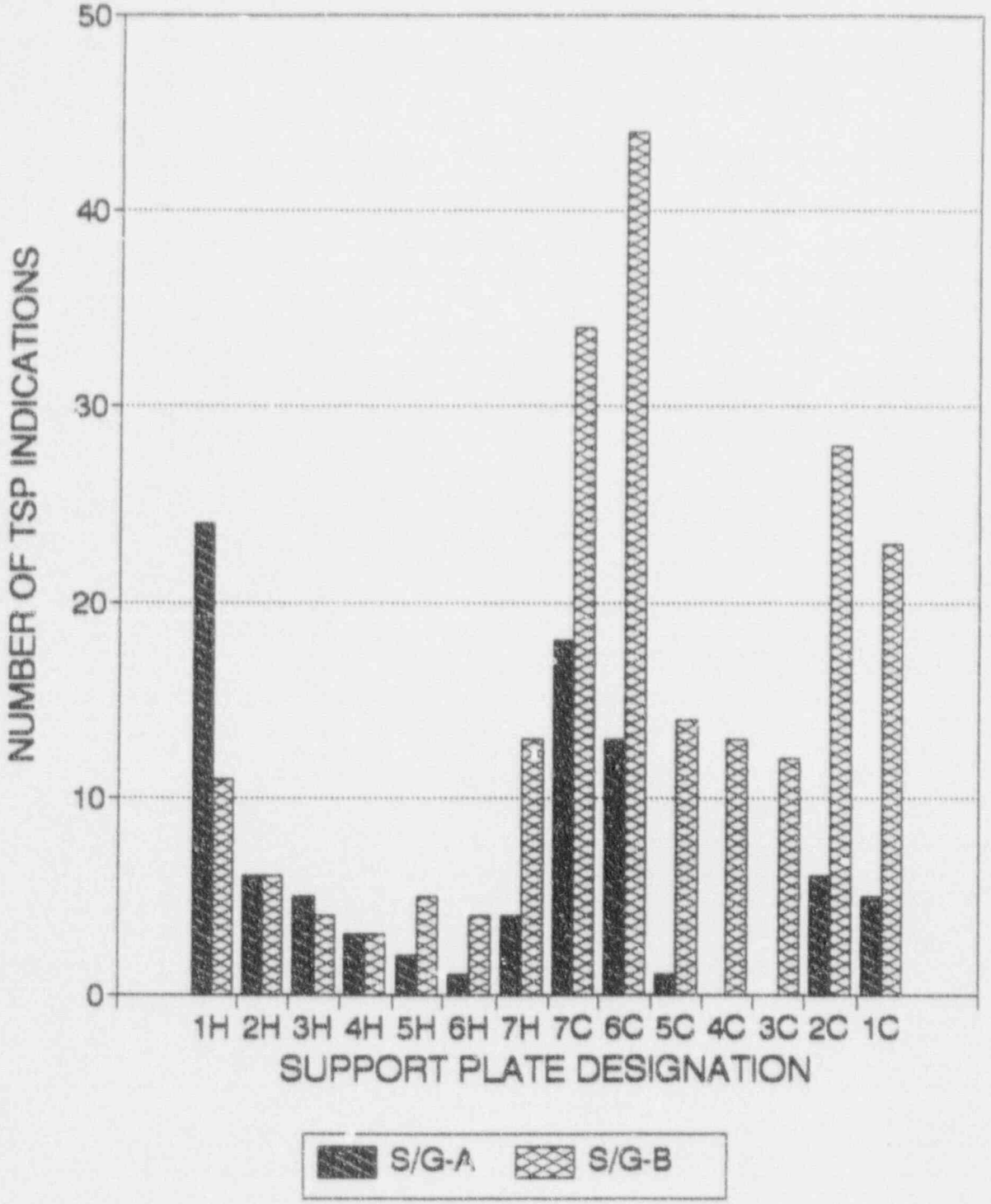

Figure 5-1. Frequency Distribution of TSP Indications by Location (March 1991 Inspection)

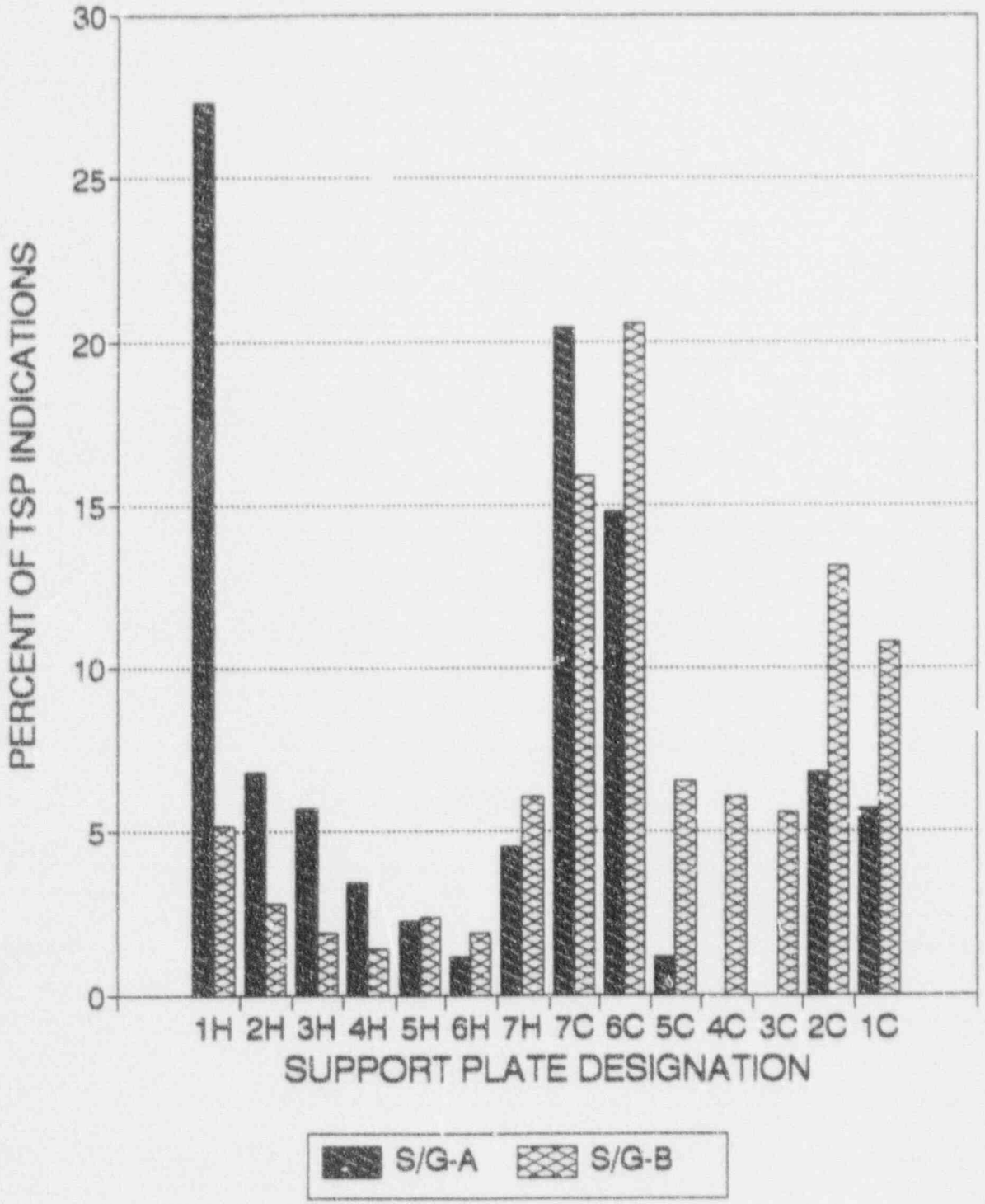

Figure 5-2. Percentage Distribution of TSP Indications by Location (March 1991 Inspection)

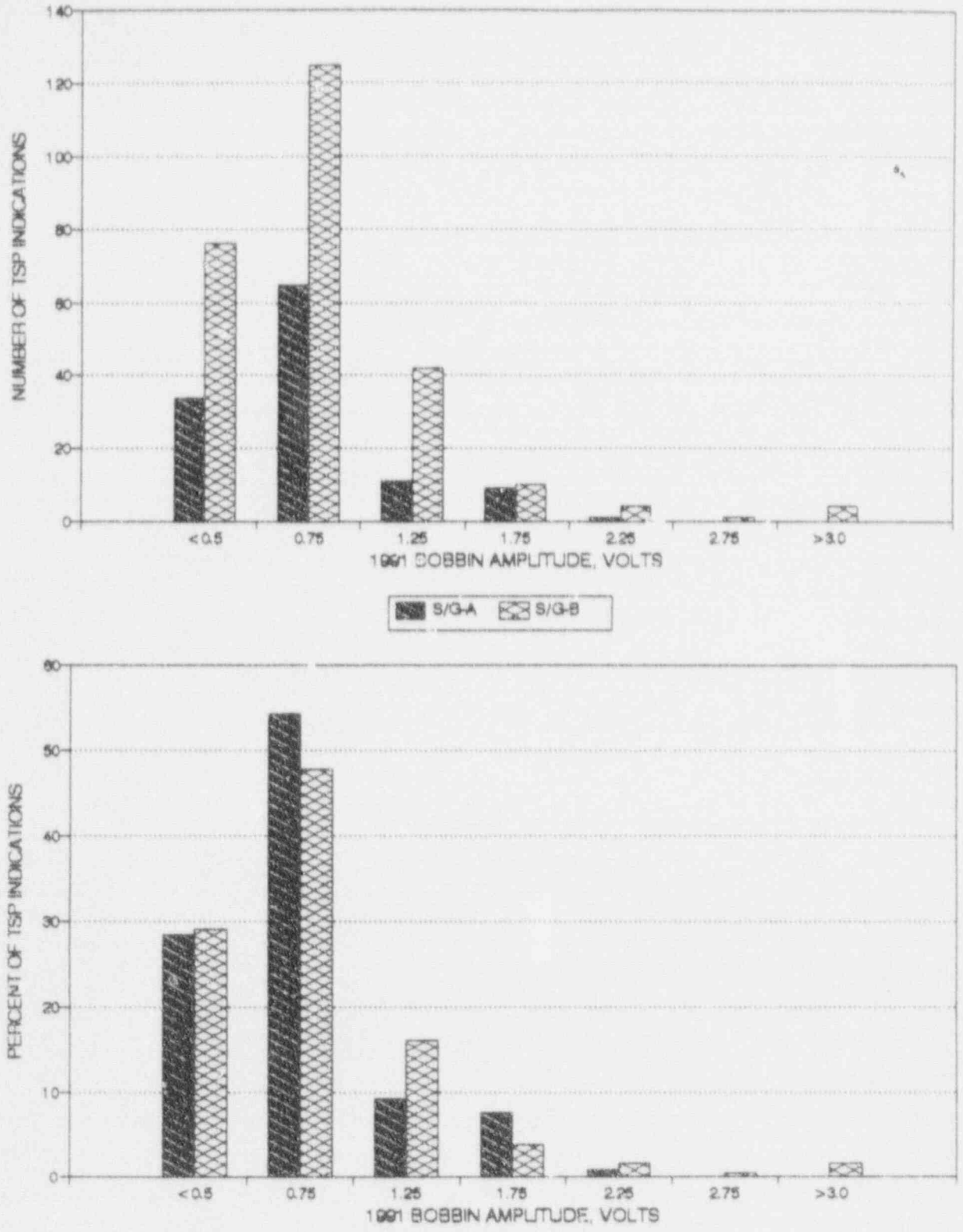

Figure 5-3. Frequency and Percentage Distribution of TSP Indication Voltage Amplitudes (March 1991 Inspection)

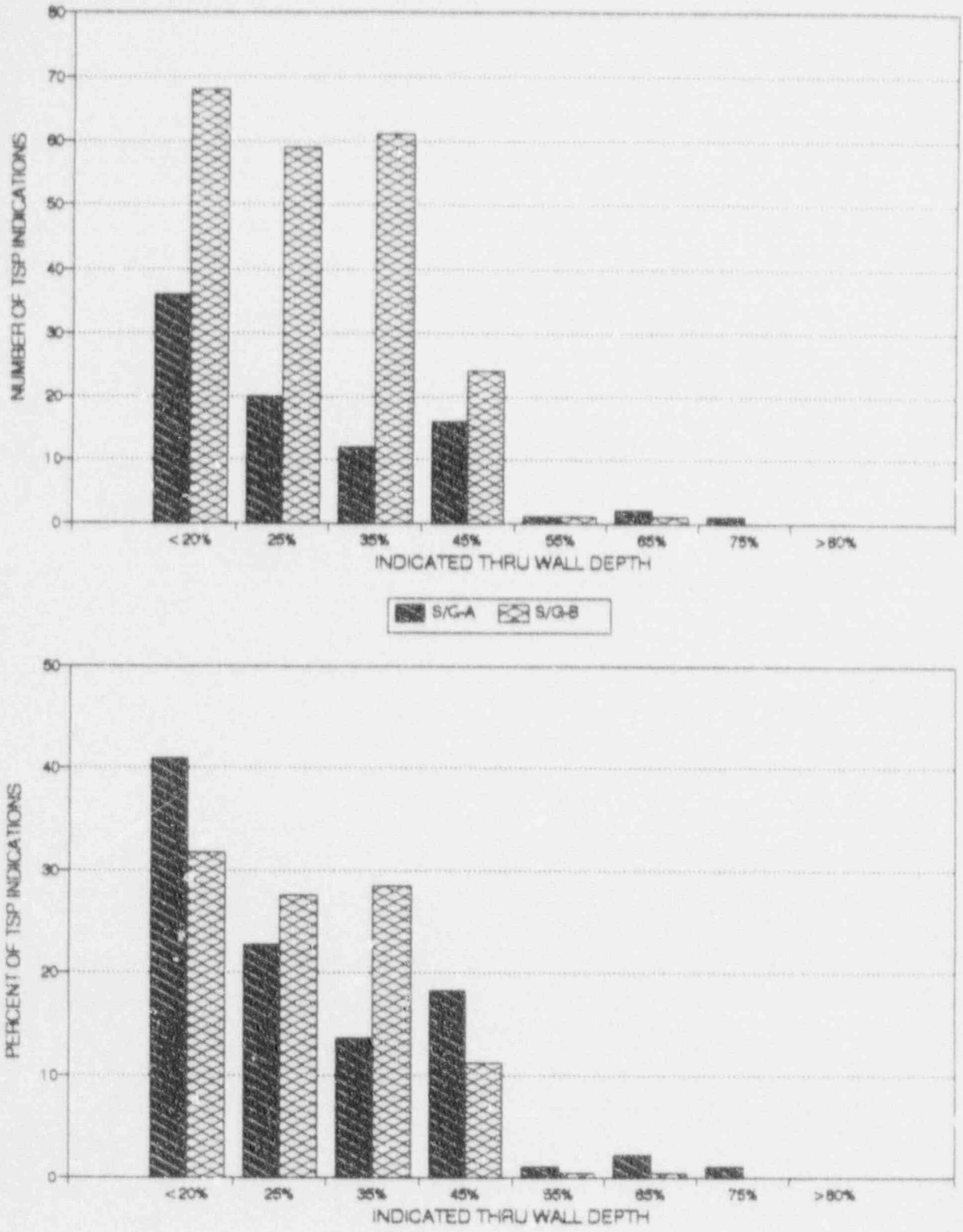

Figure 5-4. Frequency and Percentage Distribution of Indicated Depths (March 1991 Inspection)

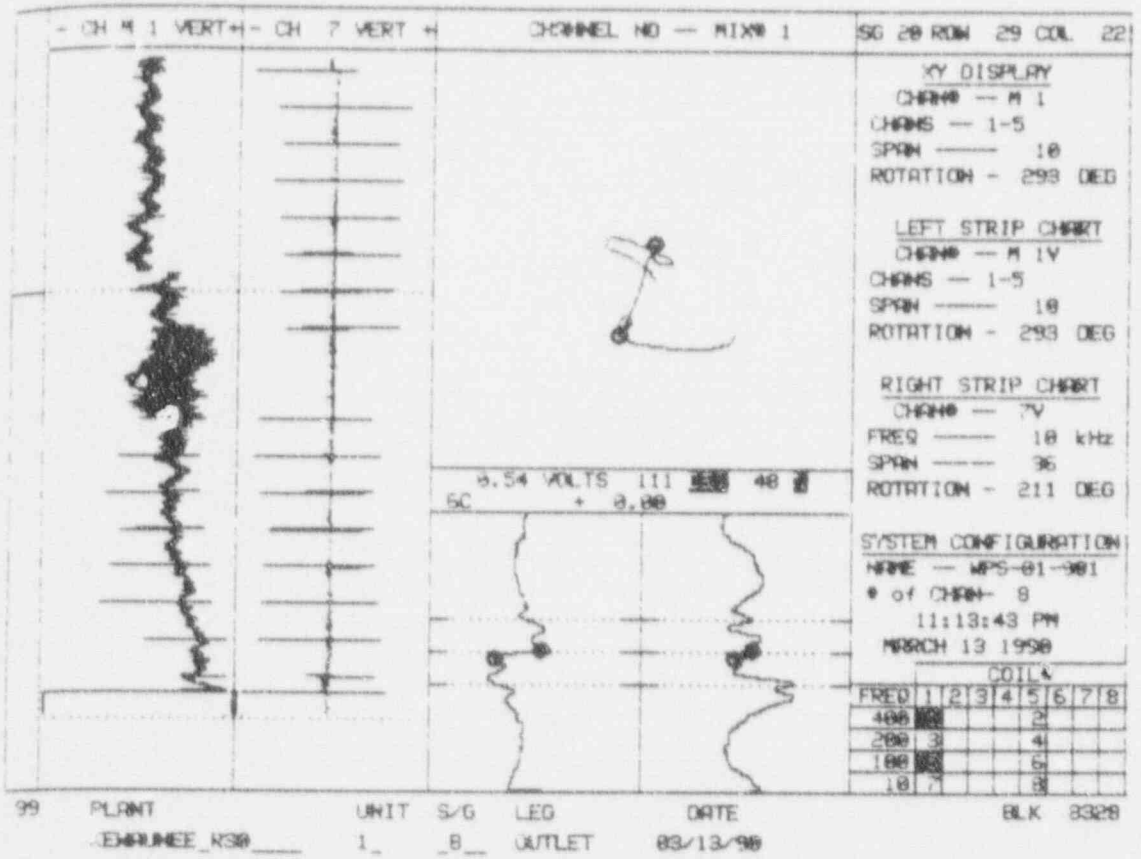

Figure 5-5. Bobbin Coil Signal Without Distortion (March 1990 Inspection)

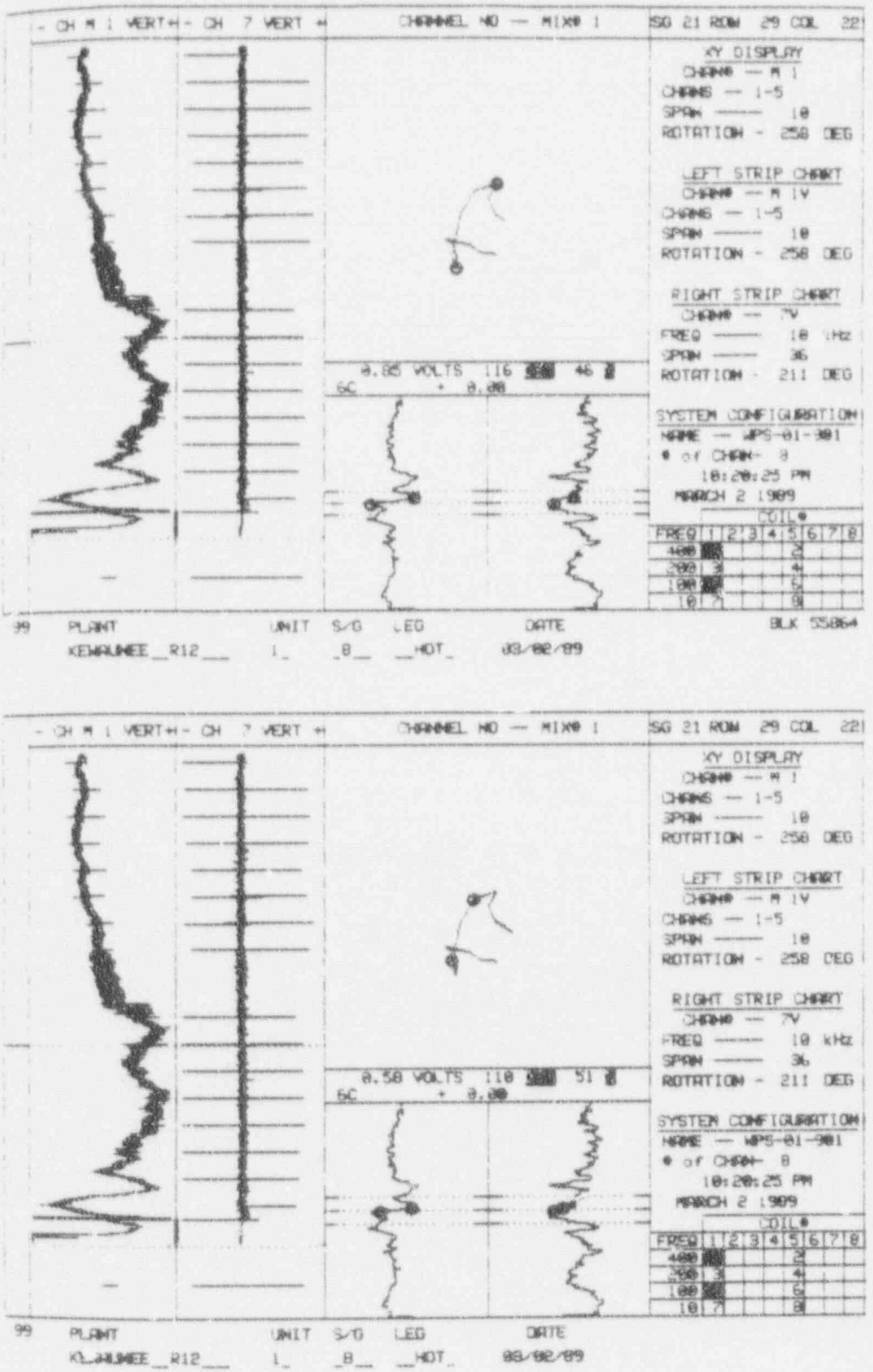

Figure 5-6. Distorted Bobbin Coil Signal (March 1990 Inspection)

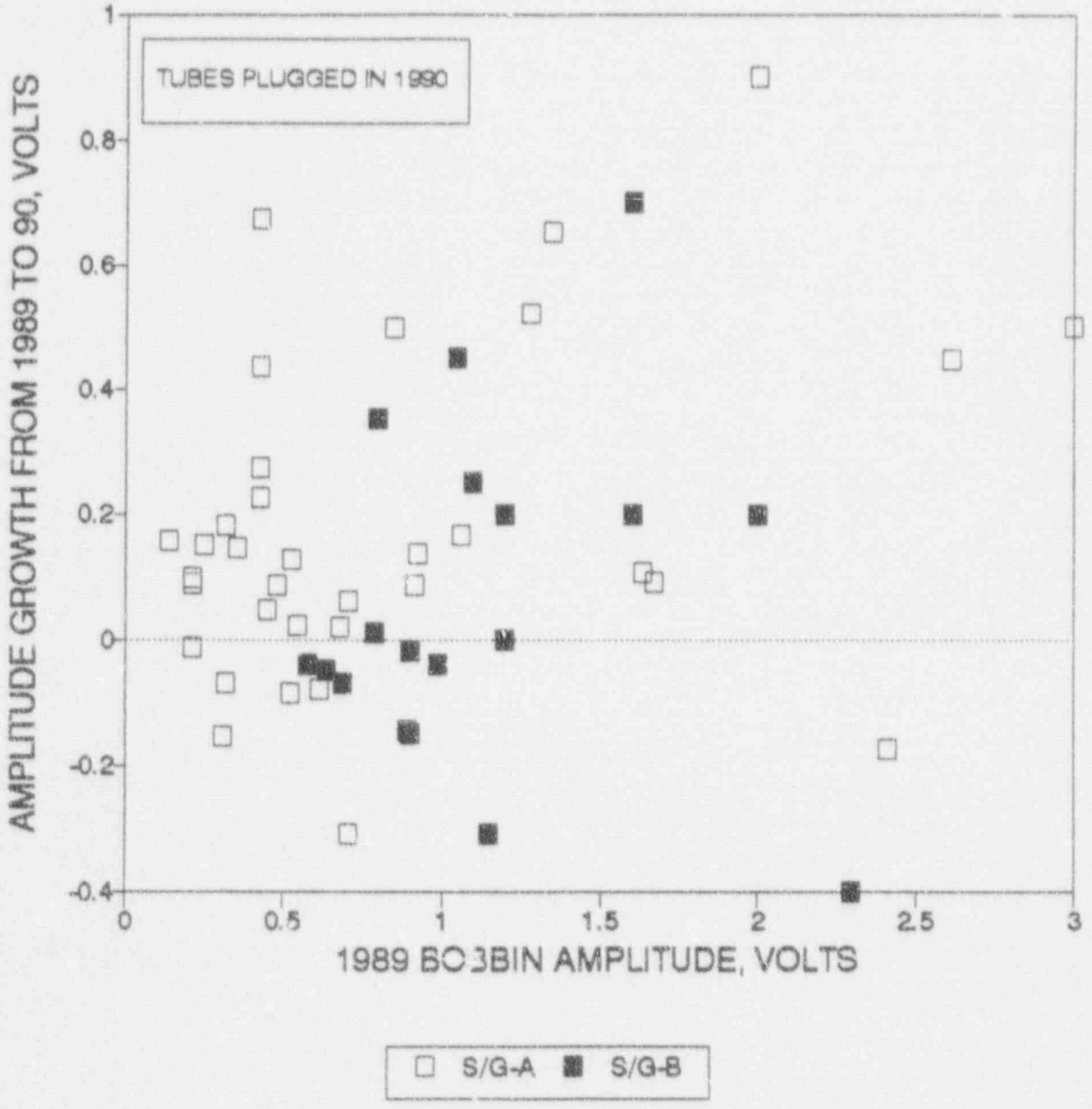

Figure 5-7. Growth in Bobbin Amplitudes from 1989 to 1990 in Kewaunee S/Gs

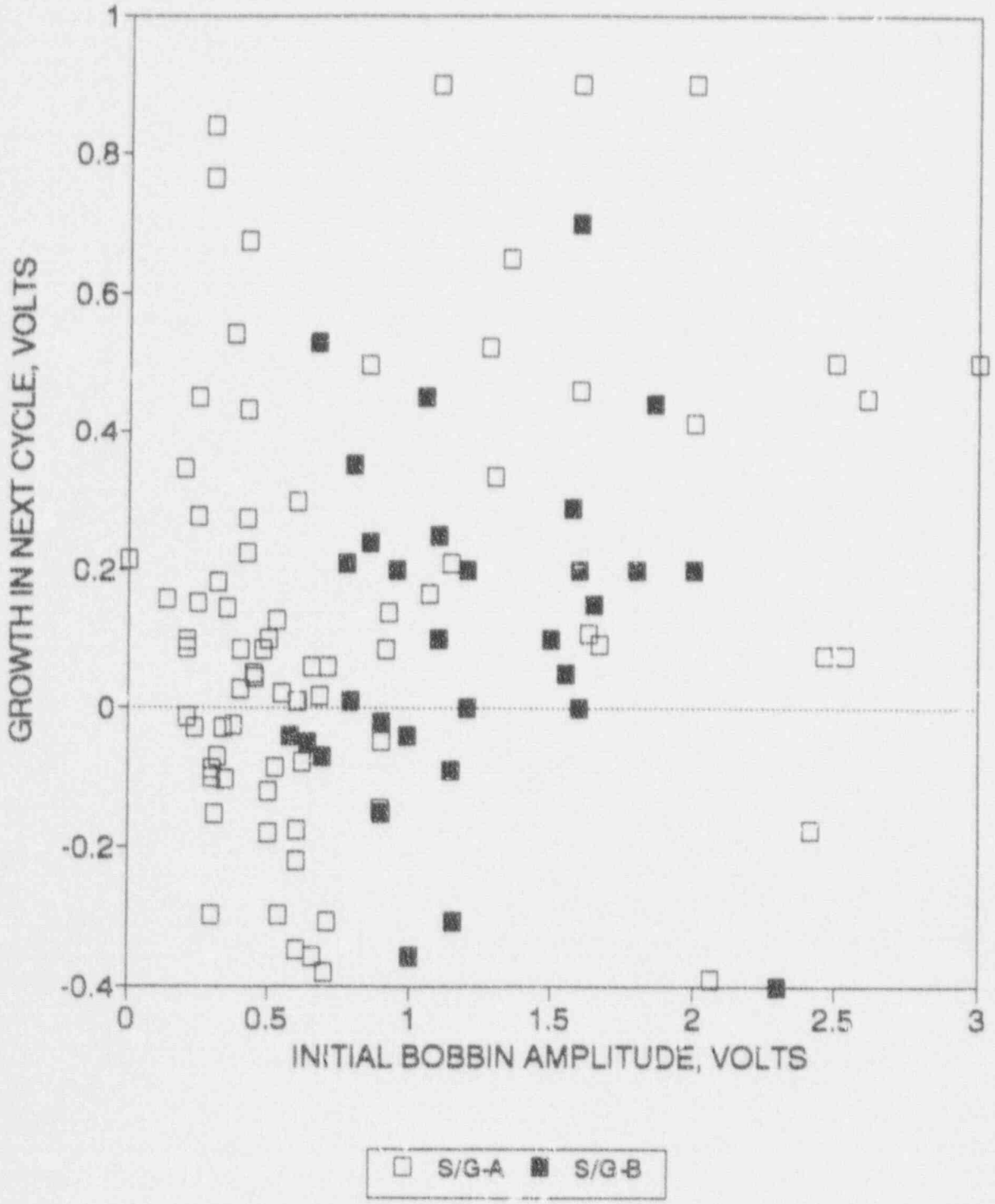

Figure 5-8. Growth in Bobbin Amplitude per Cycle from 1987 to 1990 in Kewaunee S/Gs

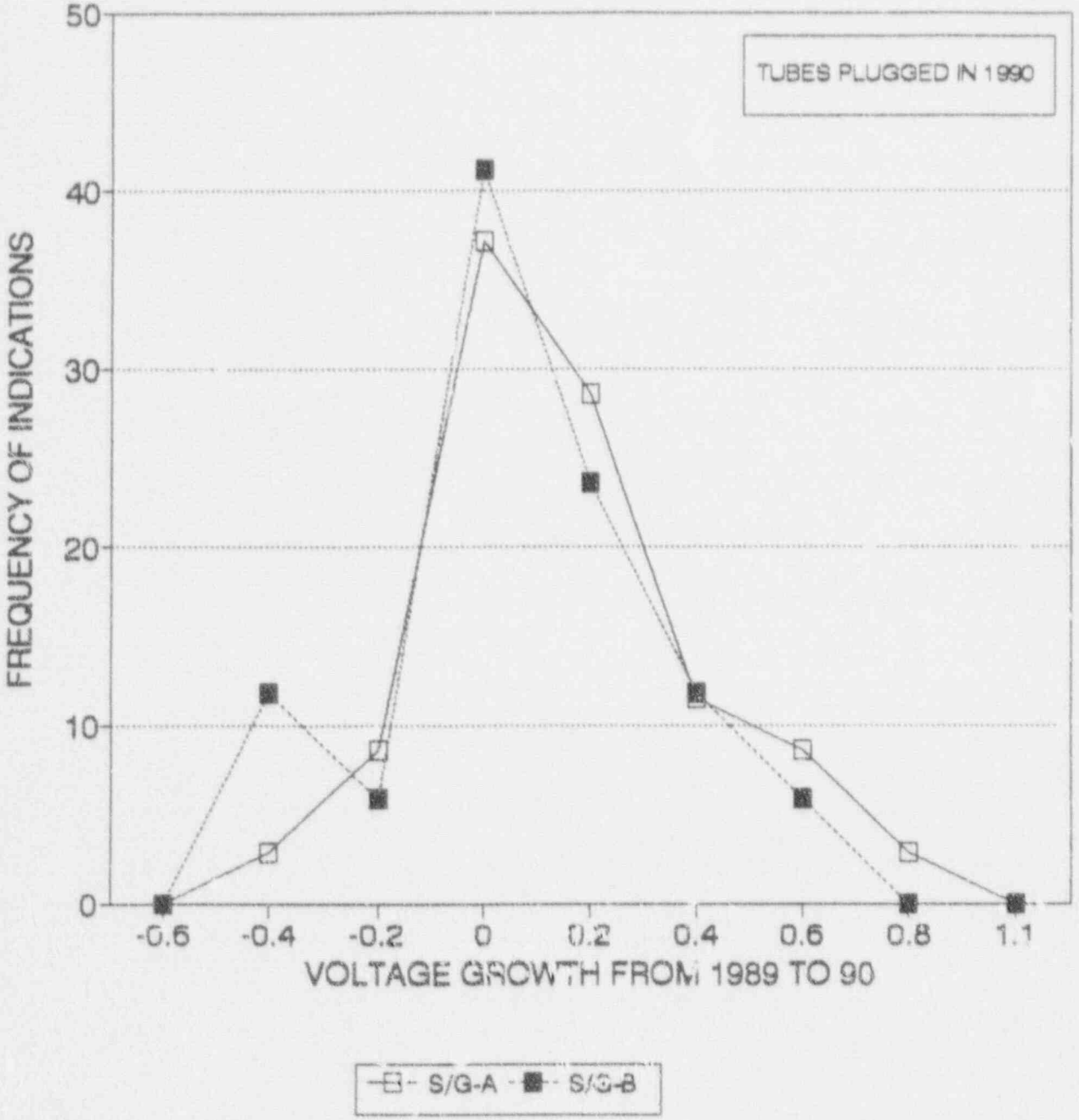

Figure 5-9. Frequency Distribution of Bobbin Amplitude Growth Rates from 1989 to 1990

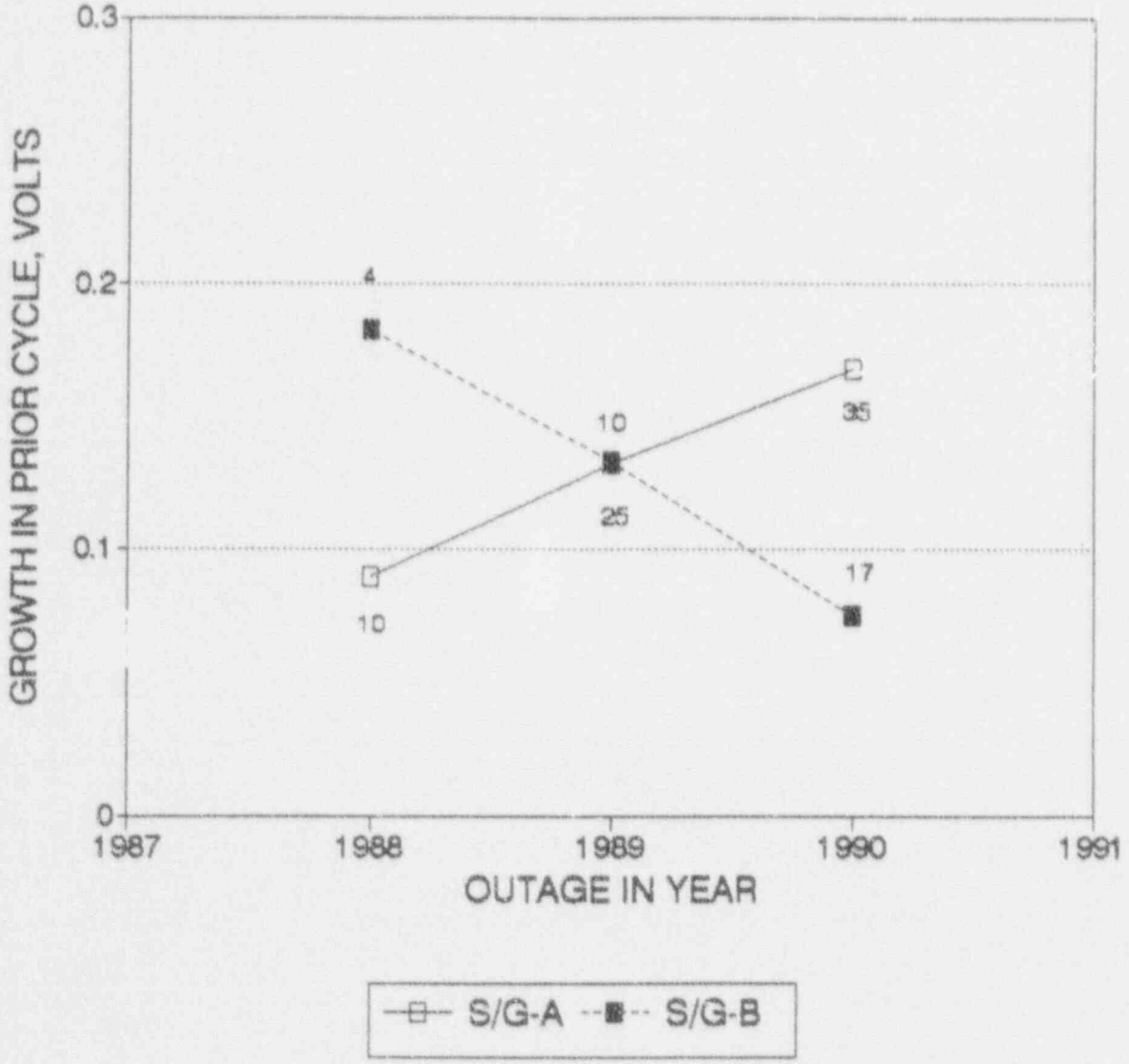

Figure 5-10. Average Growth Rates in Bobbin Amplitude from 1987 to 1990

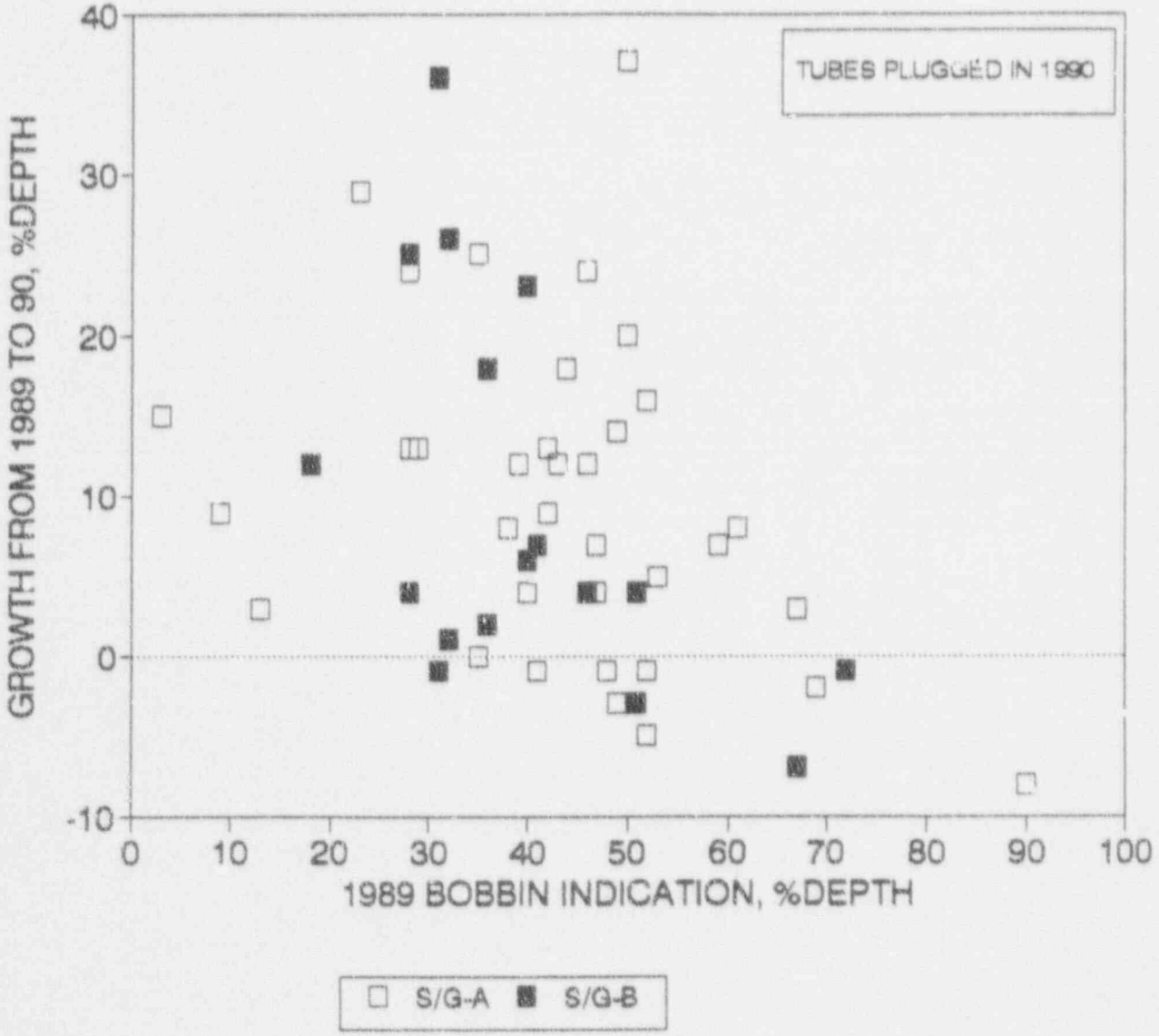

Figure 5-11. Growth in Indicated Depths from 1989 to 1990 in Kewaunee S/Gs

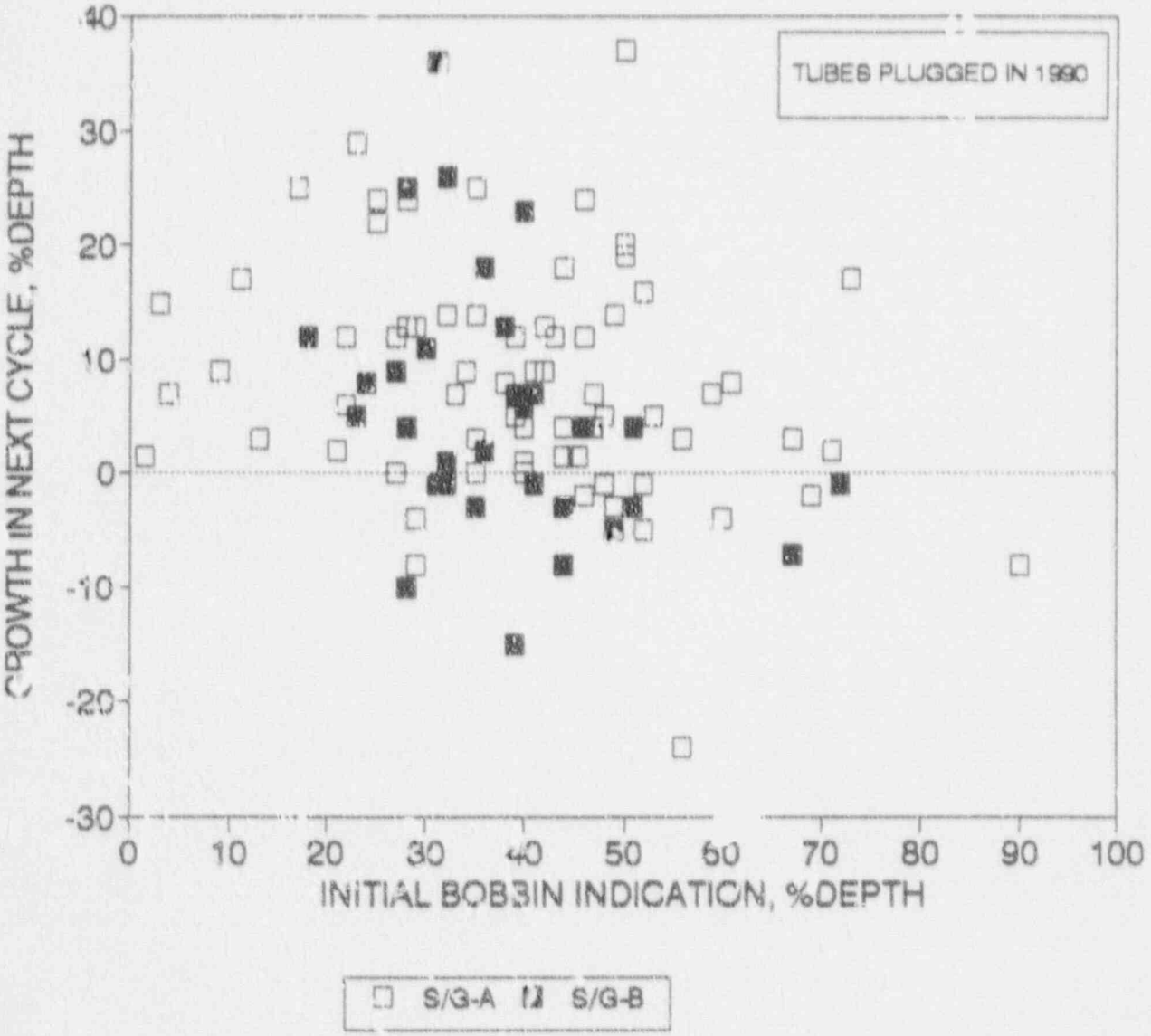

Figure 5-12. Growth in Indicated Depth per Cycle vs Prior Depth from 1987 to 1990

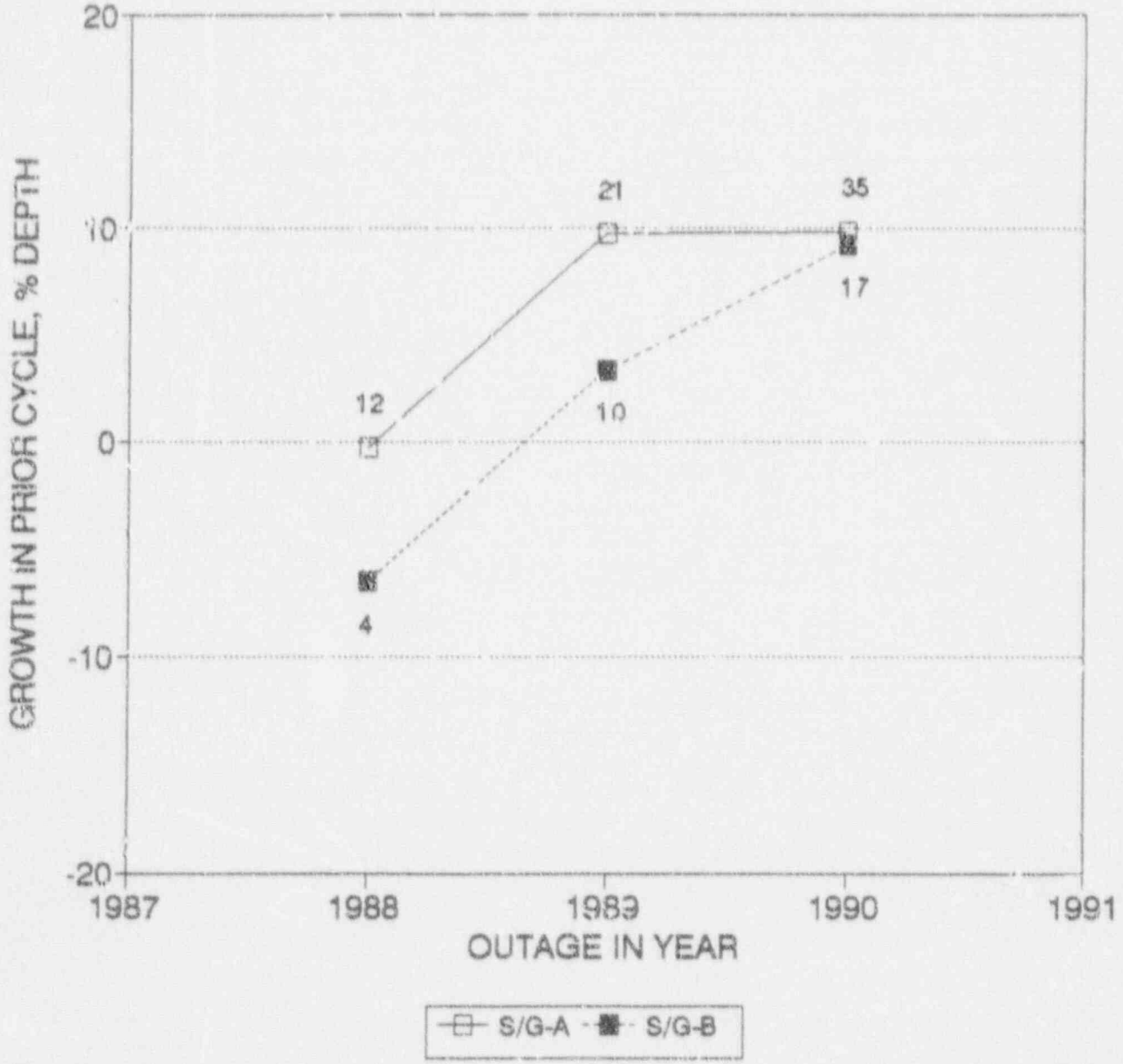

Figure 5-13. Average Growth in Indicated Depth per Cycle from 1987 to 1990

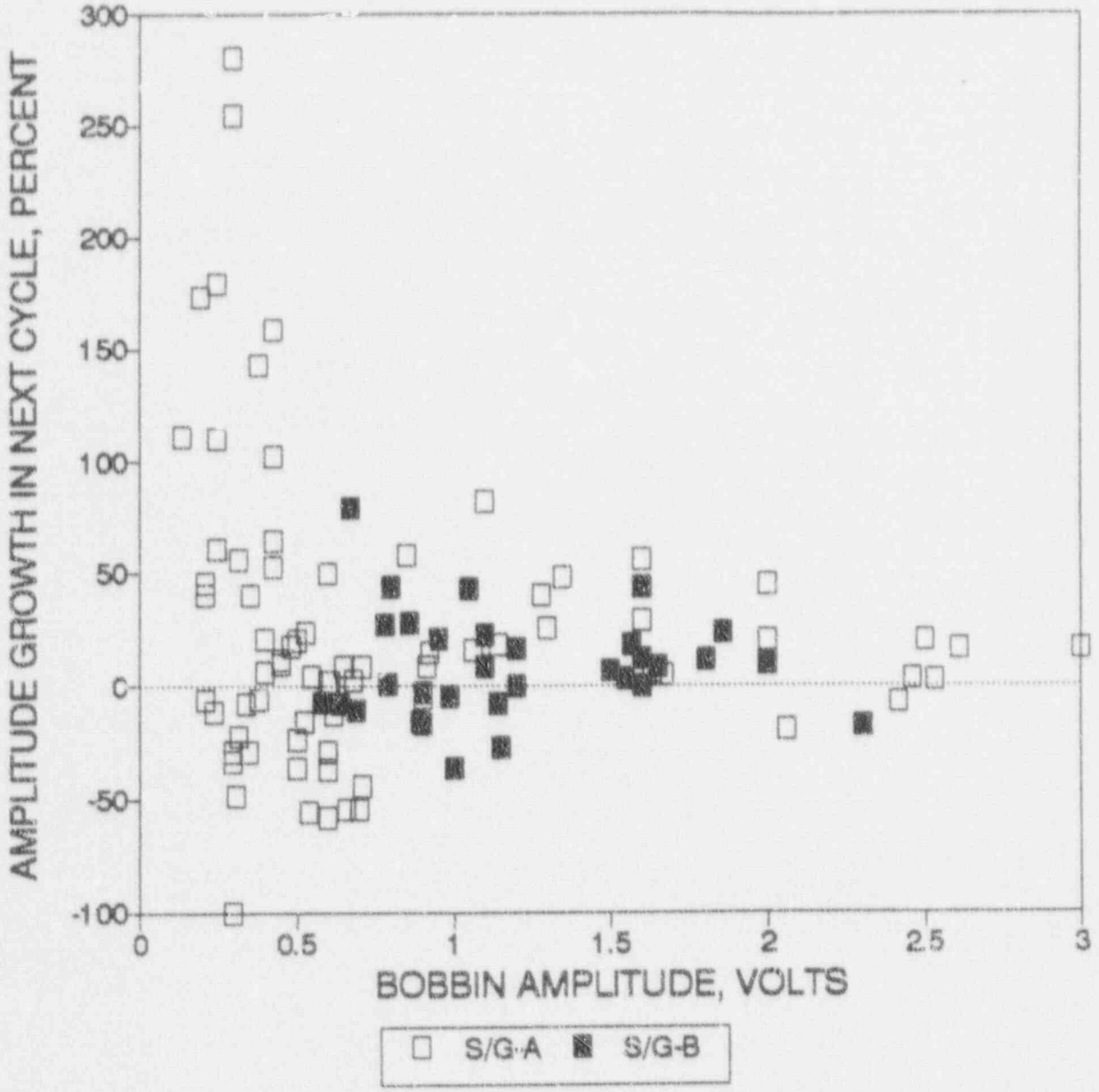

Figure 5-14. Percent Growth in Amplitude vs Prior Cycle Amplitude

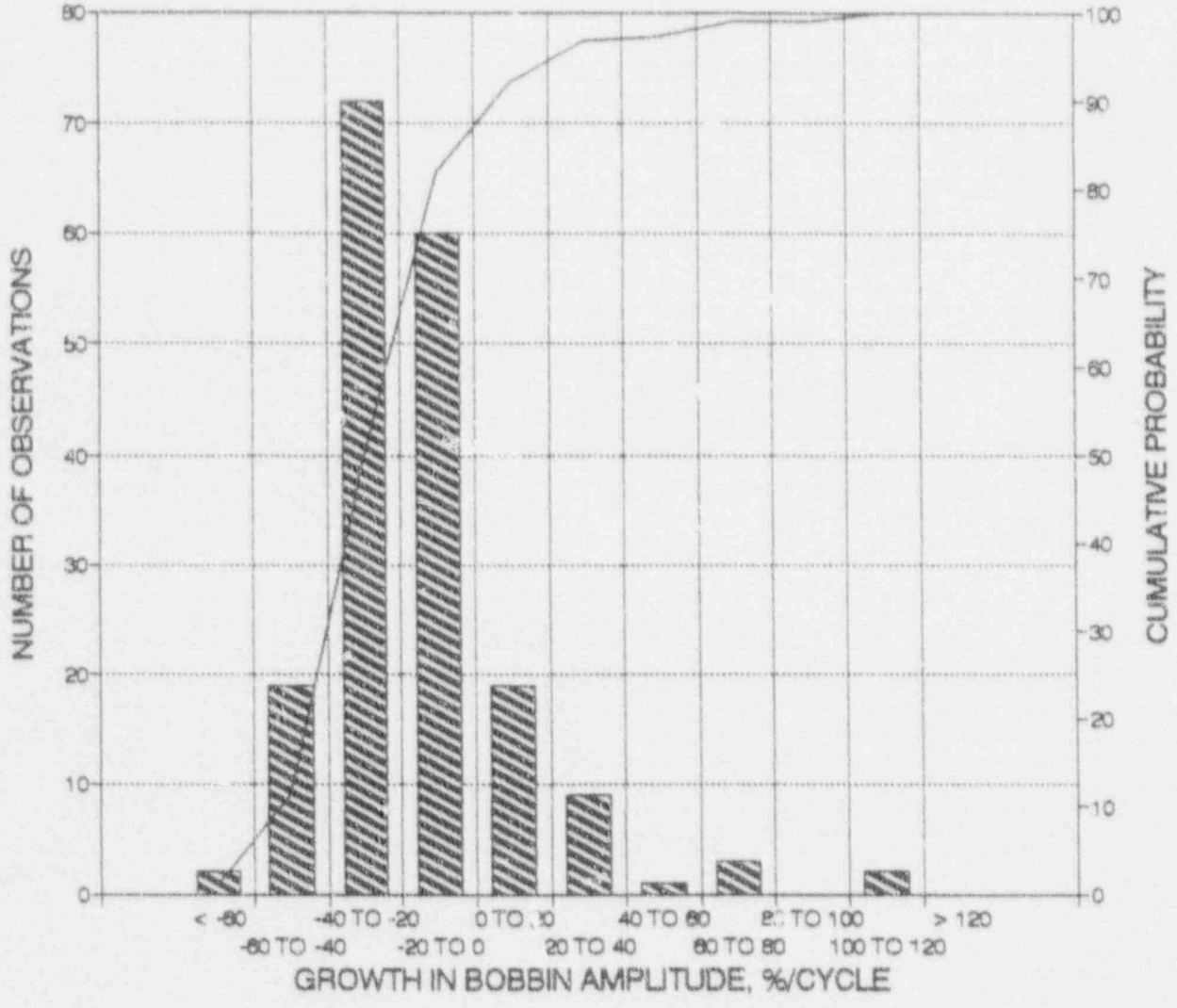

Figure 5-15. Histogram and Cumulative Probability of Voltage Growth in Kewaunee S/Gs in the Last Cycle (1990-91)

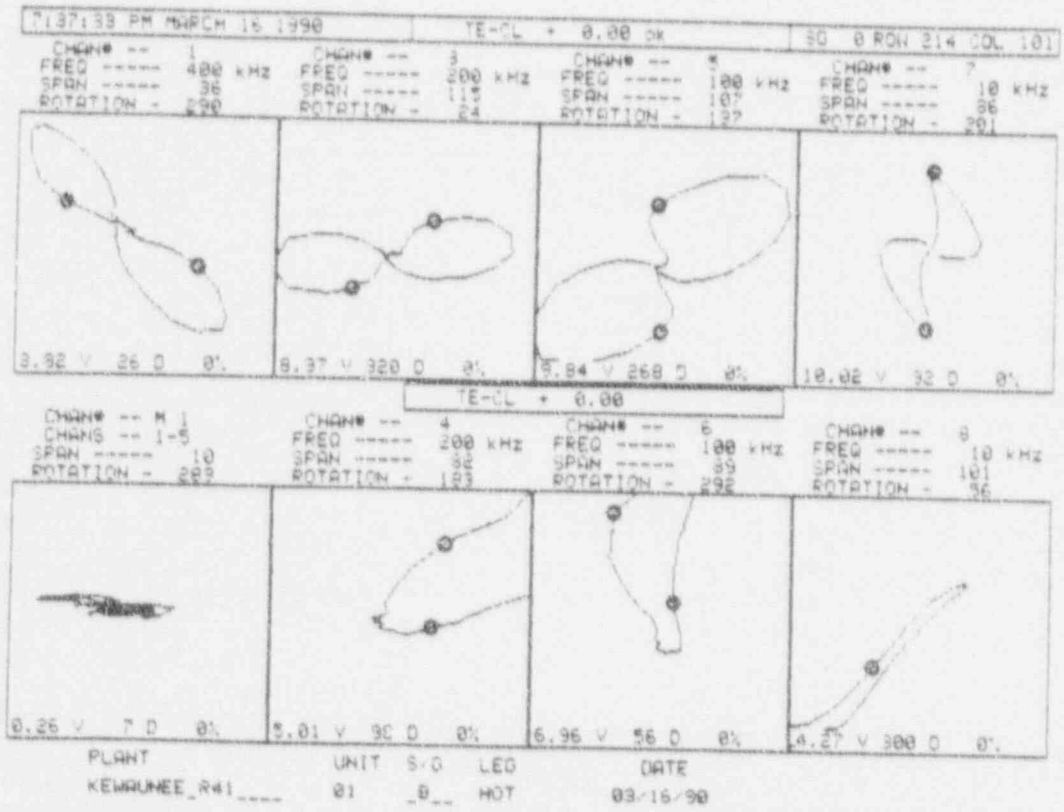

Figure 5-16. Signals from a Support Plate Calibration Standard

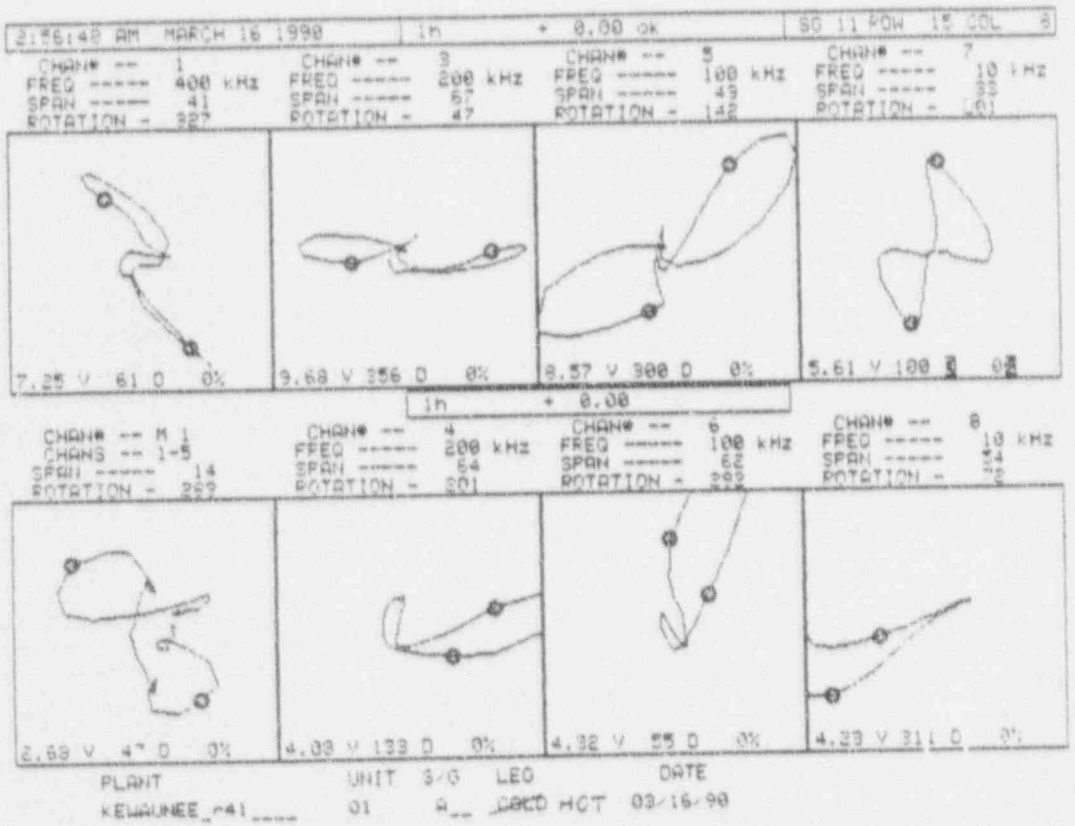

Figure 5-17. Support Plate Signals from S/G-A, R15 C8, Location 1H
(March 1990 Inspection)

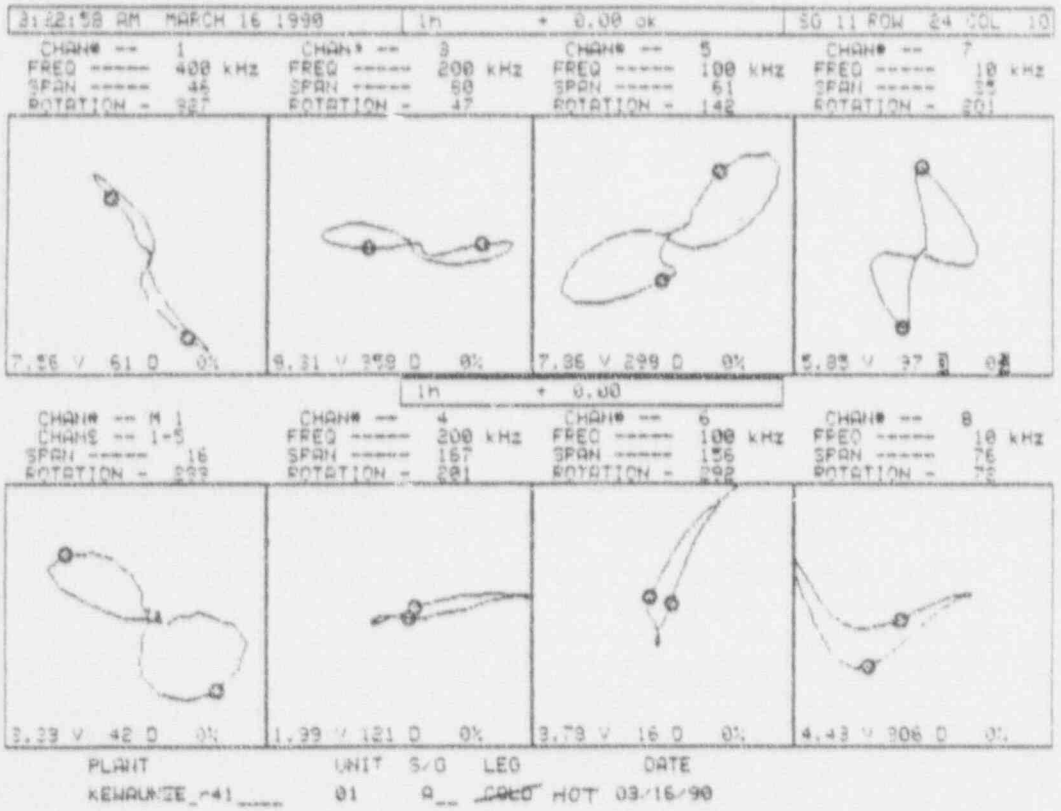

Figure 5-18. Support Plate Signals from S/G-A, R24 C10, Location 1H
(March 1990 Inspection)

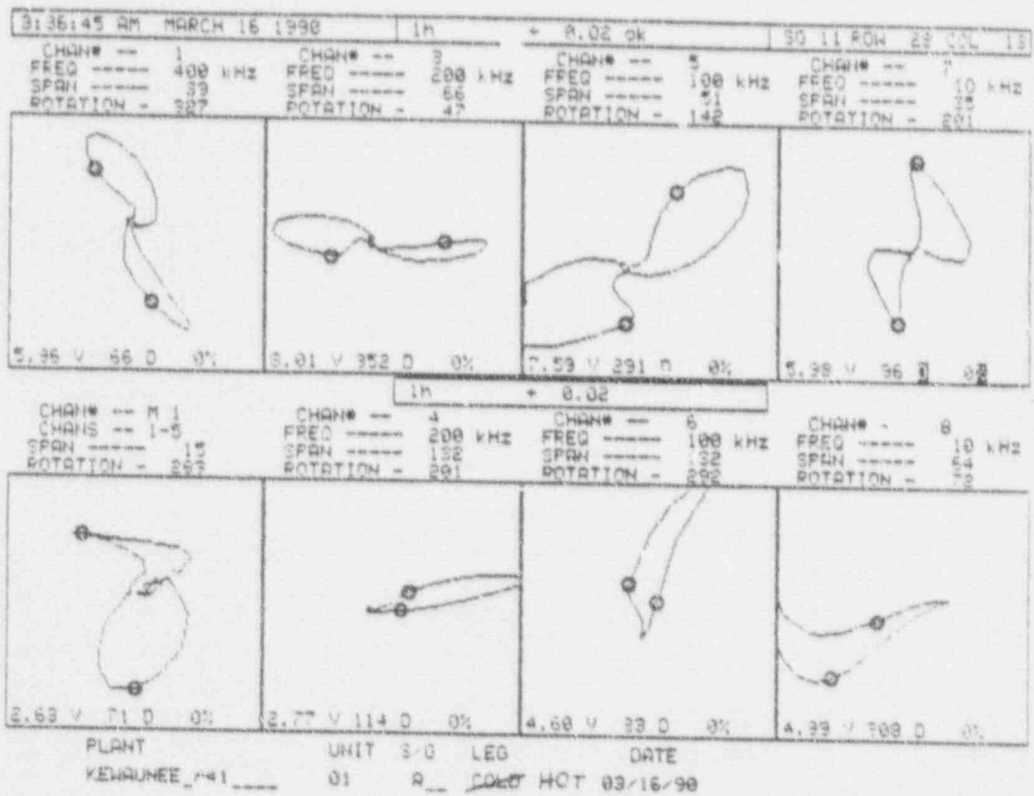

Figure 5-19. Support Plate Signals from S/G-A, R28 C13, Location 1H
(March 1990 Inspection)

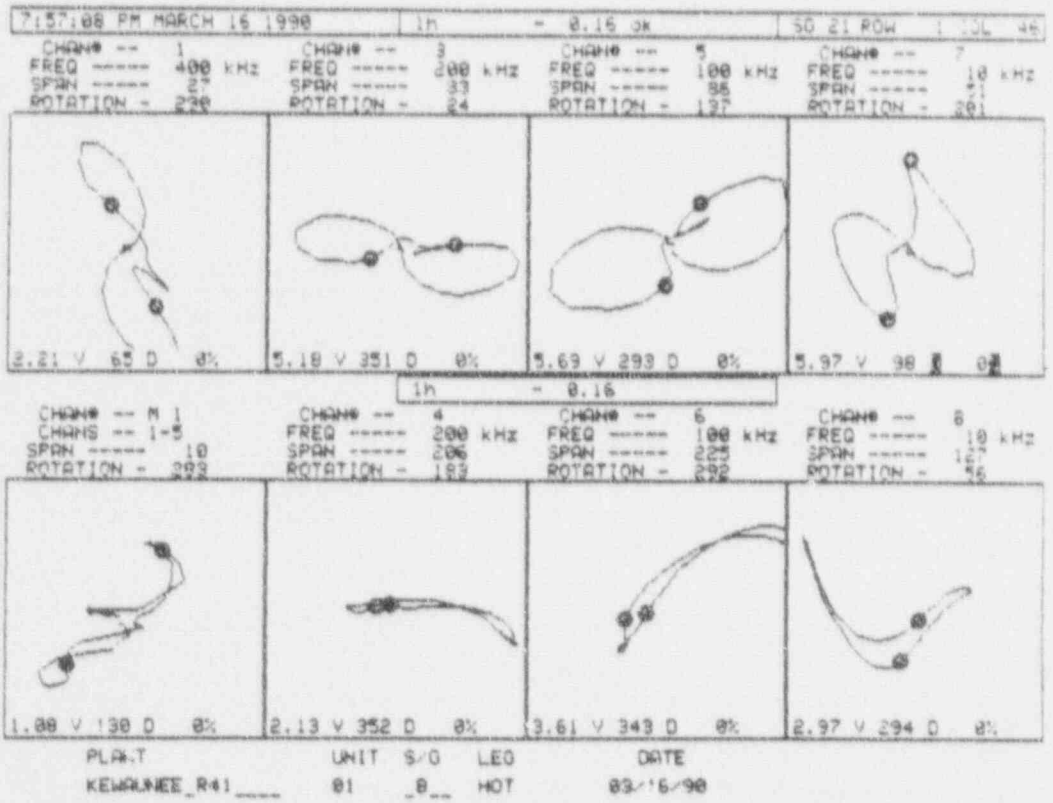

Figure 5-20. Support Plate Signals from S/G-B, R1 C46, Location 1H
(March 1990 Inspection)

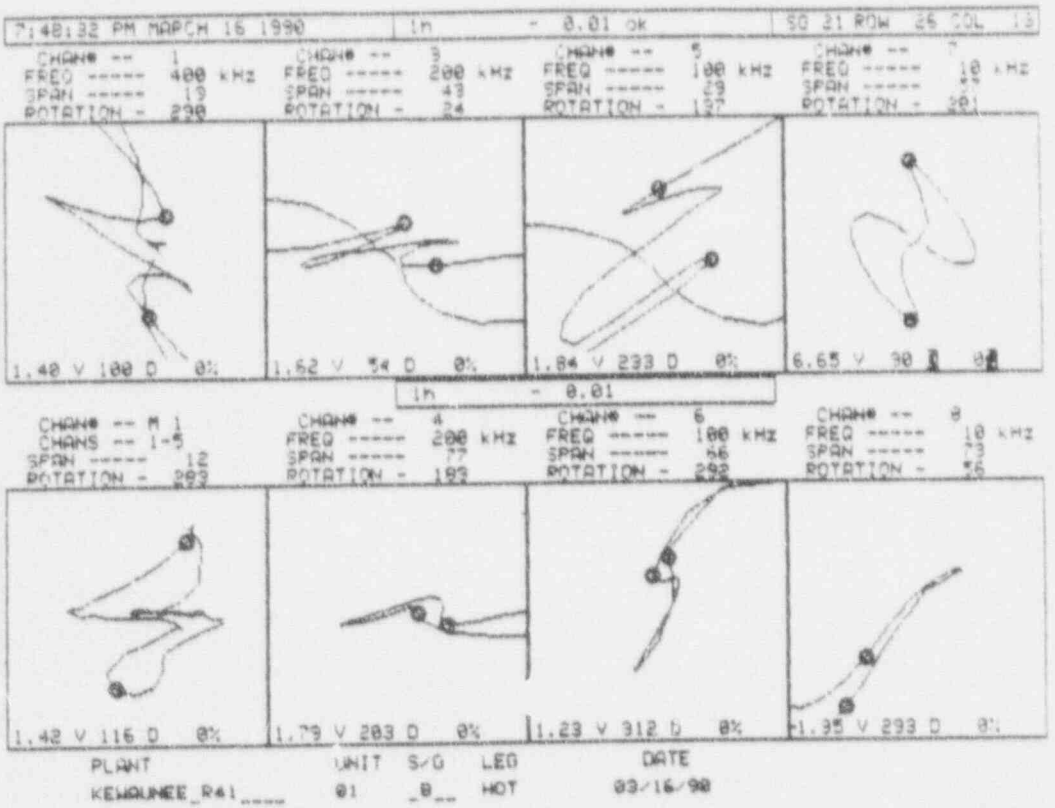

Figure 5-21. Support Plate Signals from S/G-B, R26 C18, Location 1H
(March 1990 Inspection)

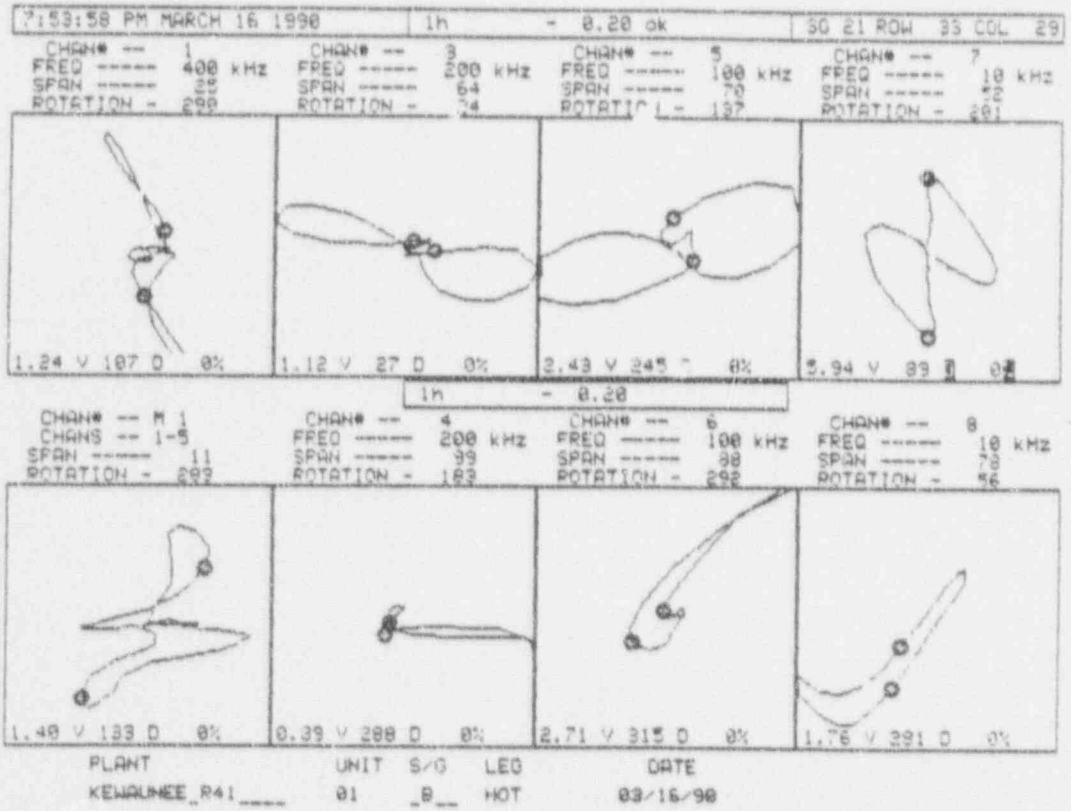

Figure 5-22. Support Plate Signals from S/G-B, R33 C29, Location 1H
(March 1990 Inspection)

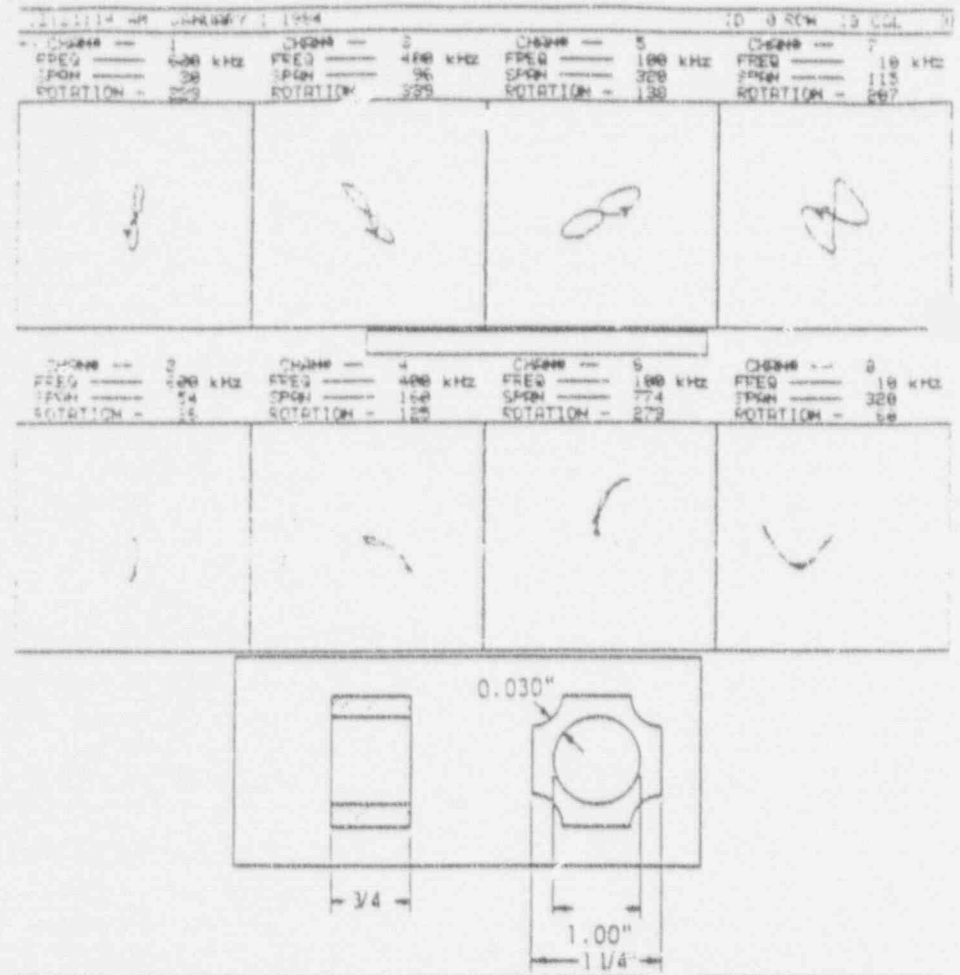

No magnetite in crevice

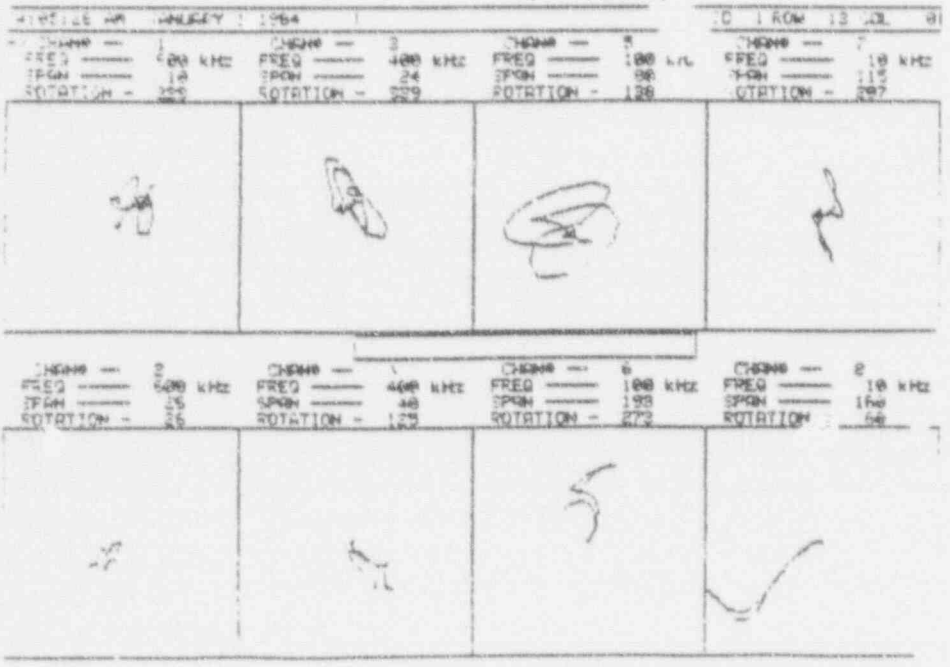

With magnetite in crevice

Figure 5-23. Influence of Magnetite on Support Plate Signals

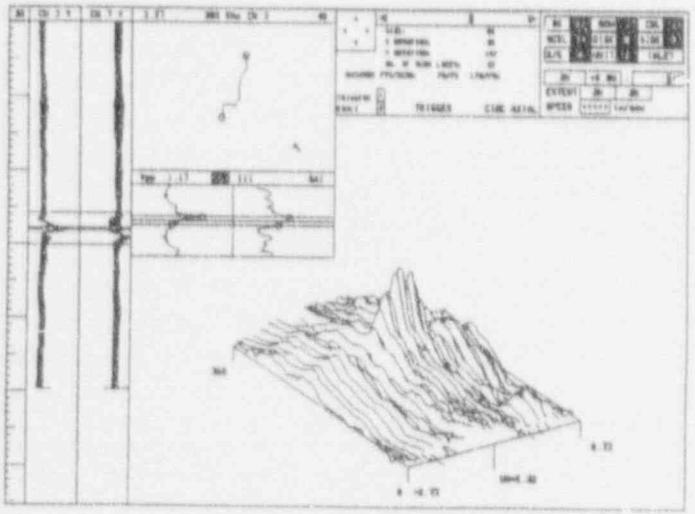

a) R37 C75, Location 2H

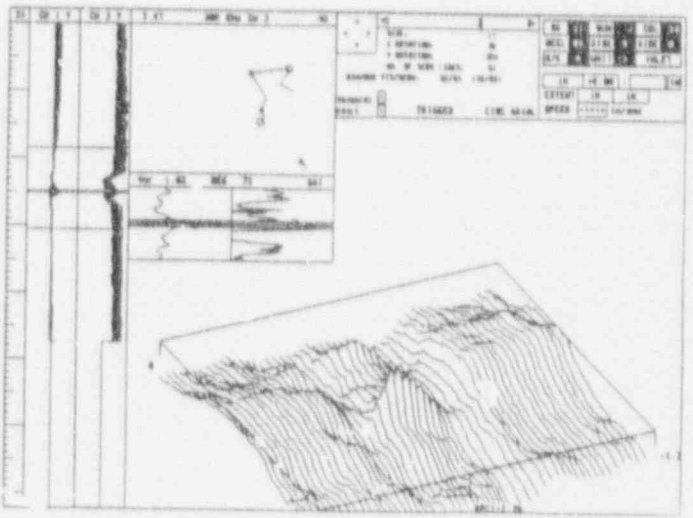

b) R2 C18, Location 1H

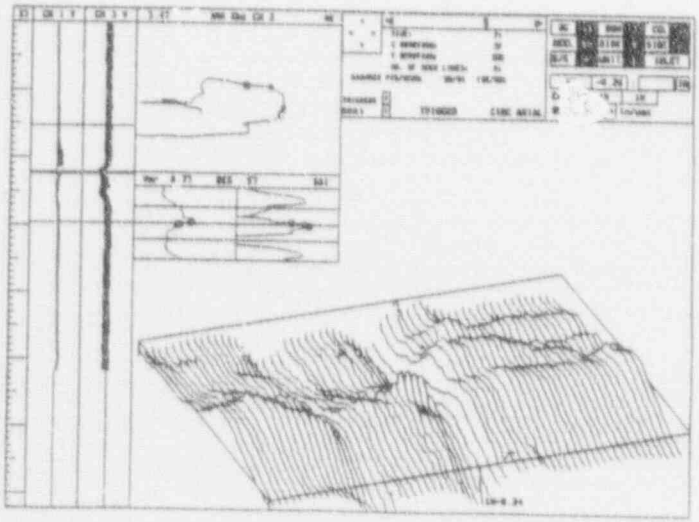

c) R33 C36, Location 1H

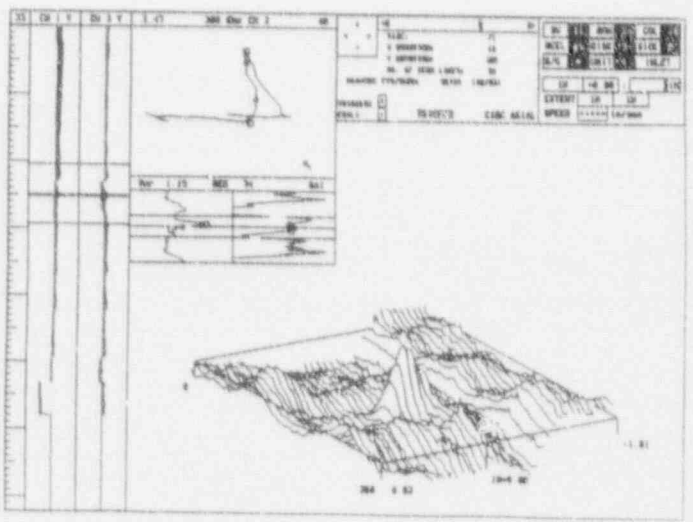

d) R26 C28, Location 1H

Figure 5-24. Example RPC Traces from Hot Leg Support Plate Locations in S/G-A
(March 1991 Inspection)

a) R38 C48, Location 6C

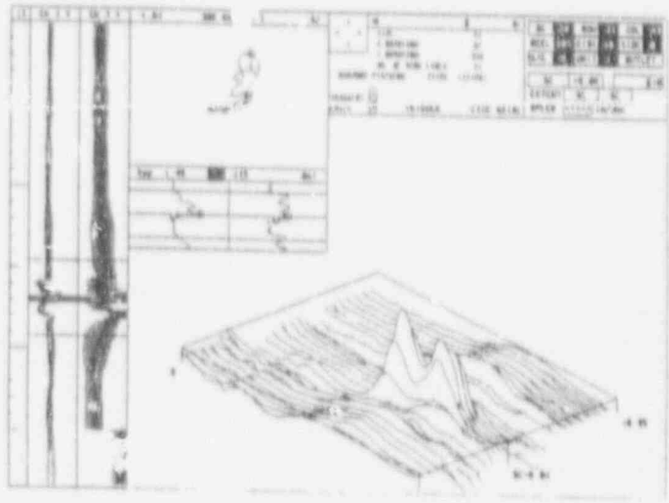

b) R21 C43, Location 5C

c) R36 C75, Location 6C

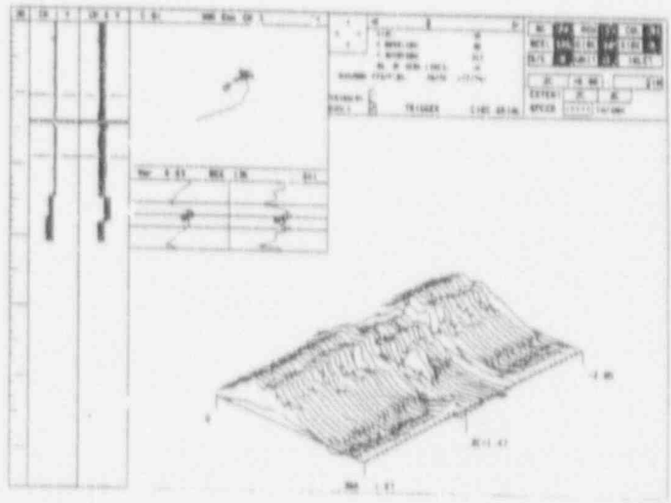

d) R15 C91, Location 2C

Figure 5-25. Example RPC Traces from Cold Leg Support Plate Locations in S/G-B (March 1991 Inspection)

6.0 FIELD EXPERIENCE SUMMARY: Pulled Tube Plant Leakage and Inspection Data

This section identifies the field experience data from operating S/Gs that are utilized in the development of tube plugging criteria for ODSCC at TSPs. The field data utilized include pulled tube examinations, occurrences of tube leakage for ODSCC indications at support plates and field inspection results for relatively large crack indications with no identifiable leakage.

6.1 Utilization of Field Data in Tube Plugging Criteria

Operating S/G experience represents the preferred source of data for the plugging criteria. Where the available operating data are insufficient to fully define plugging criteria, data developed from laboratory induced ODSCC specimens were used to supplement the field data base. Table 6.1 summarizes the utilization of field and laboratory data to develop the tube plugging criteria. The field data utilized for the plugging criteria are identified in this report section. Sections 7 to 11 describe the development of the laboratory data. The field and laboratory data are combined in Sections 9 and 12 to develop the tube plugging limits.

The overall approach to the tube plugging criteria is based upon establishing that R.G. 1.121 guidelines are satisfied. It is conservatively assumed that the tube to TSP crevices are open and that the TSPs are displaced under accident conditions such that the ODSCC generated within the TSPs becomes free span degradation under accident conditions. Under these assumptions, preventing excessive leakage and tube burst under SLB conditions is required for plant safety. Tube rupture under normal operating conditions is prevented by the constraint provided by the drilled hole TSPs with small tube to TSP clearances (typically ~ 16 mil diametral clearance for open crevices). For the plugging criteria, however, the R.G. 1.121 criteria for burst margins of 3 times normal operating pressure differentials are applied to define the structural requirements against tube rupture.

In addition to providing margins against tube burst, it is necessary to limit SLB leakage to acceptable levels based on USAR evaluations for radiological consequences under accident conditions. Thus SLB leakage models are required for the plugging criteria in addition to tube burst data.

Based on the above considerations and the plugging criteria objective of relating tube integrity to NDE measurements, the primary data requirements for the plugging criteria are the correlation of burst pressure capability and SLB leak rates with bobbin coil voltage. For plant operational considerations, it is desirable to minimize the potential for operating leakage to avoid forced outages. Thus an additional objective is to relate bobbin coil voltage to operating leakage. The field data of this section indicate very low leakage potential for ODSCC at TSPs even at voltage amplitudes much higher than the plugging limits.

Within the above overall approach, field data are utilized as follows:

A. Pulled Tube Data

The test results for pulled tubes having had leak rate and burst tests performed, such as the three Plant A-2 tubes, are used directly in supporting the plugging limits. If metallographic

data on the crack morphology is available but leak/burst tests were not performed, the crack depths and lengths were evaluated to assess the potential for leakage and to estimate burst pressure margins. However only tubes with measured burst pressure are used in the voltage/burst pressure correlation. The pulled tube data base is discussed in Section 6.2.

B. Plant Leakage Experience for ODSCC at TSPs

Domestic and international data for operating leakage within Westinghouse plants was reviewed for identification of leakers attributable to ODSCC at TSPs. No occurrences of identifiable leakage due to ODSCC at TSPs were found in domestic units. Three occurrences were identified in European units. The latter data (See 6.3 below) together with field inspection data are used to assess the potential for operating leakage at plugging limits that meet tube burst and SLB leakage requirements.

C. Field Inspection Data for Tubes With No Identified Leakage

It is shown in Section 9 that tubes with voltage levels up to about 6 - 7 volts meet the requirements for burst pressure margins under free span burst conditions. Therefore field inspection data for indications above and below this voltage level, and with no identified operating leakage, can be used to assess the potential for significant operating leakage.

The field data base for items A, B and C are described in the following sections.

6.2 Pulled Tube Data Base

The available pulled tube data base for ODSCC at TSPs in Westinghouse S/Gs includes 23 pulled tubes for which 45 tube to TSP intersections have both NDE and destructive examination results. This group includes four tubes from Plant A-2 and one tube from Plant A-1 with one intersection destructively examined for each pulled tube. None of the 23 pulled tubes have been reported as leakers during plant operation. The crack morphologies were reviewed for 14 tubes with TSP intersections having no leakage or burst test measurements. This review indicates that no leakage would be expected for these tubes even under SLB conditions and that the burst pressures would exceed 3 times normal operating conditions. The field eddy current data for all pulled tubes were reviewed for voltage normalization consistent with the standard adopted (see Sections 5.6, 8) for the plugging criteria development. Indications for 3/4 inch diameter tubing were normalized to 4.0 volts in the 550 kHz channel and evaluated for the 550/100 kHz mix.

Table 6.2 provides the leak rate and burst pressure data for the 10 pulled tubes (15 intersections) for which these tests were performed. The leak rate and burst tests were conservatively performed as free span (without collars) tests. Also shown in the table are the estimated leak rates and burst pressure based upon the actual crack morphology for the Plant A-2 tube with the 7.2 volt indication. The 1990 Plant A-2 tube leakage tests showed [ ]9 of leakage at normal operating conditions but these low values cannot be clearly separated from test system leakage. The measured SLB leak rates are [ ]9. The pulled tubes in Table 6.2, with up to 10 volt indications, all show burst pressures for the test conditions (room temperature, as-built material properties) in excess of 4590 psi, 3 times the normal operating pressure differential (adjusted for temperature, the 3 times normal operating pressure differential equivalent is 5500 psi).

The pulled tube NDE data are shown in Figure 6-1 as bobbin coil voltage versus indicated depth. All pulled tube results at normal operating pressure differential represent no leakage conditions while two small leakers at SLB conditions were found from Plant A-2. Figure 6-2 shows the same data plotted as voltage versus actual depth from destructive examination.

Correlations of the bobbin coil phase angle based depth estimates with the maximum depths from destructive examinations have shown an uncertainty of 15% for the depth indications. The pulled tubes have typically shown one dominant axial crack network with multiple, small cracks around the tube circumference. With multiple, large axial crack networks around the tube circumference, the bobbin coil depth uncertainty can be larger than 15%.

Figure 6-2 shows that below 2.8 volts the maximum depths are dominantly less than 80%. An occasional, very short, 100% through wall indication, such as the 1.9 volt indication, could potentially occur at these low voltage levels although the pulled tube examination results indicate that the associated crack length can be expected to be too short for any measurable leakage at normal operating or SLB conditions. The smallest voltage found for a through wall crack in the current pulled tube data base is 1.9 volts for a 3/4 inch diameter tube as noted in Table 6.2. Figure 6-3 shows the field bobbin and RPC data for this indication.

Between 3 and 10 volts, the limited pulled tube data indicate the potential for through wall cracks with negligible leakage at normal operating conditions and very small leaks at SLB conditions.

6.3 Operating Plant Leakage Data for ODSCC at TSPs

Table 6.3 summarizes the available information on three suspected tube leaks attributable to ODSCC at TSPs in operating S/Gs. These leakers occurred in European plants with two of the suspected leakers occurring at one plant in the same operating cycle. In the latter case, five tubes including the two with indications at TSPs were suspected of contributing to the operating leakage. Leakage for the two indications at TSPs was obtained by a fluoresceine leak test as no dripping was detected at 500 psi secondary side pressure.

For the Plant B-1 leakage indication, other tubes also contributed to the approximately 63 gpd total leak rate. Helium leak tests identified other tubes leaking due to PWSCC indications. Using relative helium leak rates as a guide, it was judged that the leak rate for the ODSCC indication was less than 10 gpd. These leakage events indicate that limited leakage can occur for indications above about 7.7 volts. No leakage at Kewaunee has been found that could be attributable to ODSCC at TSPs.

6.4 Plant Inspection Data for Tubes with No Identified Leakage

Additional guidance on the voltage levels at which significant operating leakage might be expected can be obtained from plant inspection results for tubes with large indications but no identified tube leakage. Inspection results from 8 units were reviewed to identify indications above about 1 volt with no suspected leakage. Data from this review are shown in Figure 6-4. These data show a large number of indications below 6 volts and a few larger indications that can be associated with no leakage conditions. This is consistent with the pulled tube results of Figure

6-1. The overall Plant A data support no operating leakage below about 10 volts even though the Plant A pulled tubes indicate short, through wall crack penetrations.

6.5 RPC Data Considerations

Examples of RPC indications for the Kewaunee S/Gs are given in Section 5. As per the proposed plugging criteria, RPC inspections are required for bobbin coil indications above 1.5 volts (See Section 12) to support the continued presence of ODSCC as the dominant degradation mechanism. In addition, the data obtained would support further development of SLB leakage models which may utilize leakage correlated with RPC parameters. The RPC inspection results can be optionally applied to verify the presence of the bobbin coil indication.

6.6 Voltage Renormalization for Alternate Calibrations

To increase the supporting data base, it is desirable to be able to renormalize available data to the calibration values used in this report. When 400/100 kHz mix or 400 kHz data normalized to an ASME standard are available, the renormalization is a straight forward ratio of the calibration voltage values. However, when different frequencies are used, the normalization ratio is phase angle or depth dependent and this normalization has been evaluated as described below.

For data on 3/4 inch diameter tubing, voltage renormalization has been obtained by applying a normalization of 4.0 volts for the ASME 20% holes in the 550 kHz channel and evaluated using 550/100 kHz mix. Westinghouse, under EPRI sponsorship, is further evaluating alternate voltage normalizations for 3/4 inch tubing to compare with the normalization adopted in this report for 7/8 inch tubing. Comparisons of responses to drilled holes and EDM slots as well as burst correlations will be applied to adopt a 3/4 inch tubing voltage normalization for use in alternate plugging criteria. Until this study is complete, data from 3/4 inch tubing tests are not used in the voltage/burst correlation (data from 7/8 inch tubing used) applied for Kewaunee.

The voltage normalizations applicable to the calibrations used in this report are:

ASME 4-hole, 100% deep, 0.033 ± 0.001 inch dia. = 6.4 volts at 400/100 kHz
ASME 4-hole, 20% deep, 0.187 ± 0.003 inch dia. = 2.75 volts at 400/100 kHz
ASME 4-hole, 20% deep, 0.187 ± 0.003 inch dia. = 4.00 volts at 400 kHz

The through wall hole with tighter than ASME hole tolerances has been selected as the primary voltage normalization for application of the voltage plugging limits. The through wall holes result in lower influence of manufacturing tolerances on the voltage calibration than partial depth holes. Calibration at the 400/100 kHz mix used for data evaluation is recommended to minimize potential uncertainties from normalization at other than the evaluation frequency. The above calibrations can be applied to normalize most of the domestic inspection results for 7/8 inch tubing.

In France and Belgium, a 240 kHz differential inspection is most commonly applied. Voltage renormalization was evaluated by fabricating the French and Belgian standards and comparing their procedure with that of this report. Results of this study are given in Table 6.4. The U.S. to French voltage ratio was further evaluated using an Intercontrole probe commonly used by EdF

(Electricite de France) and applying this probe as well as a domestic probe to the calibration standard and to several model boiler specimens with ODSCC. The results of this evaluation are given in Figure 6 5. These results show a consistent ratio (within ~10%) for both probes and between calibration standards and ODSCC. In Figure 6-5, phase angles of 30^{o} and 100^{o} correspond to 100% and 20% ASME hole depths, respectively.

Given Table 6.4 and Figure 6-5, most bobbin coil voltage measurements can be renormalized to the calibration applied in this report.

6.7 Comparisons With European Plant Inspection Results

The pulled tube data described in Section 6.2 and the field inspection results of Section 6.4 were obtained from domestic and European plants that apply essentially the same voltage calibration standards and comparable frequency mixes for indications at TSPs. The operating experience data base can be increased substantially by including plant data from French and Belgian plants. However, these plants utilize different voltage calibrations and frequencies for TSP indications. To compare the domestic plant data with these European data, the voltage ratios of Figure 6-5 (as a function of phase angle) have been applied. However, any conversion factor involves some uncertainties as indicated in Figure 6-5 because it depends on the varying crack responses to different frequencies as well as procedural/environmental conditions. Recognizing uncertainties in the voltage conversion factors, comparisons with the European data are particularly valuable for the following comparisons:

- Trends in indications and growth with time for equivalent voltages higher than available in domestic plants which have applied 40% depth criteria for tube plugging. None of the European data at higher equivalent voltages have had identifiable operating leakage so these data substantially increase the high voltage data base supporting negligible leakage for ODSCC at TSPs.

- Percentage growth in voltage from European plants can be used to assess growth rate trends for equivalent voltages much higher than that available in domestic plants.

For these comparisons between domestic and European experience, the domestic data for Plant A-2 and Kewaunee are compared with French and Belgian data.

Distribution of Indications

Data for ODSCC at TSPs for French Unit H-1, S/G-1 are available for four successive inspections with no tube plugging, as shown in Figure 6-6. The upper figure shows the number of indications versus voltage amplitude while the lower figure shows the percentage distribution of indications within each outage. Without tube plugging to eliminate the larger indications, the distribution becomes more heavily weighted at the larger indications with increasing operating time.

European data is currently available for French Units H-1 and J-1 and Belgian Unit K-1. It is useful to compare the percentage voltage distributions for these units with the Kewaunee data and data from two other domestic units, Plant A-1 and A-2. This is shown in Figure 6-7. The lower figure is scaled to include all available data while the reduced scale of the upper figure is included to emphasize the small voltage range of the U.S. data compared to the European data.

Plant J-1 was excluded from the upper figure since breakdown of the data into small ranges was not available. It may be noted that over 97% of the domestic data falls below 0.5 volts when normalized to the French procedure and none of this domestic plant data falls above 1 volt. The French and Belgian data, on the other hand, extends above 3 volts.

Overall, it is seen that the U.S. plants with 40% or 50% depth plugging limits are operating with voltage amplitudes notably lower than that in European units.

The European units of Figure 6-7 with higher equivalent bobbin voltage signals have operated with no identifiable leakage. This result indicates that operating leakage due to ODSCC at TSPs is expected to be insignificant. This is supported by the fact that only 3 cases of small operating leakage, as shown in Table 6.3, have been identified to date.

French Pulled Tube Data

Fourteen tubes have been removed from French units with destructive examination results currently available. Figure 6-8 shows the crack morphology for a tube with a 0.7 volt (~3.7 U.S. volts) indication. The tube exams indicate many axial cracks of comparable depth around the tube circumference. The cracks are dominantly ODSCC with somewhat more IGA participation than seen in most domestic pulled tube data such as the Plant A data. The multiple crack networks would be expected to increase bobbin coil voltage compared to one or only a few deep cracks as typical of the domestic data. Figure 6-9 shows the French data added to Figure 6-2. This figure shows the trend toward higher voltages from the French data for a given maximum depth. Similarly, the data points for Plants L, M and N, which show increased IGA with multiple cracks, also show a tendency toward the higher voltage range of the data. The data for Plant N, as described in Section 4, are from a non-Westinghouse unit with egg crate supports and were reported as IGA. Overall, the data for IGA and IGA/SCC indications show comparable or higher voltage levels than obtained for SCC with minor IGA.

6.8 Growth Rate Trends

Of particular interest to establishing the plugging limits of this report is voltage growth rate as a function of the voltage amplitude. Current domestic plugging limits result in little data on growth rates in the range of voltage amplitudes being evaluated for the plugging limits of this report. The larger voltage amplitudes of the European data provide guidance on growth rate progression. Figure 6-10 shows growth rate data for Plant H-1 both as voltage amplitude and percentage growth as a function of voltage amplitude. The data of Figure 6-10 tend to indicate percentage growth rates are not a strong function of absolute voltage amplitude. As generally expected, the spread in the data at low amplitudes is greater than for larger voltages due to the greater influence of voltage uncertainties and measurement repeatability at low amplitudes.

Figures 6-11 and 6-12 compare the percentage growth rates per cycle between domestic units Plant A-1, Plant A-2 and Kewaunee with that for Plant H-1. Figure 6-11 shows the individual data points; the lower figure is a magnification of the lower left hand corner of the upper figure. Figure 6-12 compares average growth rates and standard deviations. The averages are displayed for different ranges of the initial amplitude. The first range is 0 to 0.75 volts, the second range is 0.75 to 2.5 volts and the third is for initial amplitudes greater than 2.5 volts. In the case of the U.S. plants there is very little data above 2.5 volt amplitude; hence such data is included in the second range. The French data (Plant H-1) indicate percent growth rate nearly independent

of initial amplitude whereas the domestic units display percent growth rates decreasing with increase in initial amplitude.

The domestic plants dominate the growth rate data of Figures 6-11 and 6-12 for low amplitudes with the French data extending to larger amplitudes. The results indicate that percentage growth rates are roughly comparable between domestic and European plants. In the calculation of average growth rates, the negative growth rates (see Figure 6-11) were conservatively treated as zero growth rates. Ignoring the negative growth rates biases the average growth by including all positive but not all negative random fluctuations. Part of the apparently larger number of negative voltage growth rates for the domestic data may result from variations in calibration standards for the 20% depth normalization which may be more sensitive to fabrication tolerances than the 100% depth normalization standards employed for the European data.

6.9 Field Data Conclusions

The following conclusions can be drawn from the field data described above:

1. Burst tests performed on pulled tubes, which to date include signal levels up to 10 volts, show burst pressures exceeding 3 times normal operating pressure differential, adjusted for operating temperature effect on material properties.

2. The pulled tube, leak rate test results indicate the potential for low [

   ]9.

3. Pulled tube examination results indicate that through wall cracks can potentially occur below 10 volts but that the associated crack lengths are short with no measurable leakage at operating conditions.

4. The smallest bobbin voltage identified for a through wall crack is 1.9 volts (in a 0.75 inch OD tube).

5. Leakage at operating conditions has not been identified for bobbin coil voltage below [ ]9 volts with only 1 indication of leakage below 13 volts.

6. Negligible leakage is expected from ODSCC at TSPs based on domestic experience as well as European experience with voltage amplitudes higher than the domestic operating experience.

7. Percent growth in voltage amplitude tends to be approximately independent of voltage amplitude for the available French data while decreasing with amplitude for the domestic plants, including Kewaunee. Assuming growth in voltage is independent of amplitude appears to be very conservative for the Kewaunee S/Gs.

To supplement the above field data to define tube plugging limits, laboratory tests were performed with the following areas of emphasis:

- Improved definition of tube burst capability as a function of bobbin coil voltage to better define voltage levels that meet Reg. Guide 1.121 guidelines for burst pressures of 3 times normal operating pressure differentials.

- Improved resolution of leak rate potential for normal operating and SLB conditions above about 2 volt signal amplitudes.

- Determining NDE uncertainties associated with application of voltage plugging limits.

Table 6.1

Field and Laboratory Data Utilized forTube Plugging Criteria Development

Tube Burst Capability: Burst Pressure vs Voltage Correlation
- o Pulled Tube Data
- o Model Boiler Specimens

SLB Leakage Model
- o Pulled Tube Data
- o Model Boiler Specimens
- o Plant Inspection Results
  - ODSCC Indication Distributions
  - Growth Rates

Operating Leakage Assessment
- o Pulled Tube Data
- o Operating S/G Leakage Occurrences
- o Field Inspection Data for Tubes Without Identified Leakage
  - Larger (>1 volt) Indications
- o Model Boiler Specimens

NDE Evaluation: Specimen Characterization, Inspection Sensitivity/Uncertainties
- o Model Boiler Specimens
- o Pulled Tube Data

Influence of Tube Denting on Leakage
- o Fatigue Specimens
- o Doped Steam Specimens

Effects of SLB Loads on TSP Displacement
- o Pull Tests on Laboratory Dented Specimens
- o Thermal-Hydraulic and Structural Analyses

Table 6.2

Pulled Tube Leak Rate and Burst Pressure Measurements

Plant	Row/Col.	TSP	Bobbin Coil Volts	Bobbin Coil Depth	Destructive Exam Max. Depth	Destructive Exam Length (in.)(1)	Leak Rate (l/hr) Normal Oper.	Leak Rate (l/hr) SLB	Burst Pressure (psi)
[redacted]									

Notes:

1. Crack network length for burst crack with through wall crack length given in parentheses.
2. Negligible leak rate evaluated as no leakage for this report.
3. Measurements were not made and values are estimated based upon crack morphology obtained from destructive examination.
4. Leakage not detected as pressure increased to indicated burst pressure.
5. Field measurement using 550/100 kHz mix for 0.75 inch diameter tubing.

Table 6.3

Field Experience: Suspected Tube Leakage for ODSCC AT TSPs(1)

Plant	Inspection	Bobbin Coil Volts	Bobbin Coil Depth	Comments
[redacted]				

Notes:

1 Field experience noted is for nominal 0.750" OD tubing with 0.043" wall thickness. No data are known to be available for tubes with 0.875" OD.

2 Reported voltages were adjusted (values given in parentheses) to the normalization in this report of 2.75 volts for 20% ASME flaw and 400/100 kHz mix. The adjustment factor was developed based on voltage ratios measured between a metric calibration standard as used to obtain the original data and the reference ASME standard of this report. This adjustment provides an order of magnitude conversion to make these data roughly comparable to other data in this report. However, any conversion factor is disputable because it depends on the procedural/environmental conditions and thus may vary from case to case.

Table 6.4

Comparisons of Voltage Amplitudes Between U.S.-ASME and European Standards

	U. S. - ASME Standard						French 4-hole. 1 mm dia. holes	Belgian 4-hole. 1.25 mm dia. holes	U.S. 4-hole 33 mil dia. holes
Channel	20%	40%	60%	80%	100%	Support Plate	100%	100%	100%
U.S. Calibration Procedure ❑									
400/100 mix	2.75	2.8	5.2	5.6	8.7	<0.6	10.7	18.96	6.4
400 kHz	4.0	3.5	5.5	5.5	7.8	8.2	9.8	17.19	5.4
240 kHz	6.3	5.4	7.9	7.3	9.5	17.4	12.4*	21.15**	7.6
200 kHz	5.9	4.9	7.1	6.3	8.0	17.5	10.9	18.08	-
100 kHz	5.9	2.8	3.6	3.1	3.8	14.5	5.4	8.5	5.2
French Calibration Procedure									
240 kHz	0.66	0.56	0.82	0.76	0.99	1.8	1.3*		
Belgian Calibration Procedure									
240 kHz	0.59	0.51	0.74	0.68	0.90	1.64		2.0**	

❑ U.S. procedure involves setting up the signal for 20% ASME holes at 4 volts for 400 kHz differential channel or 2.75 volts for 400/100 kHz differential mix and then using the "Save/Store" functions of the Zetec DDA-4 software for carrying over the calibration to all other channels.

* When using the U.S. calibration procedures, the French 4-hole standard gives 12.4 volts at 240 kHz and 10.7 volts with the 400/100 kHz mix. It is 1.3 volts for the French calibration. Thus U.S. values at 240 kHz/French values at 240 kHz equals ~9.5. U.S. values at 400/100 mix/French values at 240 kHz equals ~8.2.

** When using the U.S. calibration procedures, the Belgian 4-hole standard gives 21.15 volts at 240 kHz and 18.96 volts with the 400/100 kHz mix. It is 2.0 volts for the Belgian calibration. Thus U.S values at 240 kHz/Belgian values at 240 kHz equals ~10.6. U.S. values at 400/100 kHz mix/Belgian values at 240 kHz equals ~9.5. For general data comparisons, Belgian and French data can be reasonably compared without adjustments or by multiplying the Belgian data by ~0.9 to obtain French volts.

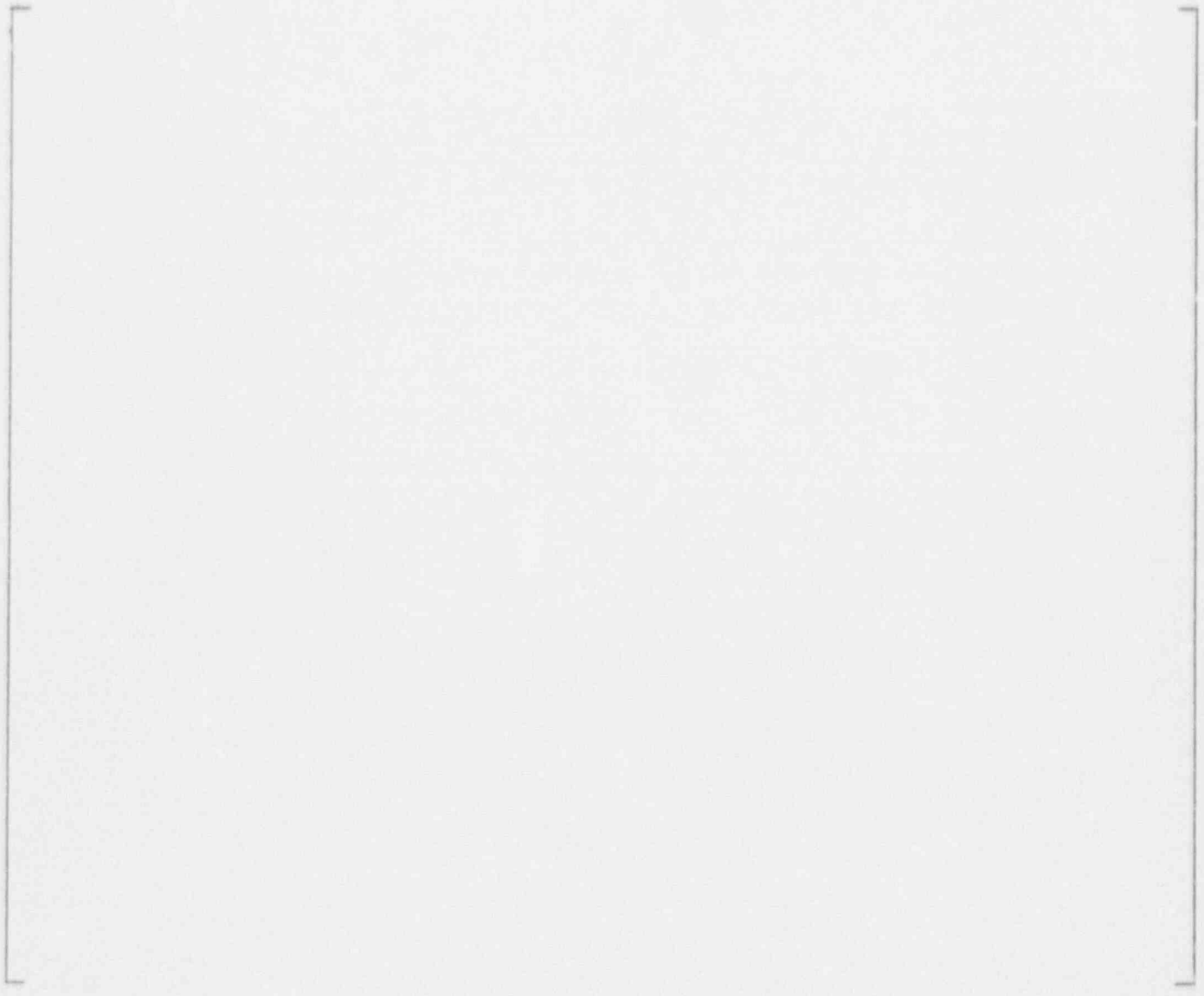

Figure 6-1. Pulled Tube Data: Bobbin Coil Voltage and Indicated Dep'h

Figure 6-2. Pulled Tube Data: Bobbin Coil Voltage and Depth from Destructive Exam

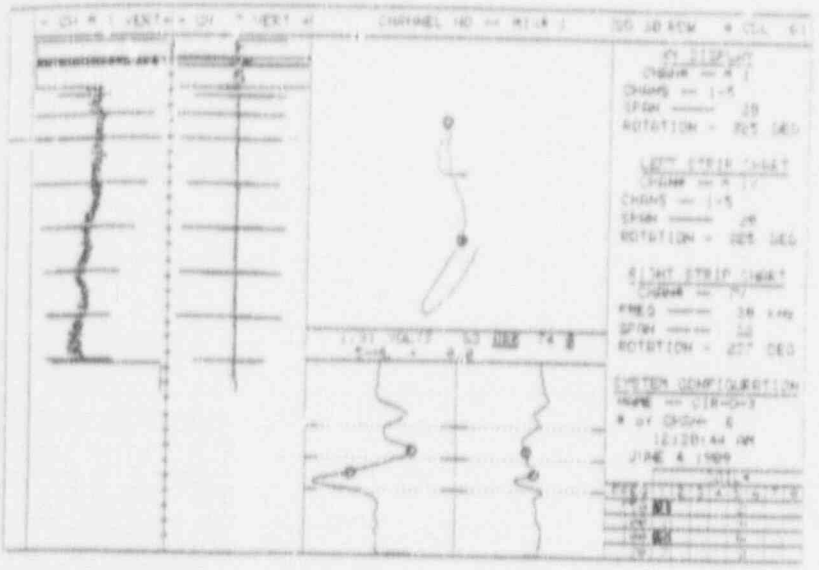

Field bobbin probe data for Plant B-1, tube R4-C61 at TSP 5, using 550/100 kHz differential mode mix. A 1.91 volt indication with 74% depth is observed.

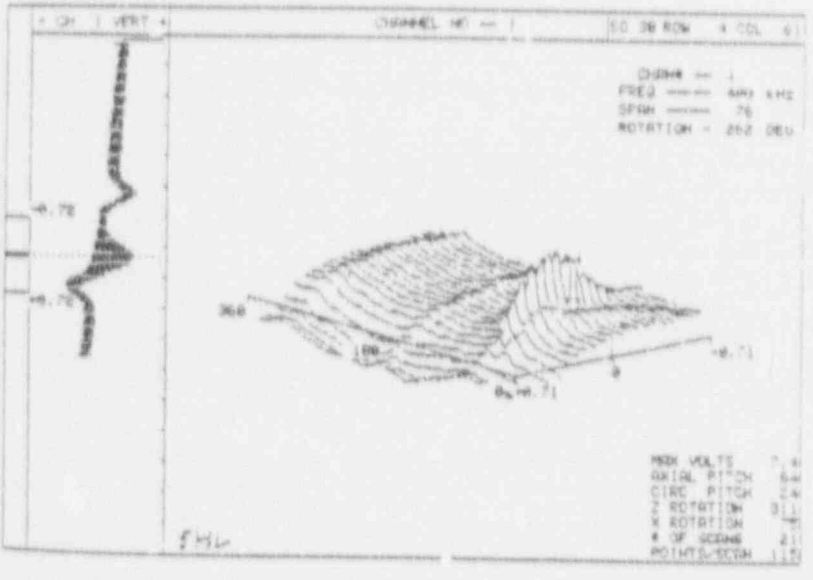

Field RPC data for Plant B-1, tube R4-C61 at TSP 5. A 0.4 inch long axial indication is observed.

Figure 6-3. Field Bobbin Coil and RPC Traces for 3/4 inch Tube

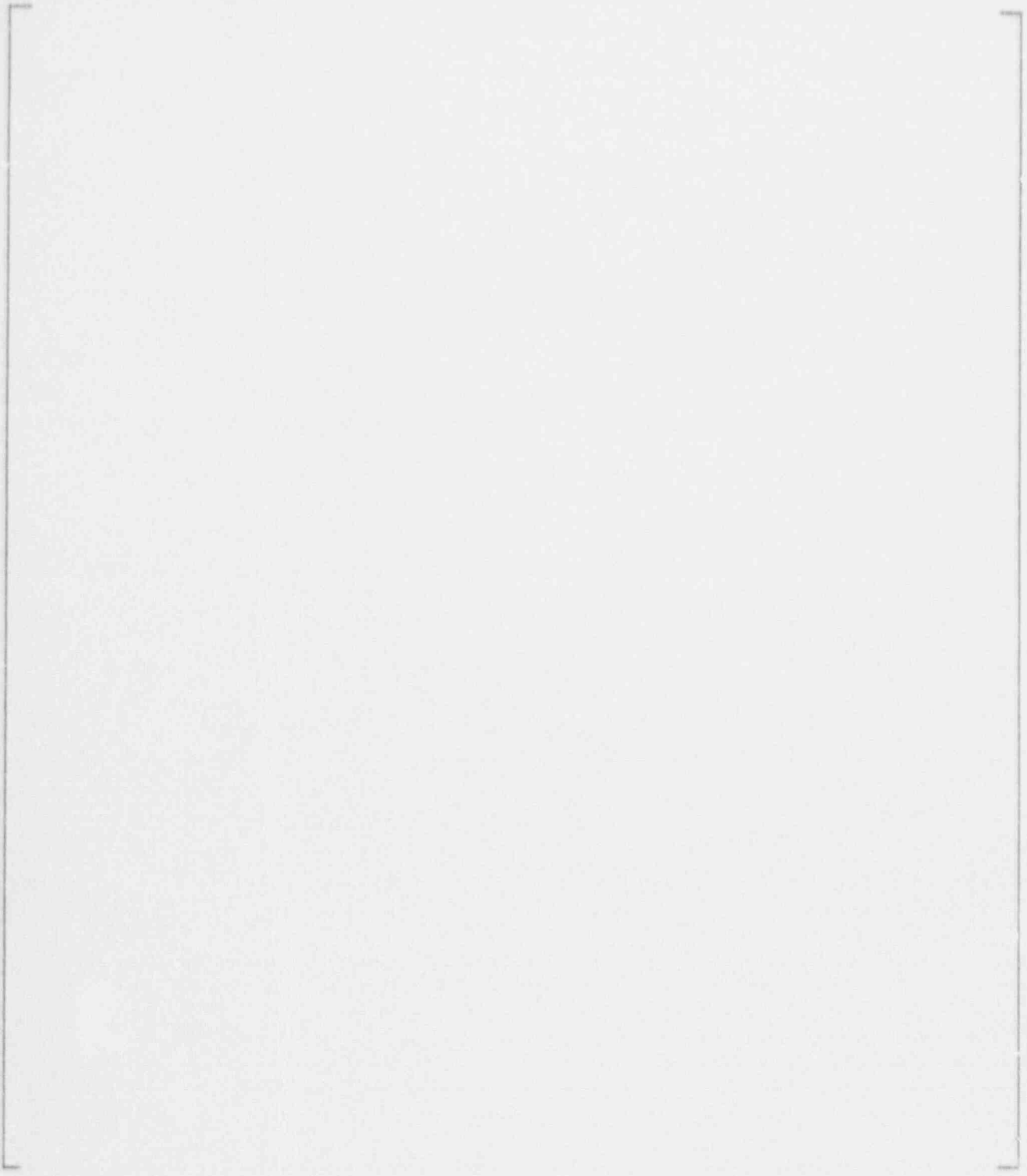

Figure 6-4. Field Inspection Data for Tubes Without Operating Leakage

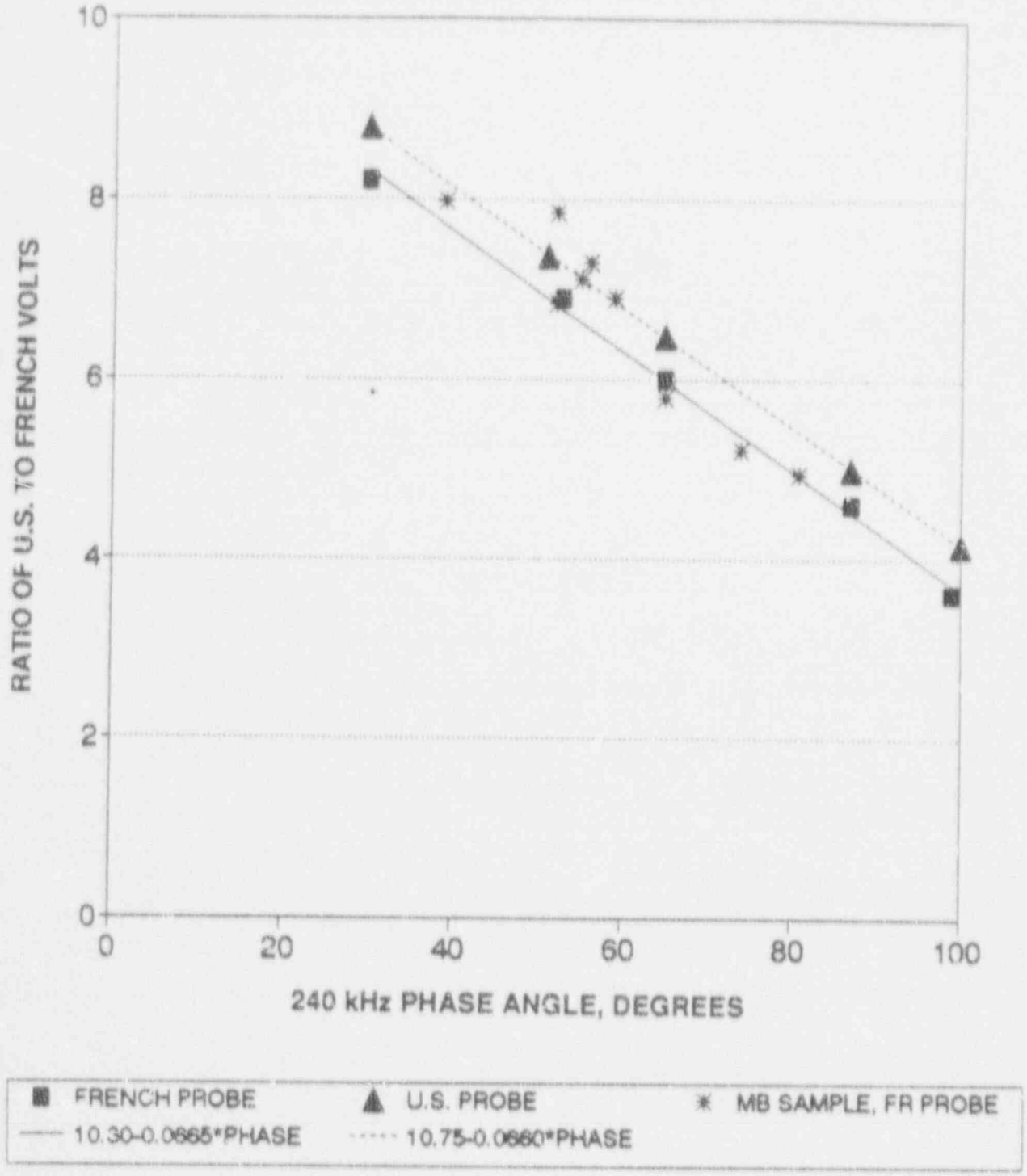

Figure 6-5. Comparison Between U.S. and French Voltage Normalization

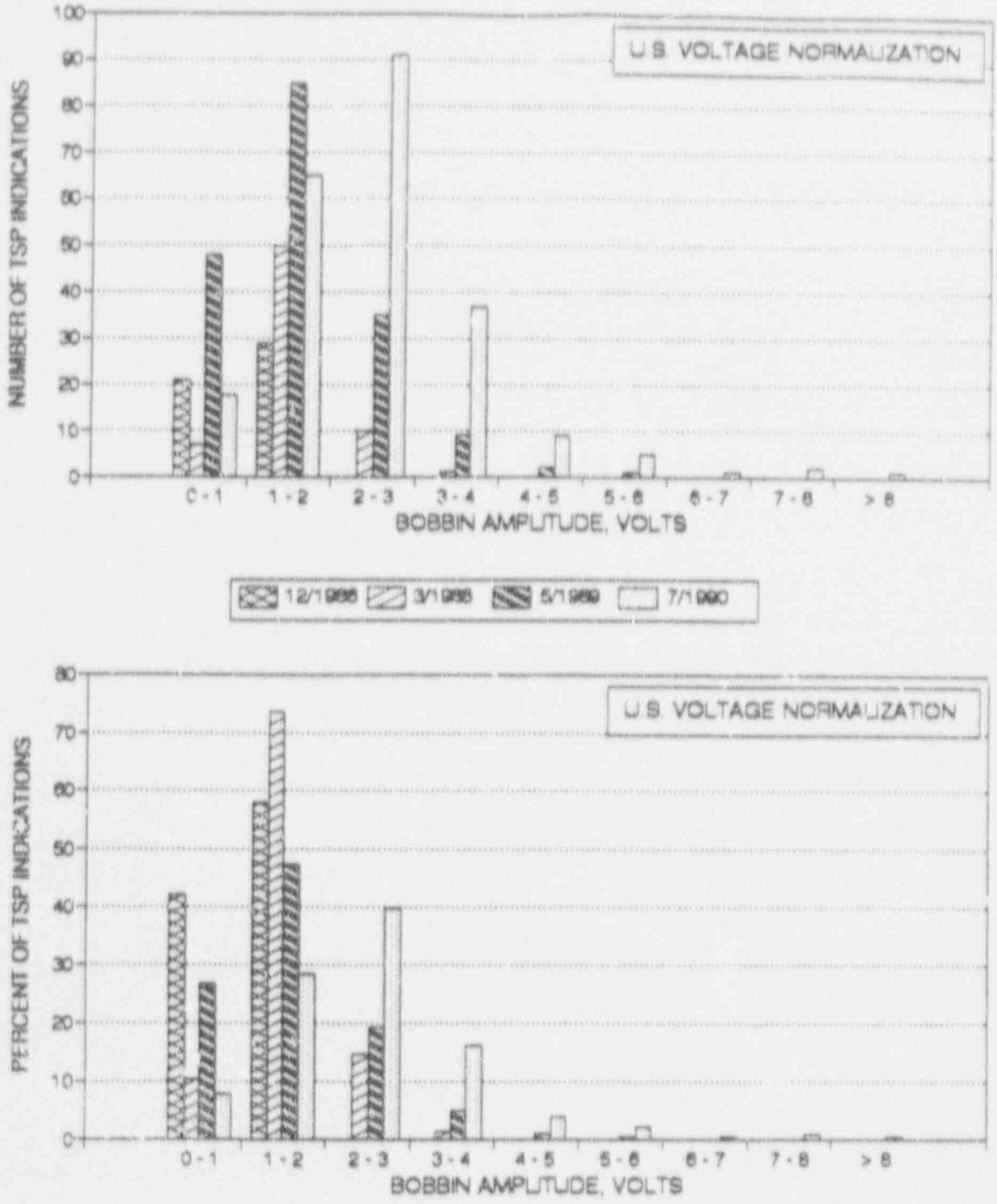

Figure 6-6. Distribution of TSP Indications for Plant H-1 (1986 to 1990)

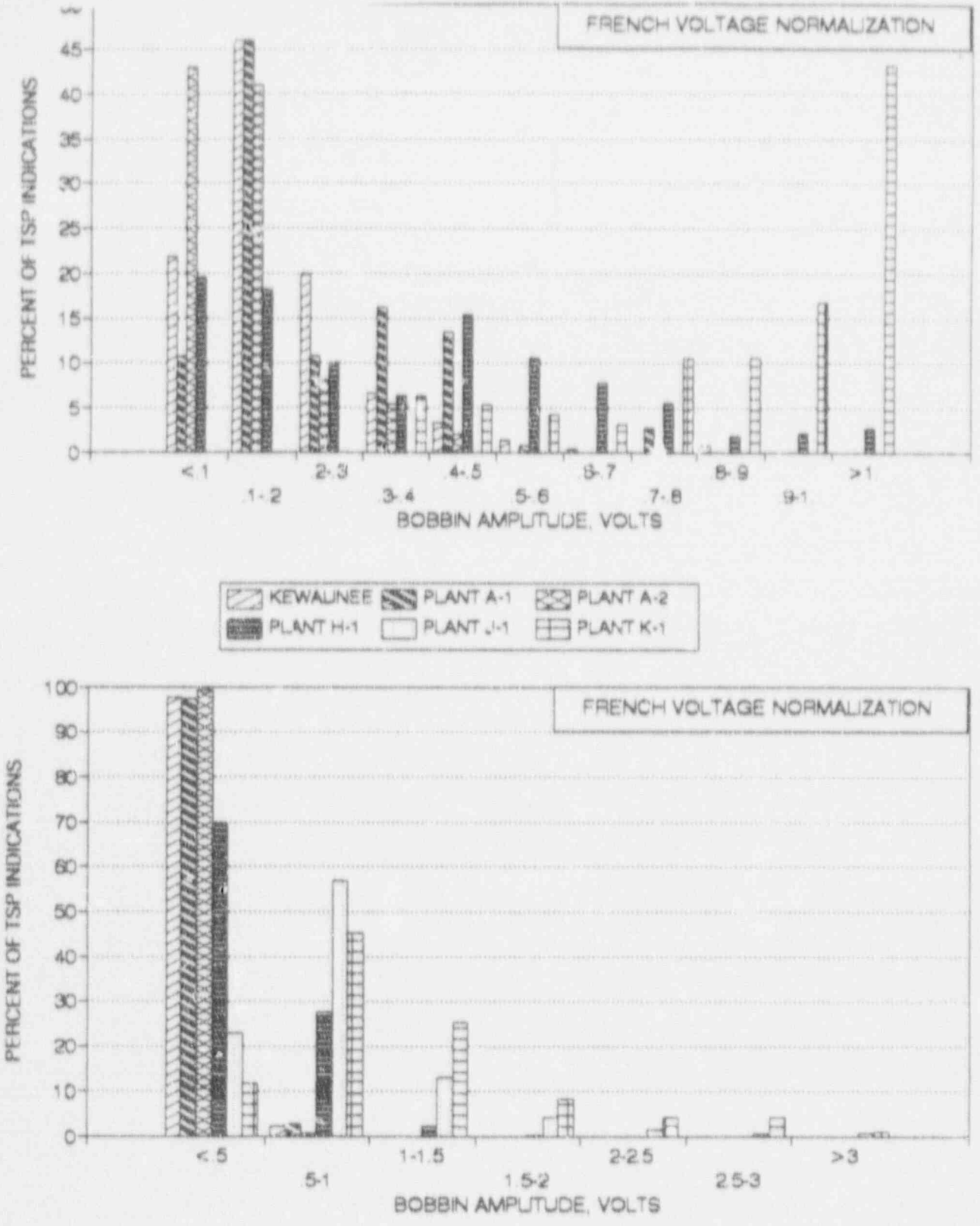

Figure 6-7. Comparison of Voltage Indications at TSPs Between U.S. and European Plants

Coupe transversale 2 (cf. annexe 8)
Aspect de la fissuration sur différents plans de polissage

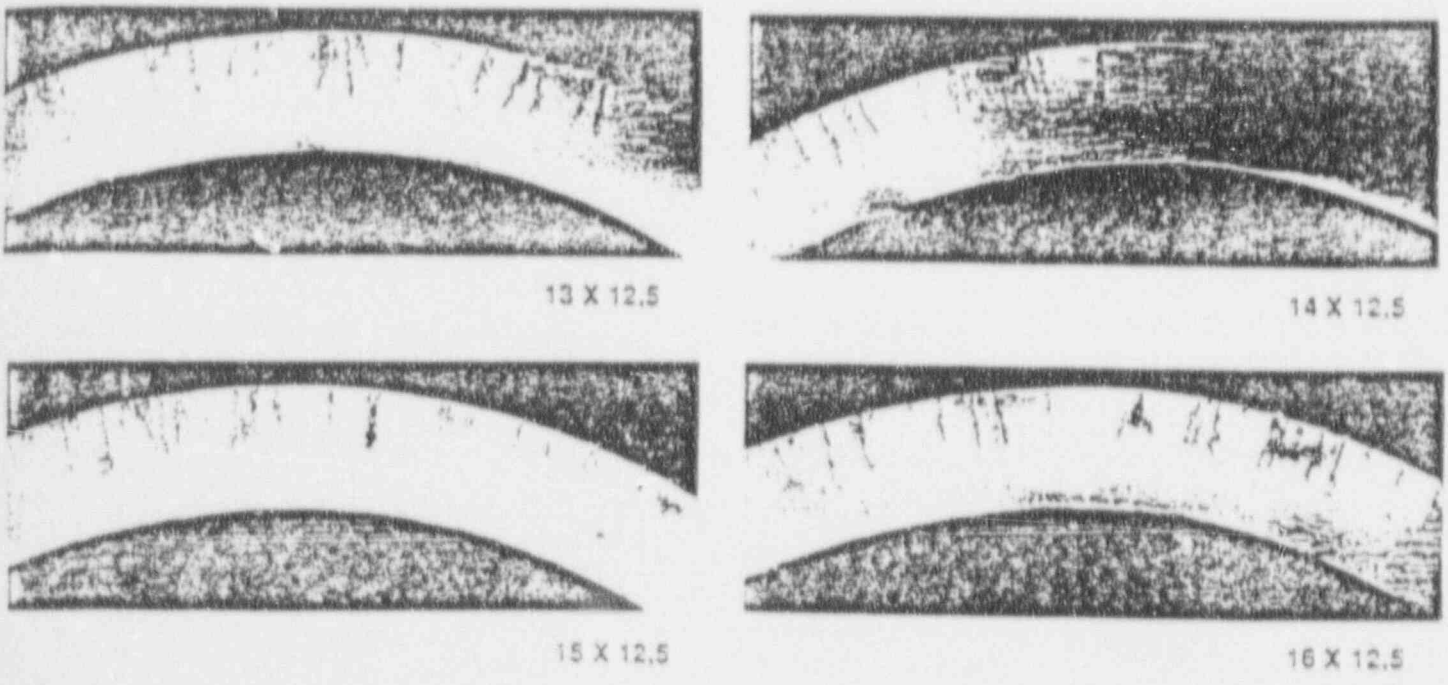

Figure 6-8. Crack Morphology for Pulled Tube from French S/G

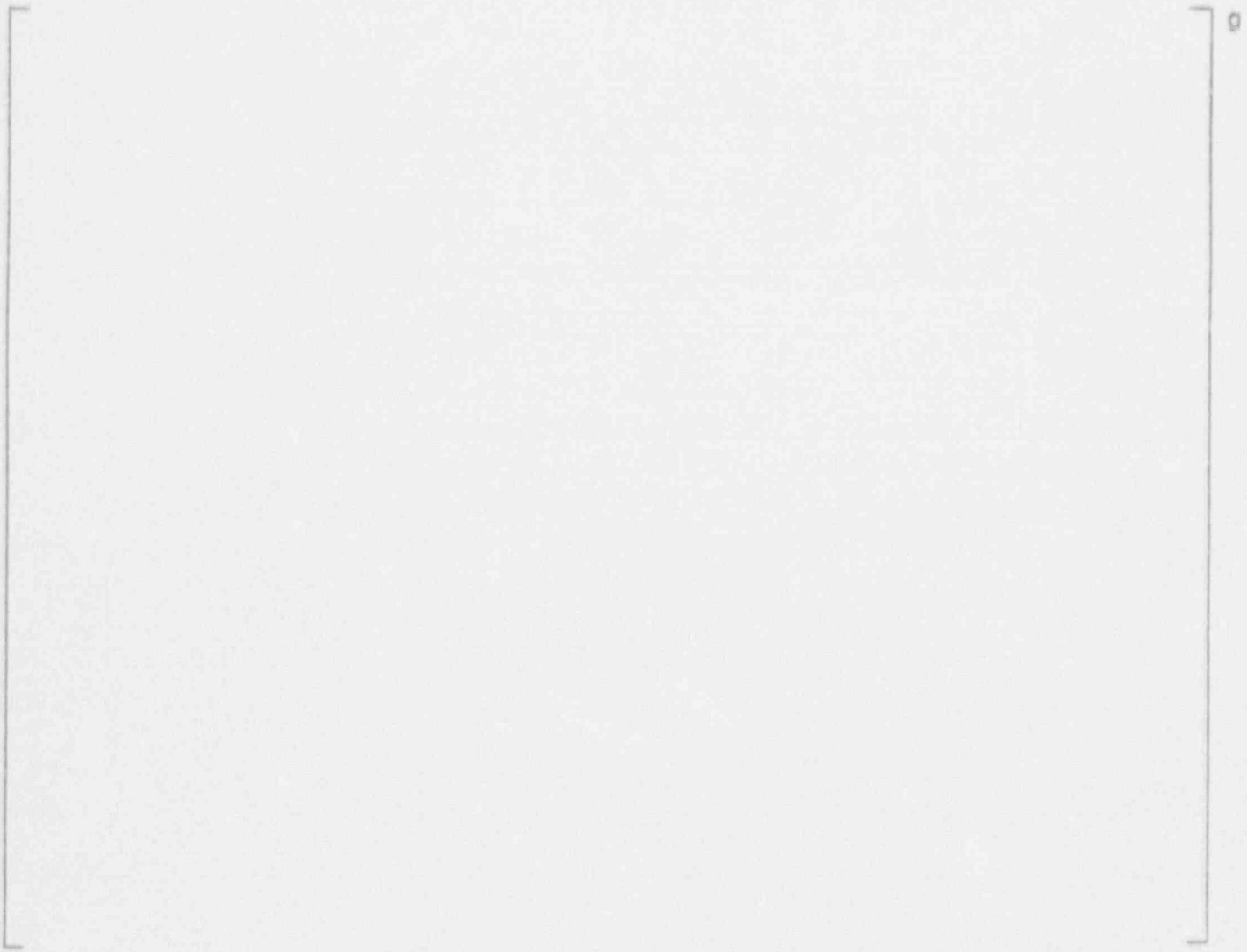

Figure 6-9. Pulled Tube Destructive Exam Data Including French Data

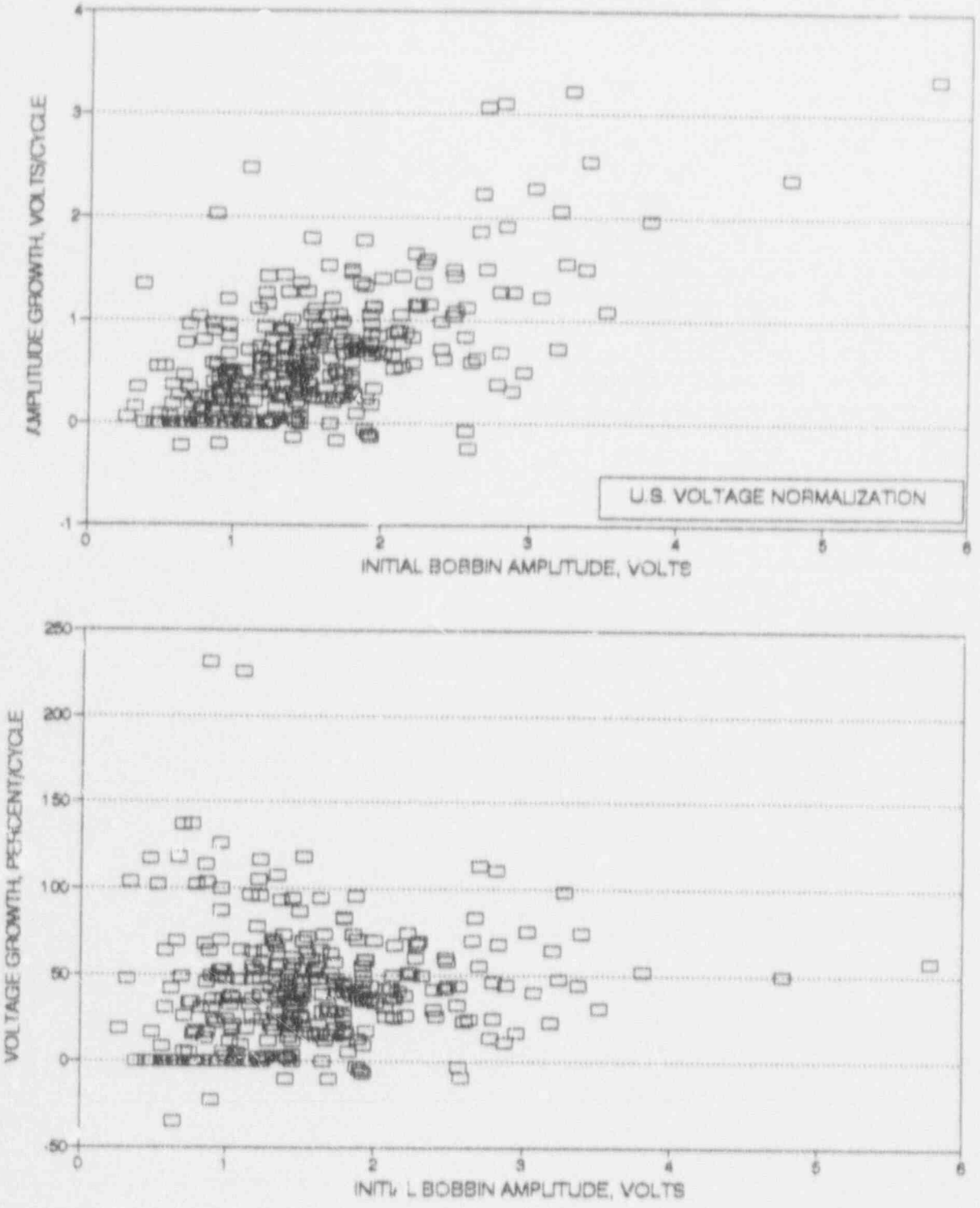

Figure 6-10. TSP Indication Voltage Growth Rates for Plant H-1

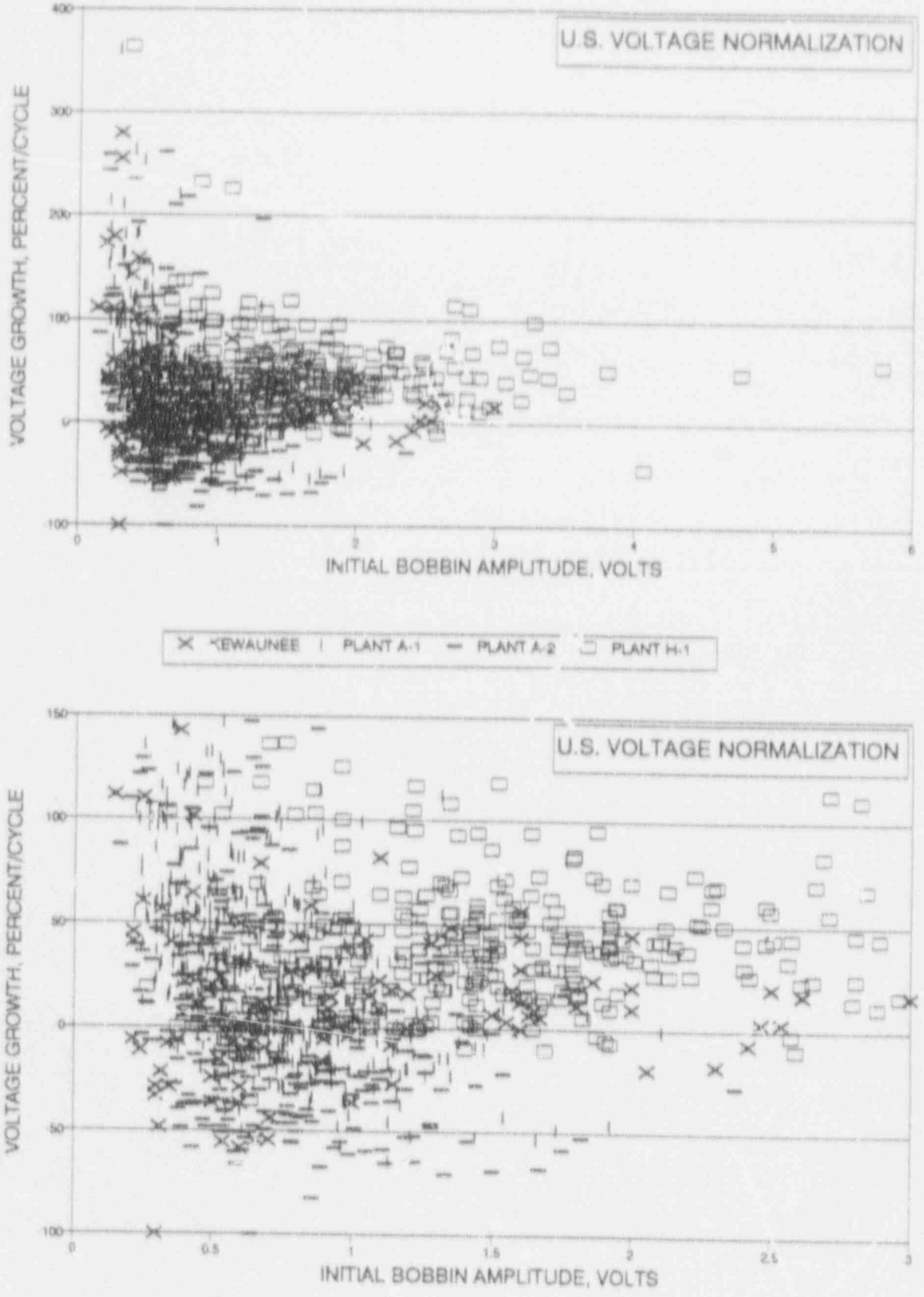

Figure 6-11. Growth Rate Data for Kewaunee, Plant A and Plant H-1

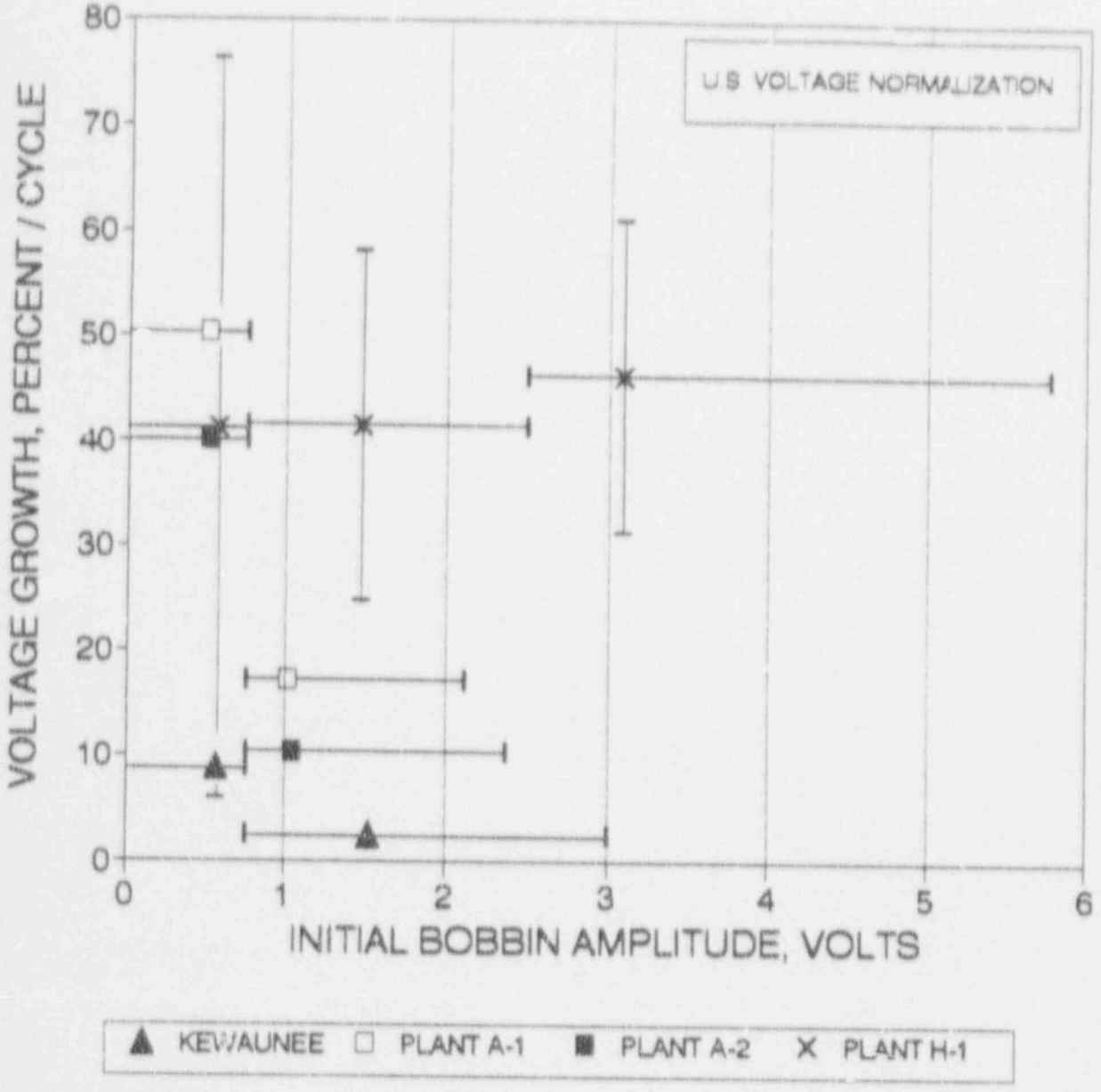

Figure 6-12. Average Percent Voltage Growth Rates for Kewaunee, Plant A and Plant H-1

7.0 LABORATORY SPECIMEN PREPARATION

7.1 Model Boiler Specimens

The Forest Hills Single Tube Model Boiler test facility consists of thirteen pressure vessels in which a forced flow primary system transfers heat to a natural circulation secondary system. Test specimens are placed around the heat transfer tube to simulate steam generator tube support plates. One to six tube support plate crevice assemblies are typically included in a given test. A schematic of the test facility is presented in Figure 7-1, and typical thermal and hydraulic specifications are presented in Table 7.1. As indicated in the table, these specifications are representative of those in a pressurized water reactor steam generator.

Four series of Single Tube Model Boiler tests have been performed to provide test pieces having through wall cracks for subsequent nondestructive examination, leak rate measurements, and destructive examination. The first series consisted of 15 archive crevice assemblies which were produced in previous Westinghouse-funded testing; the second and third series each consisted of eight crevice assemblies, while the fourth series consisted of 45 crevice assemblies. The crevices in the third and fourth series were specified so as to produce crack networks having lower bobbin probe voltages.

Series 1 Tests: A summary of the archive test pieces is presented in Table 7.2. The test pieces are listed by their tube designation and their location on the tube. The sludge type refers to the manner in which sludge was placed in the tube support plate crevices. Chemically consolidated sludge is formed by baking a mixture of sodium hydroxide, sodium silicate and sodium phosphate with the sludge; mechanically consolidated sludge is formed by hydraulically pressing the sludge into the tube support plate, drilling a hole in the sludge, and sliding the tube through the hole; the fritted design uses an Inconel sinter at each end of the crevice to hold the sludge in place. The test containing an eccentrically mounted tube support plate in which the sludge was removed from the crevice was used to simulate chemical cleaning. All tests utilized simulated plant sludge, consisting of approximately 60% magnetite, 32% copper, 5% copper oxide, 2% nickel oxide, and 1% chromium oxide.

The cracks were produced in what is termed the reference cracking chemistry, consisting of either a 600 ppb (1X) or a 6 ppm (10X) sodium carbonate solution in the makeup tank. Because of hideout in the crevices, the boiler concentration is typically about 75% of the makeup tank concentration. Hydrazine and ammonia are also added to the makeup tank for oxygen and pH control, respectively.

The tubing used for the tests was taken from Heat 2675. This heat of mill annealed Alloy 600 was fabricated by Westinghouse and has been used extensively in other stress corrosion cracking programs. The tubing has a 0.875 inch outside diameter.

Series 2 Tests: The initial program test pieces consisted of eight crevice simulants which were mounted on two tubes. These tests were specified to produce rapid through wall cracking, so that the 10X reference cracking chemistry was utilized. Heat 2675 was also used for these tests. One test utilized chemically consolidated simulated plant sludge (tube 543), while the other used mechanically consolidated sludge (tube 542). The sludge filled the entire crevice volume. Primary to secondary leakage was noted in the chemically consolidated test after 10 days of boiler operation, and in the mechanically consolidated test after 24 days of operation. During the

subsequent nondestructive examination (NDE), indications were identified adjacent to the teflon collars used to support the tube support plates, as well as within the support plates. The bobbin probe voltages were found to be higher than those typically encountered in plant eddy current examinations. As a consequence, subsequent tests were designed to produce smaller cracks.

Series 3 Tests: Since the NDE of the archive and series 2 test pieces produced higher voltages than are measured in steam generator tube support plate crevices, the sludge configuration of the series 3 tests was modified to produce shorter cracks. Two tests were specified, with each containing four test specimens. Both tests utilized chemically consolidated sludge, with the sludge occupying a 60° arc and half of the 0.75 inch height of the tube support plate crevice. As in the series 1 tests, Westinghouse heat 2675 was used for the tubing.

Tube 557 utilized simulated plant sludge and was treated with the 10X reference cracking chemistry, in order to produce accelerated SCC. Tube 558 utilized chromium oxide for crevice packing and was treated with the 1X cracking chemistry. Previous testing has found that using chromium oxide rather than simulated plant sludge promotes IGA rather than SCC. It was believed that field experience with IGA produces lower bobbin probe voltages than does SCC. The 1X chemistry was specified because it was hypothesized that it would produce less grain boundary corrosion, and therefore lower voltages.

Through wall cracking of tube 557 was produced after 16 days of operation. NDE of the tube indicated the voltages to be generally lower than in the previous tests, but still well above what is typically found in the field in TSP crevices.

Operation of tube 558 continued with the 1X chemistry for 56 days, at which time the specification was changed to the 10X chemistry in order to accelerate the corrosion rate. The test was then operated for an additional 52 days, at which time a primary to secondary leak occurred. Eddy current inspection identified a through wall crack at the bottom tube support plate elevation, with the crack producing a 6.5 volt signal and a 69% indicated depth. The voltage is typical of field indications of through wall cracks, while the indicated depth is shallower than what is typically found in the field. Following inspection, the remaining three tube support assemblies were returned to test. Testing continued for an additional 50 days, extending beyond the scheduled program completion date.

Series 4 Tests: This test series was undertaken after it was found that the test specimens produced in doped steam environments exhibited high leak rates compared to those found in tests of tubes pulled from the field. The high leak rates of the specimens produced in doped steam were attributed to the plastic deformation of the tubing required to obtain accelerated corrosion. Consequently, the series 4 tests were intended to produce both bobbin probe voltages and leak rates representative of those expected to be found in the field.

The series 4 tests contained 45 specimens, mounted on eight tubes. 23 of the specimens were fabricated from Teflon, while the remaining 22 were fabricated from carbon steel. Teflon collars were utilized because the cracks located beneath the teflon collars in the series 2 tests typically produced lower bobbin probe voltages than did the cracks located adjacent to the collars.

Unlike the series 2 and 3 tests, the series 4 tests used tubes supplied to Westinghouse by the EPRI NDE Center. Tubing Heat 96834, lot 6, was originally fabricated by another NSSS vendor, and is the same as was used in the doped steam testing (see Section 7.2). The heat of material

was changed because the doped steam testing found that this heat produced more accelerated corrosion than did the Westinghouse heat.

The design of the test specimens was also modified in order to reduce the magnitude of the eddy current voltages. These modifications are outlined in Table 7.3. The specimens in test 1 were configured to fit snugly around the tube (as did the teflon collars in the series 1 tests), but the height of the collars was varied between 0.25 and 0.7 inch. The expectation is that the shorter collars should limit the length of the cracks which can be produced.

The inside face of the specimens in test 2 were machined to produce a grid pattern to limit the crevice area between the tube and the collar. Six holes were first drilled around the periphery of the inside face of the specimen, so that the crevice would have an approximate 40° arc width. Two rings were milled on the face of three of the specimens. The rings had a width of 0.125 inch, so that the face was divided into three contact regions, with the outer regions having a 0.125 inch width and the central region having a 0.25 inch width. A helical pattern was machined into the face of the remaining three specimens, with the width of the helix being 0.125 inch and the pitch of the helix being 0.25 inch.

The specimens in test 3 all had a 0.75 inch height, but the diametral gap width was varied between a snug fit (as in test 1), a 10-mil gap, and a 20-mil gap. The gap width was varied because previous testing has found that the gap width affects the rate and location of corrosion.

Tests 4 and 5 both utilized chemically consolidated simulated plant sludge located adjacent to carbon steel tube support specimens. Two sets of specimens having thicknesses of 0.25, 0.50, and 0.75 inch were used in each test. The sludge was consolidated over a 40° arc width within the crevice. The 0.25 inch specimens contained one sludge region, which occupied essentially the full thickness of a specimen; the 0.5 inch specimens contained two sludge regions, separated by a 100-mil wide band at the center; the 0.75 inch specimens contained three sludge regions, separated by two bands.

Test 6 contained carbon steel specimens having the same range of thicknesses as in tests 4 and 5. Instead of using simulated plant sludge, however, the crevices remained empty, with the specimens being held in place with porous Inconel sinters located at each end of the crevice. This design has been used to produce accelerated intergranular corrosion in previous tests.

The 10X reference cracking chemistry was specified for use in tests 1 through 6. Because of concern that this specification may produce excessive grain boundary corrosion and therefore high bobbin probe voltages, two additional tests (7 and 8) were specified to utilize the 1X chemistry. Test 7 utilized five Teflon specimens, while test 8 utilized four carbon steel specimens. The specimens utilized a range of designs selected from tests 1 through 6.

The eight tests accumulated between 96 and 328 days of operation, depending upon the test. Through wall cracks had been produced in five test pieces, with a few additional test pieces containing partial through wall cracks. The designs of the test specimens having through wall cracks are presented in Table 7.4. As indicated in the table, three of the through wall cracks were produced adjacent to teflon simulants in test 3, while the other two through wall cracks were produced adjacent to carbon steel simulants. The only common feature of the crevice configurations which produced the cracks is that the crevice length was always 3/4 inch, perhaps suggesting that the shorter crevices could not produce sufficient superheat to promote accelerated corrosion.

Series 5 ... two additional tests were conducted when it became apparent that accelerated corrosion was not being produced in Series 4 tests. Both tests utilized tubing from heat 2675, ... heat used in ... three series, rather than heat 96834, which had been used in ... 75 ... and four tube support simulants having the same fritted design used in ... tests. ... was conducted because the test piece had been assembled for a ..., but had not been used. Since this design was known to produce accelerated ... hoped that the test could also provide additional crevice assemblies having ... through wall cracking was produced after 25 days of boiler operation, ... signals were on the order of 20 volts, so that no further evaluation of th... performed.

... produce ... cks, as was the intention of the Series 4 tests, ... local crevice superheats in the same region as in the tests which produced accel... sion. The crevices contained two sludge regions: a larger outer region of chrom... a smaller inner region of simulated plant sludge. The expectation was that the cra... would be confined to the inner region, while the outer region would increase the superheat values comparable to those in the early tests. Two of the crevice assemblies were specified to have the simulated plant sludge occupying the center of the top half of the chromium oxide region, while the other two crevice assemblies were specified to have the simulated plant sludge centered in the chromium oxide. In both cases, the inner region had a width of 0.125 inch and a height of 0.375 inch.

The test operated for 45 days with the 1X reference cracking chemistry, plus an additional 56 days with the 10X chemistry, when it was shut down because of a primary to secondary leak. Subsequent eddy current evaluation identified indications at two locations, as outlined below:

Location	Voltage	Depth
576-2	8.41	80%
576-2	8.43	86%

Both locations correspond to crevice configurations in which the simulated plant sludge was centered both axially and circumferentially with respect to the chromium oxide. An RPC evaluation identified three cracks; two were in the simulated sludge, while the third was in the chromium oxide. These results suggest that the two-region sludge configuration is a promising means of producing smaller cracks in model boiler specimens.

7.2 Doped Steam Specimens

Axial stress corrosion cracks and crack networks were produced in 30 mill-annealed Alloy 600 tubes through exposure to a doped steam environment. The steam was produced from water containing 30 ppm each of chloride, fluoride, sulfate and nitrate anions as salts of sodium. The steam pressure was 3000 psi at a temperature of 750° F. Individual specimens were eight inches in length. Stressing was accomplished by clamping the tube at mid length between two flat steel plates, as shown in Figure 7-2. Ovalization of the tube resulted in outer fiber tensile yielding on the OD surface of the tube at the maximum diameter. The tube ends were sealed to permit internal pressurization of the tube during the autoclave exposure. The OD surface of the clamped tube was exposed to the 3000 psi doped steam environment in a one gallon autoclave.

Nitrogen gas was used to pressurize the inside of the tube to 4500 psi producing a differential pressure across the tube wall of 1500 psi. The development of through wall cracking was detected by a drop in the internal pressure of the tube.

Table 7.5 summarizes the specimens tested in the doped steam environment. Two heats of mill annealed Alloy 600 tubing were used, Heat 2675 and Heat 96834L. The width of the clamp in contact with the tube was typically 0.25 inch but larger clamp widths were also used in an attempt to vary the crack morphology. All of the tube displacements were sufficient to cause outer fiber yielding. These displacements ranged from 0.030 to 0.005 inch. In general, the smaller displacements resulted in shorter crack lengths and an increase in the test exposure time. The eddy current voltages listed in Table 7.5 are preliminary values used to help decide the disposition of the tube and should not be confused with the eddy current results provided in Section 8 for the same samples using representative field inspection procedures. The crack lengths shown in Table 7.5 are from optical measurements on the tube OD surface obtained at low magnification and may differ significantly from later destructive examinations. Some attempt to control the length of crack initiation sites was made on the last 7 specimens listed in Table 7.5. Selected portions of these specimens were grit blasted. This procedure had no discernible effect on crack initiation. Selected specimens from Table 7.5 were forwarded for full NDE examination, leak and burst testing as described later.

7.3 Fatigue Precracked Specimens

Through wall axial fatigue precracks were developed in 12 mill annealed Alloy 600 tubes by cyclic internal pressurization. A starter flaw was spark machined half way through the wall of the 0.050 inch thick by 0.875 inch diameter tubing with a length of 0.25 inch. Cyclic internal pressurization then was used to grow the crack through wall. A soft plastic bladder seal was then inserted in the tube and cracks up to 0.70 inch in length were grown by a fatigue process. The pressure was adjusted during fatigue precracking to maintain the maximum applied stress intensity factor below 25 ksi-√in.. The maximum plastic blunting of the crack tip was thus kept below 0.0003 inch. Table 7.6 lists the fatigue precracked specimens, crack lengths and number of cycles. The fatigue precracked samples have well characterized leak rates from previous evaluations, although the leak rates are large compared to those for ODSCC cracks. These samples were used in studies of the effect of denting at tube support plate intersections on leak rates through cracked tubes.

7.4 Chemically Dented Tubes

Fatigue precracked tubes and tubes with stress corrosion cracks were used to simulate cracked tubes in tube support plates which are also dented. Carbon steel collars were used to simulate tube support plates. These collars were drilled with the nominal clearance hole for 0.875 inch diameter tubing. The collars were then packed with magnetite using a hydraulic press. The pressed magnetite was drilled out to a tight fit hole for insertion of a precracked tube. The final configuration was a carbon steel collar with an inside diameter of 0.016 inch, a pressed 0.014 inch layer of magnetite and then the tube wall. The ends of these specimens were sealed and the specimens were exposed to a 0.2 M cupric chloride solution in an autoclave at 572°F.

Corrosion of the carbon steel and a smaller reaction layer with the Alloy 600 tubing resulted in corrosion products which tightly packed the tube-tube support plate crevice and led to a small

amount of denting of the tube. Table 7.7 lists the dented specimens, the eddy current dent voltage and the average estimated radial dent size.

A section through the tube and collar of specimen Trial-1 is shown in Figure 7-3. The packed magnetite and the corrosion products in the crevice are clearly evident. A scanning electron photograph of the polished section in Figure 7-3a shows several layers of corrosion products along with the starting layer of packed magnetite. The EDS nickel and iron maps of Figure 7-4 show that the corrosion product adjacent to the Alloy 600 tube is enriched in nickel and some what depleted in iron. The corrosion product adjacent to the carbon steel collar appears to have the same iron content as the packed magnetite layer. The corrosion product layers in general appear to be relatively dense and any leakage path would be highly tortuous.

7.5 Crack Morphologies

Plugging criteria which are partially based upon eddy current characterization, leak rate and burst strength testing of laboratory specimens depend upon a reasonable simulation of actual service produced cracks. The crack morphologies of service tubes, doped steam test specimens and model boiler test specimens are presented in this section. An intergranular mode of cracking is common to cracks produced in these three environments. Figure 7-5 illustrates this fact with scanning electron fractographs. A further illustration of intergranular cracking is provided by the metallographic details shown in Figure 7-6.

Stress corrosion cracking patterns on the OD of Alloy 600 tubes at tube support plate intersections range from a few to many axial cracks distributed around the circumference of the tube. The model boiler test specimens also show this characteristic. Figure 7-7 shows several arrays of cracks and a larger single crack. The cracks in the doped steam specimens tend to be either a single axial network or axial cracks 180 degrees apart. This is due to the nature of loading of the doped steam specimens. Clamping of the tube leads to a 180 degree symmetry of stresses, bending across the wall thickness and outer fiber bending stresses beyond the yield point. In model boiler specimens, as in actual tube support plate intersections, the stresses are uniform around the circumference of the tube and the occurrence of single or multiple axial cracks is controlled by the crevice conditions. The differential pressure hoop stress is relatively low, about 12 ksi. Hence the model boiler specimens experience essentially prototypic loading while the doped steam specimens experience stresses far beyond actual service conditions. The doped steam environment is substantially less aggressive than that produced in the model boiler tests and thus clamping loads are required in addition to the pressure stress to produce cracking in reasonable lengths of time. The high stress clamped condition of the doped steam specimens led to a higher degree of through wall cracking for a given total axial crack network length and hence higher leak rates at a given eddy current bobbin coil voltage. Another complicating factor is the fact that relaxation of the through wall bending stresses when the clamping fixture is removed can lead to contact across the faces of the crack. This would provide an eddy current path and reduce the bobbin coil voltage relative to a crack with non-contacting faces, as in the model boiler specimens. The above considerations indicate that the clamped test condition of the doped steam specimens produced non-prototypic stress corrosion cracks, particularly as they relate to any correlation between bobbin coil voltage, leak rate and burst strength. Therefore, only the model boiler specimen test results were added to the data base used to develop tube plugging criteria.

Table 7.1

MODEL BOILER THERMAL AND HYDRAULIC SPECIFICATIONS

Primary loop temperature	327°C (620°F)
Primary loop pressure	13.8 MPa (2000 psi)
Primary boiler inlet temperature	324°C ± 3°C (610°F ± 5°F)
Primary boiler outlet temperature	313°C ± 3°C (595°F ± 5°F)
Secondary T_{sat} at 5.5 MPa (800 psi)	271°C ± 3°C (520°F ± 5°F)
Steam bleed	8 cm^3 /min (continuous)
Blowdown	1 cm^3 /min (8 hr/day)
Nominal heat flux	16.28×10^4 kcal/m^2 -hr (60,000 Btu/ft^2 -hr)

Table 7.2

DIRECTORY OF SINGLE TUBE MODEL BOILER TEST SERIES 1, 2, AND 3

TUBE-PIECE	INITIAL SLUDGE TYPE	THRU WALL	LEAK TESTED
Series 1 - Archive Test Pieces			
528-1-1	Chem. Cons.	Yes	No
528-2-1	Chem. Cons.	Yes	No
530-1-1	Chem. Cons.	Yes	Yes
530-1-2	Chem. Cons.	Yes	No
530-2-1	Chem. Cons.	Yes	No
530-3-1	Chem. Cons.	Yes	No
530-4-1	Chem. Cons.	Unknown	No
533-1-1	Mech. Cons.	Yes	No
533-2-2	Mech. Cons.	Yes	No
533-4-1	Mech. Cons.	Yes	Yes
532-1-1	Frit	Yes	No
532-2-1	Frit	Yes	No
500-1-1	Mech. Cons.	No	Yes
525-1-1	Frit	No	Yes
535-1-1	Mech. Cons.	No	No
536-1-1	Eccentric	No	Yes
Series 2 Test Pieces			
542-1-1	Mech. Cons.	Yes	Yes
542-2-1	Teflon Sup.	Yes	Yes
542-2-2	Mech. Cons.	No	No
542-3-1	Mech. Cons.	No	Yes
542-4-1	Mech. Cons.	Yes	Yes
543-1-1	Chem. Cons.	Yes	Yes
543-2-1	Chem. Cons.	Yes	Yes
543-3-1	Chem. Cons.	No	Yes
543-3-2	Chem. Cons.	No	Yes
543-3-3	Teflon Sup.	No	Yes
543-4-1	Chem. Cons.	No	Yes
Series 3 Test Pieces			
557-1-1	Chem. Cons.	No	Yes
557-2-1	Chem. Cons.	Yes	Yes
558-1-1	Chromium Oxide	Yes	Yes
558-2-1	Chromium Oxide	No	No
553-3-1	Chromium Oxide	No	No
558-4-1	Chromium Oxide	No	No

Table 7.3

SUMMARY OF SERIES 4 TEST SPECIFICATIONS

Test	Tube	Collar Material	No. of TSP's	Thick. (in.)	Crevice * Configuration	Chemistry
1	569/1	Teflon	2	0.25	Snug Fit	10X
			2	0.5	Snug Fit	
			2	0.75	Snug Fit	
2	567/9	Teflon	3	0.75	Mach'd Rings	10X
			3	0.75	Mach'd Helix	
3	568/12	Teflon	2	0.75	Snug Fit	10X
			2	0.75	10 Mil Gap	
			2	0.75	20 Mil Gap	
4	570/2	C. Steel	2	0.25	Sim. Plant	10X
			2	0.5	Sim. Plant	
			2	0.75	Sim. Plant	
5	571/4	C. Steel	2	0.25	Sim. Plant	10X
			2	0.5	Sim. Plant	
			2	0.75	Sim. Plant	
6	572/5	C. Steel	3	0.25	Frits, Empty	10X
			3	0.5	Frits, Empty	
7	573/6	Teflon	2	0.25	Snug Fit	1X
			1	0.5	Snug Fit	
			1	0.75	Snug Fit	
			1	0.75	Mach'd Rings	
8	574/3	C. Steel	2	0.75	Sim. Plant	1X
			1	0.25	Frits, Empty	
			1	0.75	Frits, Empty	

* Where a sludge type is listed, the sludge is chemically consolidated over a 40 to 60 degree arc width within the crevice; the machined rings are formed by dividing the tube support plate circumferentially into six land regions, and axially into two rings having a 1/8 inch thickness; the machined helix is formed by dividing the tube support plate circumferentially into six land regions, and axially into a helical pattern having a 1/8 inch thickness and a 1/4 inch pitch.

Table 7.4

SUMMARY OF SERIES 4 TEST PIECES HAVING EDDY CURRENT SIGNALS

Test	Tube	Collar Material	Thick. (in.)	Crevice Configuration	Thru wall Leak	Leak Tested
3	568-1-1	Teflon	0.75	Snug Fit	Yes	Yes
	568-2-1	Teflon	0.75	10 Mil Gap	Yes	Yes
	568-4-1	Teflon	0.75	Snug Fit	Yes *	Yes *
	568-5-1	Teflon	0.75	10 Mil Gap	No	No
	568-6-1	Teflon	0.75	20 Mil Gap	No	No
5	571-1-1	C. Steel	0.75	Sim. Plant	Yes	Yes
8	574-2-1	C. Steel	0.75	Sim. Plant	No	No
	574-3-1	C. Steel	0.25	Frits, Empty	No	No
	574-4-1	C. Steel	0.75	Frits, Empty	Yes	Yes

* Separate cracks were identified at the top and bottom ends of the crevice. Both cracks were included in the leak test.

Table 7.5

Summary of SCC Behavior in Doped Steam at 750°F

Specimen[a] Number	Alloy Heat	Clamp Width (in)	OD_{min} Deflection (in)	TW SCC (hours)	Crack Network Lengths (in)	Bobbin Mix Voltage
SL-FH-1	2675	0.75	0.030	143.1	1.20	5.7
SL-FH-2	2675	2.0	0.030	93.3[b]	2.67; 2.96	0.48; 0.27
SL-FH-3	2675	0.25	0.020	169.9	0.90	0.95; 8.5; 1.1
SL-FH-4	2675	0.25	0.010	261.3	0.63	7.4; 3.2
SL-FH-5	2675	0.25	0.010	170.5	0.47	4.0
SL-FH-6	2675	0.25	0.005	98.2	1.45	5.2; 7.5; 1.6
SL-FH-7	2675	0.25	0.005	175.0	1.22	6.1
SL-FH-8	2675	0.25	0.005	207.8[c]	0.27; 0.34	1.5; 0.44
SL-FH-9	2675	0.25	0.005	118.0	0.97; 1.15	1.3; 3.9; 2.0
SL-FH-10	2675	0.25	0.005	118.0	1.20; 1.16	0.69; 1.7; 1.8
SL-FH-11	2675	0.25	0.005	119.9	0.50; 1.10	2.3; 5.7
SL-FH-12	2675	0.25	0.005	119.9	0.57; 1.63	1.9; 0.48
SL-FH-14	2675	0.25	0.005	307.8	0.67	2.2; 5.2
SL-BW-1	96834L	0.75	0.030	95.1	0.72; 0.85	5.4; 1.5
SL-BW-2	96834L	2.0	0.030	35.3	1.65	6.0
SL-BW-3	96834L	2.0	0.020	58.0	0.78	7.4
SL-BW-4	96834L	0.25	0.020	64.5	1.10; 1.44	7.5; 4.1; 4.3
SL-BW-5	96834L	0.25	0.020	164.4[c]	0.37; 0.50	0.48; 0.53
SL-BW-6	96834L	0.25	0.030	71.0	2.07; 2.35	8.0; 7.2
SL-BW-7	96834L	0.25	0.010	93.8	0.72	4.2
SL-BW-8	96834L	0.25	0.005	132.8	0.28	2.6
SL-BW-9	96834L	0.25	0.005	334.0	0.65	4.3
SL-BW-10	96834L	0.25	0.005	424.0	0.62; 0.17; 0.28	7.0
SL-BW-11	96834L	0.25	0.005	213.0	0.34	2.2
SL-BW-12	96834L	0.25	0.005	693.0[d]	e	2.5
SL-BW-13	96834L	0.25	0.005	87.0	0.63	3.2; 3.4; 7.6
SL-BW-14	96834L	0.25	0.005	64.0	0.33	4.6
SL-BW-15	96834L	0.25	0.005	667.0[d]	e	1.2; 2.3
SL-BW-16	96834L	0.25	0.005	500.0	0.20	4.9; 7.7; 4.6
SL-BW-17	96834L	0.25	0.005	146.0	0.14	1.8; 1.3; 2.8
SL-BW-18	96834L	0.25	0.005	366.0[d]	e	NDD[f]
SL-BW-19	96834L	0.25	0.005	480.0[d]	e	NDD[f]
SL-BW-20	96834L	0.25	0.005	257.0[d]	e	NDD[f]
SL-BW-21	96834L	0.25	0.005	243.0[d]	e	NDD[f]

a SL-FH-13 rejected because of baseline NDE indication.
b Leaked at 750°F; did not leak at room temp.; but had visible OD cracks.
c Did not leak at 750°F. Test periodically shut down till OD cracks visible.
d Did not leak at 750°F.
e No OD cracks visible at termination.
f No detectable degradation.

Table 7.6

Fatigue Precracked Specimens

Specimen	Crack Length	Number of Cycles
FAT-1	0.500	323,700
FAT-2	0.299	85,000
FAT-3	0.300	26,100
FAT-4	0.697	1,278,000
FAT-5	0.300	22,600
FAT-6	0.302	110,000
FAT-7	0.509	410,000
FAT-8	0.707	710,000
FAT-9	0.513	370,000
FAT-10	0.701	726,000
FAT-11	0.499	226,000

Table 7.7

Summary of Dented Specimens

Specimen	Dent Voltage	Average Radial Dent (inches)	Exposure Time (hours)
Trial-1	-	-	24
FAT-1	7.39	0.00037	24
FAT-2	6.09	0.00030	24
FAT-3	12.11	0.00061	48
FAT-4	12.0	0.00061	58
FAT-5	4.55	0.00023	6
FAT-6	0.00	0.0	6
FAT-7	9.43	0.00047	24
FAT-8	17.42	0.00087	48
FAT-9	3.40	0.00017	6
FAT-10	2.50	0.00012	6
FAT-11	2.75	0.00014	6
BW-1	14.67	0.00073	24
BW-3	6.27	0.00031	24
BW-9	6.38	0.00032	48
BW-14	7.03	0.00035	48

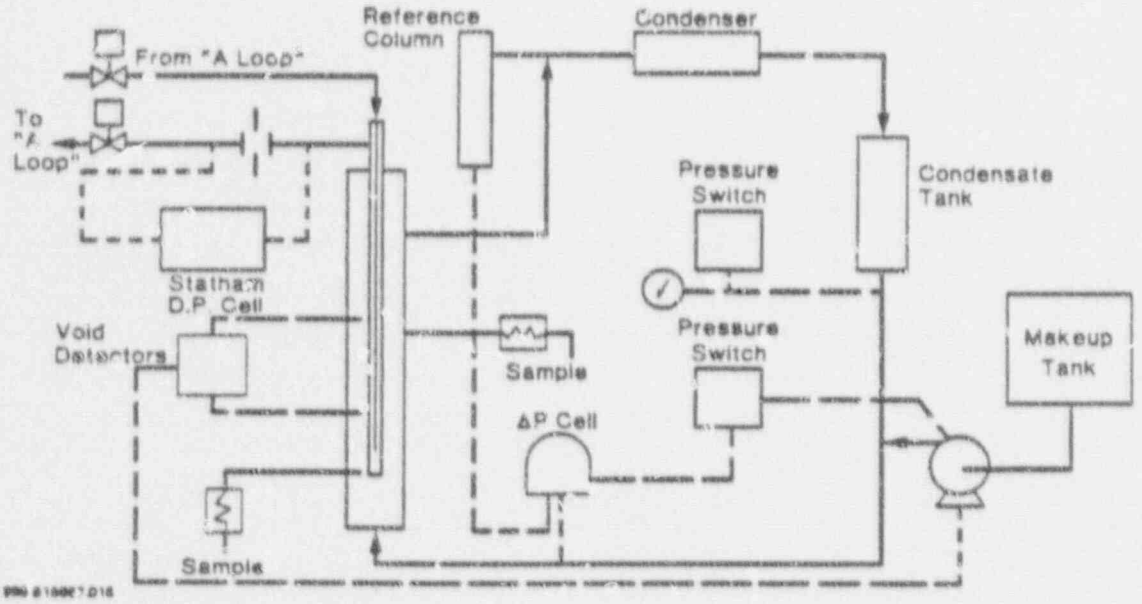

Figure 7-1. Schematic of Model Boiler Facility

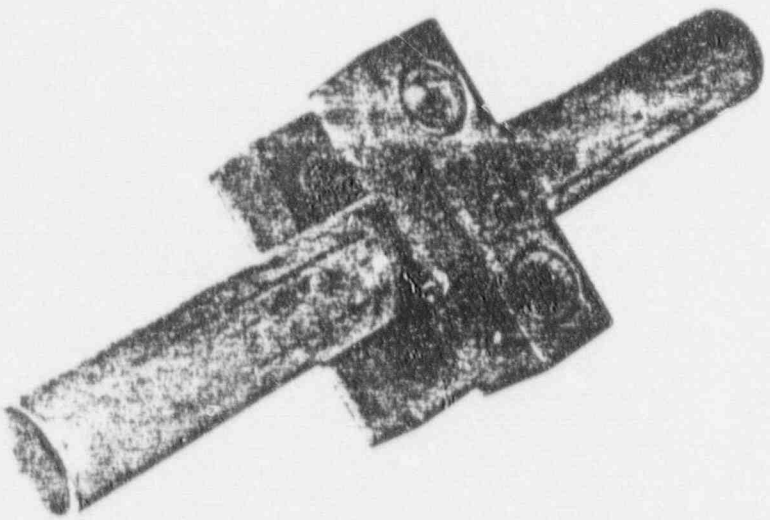

Figure 7-2. Clamped Specimen Used For Doped Steam Test

Specimen Trial-1

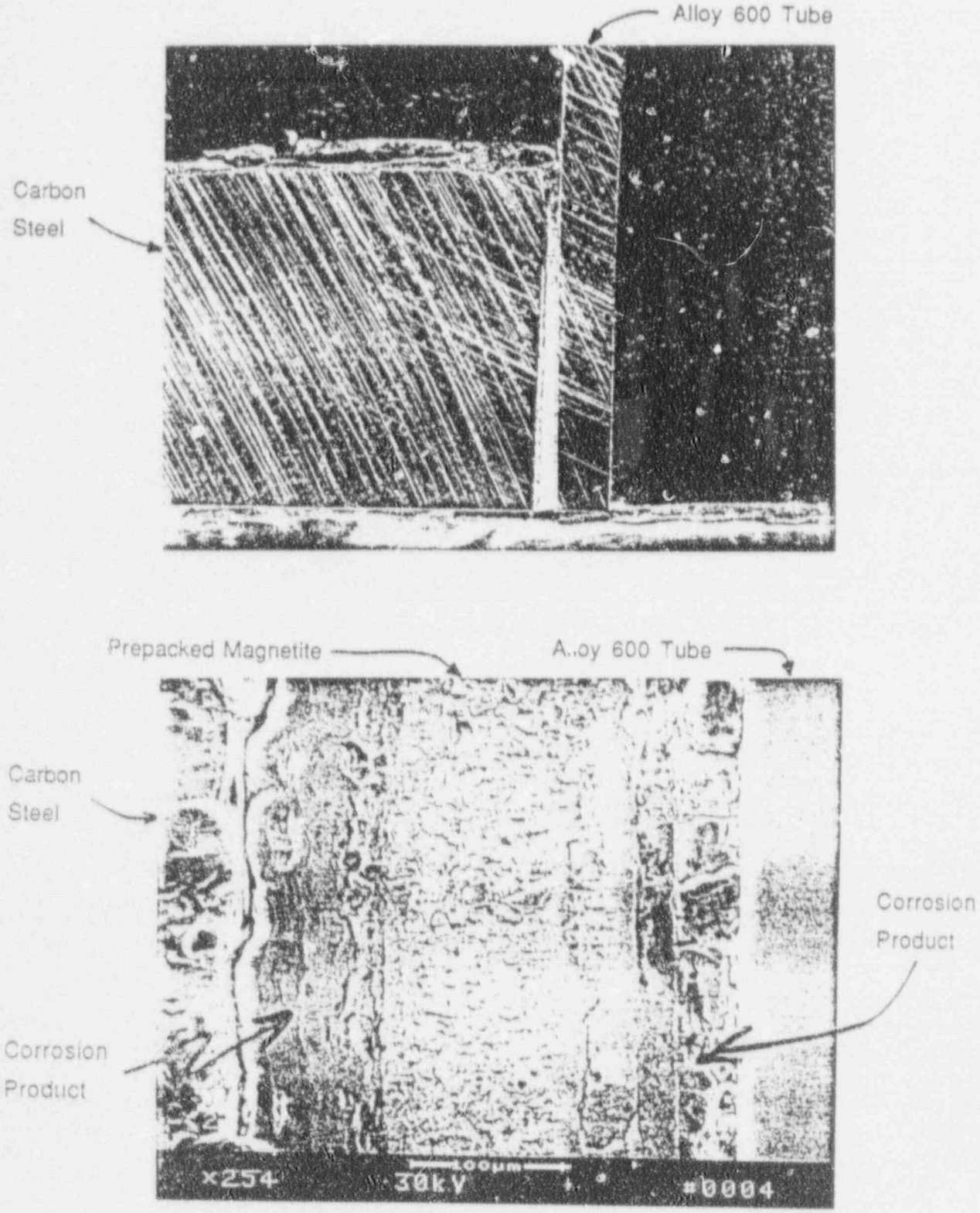

Figure 7-3. Section Through a Dented Tube Support Plate Intersection

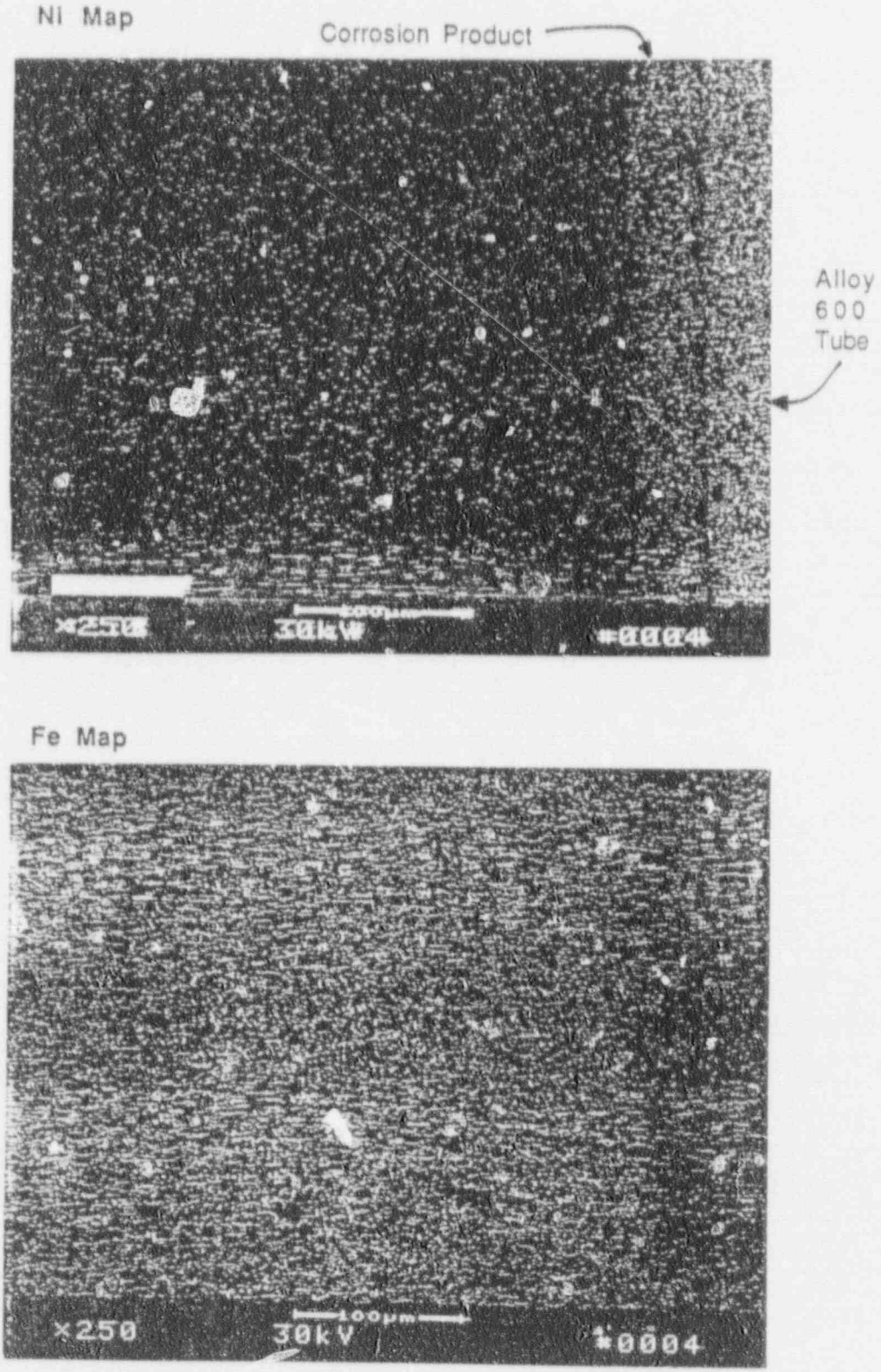

Figure 7-4 . EDS Elemental Maps Across a Dented Crevice; Specimen Trial-1

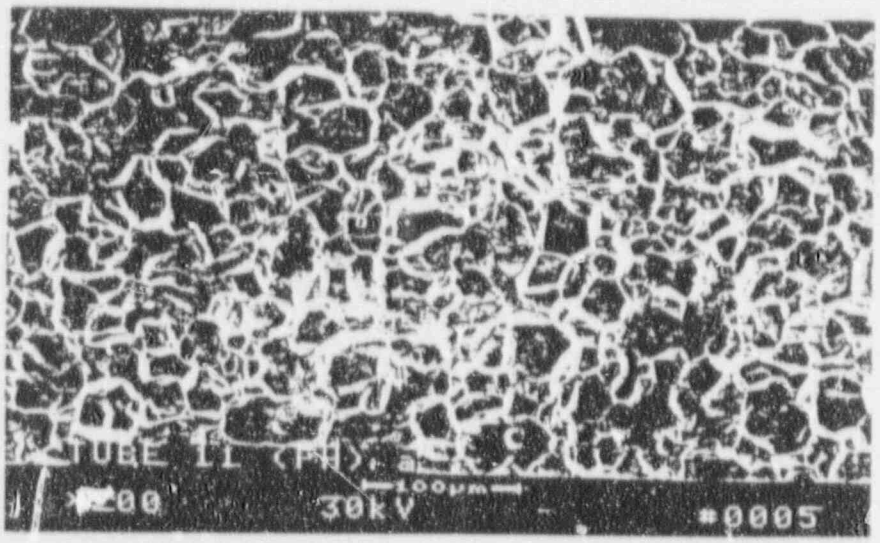

Doped Steam Specimen

200X

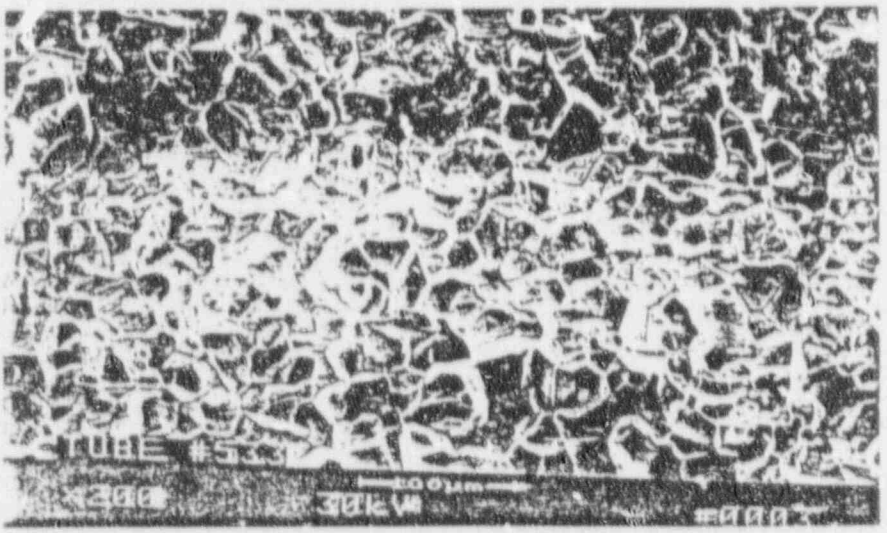

Model Boiler Specimen

200X

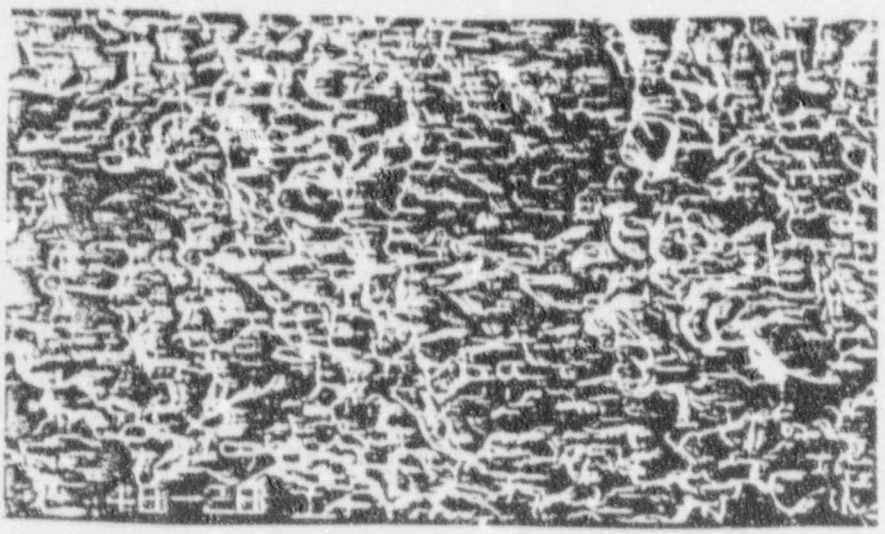

Pulled Tube (Field)

200X

Figure 7-5. SEM Fractographs of Cracks in Doped Steam Specimen, Model Boiler Specimen and Service Tube

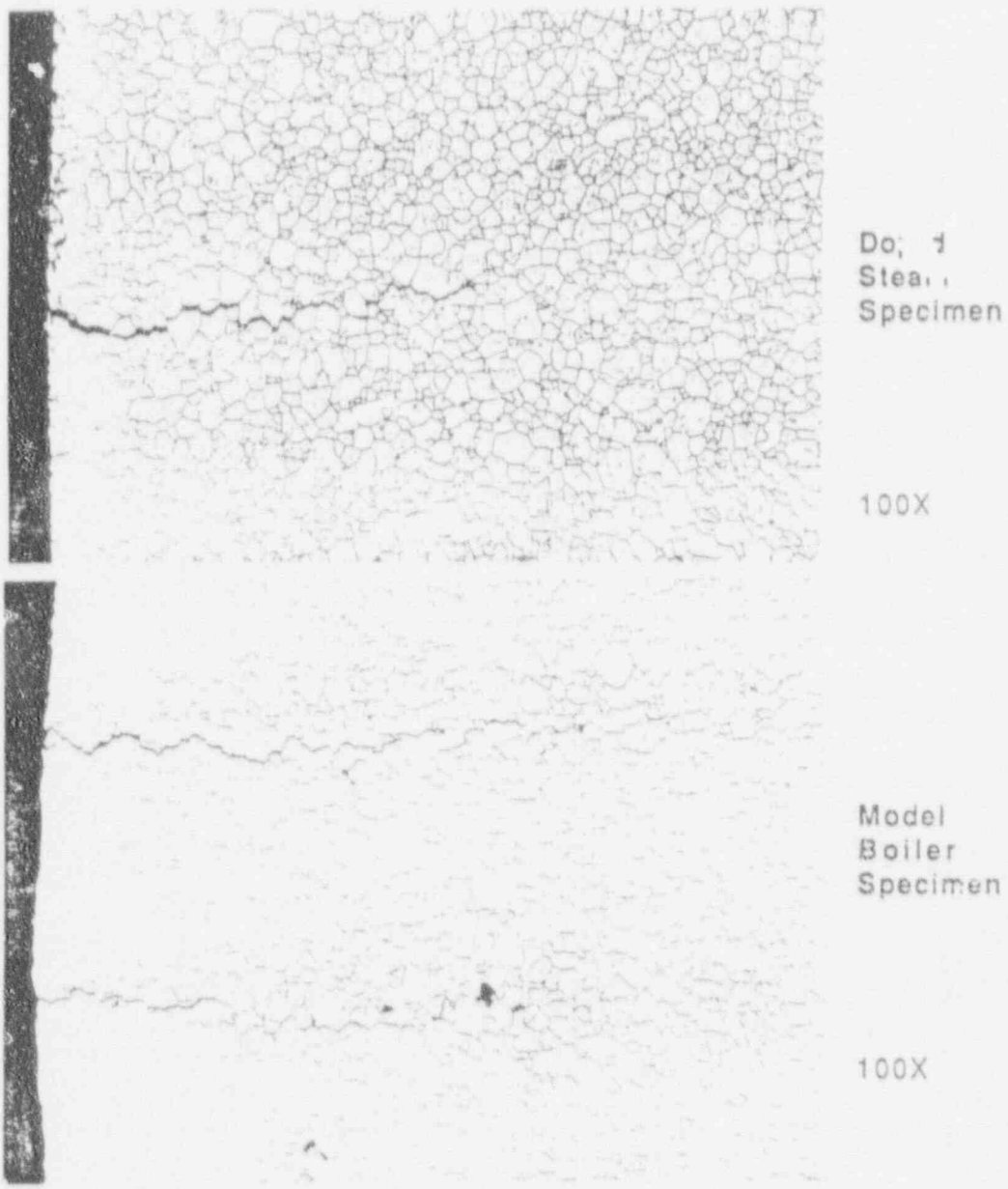

Figure 7-6. Metallograph of Cracked Specimens

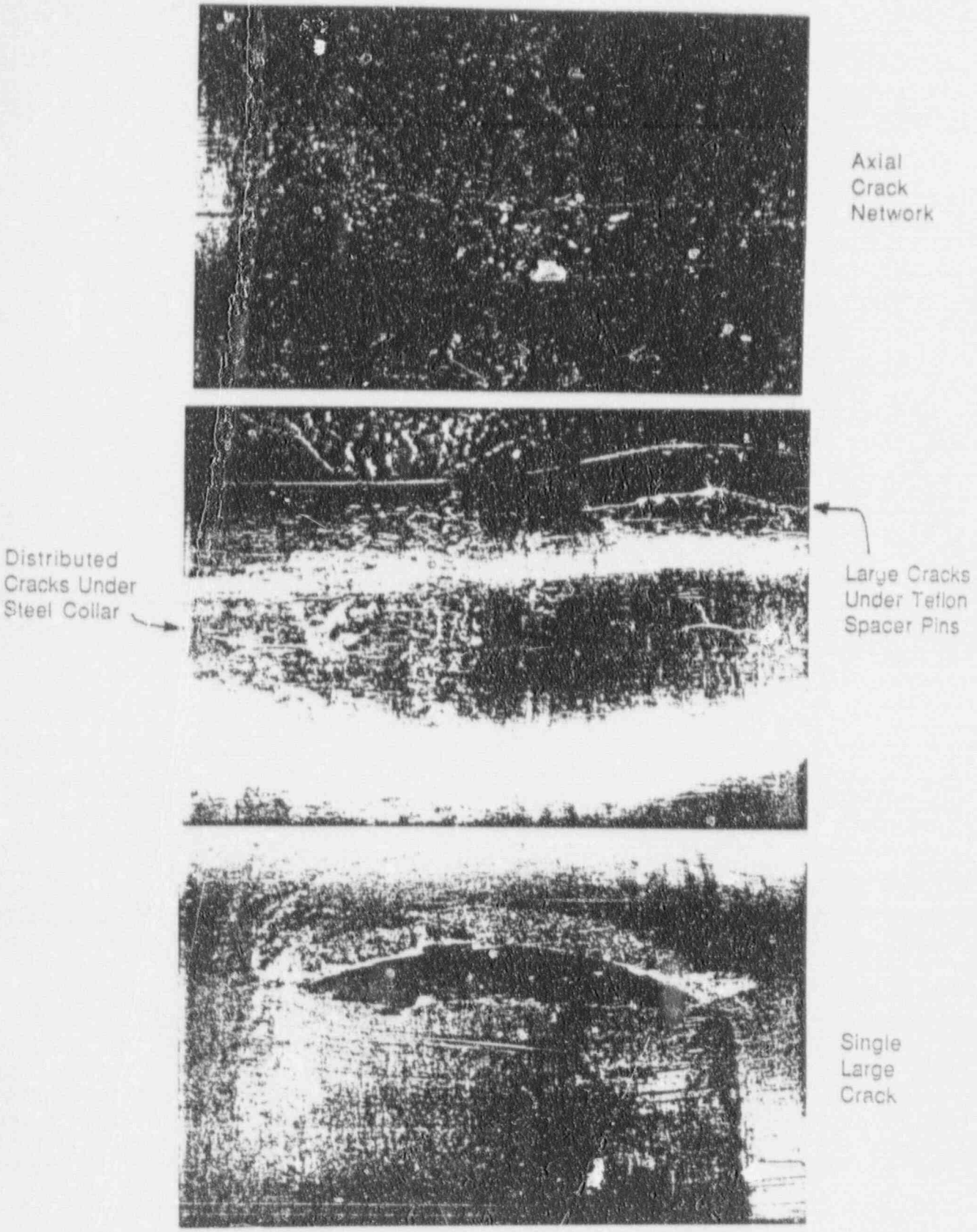

Figure 7-7. Cracks in Model Boiler Specimens

8.0 NON-DESTRUCTIVE EXAMINATION (NDE)

An extensive NDE program was implemented to characterize the laboratory cracked specimens and to assess the sensitivity associated with application of the bobbin coil voltage limits for the tube plugging criteria.

The test program included tests to address some of the variables associated with field characterization of degradation as follows:

1. Bobbin probe voltage sensitivity to the length of the cracks, depth of the cracks, presence of ligaments in the cracks and parallel cracks.

2. Multiple probes to address probe-to-probe variations utilizing probes from Echoram and Zetec.

3. Influence of tube to TSP crevice condition on bobbin coil response including open crevices, packed crevices, incipient denting and fully developed denting.

4. Bobbin probe voltage sensitivity to probe wear to establish field inspection requirements for acceptable NDE uncertainties.

5. Variability among calibration standards, and normalization of the frequency mix.

6. Use of RPC to augment bobbin probe inspections, although the RPC data are not considered essential to the development of the plugging criteria of this report.

The NDE results for the laboratory specimens are utilized in later sections to establish the relation of eddy current voltage response to potential leakage and burst pressure as the basis for the tube plugging criteria.

Establishing a relationship between the bobbin coil response and tube integrity (leakage, burst considerations) is important to inspection planning. A relationship helps determine the importance of detecting degradation with a small amplitude. That is, can "small" indications be left in service and have negligible consequences for safe operation. Degradation exceeding present plugging limits, whose bobbin coil eddy current response was not detected as readily as would equivalent size notches, has been confirmed by destructive examinations.

The morphology of the intergranular corrosion can explain the lack of an eddy current response for small cracks. The observed field degradation, multiple short cracks coupled with an intergranular nature, allows paths for the eddy currents to pass uninterrupted through the degradation. An appreciation for why this phenomenon can account for the lack of an eddy current response has come from the use of liquid metal modeling techniques. Using this technique, degradation is simulated as inserts in liquid metal, and degradation morphologies that are difficult or impossible to machine can be easily simulated. The difference in response between "real" cracks and notches have been modeled by varying the contact between the faces of the crack. In that work, interfacial contact of 50% reduced the eddy current response by a factor of 5. An example of this behavior was found for the doped steam specimens cracked with high applied hoop stresses. These specimens were found to have lower voltages than expected for the crack sizes present in these tubes. This result is judged to be the consequence of crack face

contact as a result of removing the applied stress. Similarly, the voltage sensitivity tests reported here show large voltage increases as ligaments between cracks are lost. The presence of crack ligaments and partially degraded grain boundaries provides an explanation for the lack of eddy current response associated with field induced degradation. Further, the presence of these ligaments and the low instance of primary coolant leakage associated with this degradation mode suggests that there is residual strength associated with these ligaments. Thus, significant degradation depths may result in less severe loss of strength than was assumed in determining the plugging limits based only on crack depth. For this reason, plugging criteria are based on voltage responses correlated to tube integrity through the voltage versus burst pressure and leakage correlations.

8.1 Voltage Sensitivity to Crack Morphology

A series of eddy current tests were performed to establish voltage trends with crack morphology to characterize voltage as a measure of tube integrity. In most cases, machined specimens were used to simulate degradation features. This section describes using simulated cracks and volumetric indications. In addition, voltage measurements for laboratory specimens and pulled tubes with IGA degradation are summarized to assess detectability of IGA.

Voltage Sensitivity Using Slits in Copper Foil

To establish the general trends of bobbin coil voltage amplitude to crack morphology, sensitivity tests were performed using slits in a cylindrical copper foil to simulate varying crack lengths, ligaments and parallel cracks around the tube circumference. The copper foil was placed around a plastic tube. The various crack morphologies simulated by the slits in the copper foil , and the associated voltage responses are shown in Figure 8-1. For each combination of simulated cracks in Figure 8-1, the total crack network length is equal to the TSP thickness of 0.75 inch. The vertical cuts between the parallel axial cracks simulate loss of ligaments between cracks.

The voltage trends of Figure 8-1 show that the voltage increases with:

- Increasing crack length
- Increasing number of cracks around the tube circumference, and
- Loss of ligaments between cracks.

Voltage Sensitivity Tests Using Slots in Inconel 600 Tubing

Additional information on the functional dependence of bobbin signal voltage on length and depth of axial cracks was obtained using EDM slots in 7/8 inch OD, 50 mil wall alloy 600 tubing as shown in Figure 8-2. The signal voltages for the slots represent the upper bound for the signal voltages expected for actual cracks of similar length. For the 100% deep slots, the signal voltage increases steeply with slot length up to about 0.5 inch and continues to increase up to one inch, after which it tends to level off. For the 50% deep OD slots, the signal amplitude increases with slot length up to about 0.250 inch after which it levels off. The signal amplitude increases by a factor of about 50 for 100% deep slots as the slot length increases from 0.03 inch to 1.0 inch; it increases by a factor of about 4 for the 50% deep OD slots over the same range of crack length. It may further be noted that for longer slots, there is a greater increase in the signal voltage as the depth increases from a shallow depth to 100%. For example, for 1/4" slots, the voltage increases by a factor of about 50 as the depth increases from 50% to 100% where as for 60 mil long slot it increases by only a factor of 10 for the same range of depth change. Voltage increases

in an exponential manner with depth for a given slot length. For example, the voltage for a 1/4" slot increases from about 5 volts at 80% depth to 40 volts at 100% depth. Overall, the voltage amplitude is particularly sensitive to deep wall penetration and crack length; this is the desired dependence for voltage as a severity index for tube integrity.

Figure 8-2 also shows the data for three slots with depth varying along slot length. The central 1/3 of each slot had 100% depth which tapered off to 0% at the ends. The signal amplitudes for these slots with tapered ends are, as expected, higher than for the through wall rectangular slots when plotted against the through wall slot lengths. Figure 8-3 shows a plot of percentage increase in signal amplitude above that for a uniform through wall slot resulting from the tapers as a function of the 100% deep portion of the slot length. As the through wall length increases, the influence of the partial depth slot decreases such that for lengths greater than about 0.25 inch, the partial depth slot length has negligible influence on the voltage amplitude.

Figure 8-4 shows the signal amplitudes for the axial slots obtained by using the rotating pancake probe with a 125 mil diameter coil. This data is qualitatively similar to the bobbin data of Figure 8-2. Figure 8-5 gives a plot of bobbin voltage vs. RPC voltage for the slots showing a correlation between the signal amplitudes expected from the two types of probes. It may be noted that for both the bobbin and the RPC probes, the amplitudes are dominated by the deepest part of the slots. A well defined correlation between bobbin and RPC voltages is seen for the single slot data.

The effect of ligament within the crack length on the eddy current signal voltage was studied by varying the axial distance between two 0.125 inch long 100% deep axial slots. The results are shown in Figure 8-6. The bobbin signal voltage drops by approximately a factor of 2 when a ligament as thin as 8 mils is placed in the middle of the two slots. The bobbin signal voltage is relatively insensitive to any significant increase in the spacing beyond 16 mil. RPC voltage is also seen to decrease with increasing ligament size although the rate of decrease for small ligaments is less than for the bobbin coil. Since the small 16 mil ligaments within a crack cannot be distinguished by eddy current, the voltage increase with loss of ligaments supports voltage as a severity index for tube integrity.

A variation in bobbin signal amplitude is expected in case of parallel, multiple axial cracks spaced around the circumference of the tube. This effect can again be studied using EDM slots in the Alloy 600 tubing. Figure 8-7 shows the effect on the signal amplitude of varying the spacings between four through wall axial slots. The signal amplitude increases by a factor of about three as the spacing between parallel slots increases from a few mils to 700 mils. Closely spaced parallel slots do not show an increase in voltage above that of a single slot. The signal phase angle decreased by about 10 degrees at 400 kHz for this entire range of spacing. Qualitatively, a similar result was found for 50% deep EDM axial slots.

The positioning of degradation near the end of the TSP can potentially influence the responses with the principal contribution due to the mix residual that occurs at these locations. This response is typically small compared to the voltage plugging limits so that the amplitude of significant degradation will not be influenced by this residual. To demonstrate the TSP edge effects, bobbin coil measurements were made on 1/4-inch EDM slots of 50% and 100% depth. Measurements were made for the slot at the center of the TSP and at the inside and outside edges of the TSP. Results of these measurements are given in Table 8.1. It is seen that the voltage values for the crack within the TSP are essentially the same at the center and at the inside edge of the TSP. Variations in voltage with the slot inside the TSP are <2% for both 50% and 100% deep

notches, while moving the slot outside the TSP increased voltages by 5%-10%. The bobbin coil indicated depth changed by 29% as the 50% slot was moved from the center to the outside edge of the TSP. These results support the conclusion that amplitude responses to degradation on the order of the 3-4 volt plugging limits will not be significantly impacted by the location of a crack within the TSP.

General conclusions from this eddy current evaluation of axial slots are:

- Both bobbin and RPC voltage amplitudes increase sharply with axial crack length up to about one inch for 100% deep slots.

- The voltage increase is much smaller for partial depth OD axial slots and voltage does not increase significantly with length for slots greater than about 1/4" long.

- Signal amplitude is dominated by the 100% deep portion of the slot.

- Bobbin coil signal voltage is a function of spatial separation between parallel axial slots. Very closely spaced slots show an insignificant increase in the voltage over that of a single slot.

- A correlation exists between RPC and bobbin voltages for single slots. However, bobbin voltages increase for parallel slots while RPC voltage can be isolated to a single slot provided slots are adequately separated to permit resolution of each slot.

- The presence of a small ligament between two axial slots reduces the signal voltage.

- Amplitude reponses to degradation on the order of the voltage plugging limits are not significantly influenced by the location of a crack within the TSP.

- Both bobbin and RPC voltage amplitudes from slots represent an upper bound for the voltages expected from cracks of similar length and depth.

These results demonstrate the use of the voltage amplitude as a crack severity index for tube integrity assessments. Voltages increase with increasing crack length, with increasing depth particularly near through wall penetration and with loss of ligaments between cracks.

The general concept of relating voltage to burst pressure can be demonstrated by combining data for voltage vs. slot length with burst pressure vs. slot length data. Figure 8-8 demonstrates the resulting voltage/burst correlation. Voltages for slots are not typical of cracks but the general trend and slope are similar to that later developed in Section 9.6 from burst testing of cracked tubes. As intuitively expected and shown even for machined specimens, a given voltage amplitude does not define a unique crack morphology. Thus a spread in burst pressures for a given voltage is expected. This spread is accommodated in the plugging criteria by using a voltage/burst correlation at the lower 95% confidence band of the test data. Various crack morphologies involving variables such as length, depth, ligaments, multiple cracks, etc. influence the spread of the data and thus the resulting tube plugging limit.

Voltage Sensitivity to Volumetric (Non-Crack) Indications

It is desirable to compare voltage amplitudes for volumetric indications to those associated with

plugging levels for ODSCC cracks. Given defect specific plugging criteria for ODSCC at TSPs, these comparisons help to guide the importance of distinguishing ODSCC from other types of degradation. The plugging criteria of this report establish a bobbin voltage threshold above which RPC inspection is required to facilitate identification of ODSCC from other types of degradation. These voltage comparisons provide guidance on setting the bobbin voltage threshold for RPC inspection.

Typical bobbin coil voltage amplitudes were developed from laboratory simulations of volumetric degradation as developed below and summarized in Table 8.2:

Wastage: Flat rectangular shaped flaws of different depths were machined to simulate tube wastage: the bobbin signal amplitudes as a function of maximum OD depth for 1/4" and 1/8" long machined flaws are shown in Figure 8-9. In addition, tapered flaws were machined to simulate the tube wastage shapes observed at some plates. Figure 8-9 shows the bobbin signal voltage as a function of maximum OD depth for tapered flaws.

Fretting: Flaw shapes somewhat similar to the tapered flaws shown in Figure 8-9 are observed from fretting. Thus, the data of Figure 8-9 can be used to assess the voltages expected from fretting.

Pitting: Figure 8-10 shows the bobbin signal amplitude vs diameter of machined through wall holes simulating 100% deep pits. Pitting observed in operating S/Gs occurs as multiple pits for which voltages are significantly higher as noted in Table 8.2. The data from ASME flat-bottom holes of partial depths may be used for estimating the signal voltages expected from partial depth OD pits.

Cold Leg Thinning: Pulled tube data from two different plants with cold leg thinning were reviewed and are summarized as follows. In one case, a flaw at the second TSP in the cold leg with a maximum wall penetration of 48% had a bobbin amplitude of 4 volts. Figure 8-11 shows a photograph of the OD surface at the degraded location. In the second example, which was also at the second TSP in the cold leg, a maximum wall penetration of 59% yielded a bobbin amplitude of 4.9 volts. Examination of the pulled tubes showed no cracks in these tubes and the degradation was identified as "cold leg thinning."

The data of Table 8.2 and supporting figures indicate that bobbin voltages would exceed about 2 volts, as limiting by pitting degradation, before being a concern for tube integrity. A single pit, simulated by 30 and 60 mil through wall holes would have voltages of about 2 and 7.5 volts, respectively. Pitting typically occurs as multiple pits in operating S/Gs with higher voltage levels as noted in Table 3.2. Cold leg thinning at 50% depth will yield a bobbin amplitude of over 4 volts.

Based upon the above noted voltage levels, volumetric indications with bobbin voltage amplitudes exceeding about 2 volts should be inspected using RPC probes to aid characterization of the causative mechanism. Volumetric indications less than this voltage amplitude would be expected to be acceptable for continued service and separation of the causative mechanism from ODSCC would not be critical to assure tube integrity.

IGA Detectability

Limited laboratory specimens and pulled tubes at TSP intersections with significant IGA are currently available for assessments of detectability and tube integrity. Available laboratory IGA specimens were prepared as long (to 6 inches), uniform IGA to assess detectability in unexpanded regions of tubesheet crevices. Data from three domestic tube to TSP intersections from Plant L (R12 C8), one from Plant M-2 (see Section 4), and three from Plant N-1 (non-Westinghouse) are available. Some French data obtained from EdF for TSP indications can also be assessed. The general morphology of the French indications is more like Plant L tube R12 C8 than indications in other domestic plants.

Three sets of laboratory IGA specimens are available for NDE assessments. Two are Westinghouse samples and the third represents samples prepared by Westinghouse under EPRI sponsorship (EPRI NP-5503). The two Westinghouse sets of specimens represent laboratory IGA under accelerated conditions and provide uniform wall penetration IGA over 4 to 6 inch lengths. Bobbin coil detection for these specimens is shown in Figure 8-12. Figure 8-12a represents specimens prepared using sensitized tubing and shows very high bobbin coil amplitudes. Figure 8-12b shows bobbin coil responses using non-sensitized material. The non-sensitized material shows much lower amplitudes. Methods of sample preparation were refined for the EPRI program to further improve comparisons with field experience.

The EPRI specimens were prepared using a 50% caustic and 12% chromium oxide environment at 650°F for up to 10,000 hours. Temperatures in some cases were increased to 700 °F to accelerate the corrosion rate such that 21% penetration was obtained in 35 days. Even under the accelerated laboratory conditions, the times to create IGA are very long compared to preparation of ODSCC specimens. Specimens in the range of 2 to 30% nearly uniform wall penetration were obtained in this program. Figure 8-13 shows typical NDE results for 29% deep IGA. The bobbin coil differential tests reveal the uniform IGA whereas the RPC results are not particularly revealing. Voltage amplitudes are not available for the samples that were destructively examined. Bobbin coil measurements of library samples were performed with the results given in Table 8.3 These samples show voltage amplitudes of about 1-2 volts where the IGA depth is expected to be <30% deep and are NDD (no detectable degradation) where depths of a few percent are expected. Deep cracks within the samples were detected with amplitudes of 4-40 volts. These samples are more representative of field IGA than the Figure 8-12 samples although only limited pulled tube data for uniform IGA are available for direct comparisons.

As described in Section 4.0, a pulled tube from Plant M-2 shows IGA with cracks up to 26% depth. This tube had a voltage amplitude of 1.8 volts, which is high compared to tubes with principally ODSCC at comparable depths as shown in Figure 6-9. The signal amplitude is comparable to the laboratory specimens of Table 8.3, although lower than the specimens of Figure 8-12.

Three pulled tube results from Plant N-1 with egg crate supports are also shown in Figure 6-9. These data for IGA degradation also support IGA detectability at voltage levels comparable or higher than that for ODSCC with minor IGA.

The recent pulled tube (R12 C8) indications from Plant L were detected by pre-pull bobbin coil inspection. Table 6.2 and Figure 6-9 show the voltage and maximum depth for the three Plant L indications as compared to other pulled tube results. It is seen that the Plant L voltage levels are typical of the rest of the population of pulled tubes with less IGA involvement than the Plant L

tube R12 C8 crack morphology, which shows patches of IGA with IGA/SCC cracks.

Figure 6-9 also shows voltage amplitudes for tube to TSP intersections removed from French units. The French data show voltage responses toward the high range of the data. The French crack morphology is IGA + SCC as shown in Figure 6-5. The Plant L, M and N morphologies also show IGA + SCC.

Overall, the available pulled tube results show comparable voltage responses relative to maximum depth with no definable dependence on IGA involvement within the broad scatter of the data. The laboratory uniform IGA samples show significant voltage responses at 30% depth. The available pulled tubes with significant IGA levels show IGA with cracks and have been found to be detectable indications.

8.2 Probe Comparisons

To address concerns that the results of the study might be limited to a specific probe, probes from different eddy current probe vendors (Echoram and Zetec) were used. Both probes were nominally 0.720 inch in diameter and incorporated the latest technology for centering. The coils on each probe were nominally 0.06 inch wide and were spaced by 0.06 inch. Initially each of the probes was used with two different sets of frequencies duplicating typical field inspection configurations. The first set of frequencies (configuration I) was 400, 200, 100 and 10 kHz. The second (configuration II) was 600, 400, 100, and 10 kHz. Review of the data indicated no significant differences in the results from the different probes for the different frequency configurations.

Comparisons were made between the data obtained from probe Er and probe Zt for the cracked tube specimens. The probes have different frequency response characteristics: Probe Zt gives a greater response at 100 kHz , while probe Er has a larger response at 600 kHz since it is designed for higher frequency operation than the Zt probe. This difference is not a significant issue and is noticeable only as a consequence of the way in which the voltage calibrations have been derived. Table 8.4 gives the voltage measured by probe Zt divided by the voltage measured by probe Er for the EDM calibration notches. As can be observed for each frequency, the difference between the probe responses is a constant factor for all notches. This apparent variation between the probes can be eliminated by calibrating each of the frequencies individually rather than using the 400 kHz calibration factor, or by calibration at the planned mix frequency. The latter approach is recommended as a part of the plugging criteria of this report.

The results for the 400/100 kHz Mix channel were fortuitous. Plots of the measured voltage for various indications from probe Zt versus the voltage from probe Er indicate a one to one correspondence for both amplitude and depth (Figures 8-14 to 8-16). The correspondence between the mix channels of the two probes is due to the fact that the 400 kHz channel is being used both as the "primary" mix frequency and to set the calibration factor. If another frequency is used as the primary mix frequency (i.e., 100 kHz) the apparent mix amplitudes will differ. Table 8.5 gives the measurement of the ASME holes using a 100/400 kHz mix for the two different probes. As can be seen the results from the two probes differ by a constant multiplier. As with the individual frequencies, this factor can easily be accommodated by using a different calibration procedure.

The bobbin coil inspections were supplemented by two RPC examinations, also with probes from the two eddy current probe vendors noted above. However only one set of frequencies (400, 200, 100, and 10 kHz) was used for both RPC probes. The data gathered during this phase of the program were used primarily as a qualitative tool in assessing the extent of the degradation.

8.3 Influence of TSP Crevice Condition

For some specimens, the crevice between support and the tube was packed with magnetite and the sample was inspected again with the bobbin coil. Table 8.6 compares the data from the two inspections. With the exception of sample BW-11 the amplitude of the responses from the samples changed by approximately 10 %. Sample BW-11 showed a 50 % increase in amplitude. When the support was removed from the sample the degradation response had indeed increased, indicating that the presence of magnetite in the crevice did not cause the increase in response, rather the process of packing the crevice had mechanically deformed the sample causing further loss of ligaments and a subsequent increase in response. Additional evidence for the minimal impact of the presence of magnetite in the crevice is derived from the comparison of the data from corrosion samples with tight packed crevices. A comparison of the EC data before and after the removal of magnetite with the packed support ring in place (Figure 8-17) shows a 5% increase in response in the presence of magnetite, with a scatter of approximately 10%.

As part of the test program, 6 fatigue crack and 3 doped steam corrosion crack samples were leak tested to determine the influence of the dented support plate crevice condition. Table 8.7 summarizes the results of the eddy current inspection of these samples before and after denting (note samples FAT 1, 2, and 3 had been leak tested previously). Denting resulted in a significant change in the amplitude of the fatigue crack eddy current responses. Prior to denting, all but one of the fatigue cracks had amplitudes which approached that of the through wall EDM notch (80 Volts). After denting, two of the fatigue cracks could not be distinguished from the response of the dents, despite the fact that the dent response was an order of magnitude smaller than the initial fatigue crack response. Initially the corrosion cracks produced smaller responses than the fatigue cracks. However, their responses on average, could be detected in the presence of the dent. However, these results represent large indications in the presence of small dents. In field applications, small to moderate indications typically cannot be separated from dent signals that exceed the amplitude of the indication.

The difference in the behavior of the two crack types (and further within the fatigue samples) in the presence of denting is a consequence of the heavier oxide coating on the crack faces of the corrosion samples and the leak tested fatigue cracks. Under the compressive loads of denting, the crack faces are forced together. The presence of the oxides on the corrosion crack faces prevents interfacial contact and therefore results in a minimal change in the crack response. On the other hand, the faces of a virgin fatigue crack, being free of oxides, come into intimate contact permitting the eddy currents to flow unimpeded across the crack, significantly reducing the response. The significant loss in response of the fatigue cracks demonstrates that interfacial contact does indeed result in a reduced eddy current response. However, it is not expected that service-induced degradation will respond to denting as have the fatigue cracks. Rather, it is expected that the compressive stresses from denting would not play a direct role in providing interfacial contact such that field induced cracking would respond as did the doped steam samples, with little change in amplitude. However, it is recognized that bobbin coil detection of cracks at dented intersections is unreliable when the degradation amplitude is smaller than the dent amplitude.

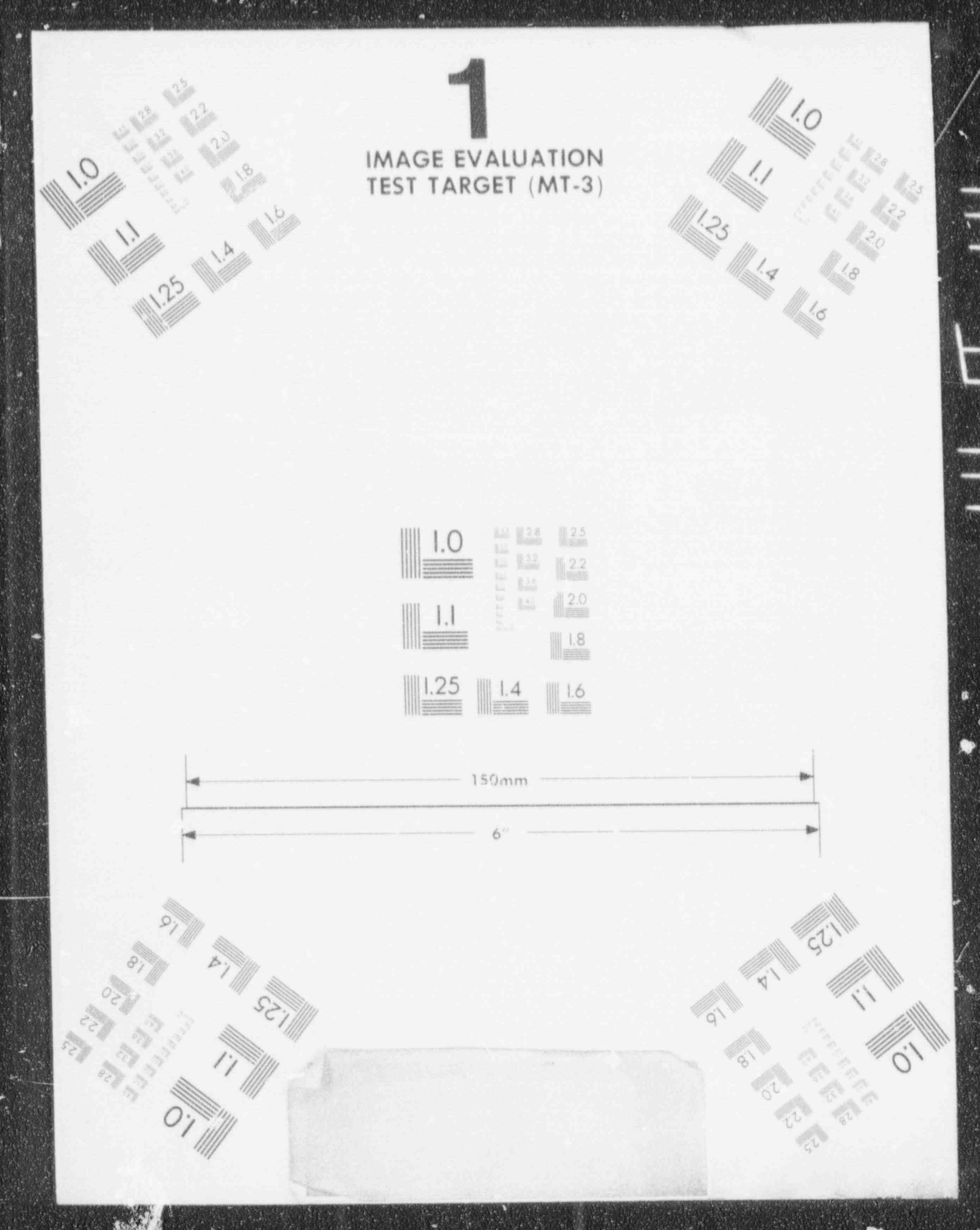
1
IMAGE EVALUATION
TEST TARGET (MT-3)
1.0
1.1
1.25
1.4
1.6
1.8
2.0
2.2
2.5
2.8
3.2
3.6
4.0
150mm
6"

1

IMAGE EVALUATION
TEST TARGET (MT-3)

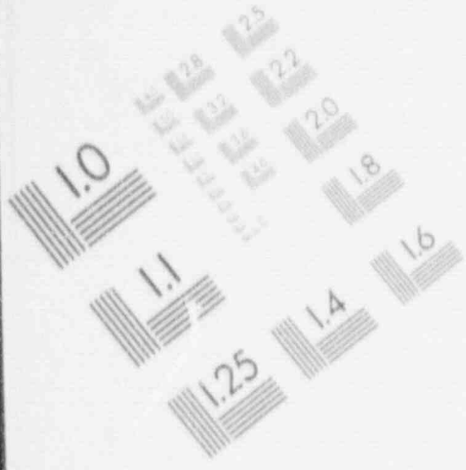

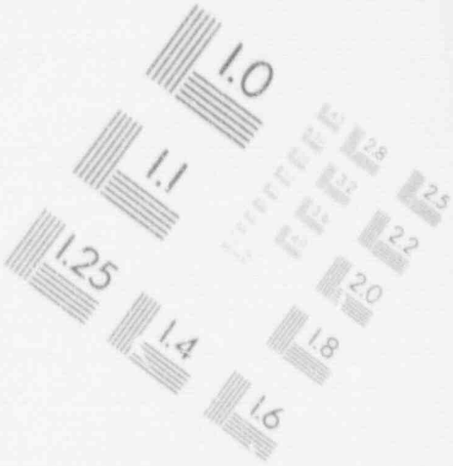

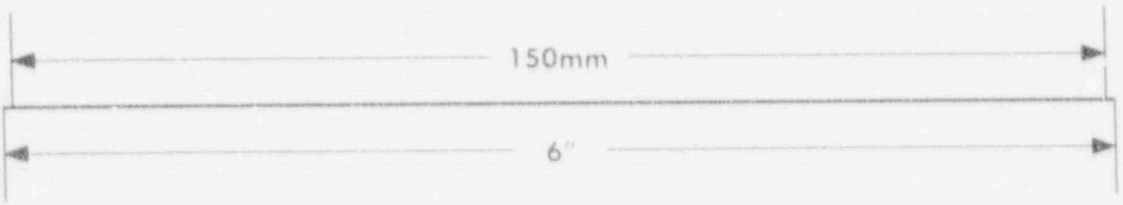

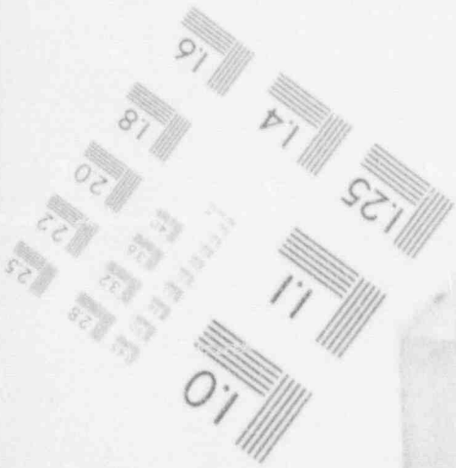

1

IMAGE EVALUATION TEST TARGET (MT-3)

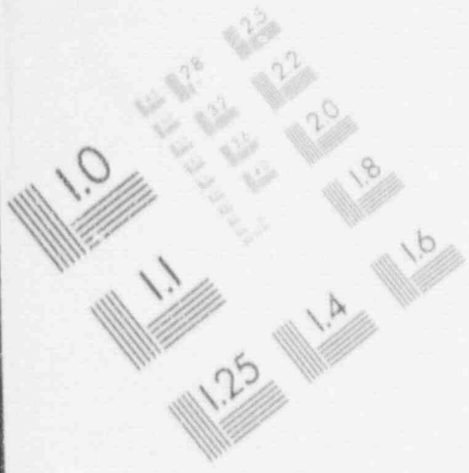

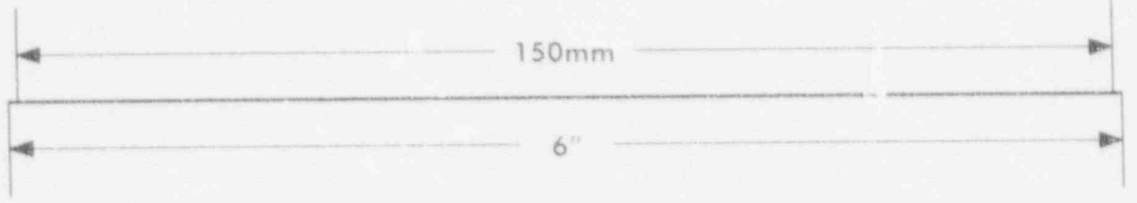

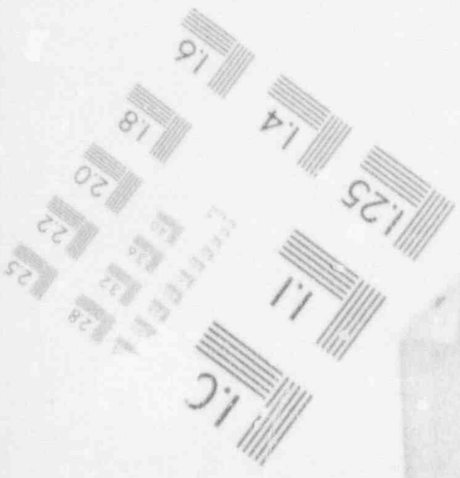

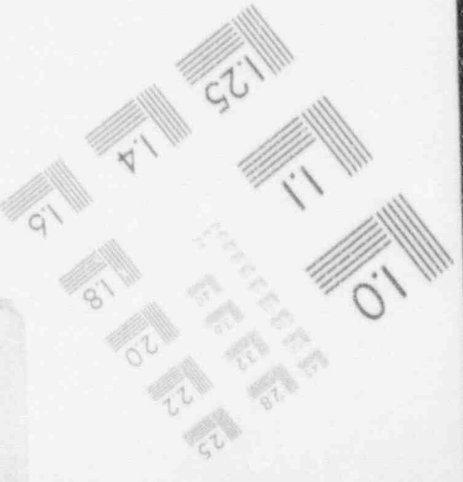

8.4 Sensitivity to Probe Wear

Eddy current test parameters can exist over which there is little systematic control and which may vary between tubes or along the length of a tube. The centering of the eddy current probe as it passes the degradation poses the greatest concern of this type. This study has shown that probe centering can vary the amplitude of a signal, in the worst case, by a factor of two. The laboratory study used field probes which had excellent centering characteristics. At the beginning of a field inspection sequence, the probe centering characteristics would mimic those found in the laboratory. As the inspection continues the probe is expected to wear and its centering capability to degrade. The time frame for this to occur is unknown because it is a complex function of inspection extent, tube geometry, the presence of oxides, etc.

A means of assessing the probe's centering capability is through the use of an appropriate verification standard as illustrated in Figure 8-18. Such a standard can be as simple as four holes drilled in a segment of tubing. The holes are displaced axially in different planes with each spaced 90 degrees around the circumference from its neighbor. The amplitude ratio between the holes then determines the degree of centering of the probe. A standard of this type could be put in-line to provide continual verification of probe centering during the inspection.

The bobbin probe centering mechanism wears with usage. This could affect the eddy current signal. The effect of wear on signal voltage was evaluated using a "4-hole standard." The four holes were 87 mils in diameter, 100% deep, 90 degrees apart circumferentially, and 1.5 inches apart, axially. A 0.720 inch diameter probe fabricated by Echoram was used for this evaluation. The centering mechanism in this probe consists of three sets of spring loaded plastic buttons (hemispherical) 120 degrees apart and protruding approximately [ ]^{a} mils from the probe body. The test runs were made with the tubes in a vertical position. The probe pull speed was approximately 12 inches per second. The tubes were rotated 90 degrees after each run to provide for the randomness in the probe to tube orientation expected in the field. For the new probe, the scatter in the voltages obtained from the four identical holes for repeated test runs was [ ]^{a}.

The centering buttons of the probe were worn by repeatedly running the probe through a tube with an abrasive tape on the tube ID. The data from the 4-hole standard was collected for different levels of probe wear. At the level of probe wear represented by a 50% reduction in height of the centering plastic buttons (ie, about [ ]^{a} mils), the scatter in the voltage for the four holes was found to be within [ ]^{a}. Increasing the probe wear beyond this level resulted in rapid deterioration of the quality of the data. The results of the tests are shown in Figure 8-19. The 50% reduction in height of the centering buttons apears to envelope typical field wear between probe changeouts during an inspection. Thus an allowance of [ ]^{a} uncertainty for probe wear is consistent with current field experience.

The remaining concerns over probe centering are the impact of tube to tube variations in diameter and ovality. Neither of these are anticipated to be major sources of variability.

8.5 Eddy Current Inspection and Analysis Practices

To lay the foundation for field application of the results of the tests, the data collection and analysis procedures were made as close to those used in the field as possible, while conducted

under laboratory conditions. A formal procedure for instrument calibration, data acquisition and analysis was developed. The key point to note from the procedure is that the analysis of the bobbin coil data was conducted from a 400/100 kHz mix data channel. The mix was established by eliminating the response from the support ring on the calibration tube. The voltage for all channels was calculated from the conversion factor found by setting the response of the 20% ASME calibration holes at 400 kHz to 4 volts (save/store mode). This corresponds to setting the 400/100 kHz mix channel voltage of the 20% holes to 2.75 volts or to 6.4 volts for the four-100% hole standard. A similar procedure, in which the 400 kHz response of a through wall EDM notch was set to 20 volts and the voltage of all other channels established using the Save/Store mode, was used to calibrate the RPC probes.

Because each calibration standard is potentially unique, a system to assure consistency of the data must be established. Currently, the field data is tied to the calibration tube used during an inspection and the correlation between that standard and all others used in the industry is through the certification provided by the manufacturer of the standard. Typically, the controlled parameters of the standards are the depth of the calibration holes and whether the phase response of the machined holes is within acceptable tolerance. The amplitudes of the hole responses are not controlled parameters. Small changes in tube dimensions, hole placement and other subtleties can cause variations in the hole response and therefore systematic offsets in the measured degradation response with respect to the data obtained in this study. An examination of a limited number of field standards has found a variation in the 20% hole response as large as 18% above that of the standard used in the laboratory work.

Evaluations of alternate practices for voltage normalization have found minimum uncertainties between standards when the 4 in-plane hole standards are utilized. This eliminates the depth variation between standards and limits voltage variations to principally the hole diameter tolerance. Consequently, the recommended voltage normalization is 6.4 volts for the 4 hole (0.033" dia.) ASME standard. For further limitation on the uncertainty, the ASME allowable hole tolerance of 0.003" is reduced to 0.001".

8.6 Alternate Inspection Methods: Rotating Pancake Coil (RPC)

The primary objective of this program was to arrive at inspection and plugging criteria based upon the bobbin coil inspection. However supplemental RPC data was also acquired from the test samples. This data served two objectives: (1) to establish a data base that if needed could be used to augment the bobbin coil data in establishing tube plugging criteria, and (2) to gather information that might be used as additional support for the current practice of using RPC data as the final arbiter for determining tube plugging.

It is believed that combinations of deposits and other spurious conditions can result in bobbin coil responses that have degradation-like characteristics. To minimize plugging tubes with such responses, the philosophy of using the bobbin coil as a screening tool and the RPC as a confirmatory tool has developed. For the samples that were leak checked, indications were present in both the bobbin and RPC data. Table 8.8 contains a comparison of the bobbin coil and RPC results respectively for the leak tested model boiler samples. It is noted that the samples with the largest bobbin responses generally had large multiple RPC responses. It can be noted that specimen 568-4 had a crack length greater than the 0.75 inch TSP thickness. In this case, the crack extended below the TSP into a teflon spacer used to support the TSP in the test. Figure 8-20 shows examples of RPC traces for typical model boiler specimens at 6.5, 12.7, 26.5, and

67.7 volts (bobbin coil). It can be seen that for bobbin coil voltages above about 25 volts, multiple axial cracks of comparable amplitudes are found. Specimen 543-2 (67.7 volts) shows closely spaced, long axial cracks with large RPC amplitudes.

An example of an apparently spurious bobbin response, similar to those observed in pulled tubes, was identified in the model boiler tests (Model Boiler 568). During interim inspections these samples displayed the characteristic of having bobbin coil indications without showing discrete RPC indications. The bobbin coil mix response had amplitudes on the order of one volt, with depths based upon phase measurements on the order of 80% through wall. However, the phase of the indications did not change as a function of frequency consistent with that of the calibration tubes. Rather, as the frequency was decreased the phase remained essentially constant such that the apparent depth of the indication decreased. RPC inspection gave a response indicating a band of material with electromagnetic properties different from that of the remaining portion of the tube but with no discrete indications. When the pancake probe was pulled axially through the band, a response was obtained which behaved similar to the bobbin coil response. That is, as the inspection frequency is decreased the apparent depths of the indications appeared shallower. The underlying mechanism which causes this shift in the tubing's electromagnetic properties has not been identified. Ultimately the samples showed both significant bobbin coil responses and RPC indications. Post burst examination of the specimens showed no apparent degradation apart from that identified in the RPC results. This example tends to lend support for the RPC probe as arbiter of bobbin coil indications for identifying discrete crack responses.

8.7 Field Considerations

Proper implementation of the tube plugging criteria depends on consistent data acquisition between the field and the laboratory. Although field NDE procedures were utilized in the laboratory, the test program yielded the following modifications to the field eddy current procedures which are necessary to assure proper control of the uncertainties in the data acquisition:

1. The 4-hole ASME (Section XI, Article IV-3220) standard with 0.033 inch diameter holes spaced 90° apart in a single plane should be used for field voltage normalizations. However, hole diameter tolerance must be ±0.001 inch rather than the ASME value of 0.003 inch.

2. An additional standard should be used in line with the ASME standard to limit the effect of probe wear (probe centering) on the field data. Use of this standard indicates when data uncertainties due to probe wear become greater than acceptable for the tube plugging criteria, requiring use of a new probe.

3. The calibration should be normalized to 6.4 V for the 400/100 kHz mix channel for the 100% 4 hole ASME standard to eliminate the uncertainties introduced by depth uncertainties in the standards and by calibration to 4 V for the 400 kHz channel and carrying over the conversion factor for the mix channels.

8.8 Eddy Current Uncertainties for Tube Plugging Criteria

In most prior evaluations, S/G NDE uncertainty is determined as the difference between bobbin

coil indicated depth versus actual depth from destructive tube examinations. This is not the case for voltage measurements such that the NDE uncertainties for voltage do not have such a unique interpretation. For voltage plugging criteria based upon voltage versus burst pressure correlations, the NDE voltage "uncertainties" affect both the voltage measurement and the spread or uncertainty in the burst pressure correlation. The goal for the voltage measurements is to minimize the uncertainty on repeating a measurement so that the uncertainty on the burst correlation is reduced to the extent practical. The remaining voltage measurement uncertainties end up as part of the burst correlation uncertainty. For example, assume that a number of perfectly identical samples were prepared such that burst pressures would be identical. If voltage measurements were then made with different probe diameters, calibration standards, open crevices, packed crevices, copper deposits in crevices, etc., the voltage measurement variability would then result in a spread in the voltage versus burst correlation. Clearly the goal is to minimize the burst correlation uncertainty (lower 95% confidence limit used for plugging criteria) by controlling the voltage variability. The voltage measurement procedures must be consistent between laboratory and field implementation so as to apply the laboratory specimen NDE/burst data for developing plugging limits. Inclusion of field voltage measurements for tubes pulled prior to implementating the procedures to improve measurement repeatability tend to increase the spread in the burst correlation. The NDE voltage uncertainty is defined as the uncertainty in voltage repeatability emphasizing differences between the laboratory and the field measurements.

As applied for the plugging limit development, the variables affecting the burst correlation are split into NDE uncertainties for determining voltage and burst correlation uncertainties as given in Table 8.9. The potential contributors to the NDE repeatability uncertainty are probe centering (principally probe wear), calibration standards, probe design differences and eddy current system variability. Eddy current system variability results from noise due to instrumentation and cabling. This contributor is on the order of 0.1 V and can be ignored when combined with the probe wear uncertainty for applications to plugging limits above a few volts.

Probe design differences are eliminated by requiring that only bobbin coil probes with 0.06 inch coils and 0.06 inch spacing between coils be used for voltage measurements. These values are commonly used by nearly all probe vendors. The voltage amplitude is a function of coil to coil spacing. For differential responses and a center to center coil spacing of 0.12 inch, the influence of small changes in coil spacing such as associated with manufacturing tolerances is small. This sensitivity is shown in Figure 8-21.

The calibration uncertainty results from dimensional tolerances in fabricating the standards. The effects of dimensional tolerances in S/G tubing result in a spread of the voltage/burst correlation as the tolerances may affect both voltages and burst pressure and thus are not categorized as an NDE uncertainty. The calibration standard variability for Kewaunee S/G applications is eliminated by requiring that the field standards be calibrated against the laboratory standard. The differences between calibration correction factors have been minimized by normalizing voltages to a four through wall hole ASME standard rather than the 20% depth holes. Voltage sensitivity to manufacturing tolerances for the through wall holes is expected to be smaller than found for 20% depth holes.

The probe centering uncertainty is limited by requiring probe replacement if individual hole voltages for an axially staggered, four through wall hole wear standard vary by more than a probe wear allowance between the initial or new probe values and subsequent measurements. Thus this uncertainty is limited by field data collection requirements. The probe wear allowance

includes voltage repeatability uncertainties (found to be ~ 5% as shown in Figure 8-19) for a new probe and a wear allowance for additional repeatability variation. For the Kewaunee data acquisition requirements, the probe wear allowance represents the total significant NDE voltage uncertainty. Pending additional field experience with the probe wear standard, an expected 10% NDE uncertainty for probe wear has been increased to a 15% objective for the EC guidelines and conservatively included as 20% in establishing the Kewaunee S/G plugging limits in Section 12.

Table 8.9 identifies variables which led to spread or uncertainties in the voltage/burst correlation. Crack morphology variations are the principal contributor to spread in the burst correlation. Voltage amplitude does not define a unique crack morphology but rather a range of morphologies and associated burst pressures with the empirical relationship established by the voltage/burst correlation. The correlation relates the EC sensitivity and burst pressures to the degradation morphology. To date, emphasis in developing the burst correlation has been placed on axial ODSCC with crack branching and limited IGA which represents the Kewaunee S/Gs and many other plants. Assessments of increased IGA involvement will be performed as data become available. Currently available data for IGA involvement indicates that the current burst correlation tends to envelope IGA and IGA/SCC modes of degradation. Section 8.1 shows comparable voltage responses, Section 9.8 includes available Plant L data with IGA/SCC in the burst correlation, and Section 9.9 shows that burst results for uniform IGA specimens are consistent with the burst correlation.

Human factor variability in interpreting signal amplitudes becomes less significant for application of the voltage plugging limits than for 50% depth limits, for which indications are evaluated at or near the detection threshold such that many of the indications have a poor signal to noise ratio. Under these circumstances, it is expected that the human factor plays a greater role in determining the accuracy of the inspection. The voltage limits move the amplitude of concern for tube plugging to generally higher signal to noise ratios so that human factors and details of interpretation guidelines become less significant. The variability in voltage growth rates found in Section 5 from prior Kewaunee operating experience reflects the nature of corrosion as well as the variability of measurements. Given that the indications are on the order of the detection limit as noted above and that no criteria were applied for assuring probe centering or calibration standards, the trends in these figures are to be expected. As noted in Table 8-9, the use of field voltage measurements for pulled tubes obtained prior to implementing the present voltage calibration requirements contributes to the spread or uncertainty in the burst correlation. The fluctuations in growth are expected to decrease as the voltage amplitude increases and as the voltage calibration standards are implemented. The field experience on voltage growth shown in Figure 6-12 reflect this trend.

Uncertainties associated with field crevice conditions, like the human factors, are more significant at the low amplitudes near detection thresholds than at the voltage plugging limits. This has been the experience in Kewaunee S/Gs where distorted indications have been primarily low amplitude indications. Again, the larger amplitudes near voltage plugging limits provide more reliable quantification of the indications than associated with current experience with depth limits for tube plugging.

An uncertainty in the burst correlation that adds some measure of conservatism to the correlation is the effect of tube pull forces on crack morphology and potential reduction in burst pressures. Although not a major concern for axial indications, effects of the tube pull such as loss of ligaments can occur. Since pre-pull field voltage amplitudes rather than post-pull values are used in the burst correlation, the pull force effects add conservatism. Post-pull

voltages are commonly higher than pre-pull values.

The NDE uncertainties are utilized in SLB leakage analysis as well as to establish the tube plugging limits. For probabilistic leak rate evaluations, such as described in Section 11.4, a distribution for the NDE uncertainty is required. As noted, the uncertainty is bounded at 15% by the requirements for probe replacement. The distribution can be conservatively developed from the data of Figure 8-19 using the test results for 0.02" probe wear. The standard deviation is ~10% of the measurement average. The NDE uncertainty distribution can then be represented as a normal distribution centered at the measured voltage with a standard deviation of 10%, but with the distribution cutoff at ±15% or 1.5 standard deviations.

Overall, the NDE uncertainty reflects measurement repeatability and is dominated by probe wear allowances which can be limited to [ ][a] by field implementation of a probe wear standard. Burst correlation uncertainties are dominated by crack morphology variations which are accounted for by application at the lower 95% uncertainty on the burst correlation for tube plugging limits.

8.9 Smaller Diameter Probe

The 720 mil diameter bobbin coil probe is normally used for EC testing of the 0.875 inch OD tubes. At Kewaunee, this size probe cannot pass through hot leg sleeves or small radius U-bends for inspection from the cold leg. Under such conditions a smaller diameter probe has been utilized. A 680 mil diameter probe was tested as follows to derive the plugging criterion for the smaller diameter bobbin coil probe.

The probe was tested in an ASME standard in both vertical and horizontal configurations. The tests in the vertical position were conducted by manually pulling the probe through the standard. The horizontal tests were performed by machine pulling of the probe which provides a uniform probe speed. In each configuration, the tests were repeated several times with the standard rotated (around its own axis) between tests. In the horizontal position, due to gravitational force, the probe will be located adjacent to the bottom wall of the standard. Hence the signal amplitude will be influenced by the orientation of the standard, i.e., the location of the hole in the standard in relation to the probe. Therefore, a larger variation in amplitude may be expected when tests are conducted in the horizontal position with different orientations of the standard. In the vertical position, the probe is likely to be more concentric with the wall of the standard. Hence a smaller variation in amplitude may be expected from repeat tests. Since the tubes in the S/G are vertical, the vertical configuration is more representative of the field conditions.

Results were evaluated for both the 20% holes and the 100% (through wall) hole in the ASME standard. Proper inderstanding of the results requires recognition that in the standard, the 100% hole consists of a single hole whereas the 20% hole configuration is made up of four holes in the same axial position, located 90 degrees apart. As a consequence, the results from the 20% holes are likely to show less variation and are of limited significance in the current discussion.

For the 100% through wall hole in vertical configuration, the standard deviation of signal amplitudes was [ ][a] of the mean amplitude (mean of results from the vertical position). The minimum (lowest amplitude tested) was [ ][a] less than the mean. In the horizontal configuration, the standard deviation of the signal amplitudes was [ ][a] of the mean (mean of results from the horizontal position). The minimum signal in this configuration was [ ][a]

less than the mean. As expected, the variation is much greater in the horizontal position. The maximum amplitudes are not listed here since they are not relavent (nonconservative) in the development of the plugging criteria. Since eddy current testing of the S/G tubes is conducted with the tubes in the vertical position, results of tests in the vertical configuration are more relevant for field application. This suggests an NDE uncertainty of 17% (standard deviation) for the 680 mil diameter probe.

The results for the 20% holes are provided below although they are not used in the development of the criteria for reasons discussed above. In the vertical position, the standard deviation of signal amplitudes was [ ]^{a} of the mean and the minimum amplitude was [ ]^{a} less than the mean. In the horizontal configuration, the standard deviation of the amplitudes for the 20% holes was [ ]^{a} of the mean and the minimum signal was [ ]^{a} less than the mean. The test deviations are higher for the vertical than for the horizontal configuration. This is believed to be attributable to the hand pulling of the probe in the vertical configuration resulting in variable pull speeds.

Based on the above results, an NDE uncertainty of 17% may be applied for the smaller diameter (680 mil) probe for the development of the plugging criteria. It is expected that the additional uncertainty arising from probe wear will be small for the 680 mil diameter probe because 1) it has greater clearance between the probe and the tube ID thereby resulting in smaller wear rate and 2) some of the wear related (i.e., due to greater distance between the probe and the flaw) uncertainty is already reflected in the 17% uncertainty value. Therefore, the NDE uncertainty value of 20% conservatively applied for the 720 mil diameter probe may also be used for the 680 mil diameter probe. Further, in light of the substantial conservatism included in the voltage growth rate estimates (see Table 12.2), it is believed that additional increases in the NDE uncertainty estimate above 20% is not warranted.

8.10 Conclusions

1. The use of probes from Echoram or Zetec has negligible influence on the data acquisition for the tube plugging criteria.

2. For indications with amplitudes greater than 2 volts the presence of the tube support causes only small changes in indication response for the ODSCC specimens.

3. Small indications, where their amplitude approaches the size of the mix residual, can be influenced by the presence of the support.

4. The eddy current response is essentially unaffected for a packed tube to tube support plate crevice as compared to an open crevice.

5. Large amplitude cracks which are likely to have oxide coating on the crack surfaces remain detectable by eddy current in the presence of minor denting. Small amplitude cracks and cracks with clean crack surfaces (i.e., fatigue generated cracks) may be masked by the dent signal for dented intersections.

6. Probe centering characteristics, related to probe wear, can contribute to the uncertainty of the eddy current signal. This uncertainty was found by probe wear test simulations to be about [ ]^{a} to envelope typical field probe replacements. Probe wear influence on the

signal uncertainty can be controlled by the use of an appropriate wear standard. The staggered 4-hole standard will be applied at Kewaunee to limit the voltage amplitude uncertainties from probe wear to [ ][a] for the 720 mil diameter probe.

7. Use of a reference ASME standard for voltage calibration and calibration of the 400/100 kHz mix channel are recommended for application of the tube plugging criteria. Calibration at the mix frequency is recommended to minimize effects of variations in frequency response between probes.

8. NDE uncertainties contribute to the spread or uncertainty in the voltage vs burst pressure correlation and tend to lower the structural limit for tube burst which is based on the lower 95% confidence interval. The use of reference calibration standards, frequency mixes, etc. are directed toward minimizing the NDE uncertainties associated with voltage measurement repeatability. Other NDE considerations remain as part of the burst correlation uncertainty although the principal variable in the burst uncertainty is crack morphology differences.

Table 8.1

Effect of Flaw Location on Bobbin Coil Measurements*

Flaw Location	50% Deep Slot		100% Deep Slot	
	Voltage	Depth	Voltage	Depth
1. Slot centered in TSP	0.95	43%	47.4	100%
2. Slot extending from TSP edge inside TSP	0.95	72%	48.1	100%
3. Slot extending from TSP edge outside of TSP	1.07	36%	49.3	99%
4. Slot without a TSP	1.07	49%	48.7	99%

* Measurements for 0.25 inch long EDM slot in 0.75 inch diameter tubing.

Table 8.2

Typical Voltage Amplitude for Volumetric Types of Degradation

Type of Degradation	Voltage Examples	Comments
Wastage		
o Characterized by machined rectangular flaws	~4.5-7.5 volts @60% depth(1)	Data of Figure 8-8
Fretting		
o Characterized by machined, tapered flaws	~10 volts @60% depth(1)	Data of Figure 8-8
Pitting		
o Single drilled hole simulation	~7.5 volts for 60 mil dia., 100% deep	Data of Figure 8-9
	~5.3 volts for 109 mil dia., 60% deep	Data of Table 6.4
	~2 volts for 30 mil dia., 100% deep	Data of Figure 8-9
o Multiple pits	~2 volts multiple indications for multiple pits up to 60 mils in diameter and 64% deep	Pulled tube example

Note 1. Typical limiting depths for continued service allowing 10% for EC uncertainty and about 5% for growth between inspections.

Table 8.3

Bobbin Coil Detectability of EPRI IGA Samples

Specimen No.	Differential B. C. Volts	Differential B. C. Depth	Absolute B. C. Volts	Absolute B. C. Depth	Comments
[redacted]					

* Voltage measurement represents the peak at the start or end of the IGA. Peak to peak differential voltage would be about twice the single peak value for comparison with the absolute voltages and for comparison or correlation with ODSCC degradation at TSPs.

Table 8.4

Comparison of the EDM Notch Amplitude Response of Probe ZT and Probe ER (Ratio Probe ZT /Probe ER)

Notch Depth	400 kHZ	200 kHz	100 kHz	Mix 400/100 kHz
100 %	1.07	1.70	1.94	1.01
80 %	0.98	1.67	1.93	0.94
60 %	1.05	1.67	1.90	0.94
40 %	1.04	1.70	1.87	0.91

Table 8.5

Comparison of ASME Hole Amplitude Response of Probe ZT and Probe ER (Ratio Probe ZT/ Probe ER)

Hole Depth	Response Ratio 100/400 kHz Mix
100 %	1.58
80 %	1.54
60 %	1.55
40 %	1.53

Table 8.6

Comparison of Tight (Magnetite Packed) and Open Crevices for Probe Z and Probe ER (Ratio Tight/Open)

Sample	400/100 kHz Mix	
	Probe Zt	Probe Er
BW-8	1.05	1.08
BW-10	1.01	1.03
BW-11	1.51*	1.54*
BW-14	0.95	0.97
BW-17	0.96	0.94
BW-12	0.91	0.93

* Caused by process of packing the crevice as verified by comparing the pre-packed response with the tube response after removal of the magnetite packing.

Table 8.7

Influence of Denting on Indication Response

Sample	400/100 Mix Amplitude		
	Before Denting volts	After Denting volts	Dent Size volts
Fatigue			
FAT-1	61.5	18.6	7.39
FAT-2	14.6	5.42	6.09
FAT-3	NT	2.39	12.1
FAT-4	59.0	NDD	12.08
FAT-7	NT	1.24	9.43
FAT-8	69.0	NDD	17.4
Doped Steam			
BW-1	8.9	18.0	14.7
BW-3	12.5	3.97	6.27
BW-9	4.21	4.9	6.36

NT No Test
NDD No Detectable Degradation

Table 8.8

Laboratory Specimen NDE Summary(1)

Sample Number	Probe Type	Flaw Amplitude (V)	Phase (°)	Flaw(4) Depth (%)	Flaw(4) Length(in)	No. of Flaws
[redacted]						

(1) As received Specimens, Prior to Leak Test. Data are average results for Echoram EE-720-FsbM-UF and Zetec A-720-ULC(775) Bobbin Probes and Echoram EB-720-2XSRPC and Zetec 720-MRPC Pancake Probes.
(2) Specimen had multiple axial indications.
(3) Second NDE after initial leak testing.
(4) RPC depth is for the deepest crack and length for the total crack network.

Table 8.8 (continued)

Laboratory Specimen NDE Summary(1)

Sample Number	Probe Type	Flaw Amplitude (V)	Phase (°)	Flaw(4) Depth (%)	Flaw(4) Length(in.)	No. of Flaws
[redacted]						

(1) As received Specimens, Prior to Leak Test. Data are average results for Echoram EE-720-FstM-UF and Zetec A-720-ULC(775) Bobbin Probes and Echoram EB-720-2XSRPC and Zetec 720-MRPC Pancake Probes.
(2) Specimen had multiple axial indications.
(3) Second NDE after initial leak testing.
(4) RPC depth is for the deepest crack and length for the total crack network.

Table 8.8 (continued)

Laboratory Specimen NDE Summary(1)

Sample Number	Probe Type	Flaw Amplitude (V)	Phase (°)	Flaw(4) Depth (%)	Flaw(4) Length(in.)	No. of Flaws
[redacted]						9

(1) As received Specimens, Prior to Leak Test. Data are average results for Echoram EE-720-FsbM-UF and Zetec A-720-ULC(775) Bobbin Probes and Echoram EB-720-2XSRPC and Zetec 720-MRPC Pancake Probes.

(4) RPC depth is for the deepest crack and length for the total crack network.

Table 8.9

Variables Influencing NDE Voltage and Burst Correlation Uncertainties

NDE Voltage Uncertainties (Voltage Repeatability)

- Probe centering: probe diameter and wear considerations(1)
- Calibration standards: dimensional tolerances(2)
- Probe design differences(3)

Burst Correlation Uncertainties

- Crack morphology (length, depth, ligaments, multiple cracks, IGA involvement) variability for same voltage amplitude
- Tubing dimensional tolerances(4)
- Human factors affecting voltage repeatability that are not adequately controlled by data analysis guidelines
- Variations in field crevice conditions (open, packed, deposits, TSP corrosion, small dents, etc.)(5)
- Effects of tube pull forces on crack morphology and associated burst pressures(6)
- Utilization of voltage measurements for pulled tubes obtained prior to implementing voltage measurement standards of this report

Notes:

1. Eliminated in laboratory specimens by using 0.720" diameter probes with minimal wear and a single calibration standard.
2. Insignificant for Kewaunee application as standards are calibrated against reference laboratory standard.
3. Significant uncertainty eliminated by specifying coil to coil spacing.
4. The influence of tubing dimensional tolerances as they affect burst pressure are inherently included in the spread of burst pressures from pulled tubes and laboratory specimens. The dimensional tolerances on calibration standards are eliminated by calibrating the field standards to the laboratory reference standard.
5. Assumes an adequate number of pulled tubes contribute to spread of burst correlation (see text discussion).
6. Results as pre-pull field measured voltages rather than post-pull voltages are used in burst correlation.

Figure 8-1

Voltage Sensitivity to Crack Network Morphology

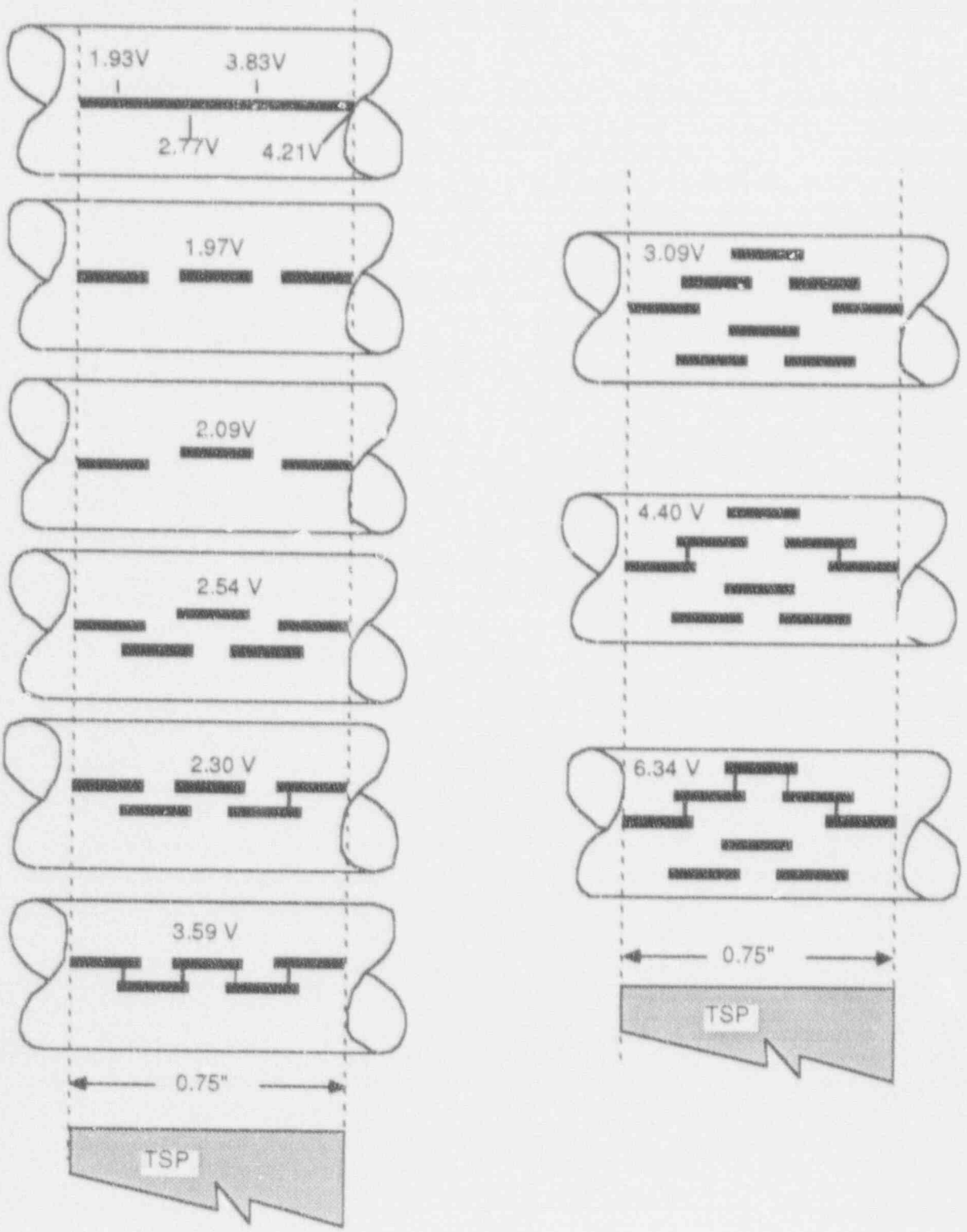

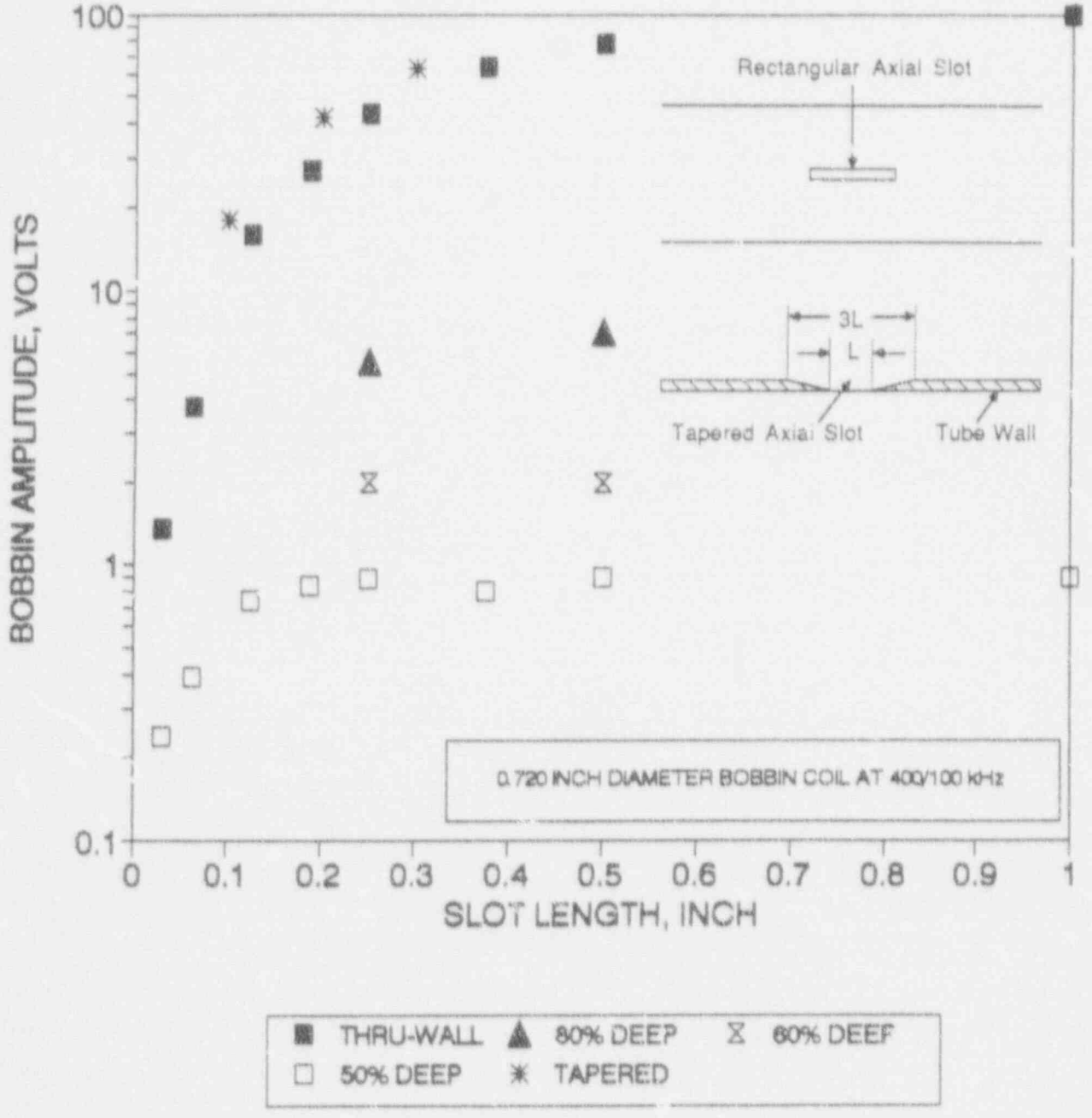

Figure 8-2. Bobbin Coil Voltage Dependence on Slot Length and Depth

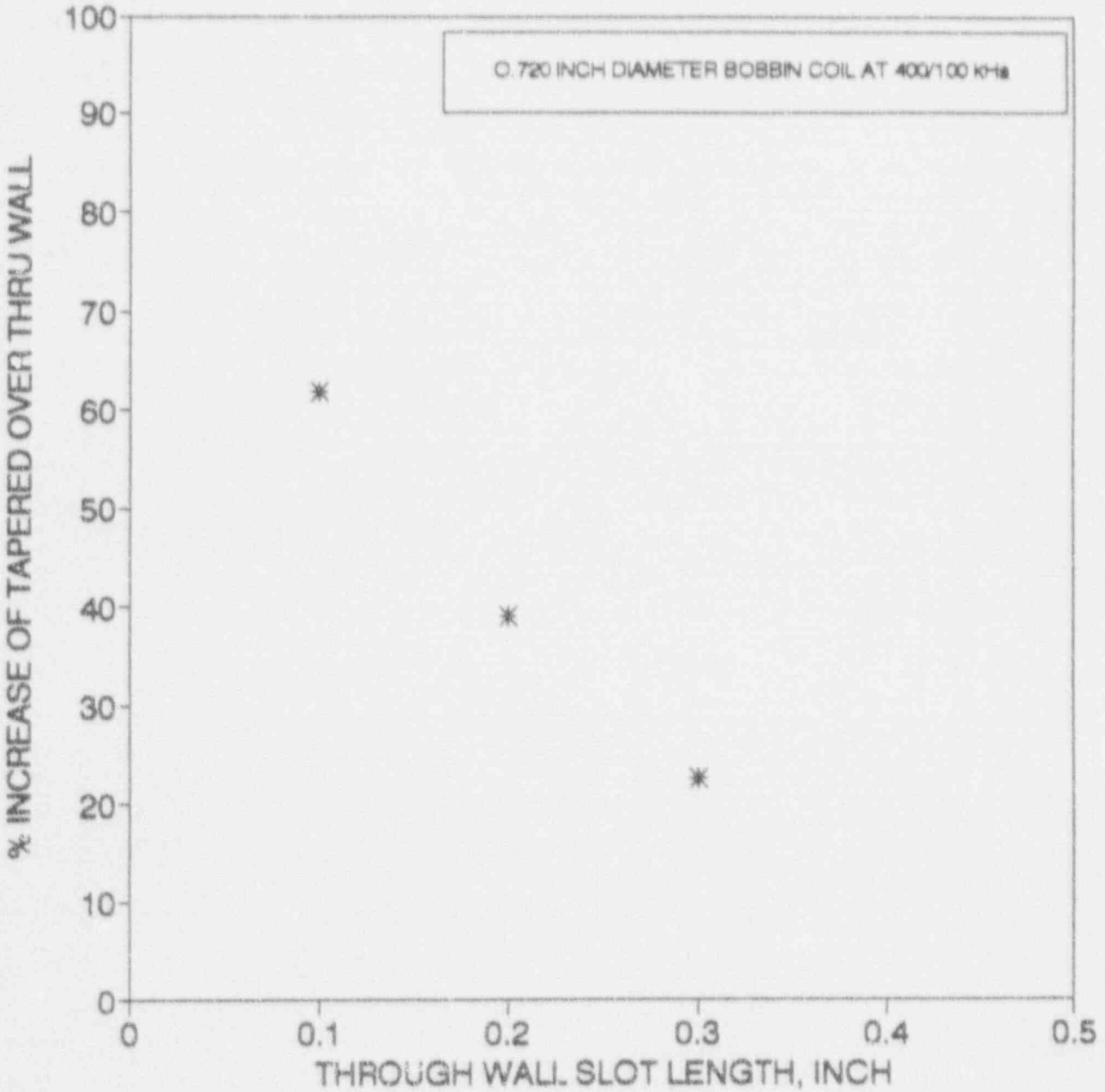

Figure 8-3. Bobbin Coil Voltage Increase due to Tapers at Ends of Through Wall Axial Slots

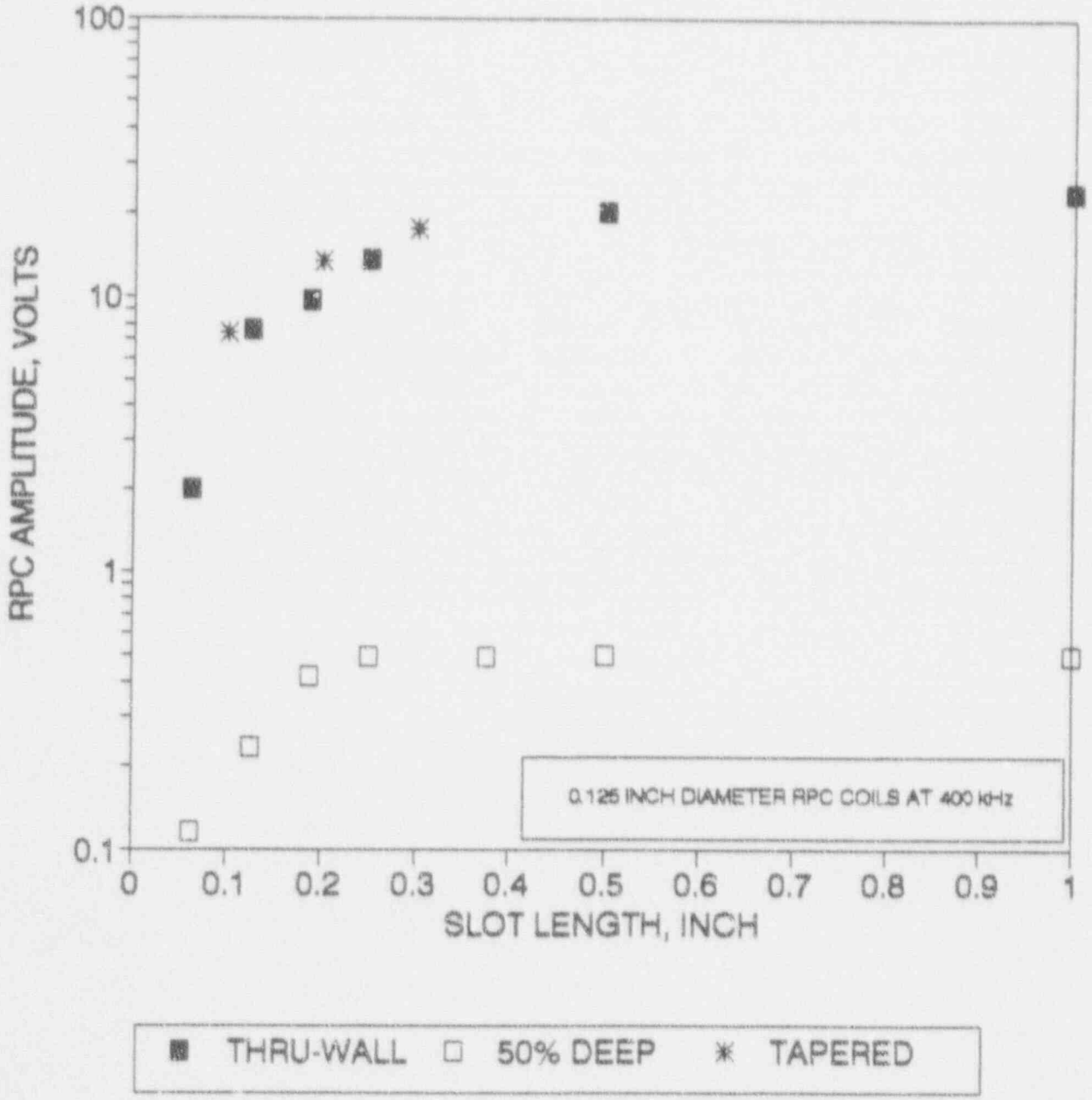

Figure 8-4. RPC Voltage Dependence on Slot Length and Depth

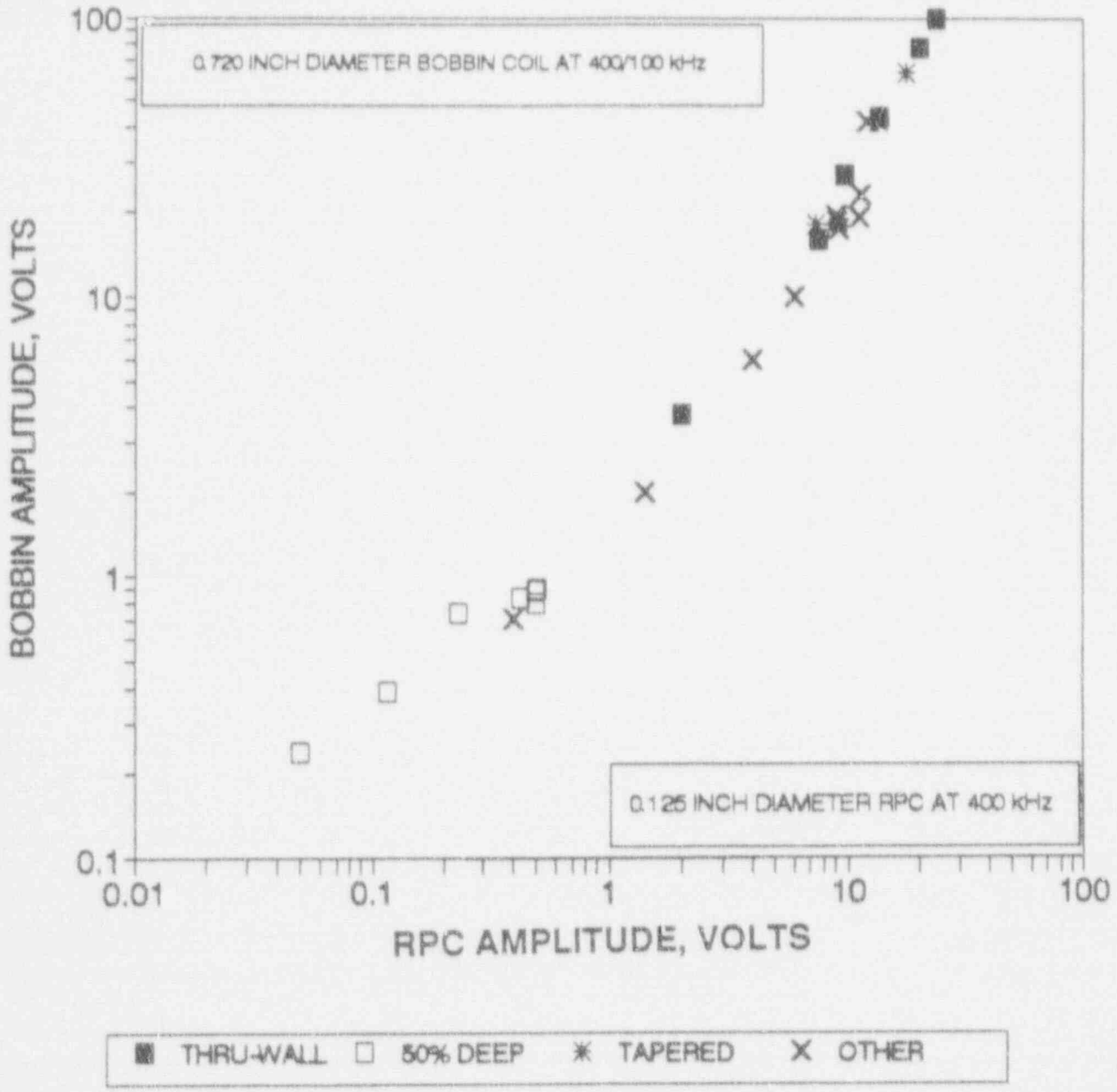

Figure 8-5. Correlation of Bobbin Coil to RPC Voltage

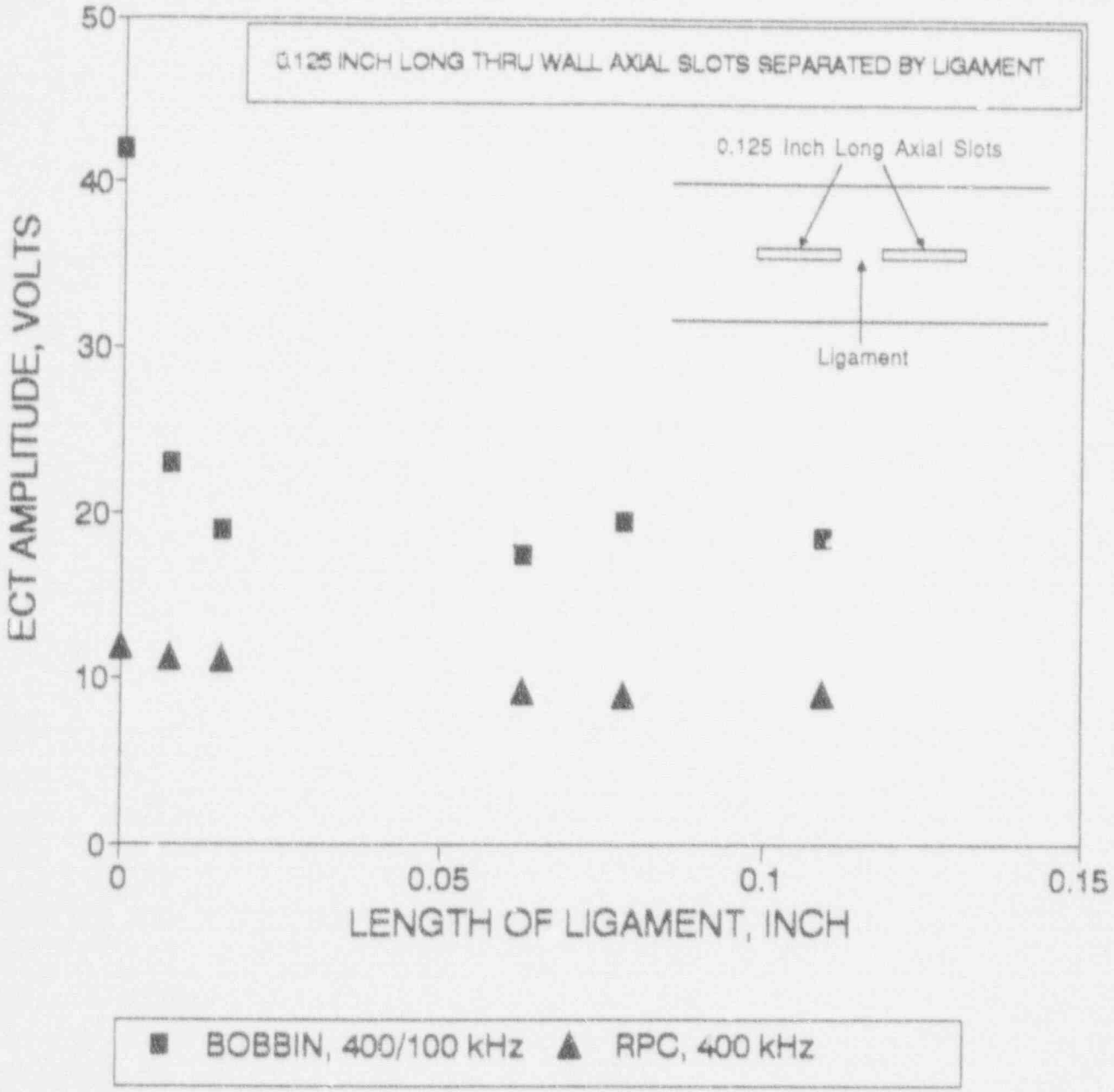

Figure 8-6. Bobbin Coil Voltage Dependence on Ligament Size Between Axial Slots

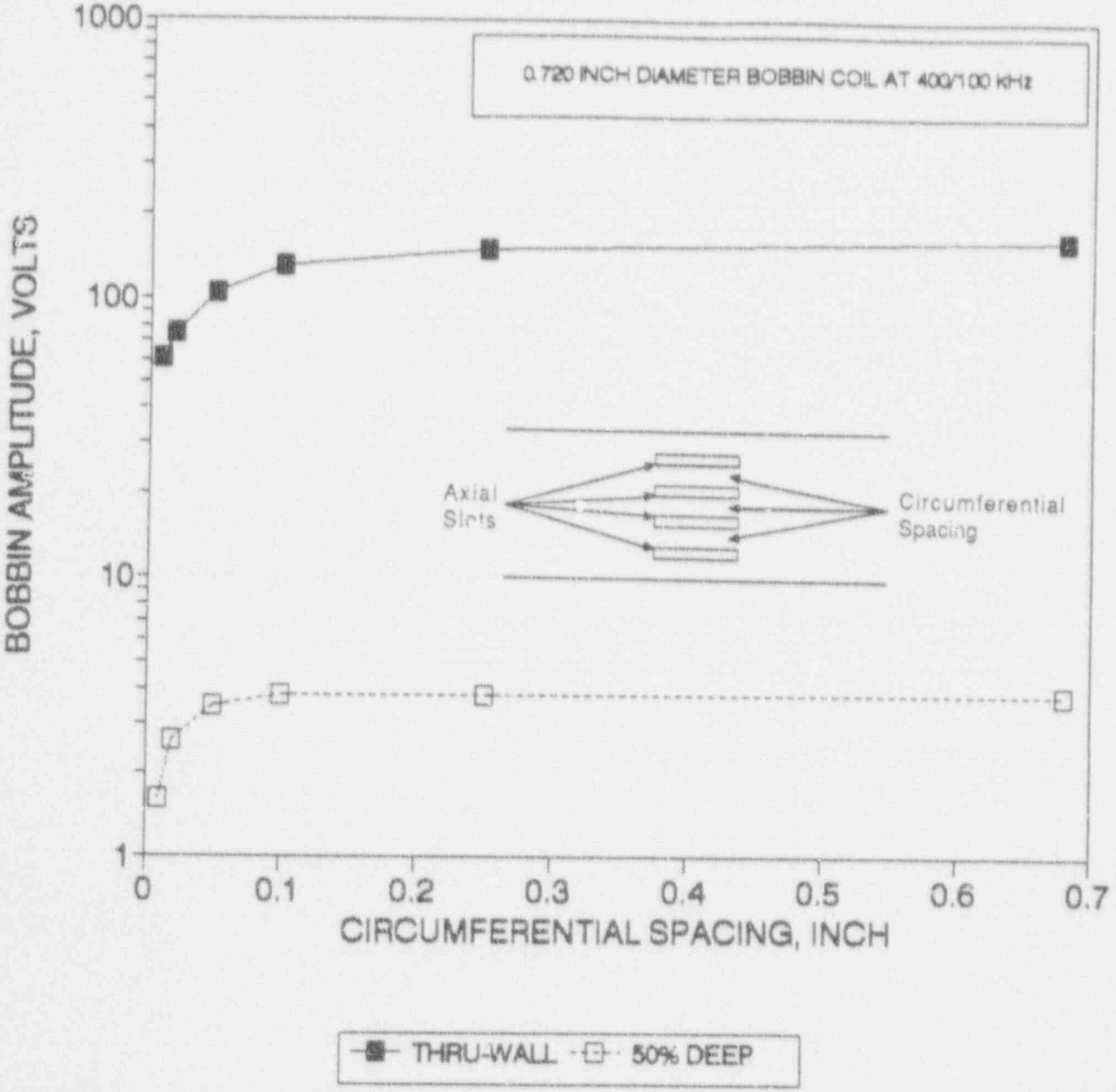

Figure 8-7. Bobbin Coil Voltage Dependence on Circumferential Spacing Between Axial Slots

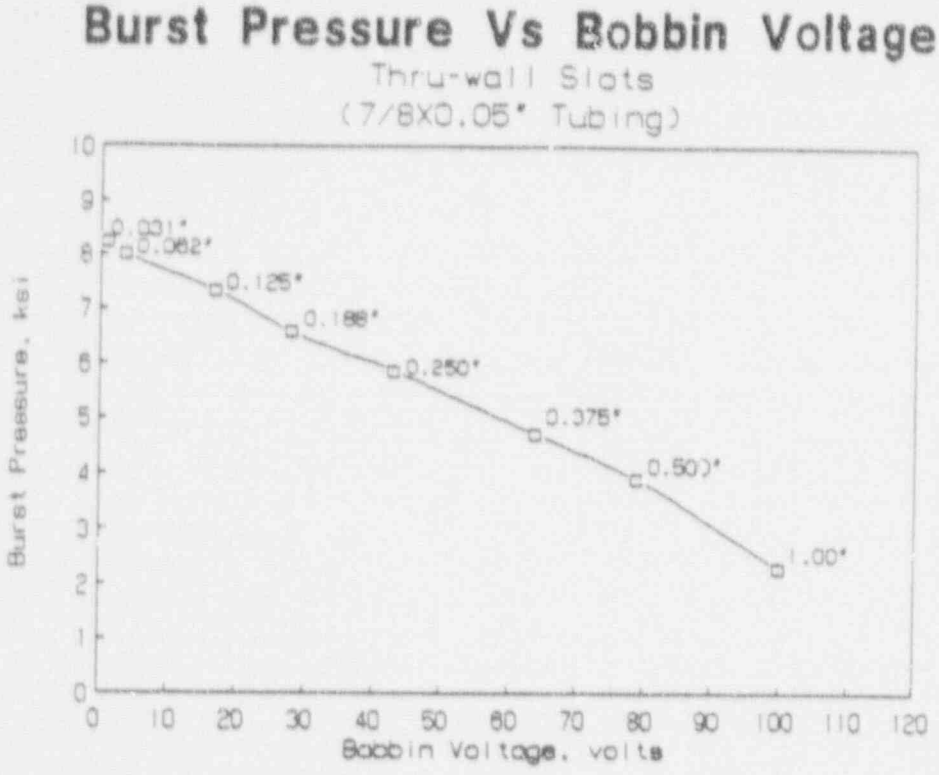

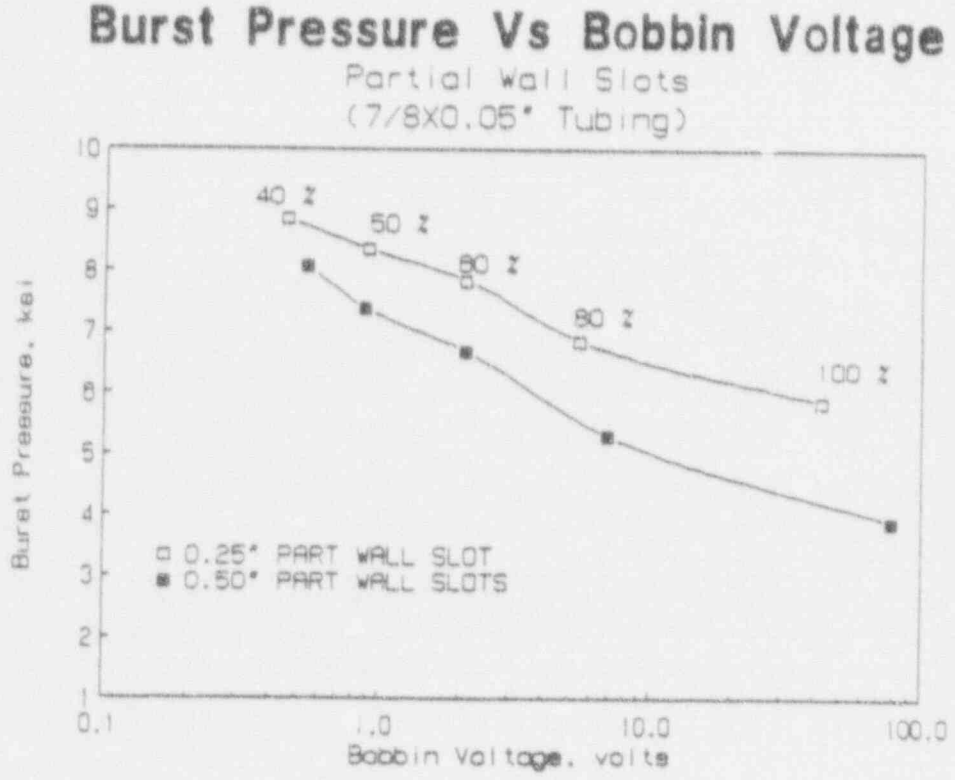

Figure 8-8. Burst Pressure vs Bobbin Coil Voltage for EDM Slots

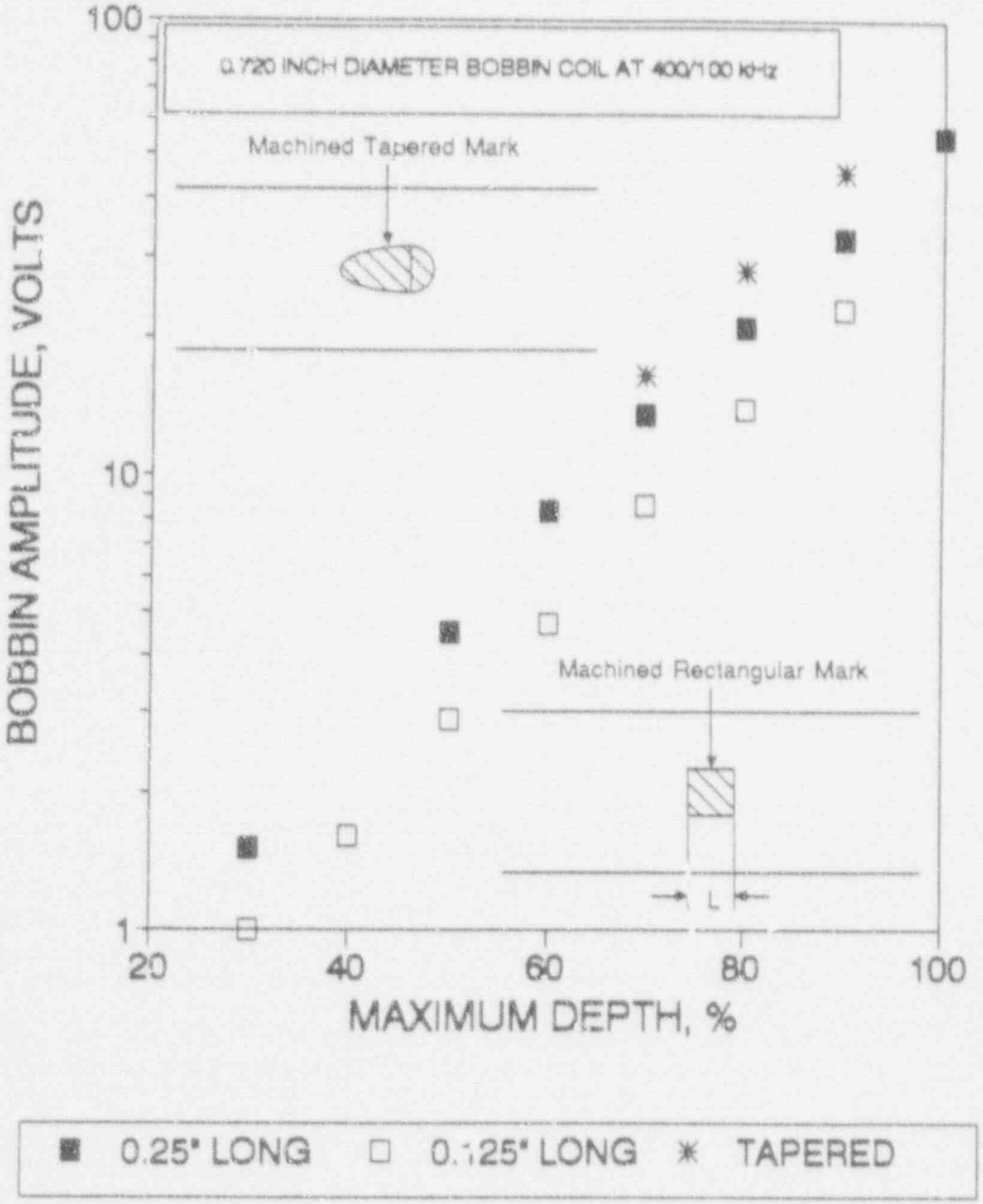

Figure 8-9. Bobbin Coil Voltage vs Depth for Simulated Volumetric Tube Degradation

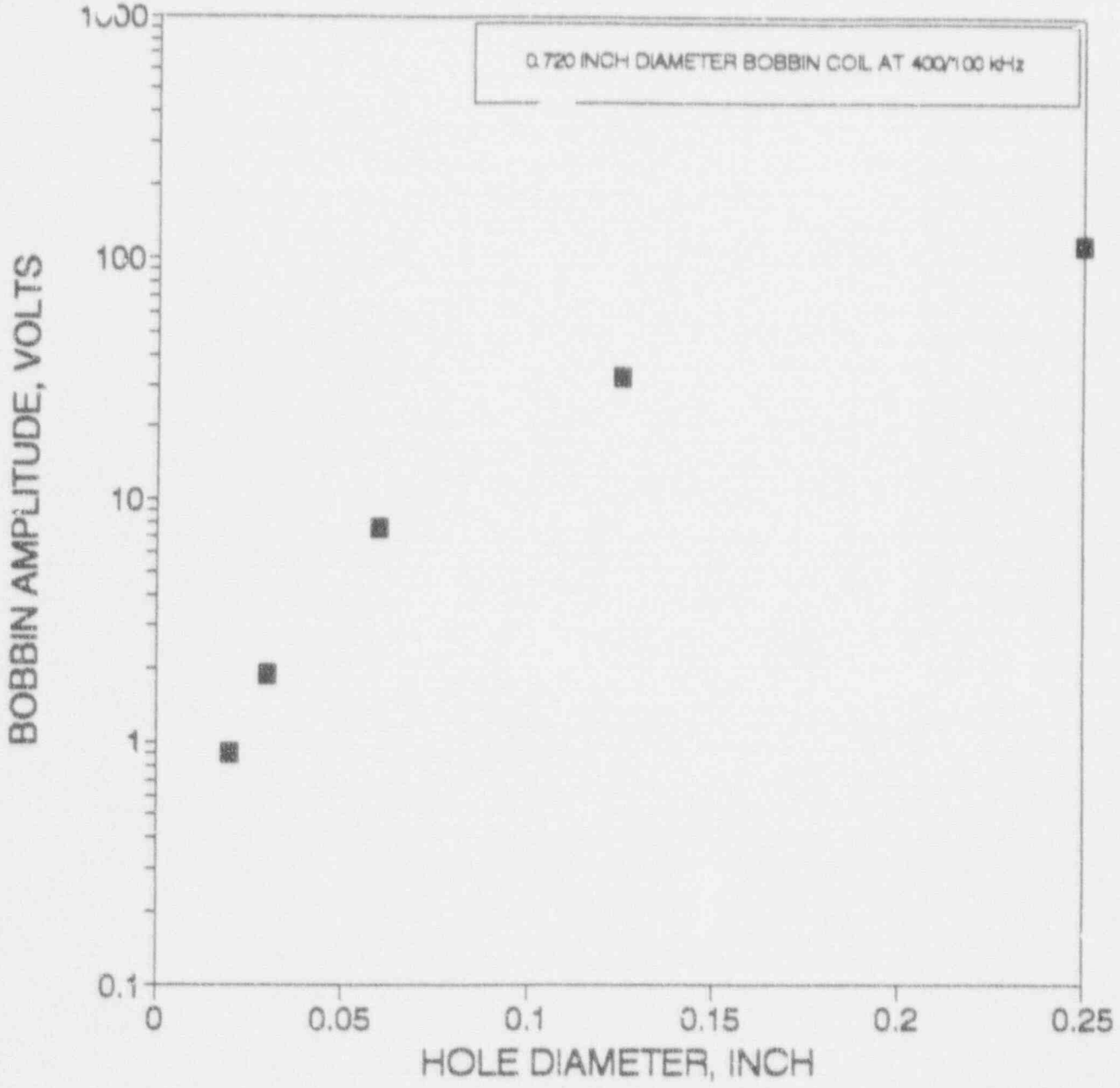

Figure 8-10. Bobbin Coil Voltage Dependence on Diameter of Through Wall Holes

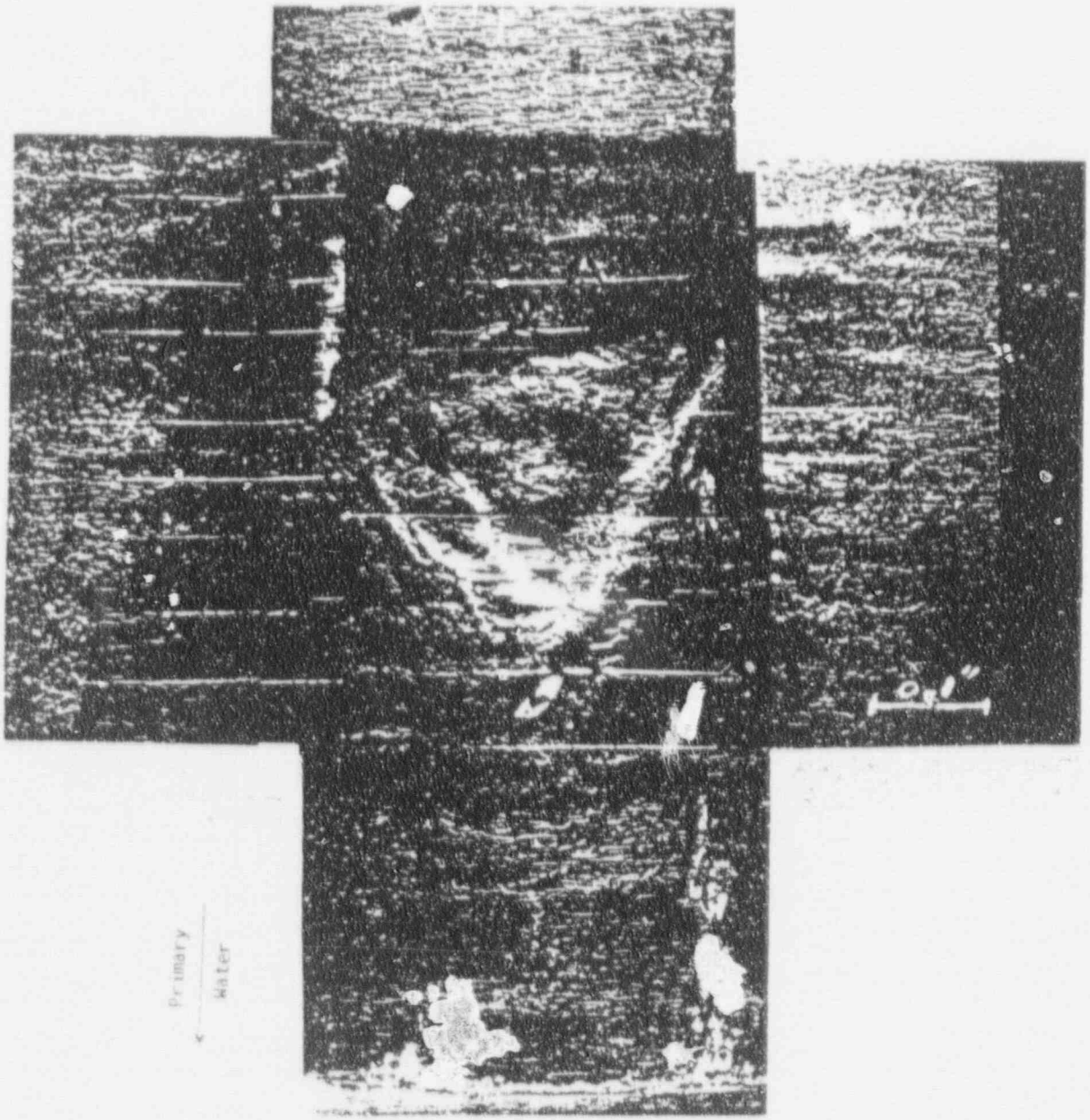

Figure 8-11. Photograph of Plant P-2 Pulled Tube With Cold Leg Thinning

Figure 8- 12a

Bobbin Data and Typical Metallographic Sections of Simulated IGA Specimens Using Sensitized Alloy 600MA Tubing

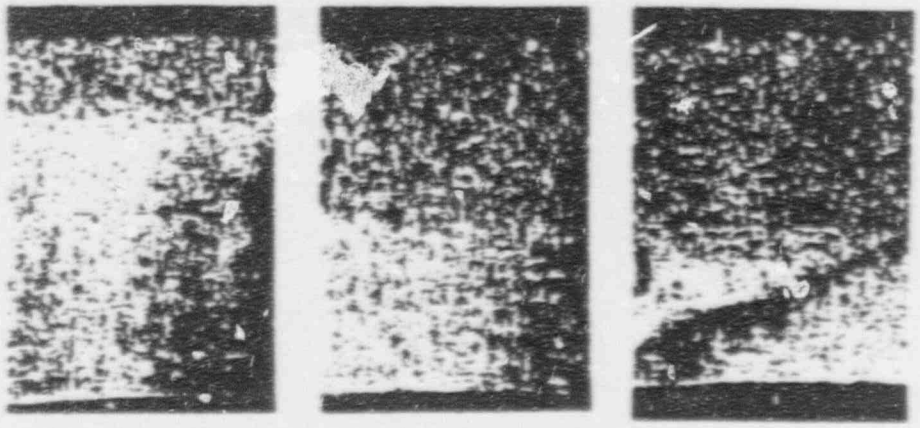

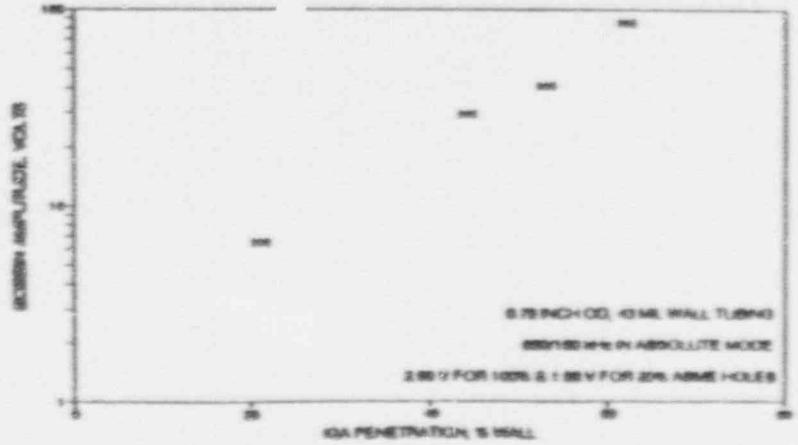

Figure 8- 12b

Bobbin Data from Simulated IGA Specimens Using Non-Sensitized Alloy 600MA Tubing

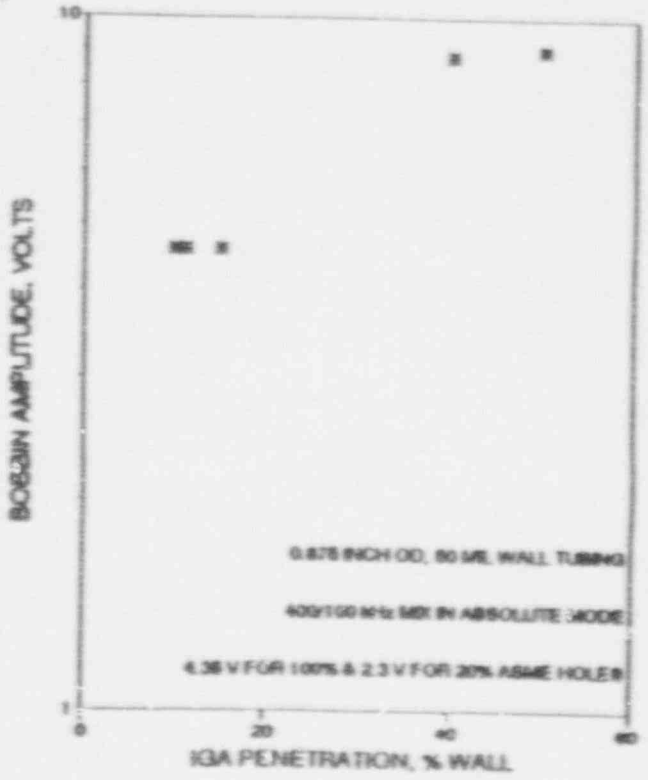

Figure 8- 12. Bobbin Coil Results for Laboratory IGA Specimens

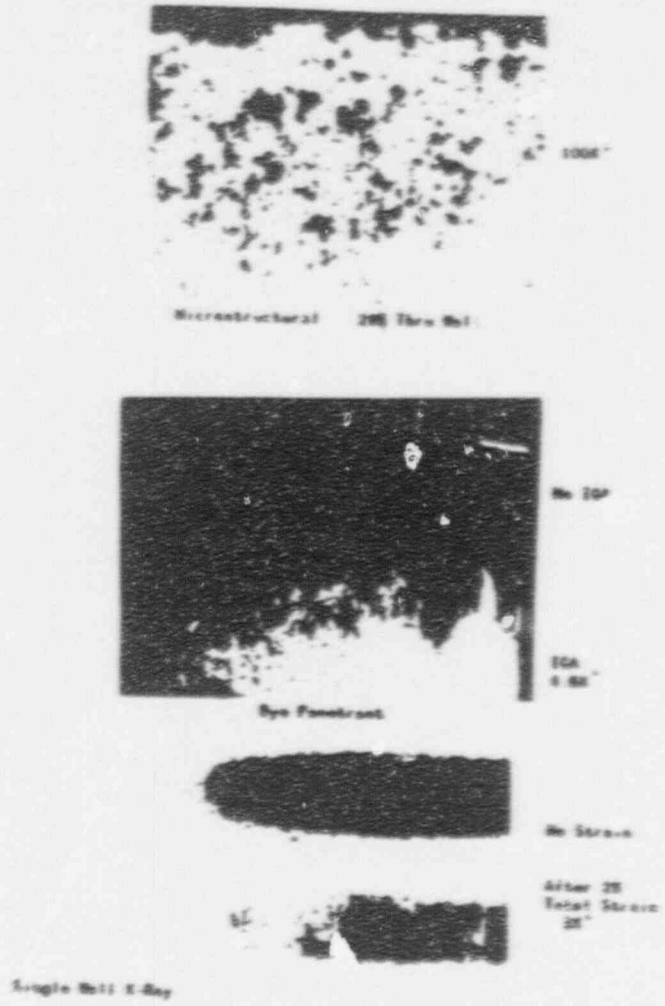

Figure 8- 13a. NDE Results for a Type 1 (IGA) Sample (Dye Penetrant and X-Ray)

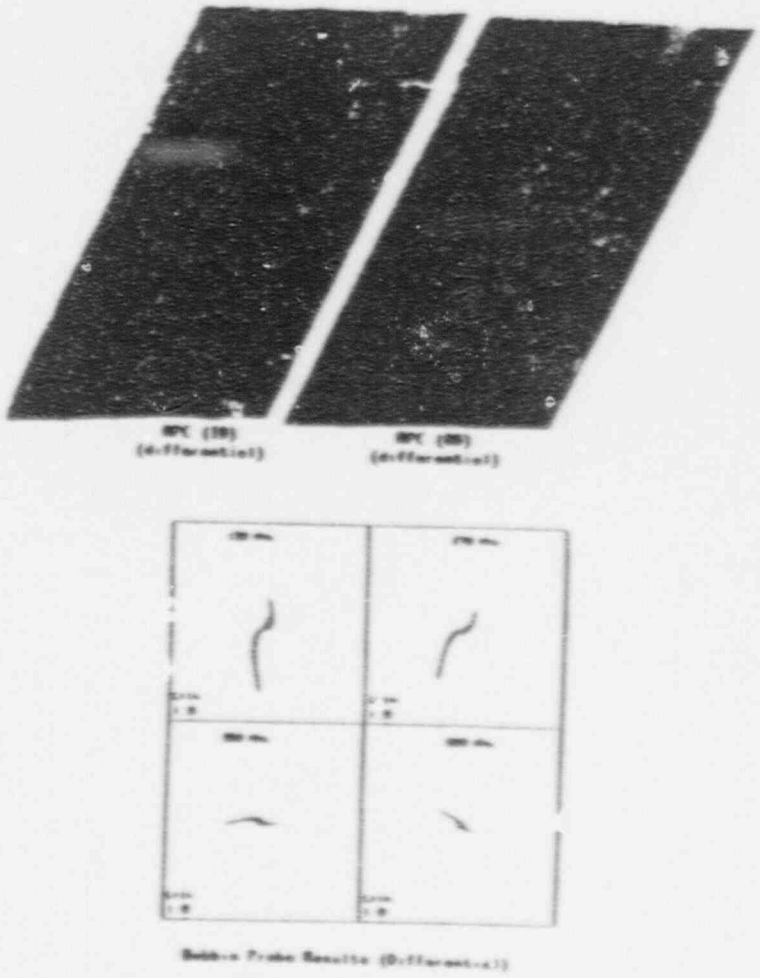

Figure 8- 13b. NDE REsults for Type 1 (IGA) Damage (Eddy Current)

Figure 8- 13. Inspection Results for Laboratory IGA Samples from EPRI Program

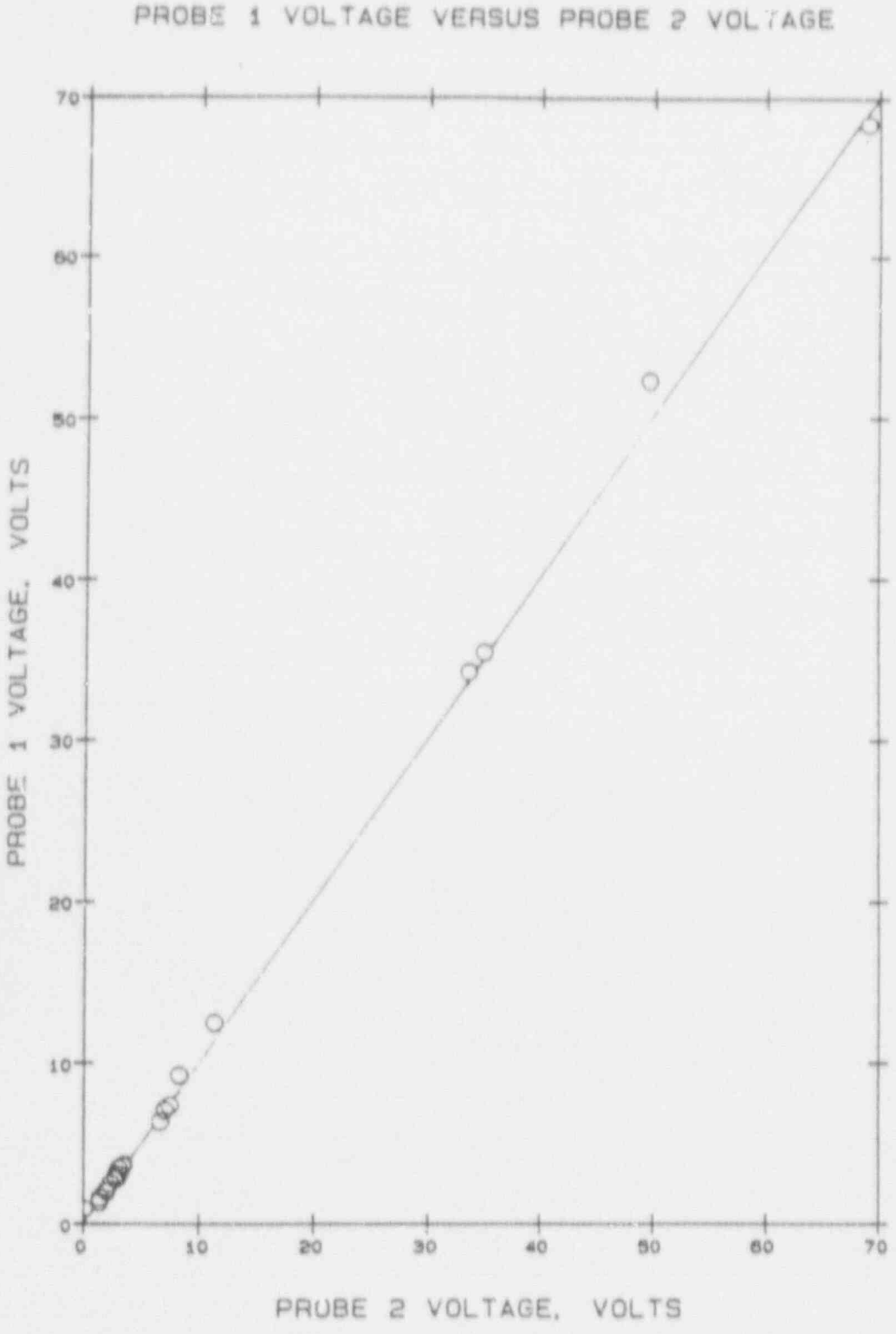

Figure 8-14. Voltage Comparison of Indications Found With Two Eddy Current Probes (400/100 kHz Mix)

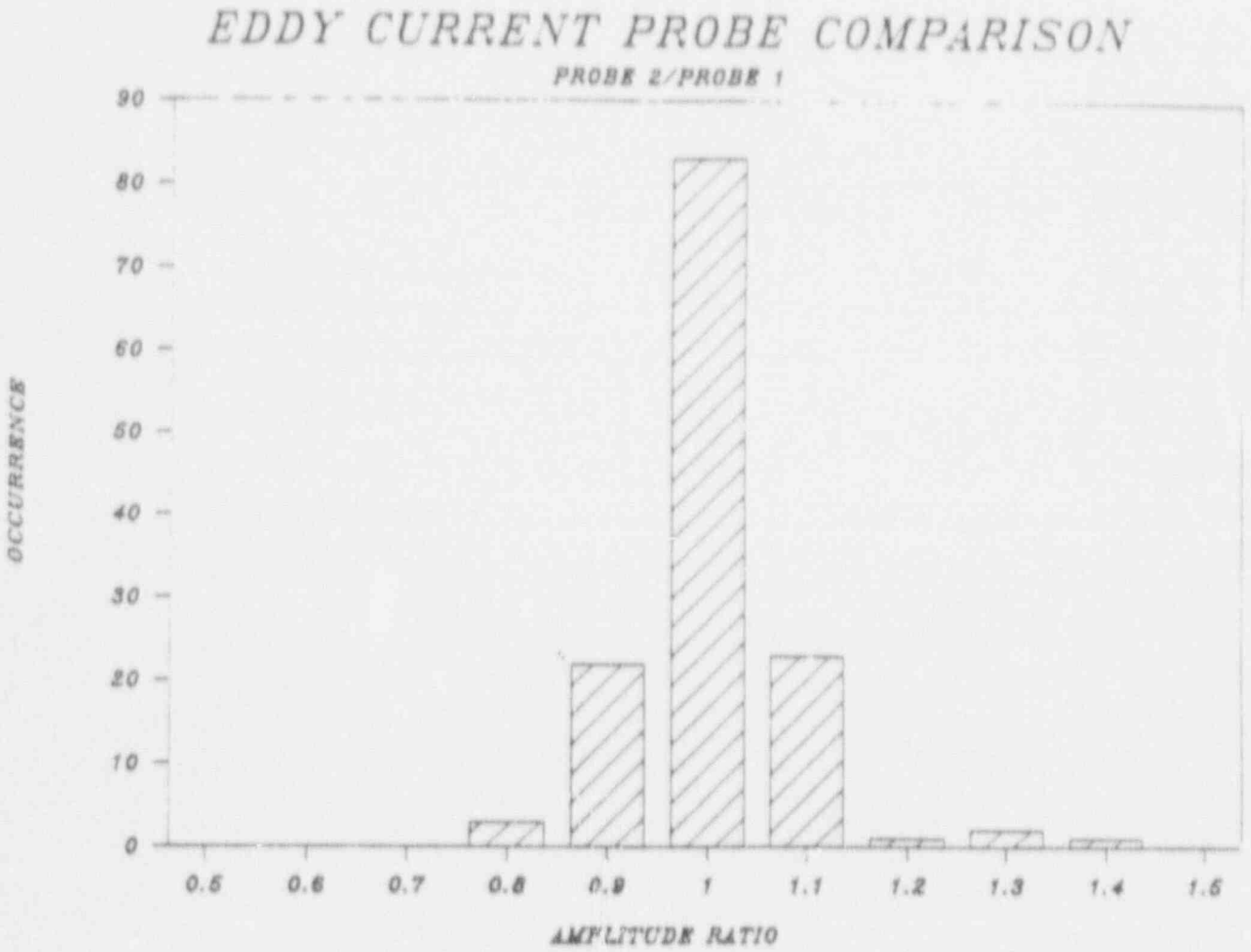

Figure 8-15. Comparison of 400/100 kHz Mix Amplitude Response from Two Probes (Model Boiler Sample)

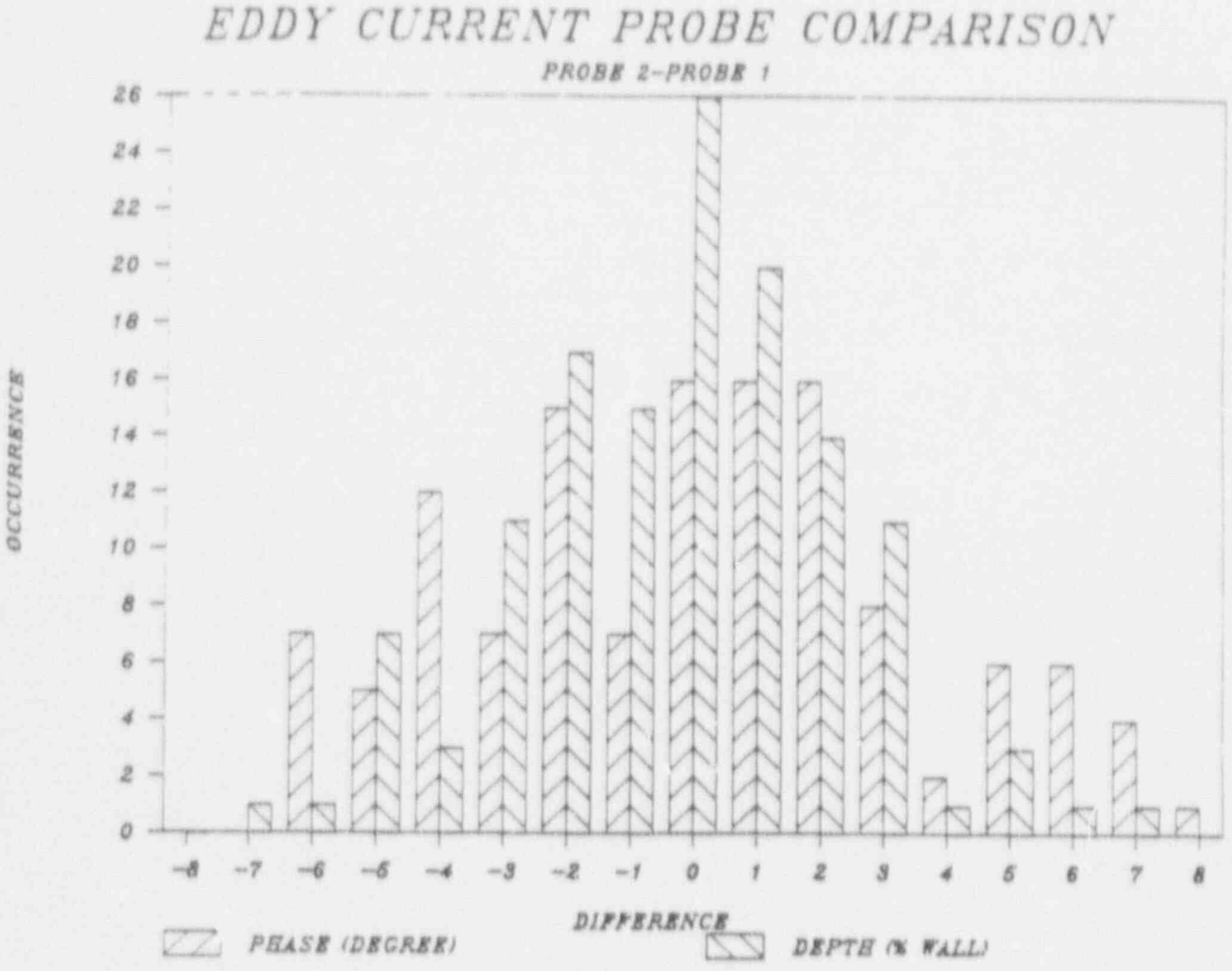

Figure 8-16. Comparison of 400/100 kHz Mix Phase Response form Two Probes (Model Boiler Sample)

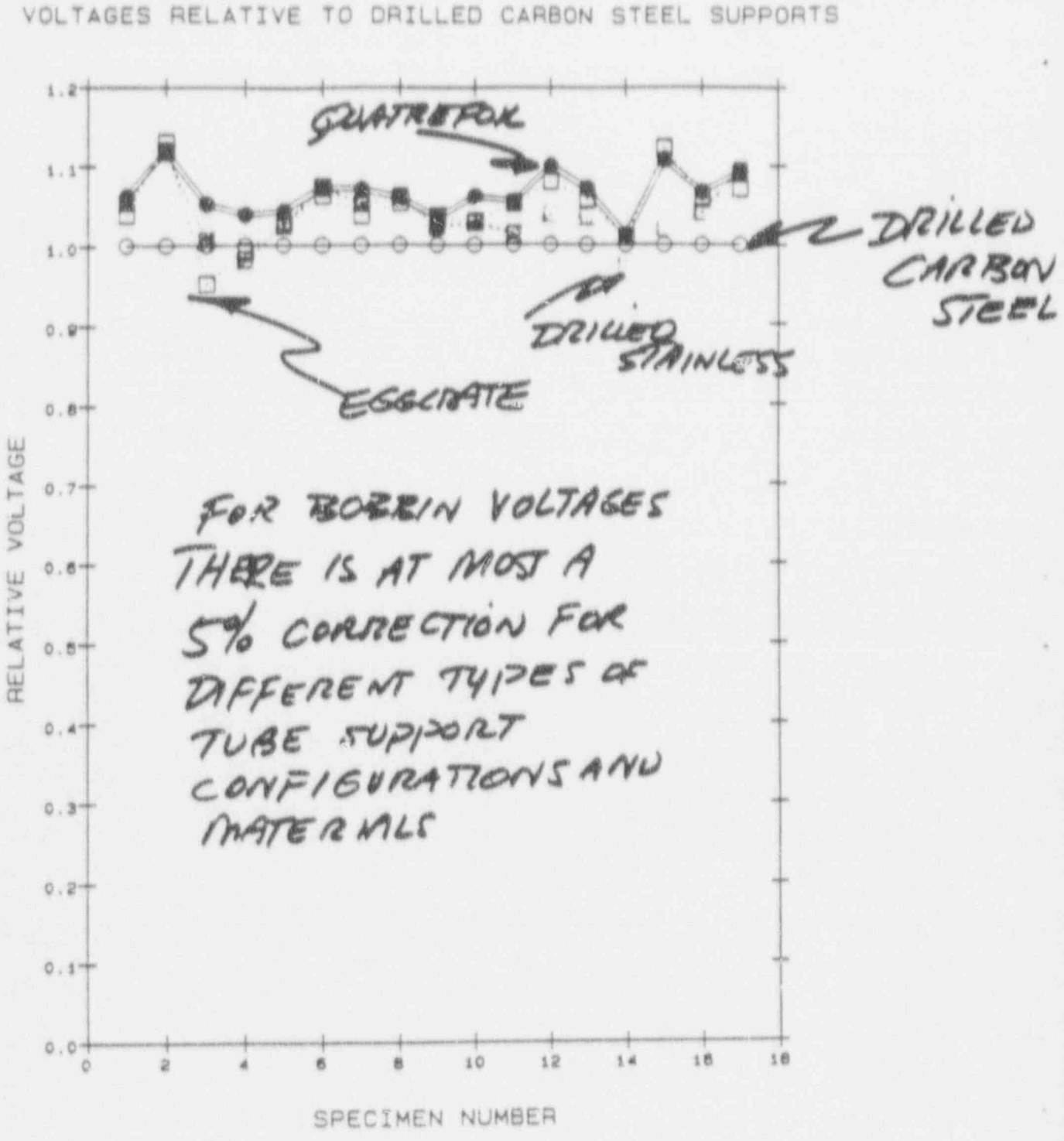

Figure 8-17. Comparisun of Tight and Open Crevice Indication Response

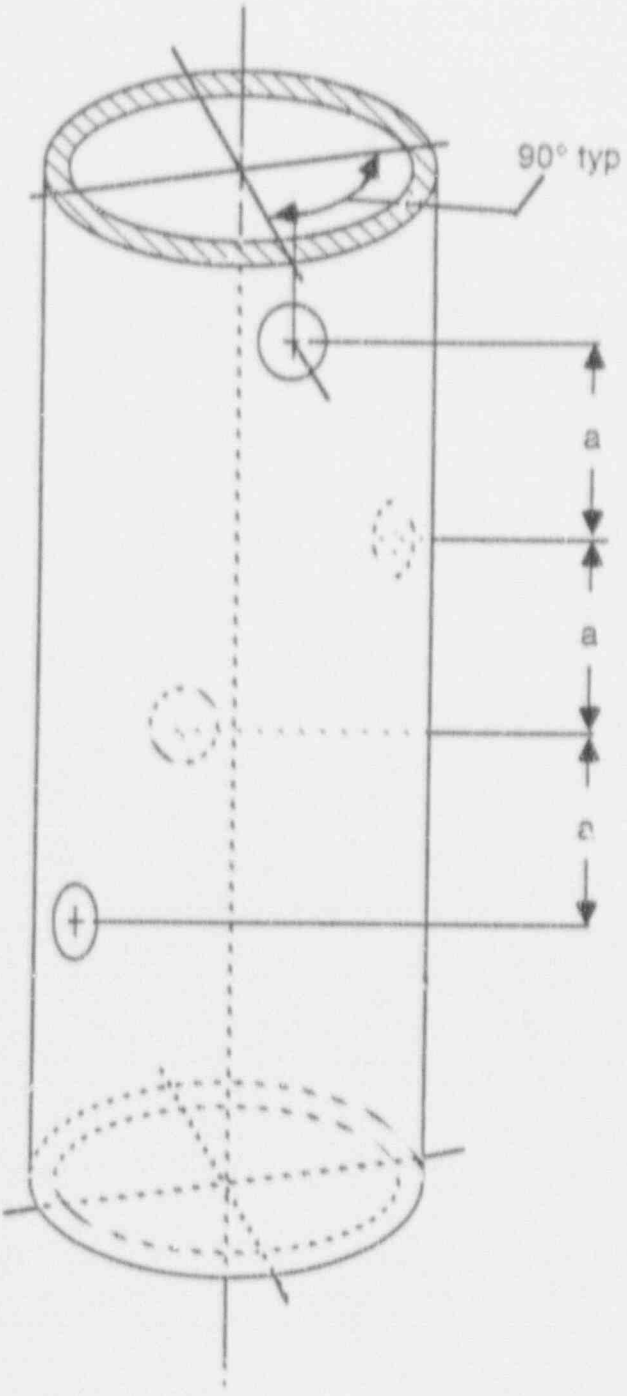

Figure 8-18. Probe Wear Calibration Standard

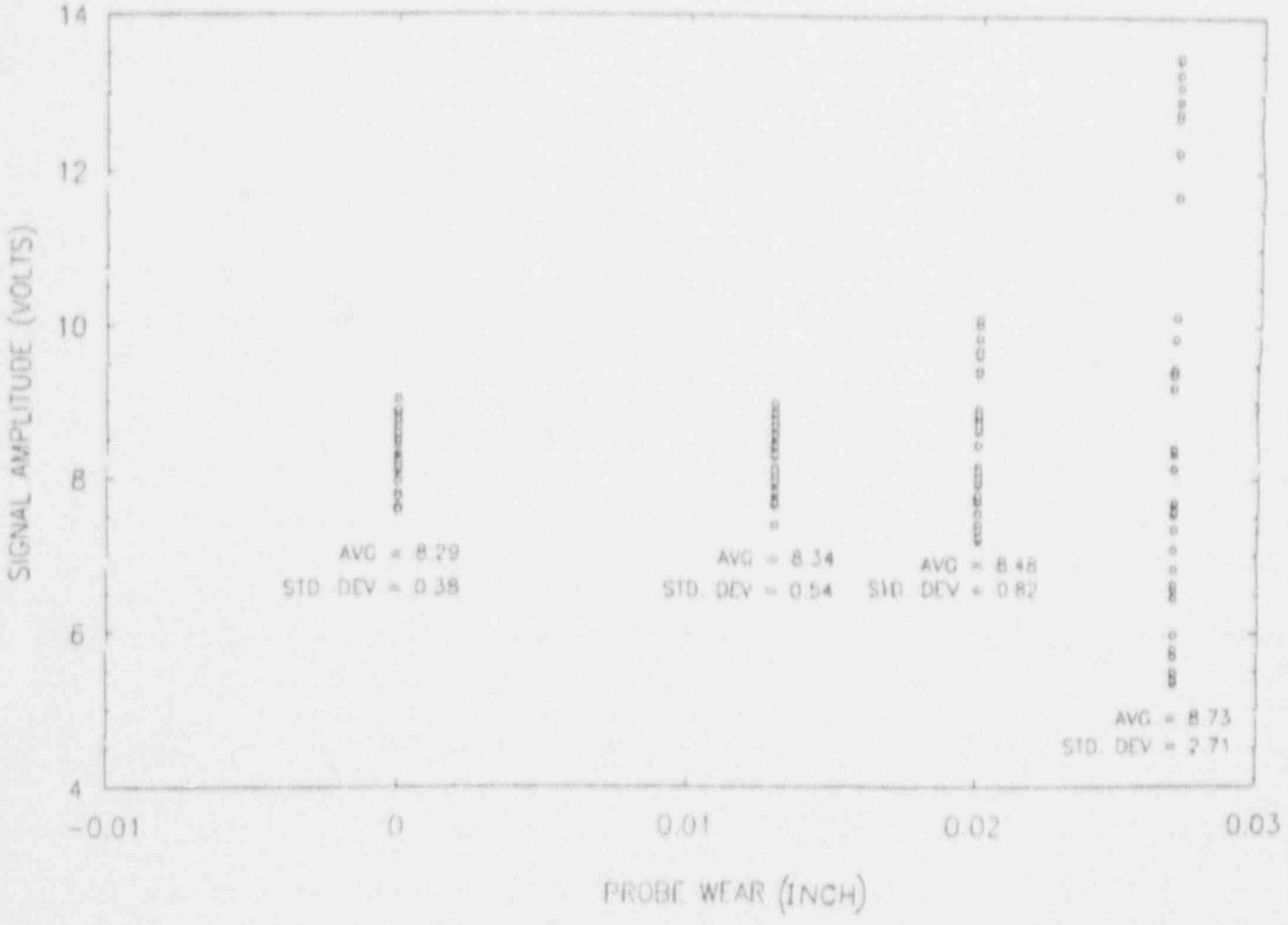

Figure 8-19. Bobbin Coil Amplitude Dependence on Probe Wear

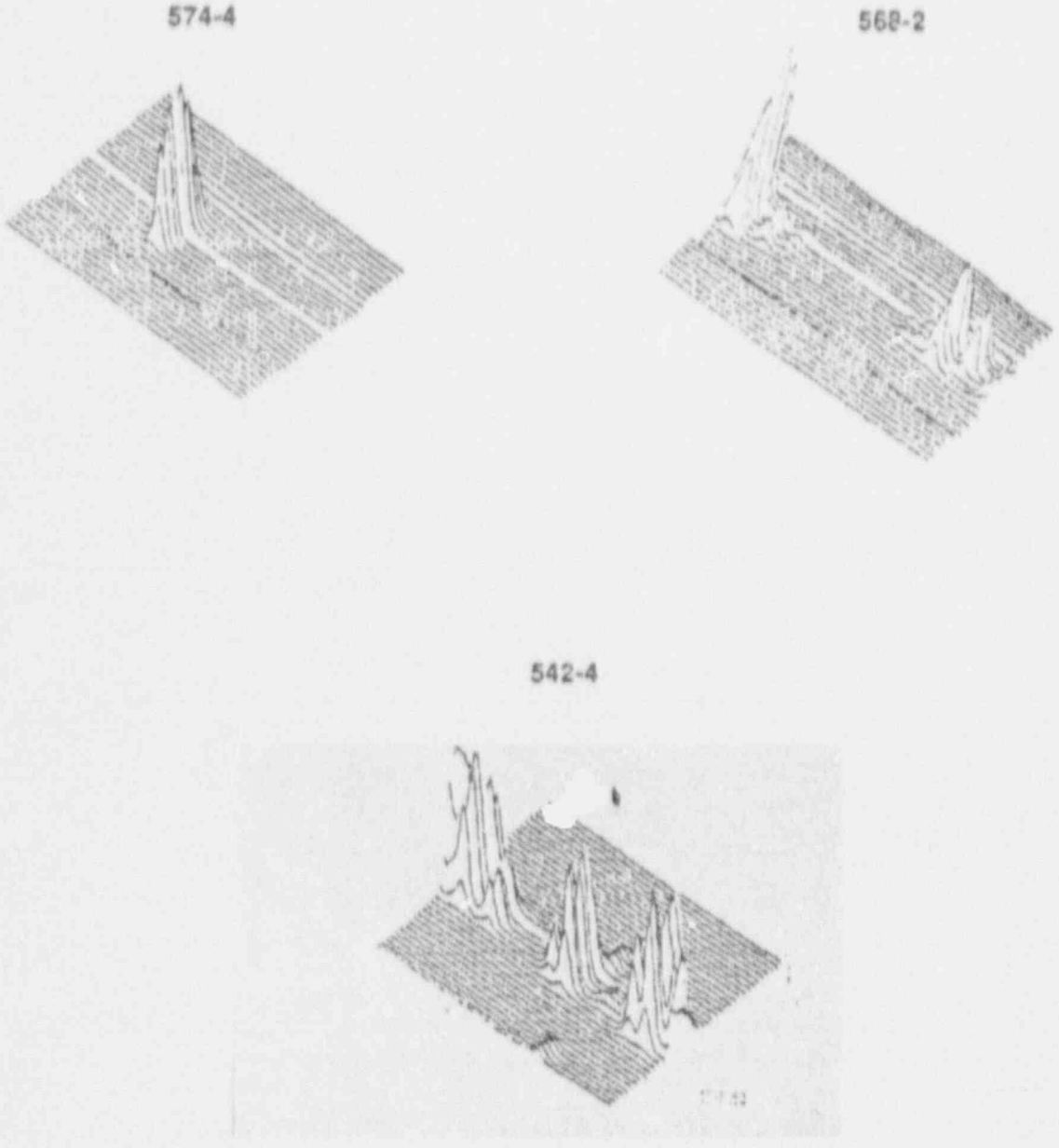

Figure 8-20. RPC Traces of Typical Model Boiler Specimens

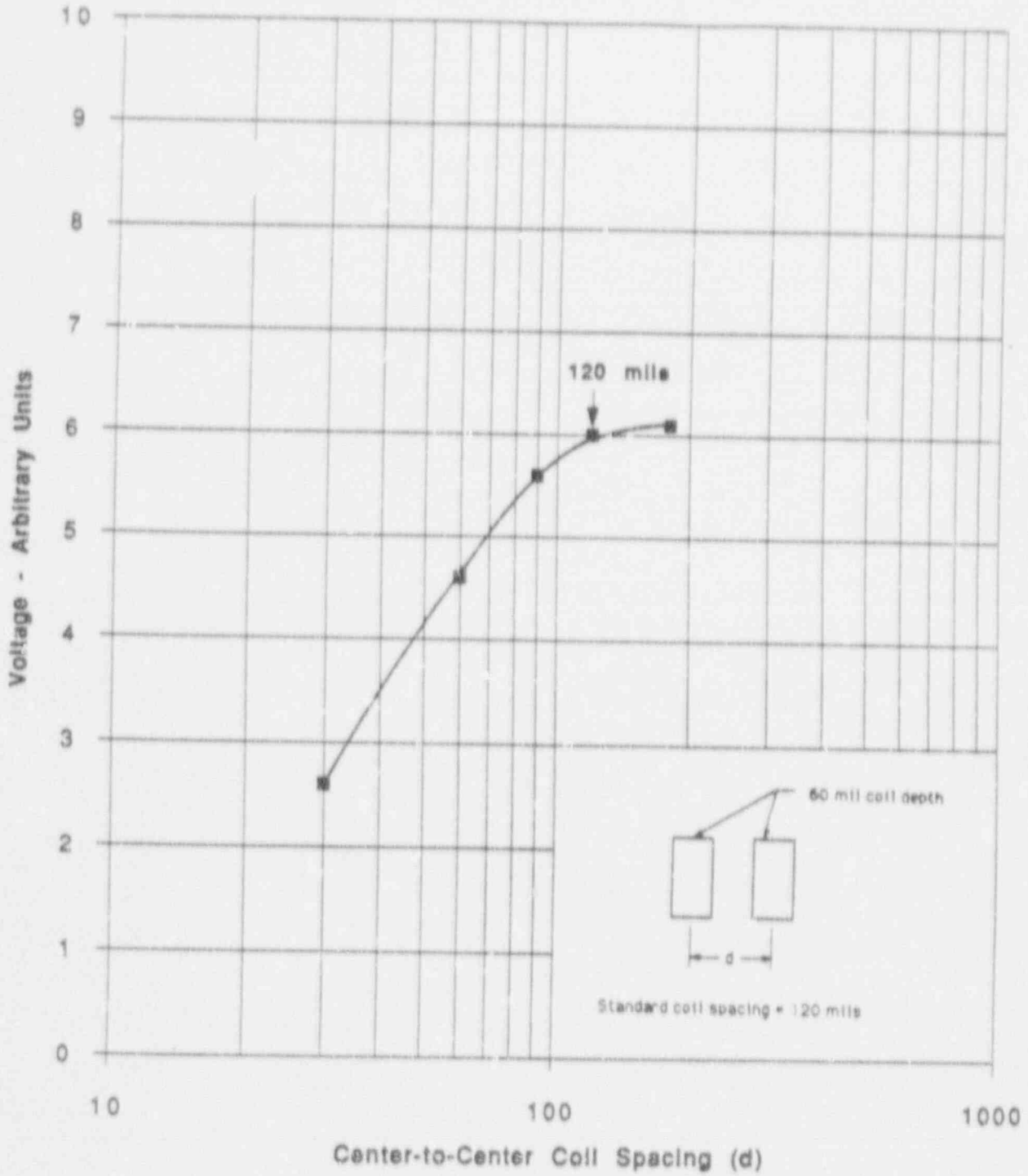

Figure 8-21. Bobbin Coil Amplitude Dependence on Center-to-center Coil Spacing

9.0 LEAK AND BURST TESTS

9.1 Objectives

The objective of the leak rate tests is to determine the relationship between eddy current characteristics and the leak rates of tubes with stress corrosion cracks. Leak rates at normal operating pressure differentials and under steam line break conditions are both of interest, since leakage limits are imposed under both circumstances. The SLB leak rate data are used to develop a formulation between leak rate and bobbin coil voltage.

Crevice condition is another important factor. Tightly packed or dented crevices are expected to significantly impede leakage through cracked tubes. Since denting is readily detectable by non destructive means while crevice gaps cannot be readily assessed, the emphasis is placed upon open crevices and dented crevices as the limiting cases.

Given the assumption that significant support plate displacements cannot be excluded under accident conditions, burst tests of tubes with stress corrosion cracks are conducted in the free span condition and burst pressure is correlated with bobbin coil voltage. This burst pressure correlation is then applied to determine the voltage amplitude that satisfies the guidelines of Reg. Guide 1.121 for tube burst margins.

9.2 Leak Test Procedure

Leak testing of cracked tubes is accomplished as follows. The ends of the tube are plug welded. One end has a fitting for a supply of lithiated (2 ppm Li), borated (1200 ppm B) and hydrogenated (1 psia) water to the tube inner diameter. The specimen is placed in an autoclave and brought to a temperature of 616 °F and a pressure of 2250 psi. The pressure on the outer diameter is brought to 1000 psi. A back pressure regulator on the secondary side maintains the 1000 psi pressure. Any leakage from the primary side of the tube tends to increase the secondary pressure because of the superheated conditions. The back pressure regulator then opens, the fluid is released, condensed, collected and measured as a function of time. This provides the measured leak rate. The cooling coil is located prior to the back pressure regulator to prevent overheating and to provide good pressure control. Typical leakage duration is one hour unless leak rate is excessive and overheating of the back pressure regulator occurs. Pressure is controlled on the primary side of the tube by continuous pumping against another back pressure regulator set at 2250 psi. The bypass fluid from this regulator is returned to the makeup tank.

To simulate steam line break conditions the primary pressure is increased to 3000 psi by a simple adjustment of the back pressure regulator and secondary side is vented within one to three minutes to a pressure of 350 psi. The pressure differential across the tube is thus 2650 psi. Temperature fluctuations settle out in several minutes and the leakage test period lasts for approximately 30 minutes.

9.3 Leak Test Results

A summary of leak test results is provided in Table 9.1. The first series of leak rate tests were conducted at the normal operating pressure differential. Some of the model boiler specimens had tightly packed crevices as a result of corrosion product buildup. These specimens were tested as is. Following this first series of leak rate tests, the welded end plugs were cut from the leak specimens. Because of the crack location and short length of some specimens additional leak rate testing could not be performed. Specimens with tight collars were subjected to extensive eddy current testing. This required removal of the tight collars. Hence all repeat testing of the first series of test specimens was performed under open crevice conditions. Repeat testing led to higher leak rates either as a consequence of the test itself, handling or forceful removal of tight collars. Only in one case did a non-leaker become converted into a leaker as a result of retesting. This case, 533-4, is one of forceful removal of a tight collar.

The steam line break conditions increased the leak rates by about a factor of three compared to normal operating conditions. More variation in this factor can be expected. Prolonged leak rate testing under operating conditions is expected to lead to lower rates. The increase in the leak rate upon transition to accident conditions then becomes more variable.

From Table 9.1, tight crevices are seen to be sometimes of benefit in reducing leak rates. Specimen 542-4 had a very high eddy current voltage and a low leak rate of [ ]9, while specimen 543-2 had a high voltage and a leak rate of [ ]9. The four other tight crevice specimens were non-leakers. Three of these remained non-leakers after removal of the tight collars. Damage during removal of the tight collar is suspected as the reason the fourth non-leaker became a leaker. Tight crevices can be of benefit in reducing leak rate but cannot be relied upon. Further, pending future developments, eddy current techniques have not been shown to be able to confidently distinguish between open and tight crevices although the presence of magnetite can often be detected in the crevice.

Eddy current inspection techniques are very sensitive to denting at tube support plate intersections. Dents of a fraction of a mil are easily detectable. Specimens with large through wall cracks which were then dented to less than one mil have not leaked significantly either at operating pressure or under steam line break conditions. A tight through wall fatigue crack 0.50 inch in length will leak at more than the typical tech spec limit of 0.35 gpm. From Table 9.1 it is evident that a small dent has turned such a cracked tube into a non-leaker. [

]9

9.4 Burst Test Procedure

Burst tests were conducted using an air driven differential piston water pump at room temperature. Pressure was recorded as a function of time on an X-Y plotter. Sealing was accomplished by use of a soft plastic bladder. Burst tests of tubes with stress corrosion cracks were done in the free span condition. No foil reenforcement of the sealing bladders was used since the crack location which was to dominate the burst behavior was not always readily apparent. Some of the maximum openings developed during burst testing were not sufficient to cause extensive crack tearing and thus represent lower bounds to the burst pressures. The openings were large enough in all cases to lead to large leakage.

9.5 Burst Test Results

Burst test results are summarized in Table 9.1. Figure 9-1 illustrates a plot of burst pressure versus bobbin coil voltage for specimens from model boiler and pulled tube tests which are considered reasonably representative of the range of field observations of ODSCC of tubes at tube support plate intersections. Note that some of the burst data points are lower bound estimates since extensive crack tearing did not develop. In these cases the crack openings were large enough to cause large leakage events in service. From Figure 9-1 it is seen that burst pressures remain above about [ ]9. As discussed later, reasonable limits on bobbin coil voltage can assure maintenance of required burst pressure margins with respect to both operating and accident pressure differentials.

9.6 Correlation of Burst Pressure with Bobbin Coil Voltage

As noted in an earlier section, a broad interpretation of the physical significance of the voltage of an eddy current bobbin coil indication is that the voltage reflects the volume of material over which eddy currents are perturbed by the geometrical configuration producing the indication. Hence, there is a very broad range of different geometries which can produce the same voltage indication. In the case of ODSCC in the tube support plate crevices of steam generator tubes, the bobbin coil indication voltage reflects the volume of material where eddy currents are perturbed by cracking. Obviously at a given indication voltage any one of a broad range of crack morphologies can be present. From past experience with pulled tubes it is known that cracking patterns are typically confined to the crevice region and thus restricted in length. Additionally, the typical cracking pattern consists of an array of essentially axial cracks. Thus, at a given indication voltage one of many crack patterns can be present but there are observed restrictions in these patterns. Other restrictions to cracking patterns, within perhaps rather wide limits, are expected from the operation of a given SCC cracking mechanism. Just as crack morphologies are many valued but bounded at a given indication voltage, burst pressures will be consequently many valued but bounded.

The burst data of Table 9.1 (model boiler samples) and of Table 6.2 (pulled 7/8-inch tubes) provide a total of 34 data points that have been used to develop a correlation between bobbin coil voltage and burst pressure. The data used in the correlation for 7/8-inch tubing are as follows:

Bobbin Voltage (V)	Burst Pressure (ksi)
[	]9

An higher order regression analysis of this data has been performed providing an equation for the mean curve using a third order polynomial equation. The equation for burst pressure (BP) as a function of volts (v) obtained is:

[ ]9

The coefficient of correlation for this regression fit is 0.92 and the error of the BP estimate is 0.935. A -95% prediction interval is established using the expression:

[ ]9

where,

[

]9

Since the burst tests were peformed at room temperature conditions, the -95% prediction interval curve was factored by the LTL-to-room temperature strength property ratio of 0.857, the Lower Tolerance Limit (LTL) strength properties of Alloy 600, 7/8 x 0.050 inch, mill annealed tubing at 650 °F divided by the strength at room temperature of the tubing material tested. The strength properties utilized are the sum of the yield and ultimate strengths. The LTL strength (yield + ultimate) of the tubing material at 650 °F is 126.0 ksi and the room temperature strength of the material tested is 147.0 ksi giving a ratio of 0.857.

The curves and data points are plotted in Figure 9-2. The -95% prediction interval, LTL, is used to establish the voltage corresponding to the burst pressure capability required of three times normal operation pressure differential (4590 psi), 3Δp. The 3Δp voltage at the -95% prediction interval is [ ]a. The voltage corresponding to steam line break (SLB) pressure (2650 psi) is [ ]a. It should be noted that the burst capabilities developed conservatively assume no potential benefit of interaction with the tube support plate.

9.7 Correlation of Leak Rates with Bobbin Coil Voltage

The distribution of crack morphologies at a given indication voltage gives rise to an associated distribution of burst pressures. Since some of these crack morphologies may involve through wall cracking, a distribution of leak rates will be also associated with each indication voltage level. The expected total leak rate from a given population of eddy current indication voltages can be determined in a statistical fashion from a knowledge of the distribution of possible leak rates at each voltage level. This is accomplished by performing a probabilistic analysis for SLB conditions as described in section 11.4. The basis for the probabilistic analysis is the correlation of leak rates at SLB conditions to bobbin coil voltage. The correlation is established utilizing linear regression analysis of the logarithms of the corresponding leak rates and voltages thereby establishing a leakage rate model of the form

[ ]g

where,

[

]g

Prediction intervals for leakage rate at a given voltage are then established to statistically define the range of potential leakage rates.

The SLB leakage rate data listed below from Table 6.2 for pulled tubes and Table 9.1 for model boiler samples are used to establish the correlations for 7/8-inch tubing:

Bobbin Volts (v)	Leak Rate (l/hr)
[	] g

[

]

Linear regression analysis of the logarithms of this data results in the following mean leakage rate correlation:

[ ]^{a}

The coefficient of correlation for this regression fit is 0.71 and the error of the estimate is 1.552. A prediction interval is established using the expression:

[ ]^{a}

where,

[

]^{a}

Figure 9-3 is a plot of the SLB leakage rate correlation versus bobbin voltage showing the data, the linear regression fit and ± 95% confidence prediction intervals. Since a fit using logarithms of voltage and leakage is required to obtain the correlation, the zero leakers were input with a leak rate of 0.0001 liters per hour, three orders of magnitude below the lowest measured leak rate. This is judged to be sufficiently low to maximize the slope of the curve providing

conservative predictions of leakage rate in the higher voltage range. In addition, only the zero leakage tubes with 90% or greater through wall penetration are included, again, maximizing the slope of the curve.

At sufficiently low voltages the degree of through wall cracking will not be sufficient to lead to measurable leakage. There will be a threshold voltage below which leakage is not expected.
[

]9

Section 12 discusses the application of burst pressure and leakage correlations in the formulation of plugging criteria. The subsections above show that burst pressure margins can be maintained by limiting maximum allowable bobbin voltage indications and that any associated leak rates with a given population of voltage indications can be appropriately determined.

9.8 Burst Testing of IGA Specimens

Section 8.1 addresses IGA detectability of laboratory prepared specimens about 4 inches in length with uniform IGA depths and no cracking. Figure 8-12 shows bobbin coil voltage amplitudes for these specimens. The IGA specimens from Figure 8-12b with depths of 9%, 36% and 52% in non-sensitized, 7/8 inch OD tubing were burst tested to compare the voltage vs burst characteristics of IGA to that of the available data base of Figure 9-2. In addition, a 3/4 inch diameter, sensitized specimen of Figure 8-12a with 58% deep uniform IGA was burst tested. These specimens had IGA from one end of the tube to the other and hence differential bobbin coil measurements could not be made. As noted in Figure 8-12, the bobbin amplitudes were measured in the absolute mode. It is expected that for uniform step change in depth, the peak to peak differential voltages would be a factor of 1 to 2 higher than the absolute voltages which are typical of single peak amplitudes. Thus using the absolute amplitudes of the specimens appears to be a conservative representation of the differential amplitudes. However, due to the associated uncertainty on the voltage amplitudes, the burst results for these specimens are provided for information only and are not included in the voltage/burst correlation used to establish tube plugging limits.

Figure 9-4 shows the IGA burst results added to the data of Figure 9-2. From Figure 9-4, it is seen that the IGA specimen burst pressures are near or above the mean fit to the Figure 9-2 data even though the IGA specimens are 4 inches long compared to the 0.75 inch TSP thickness which bounds the ODSCC lengths for the data points of Figure 9-2. These results indicats that the burst pressure correlation of Figure 9-2 represents a lower bound for uniform IGA tube degradation. In general, this result is expected at least for IGA depths up to about 65%. The voltage amplitude for uniform IGA is expected to be as high or higher than for a single ODSCC crack of the same depth due to the greater volumetric involvement of the IGA. Burst test results for uniform thinning of 0.75 inch length show higher burst pressures than for a 0.75 inch long crack of the same depth for depths up to about 65% while cracks are more limiting above ~65% depth. Thus the higher burst pressures for uniform IGA together with equal or higher voltage amplitudes would yield the Figure 9-4 results showing IGA burst pressures at or above the ODSCC results.

The IGA burst test results show that uniform IGA behaves effectively as uniform thinning of a tube. That is, the burst pressures of uniform IGA correlate well with results obtained for uniform wall thinning. For local IGA patches of limited circumferential involvement, the burst pressures would be expected to approach that of a crack. Thus an IGA patch combined with an SCC emanating deeper than the IGA, as commonly found in pulled tubes, would be expected to reflect burst properties associated with the crack depth. Similarly, the bobbin coil voltage responses are expected to be comparable. The results for the Plant L tube R12-C8 of Table 6.2 reflect this effect. Uniform IGA was about 30% deep for this tube in the region of the maximum 55% crack depth. The voltage amplitude was 0.5 volts with a burst pressure of 10,500 psi. This data point lies just above the mean fit to the data of Figure 9-2. Overall, the results to date for IGA and IGA/SCC types of degradation are enveloped by the burst pressure correlation of Figure 9-2.

Table 9.1

Summary of Leak and Burst Test Results

[redacted]

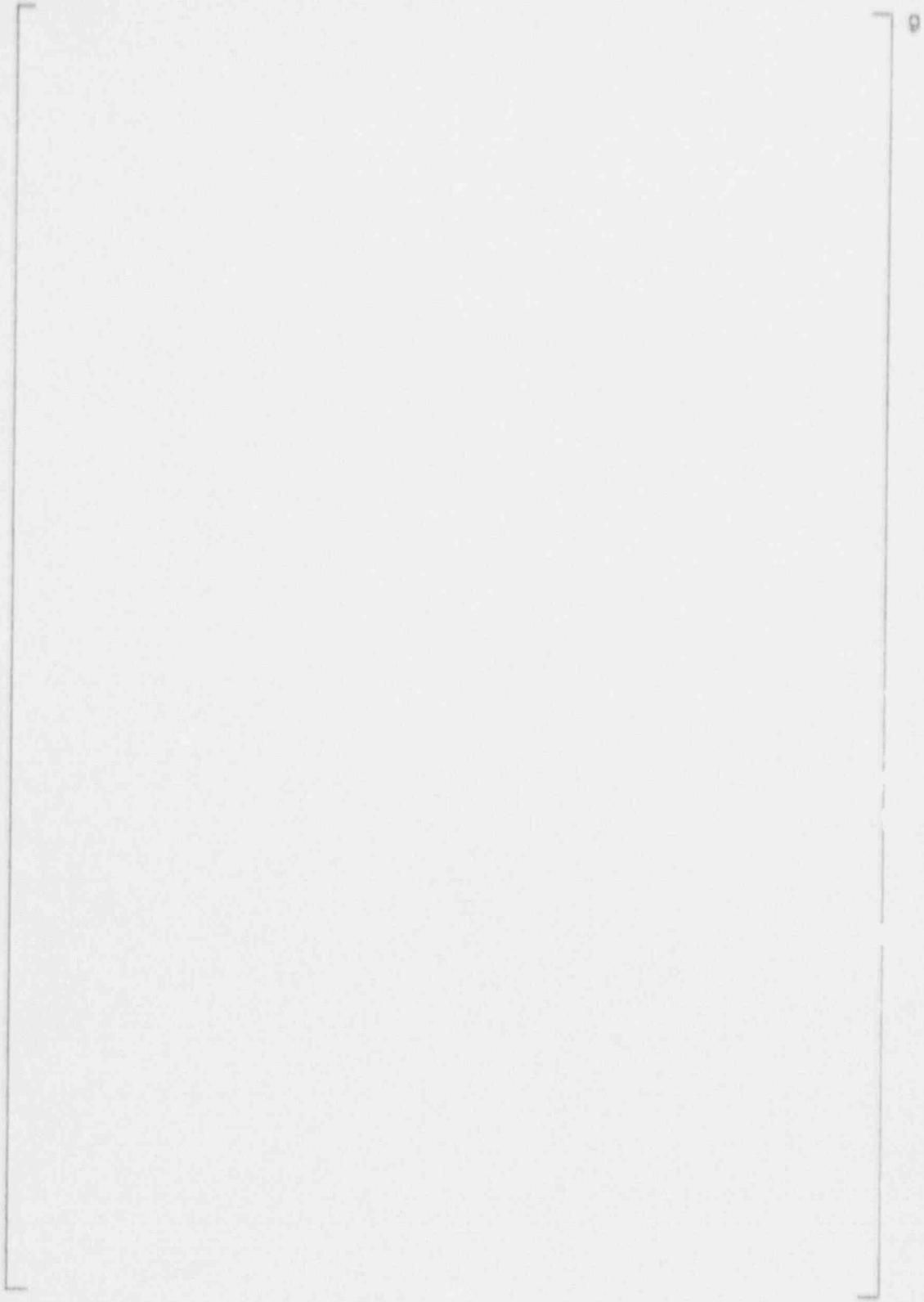

Figure 9-1. Burst Test Results Versus Bobbin Coil Voltage

Figure 9-2. Burst Pressure Correlation With Bobbin Voltage

Figure 9-3. SLB Leak Rate Correlation With Bobbin Voltage

Figure 9-4. Burst Pressure Correlation of Fig 9-2 and Data from IGA Specimens

10.0 SPECIMEN DESTRUCTIVE EXAMINATIONS

10.1 Objective

The objective of this task is to characterize the size, shape, and morphology of the laboratory created corrosion in Alloy 600 tube specimens which have been tested for leak rate and burst pressure. The crack morphology is also to be compared generally to the corrosion morphology observed in tubes pulled from operating steam generators. A summary of the results is presented in this section. From information in Section 9, one can compare the leak rate and burst pressure data to the actual size of the crack opening and relate eddy current voltage to crack aggregate size and corrosion morphology.

10.2 Examination Methods

Examination methods included visual examinations, macrophotography, light microscopy and/or SEM (scanning electron microscopy) examinations, SEM fractography, and metallography. A total of seven model boiler test specimens and one doped steam specimen were selected for destructive examinations. Six of these were examined following leak and burst testing (all model boiler specimens), one following leak testing but without burst testing being performed, and one (the doped steam specimen) with neither leak nor burst testing being performed. The six model boiler specimens were 543-4, 525-1, 533-4, 536-1, 558-1, and 571-1. The leak and burst data for these specimens are given in Table 9.1 which also lists the eddy current (bobbin coil) test results. The two specimens without burst test data were 533-3 (model boiler specimen) and SL-FH-11 (doped steam specimen).

The specimens were initially examined visually and with a low power microscope. The burst opening and visible cracks around the circumference of the tube within the tube support plate intersection were photographed and their location in relation to the burst crack noted. The major burst crack was then opened for fractographic observations including crack surface morphology, crack length, and crack depth using SEM. One metallographic cross section containing the majority of secondary cracks within the tube support plate region was selected for each tube specimen. The location of the cracks within this metallographic cross section was noted, the cracks measured as to their depth and a crack was photographed to show the typical crack morphology. Note that the one metallographic section through each specimen will provide the secondary crack distribution at that location. Secondary cracks at other elevations would not be recorded unless the burst test happened to open the secondary cracks sufficiently for visual examination to record their location.

10.3 Results

Tube 543-4

Visual examination was performed on the secondary cracks adjacent to the main burst opening. The short secondary cracks were orientated axially, inclined, and in some instances circumferentially.

Fractography of the burst crack showed that the environmental cracks were intergranular and typical of stress corrosion cracking (SCC). The macrocrack was 0.52 inch long and did not penetrate the ID wall although it was at many locations up to 98% through wall. The macrocrack was composed of at least six microcracks, all of which had joined together by intergranular SCC. A metallographic cross section through many of the secondary cracks observed on the circumference within the tube support plate intersection revealed five cracks with depths ranging from 45 to 98% through wall. A sketch of the location of these cracks relative to the burst fracture is shown in Figure 10-1. A typical crack morphology of a secondary crack is shown in this figure. A summary of the observed OD origin secondary cracks and morphology of the main crack are shown in Figure 10-2.

Tube 525-1

The burst crack was relatively short (0.16 inch long) but deep, 95% through wall. The secondary cracks were all short and axially orientated. A summary of the shape, morphology and distribution of cracks found in Tube 525-1 is presented in Figures 10-3 and 10-4.

Tube 533-4

A network of axial and circumferential secondary cracks was observed near the burst crack. The axially orientated burst crack was composed of at least five microcracks which joined to form the macrocrack. Ledges separating these microcracks showed partially ductile features (shear dimples) while the crack face was entirely intergranular. The OD origin major crack was 0.34 inch long and penetrated the ID wall for a length of 0.14 inch. The secondary crack distribution found in the metallographic cross section is shown in Figure 10-5, and a summary of the cracks observed in the support plate region of the tube is presented in Figure 10-6.

Tube 536-1

Many secondary cracks were observed clustered around the burst opening. Other larger secondary cracks were found at a location 95 and 145 degrees from the burst opening. The main burst crack and the largest of the secondary cracks located at 95 degrees were opened and examined by SEM. In both cases the OD origin cracking morphology was intergranular and typical of SCC. The burst crack was 0.4 inch long and 90% through wall. The macrocrack consisted of at least five microcracks which joined to form the macrocrack. The largest secondary crack was 0.3 inch long and 95% through wall. It was also formed by several microcracks. A metallographic cross section through the remaining piece of the tube at the support plate intersection showed two intergranular OD origin stress corrosion cracks (Figure 10-7). The larger of these two cracks was 40% through wall. A summary of crack observations on Tube 536-1 is shown in Figure 10-8.

Tube 558-1

The major burst crack originated from a cluster of smaller secondary cracks which joined in an irregular pattern to form the macrocrack. Visual examinations of the remaining tube support plate region indicated that no other secondary cracks existed. The opened fracture face of the burst crack revealed more clearly the irregular cracking pattern of this major crack caused by the joining of the widely separated microcracks. The macrocrack showed at least five major ledges which separated six microcracks. The features of the OD origin macrocrack were intergranular. The crack was 0.4 inch long and it penetrated the ID wall for approximately 0.32

inch. A summary of the crack observations is shown in Figure 10-9. No metallography was done on this tube since no secondary cracks away from the burst opening were observed.

Tube 571-1

The burst crack may have consisted of one major axial crack whose length was 0.44 inch. No obvious separation of the macrocrack into different microcracks was found within the burst crack, alternatively there were hints of four microcracks which nucleated in almost identical planes. The OD origin crack penetrated the wall for a length of 0.36 inch. It was entirely intergranular and typical of stress corrosion cracking, based on examination of the fractographic details. No other secondary cracks were observed along the circumference of the tube. A metallographic cross section through the center of the support plate region found no secondary cracking. A summary of crack observations is shown in Figure 10-10.

Tube 533-3

The collars of this model boiler specimen were removed. Several small axial cracks were observed at the support intersections. One was located under the Teflon collar and a few were located under the top steel collar. The crack within the Teflon collar intersection was opened and examined by SEM. The macrocrack face exhibited intergranular features with some ductile tearing on a ligament separating two microcracks. The macrocrack was 0.27 inch long and was composed of four microcracks. The OD origin crack penetrated the ID wall for a length of 0.17 inch. A metallographic cross section through the center of the Teflon collar intersection revealed numerous small intergranular stress corrosion cracks. The location (on the tube) and depth of these cracks is shown in Figure 10-11, together with one micrograph. A metallographic cross section through some of the cracks within the steel collar intersection revealed the crack distribution shown in Figure 10-12. The characterization of the through wall crack found under the Teflon collar and the crack distribution around the tube within the Teflon support is shown in Figure 10-13.

Tube SL-FH-11

Doped steam specimen SL-FH-11 developed a large number of OD origin cracks. The largest agglomeration of these cracks was opened for fractographic examinations and cross sectional cuts made above (A) and below (B) the opened section of the macrocrack for metallographic examinations. The opened section of the tube showed an intergranular macrocrack, 0.37 inch long. The ligaments separating the 4 microcracks of the macrocrack had only intergranular features. The crack penetrated the ID wall for a length of 0.23 inch. The cross sectional cuts made through planes A and B produced the crack distributions and typical crack morphologies depicted in Figures 10-14 and 10-15. A summary of the crack observations made at this location is shown in Figure 10-16.

A longer but more shallow crack network was found on the opposite side of the tube from the crack described above. The crack network was opened and examined fractographically. The macrocrack was 0.46 inch long and was composed of at least three microcracks. It penetrated the ID wall locally for a length of only 0.03 inch. The crack morphology was intergranular with some ductile features at ligament locations. A summary sketch of the crack profile and character is shown in Figure 10-17.

Tube 528-2

A grouping of many small, OD origin, axial cracks, interconnected by ligaments and by circumferential extensions, formed the curved major burst opening shown in Figure 10-18. Other small axial cracks with circumferential involvement were observed in other areas of the simulated tube support plate crevice region. Fractographic observations of the major burst opening revealed that the corrosion crack consisted of at least six microcracks with intergranular ligaments. These ligaments often ran in the circumferential direction. The combined length of the microcracks that formed the macrocrack was 0.67 inch. Through wall cracking extended for 0.50 inch. The morphology of the macrocrack was IGSCC with no IGA or with negligible IGA components, as shown in Figure 10-19. Circumferential, intergranular extension of the axial crack can be observed in this figure. Transverse metallography through the center of the crevice region revealed the crack distribution shown by a sketch in Figure 10-20. An example of the morphology of one of the secondary OD cracks is also shown in this figure; the morphology is again that of IGSCC with negligible IGA aspects. A summary of the major crack shape and corrosion morphology and the distribution of OD cracks observed within the crevice region of tube 528-2 is shown in Figure 10-21.

Tube 532-1

A large number of long and short, OD origin, axial cracks were observed in the simulated tube support plate crevice region of tube 532-1, many of which were through wall. Figures 10-22 and 10-23 show photographs of the burst tube and convey the extensive cracking around the tube within the crevice region. A grouping of small axial cracks combined to form two of the burst crack openings which were examined in some detail. The longer of the two was 0.70 inch long and was formed from five microcracks interconnected with ledges having intergranular features. The length through wall was 0.52 inch. The crack morphology was IGSCC. Cracks seen on a metallographic cross section through the center of the crevice are depicted in a sketch in Figure 10-24 together with two micrographs showing typical crack morphologies of secondary cracks. A summary of the major burst crack and its morphology together with a distribution of cracks seen the crevice region is shown in Figure 10-25.

Tube 532-2

OD origin cracking within the simulated tube support plate crevice region of tube 532-2 can be seen in the post-burst test photographs of the tube in Figures 10-26 and 10-27. Many of the axial cracks were through wall. A group of many through wall microcracks formed the weakest area in the tube where the main burst fracture occurred. Fractography of this macrocrack showed at least six microcracks combined to form the main burst fracture. The total length of the macrocrack was 0.75 inch and it was through wall for 0.58 inch. While most ligament features were intergranular, occasional areas had ductile features, indicating that the ligaments had not completely interconnected by intergranular corrosion. The corrosion crack morphology of the main burst crack was that of IGSCC. A metallographic cross section through the center of the crevice region revealed many cracks shown by a sketch in Figure 10-28. Typical crack morphologies are also shown in photomicrographs for two secondary cracks in this figure. A summary of the main burst crack description and morphology are given in Figure 10-29.

Tube 535-1

The burst opening in tube 535-1 formed from a cluster of small axial OD origin cracks.

Numerous secondary, but small, microcracks were observed around the circumference within the crevice region. Fractography of the burst crack showed that it was composed of three microcracks which joined together by intergranular corrosion to form the macrocrack. The morphology of the macrocrack was IGSCC with negligible IGA aspects. The macrocrack was relatively short (0.28 inch in length) and penetrated through wall for 0.11 inch. A metallographic cross section through the center of the crevice showed numerous secondary cracks, some of which had negligible to minor IGA aspects. The distribution of cracks from the cross section is shown in Figure 10-30 along with a photomicrograph of a secondary crack. A summary of the of burst crack description and of the overall crack distribution is given in Figure 10-31.

Tube 555-3

The most degraded area in tube 555-3 was confined to one location within the crevice region, the location where the burst opening occurred. The crack distribution was complex in this region, with numerous parallel axial cracks with short circumferential branches. All cracks were of OD origin. Fractography showed the major macrocrack to be composed of two or three microcracks which joined in an irregular pattern to form the burst crack. The connecting ligaments showed a ductile fracture features, while the individual microcracks had intergranular features. The macrocrack was 0.75 inch long with a through wall length of 0.42 inch. Metallography of a tube cross section through the region with the highest crack density showed a morphology of IGSCC with some IGA or SCC branch characteristics near the main fracture. A photograph of the burst opening and a photomicrograph of the fracture face at the burst opening is shown in Figure 10-32. Other crack details are summarized in Figures 10-33 and 10-34.

Tube 576-2

Only one, OD origin, single axial crack was observed after burst testing of tube 576-2. Fractography showed the crack to be 0.30 inch long and it was through wall for 0.22 inch. The macrocrack appeared to be composed of a single microcrack and its morphology was that of IGSCC. A metallographic cross section through the center of the crevice region found no secondary cracks around the circumference. Crack details and crack morphology data are shown in Figures 10-35 and 10-36.

Tube 576-4

Tube 576-4 also burst with a single crack. Fractography showed the crack to be 0.60 inch long and it was through wall for 0.43 inch. The OD origin intergranular macrocrack was composed of three axial microcracks joined together by ligaments with intergranular features. Visual examination showed a few small axial cracks nearby the burst crack. The morphology of the burst crack was IGSCC with negligible IGA aspects. A metallographic section cut through the center of the crevice found only the burst crack. Crack details and crack morphology data are shown in Figures 10-37 and 10-38.

10.4 Comparison with Pulled Tube Crack Morphology and Conclusions

Section 4.0 of this report describes the crack morphology observed on tubes pulled from operating steam generators. Most of the support plate cracking was OD origin, intergranular stress corrosion cracking that was axially orientated. Most cracks had minimal IGA features in

addition to the overall stress corrosion features. Even when the IGA was present in significant amounts, it usually did not dominate over the overall SCC morphology. Large macrocracks were composed of numerous short microcracks (typically < 0.1 inch long) separated by ledges or ligaments. The ledges could have either intergranular or dimple rupture features depending on whether or not the microcracks had grown together during plant operation.

It is concluded that the laboratory generated corrosion cracks described in Section 10.3 have these same basic features. The laboratory created specimens possibly had even less of a tendency to develop IGA components to the overall stress corrosion crack features.

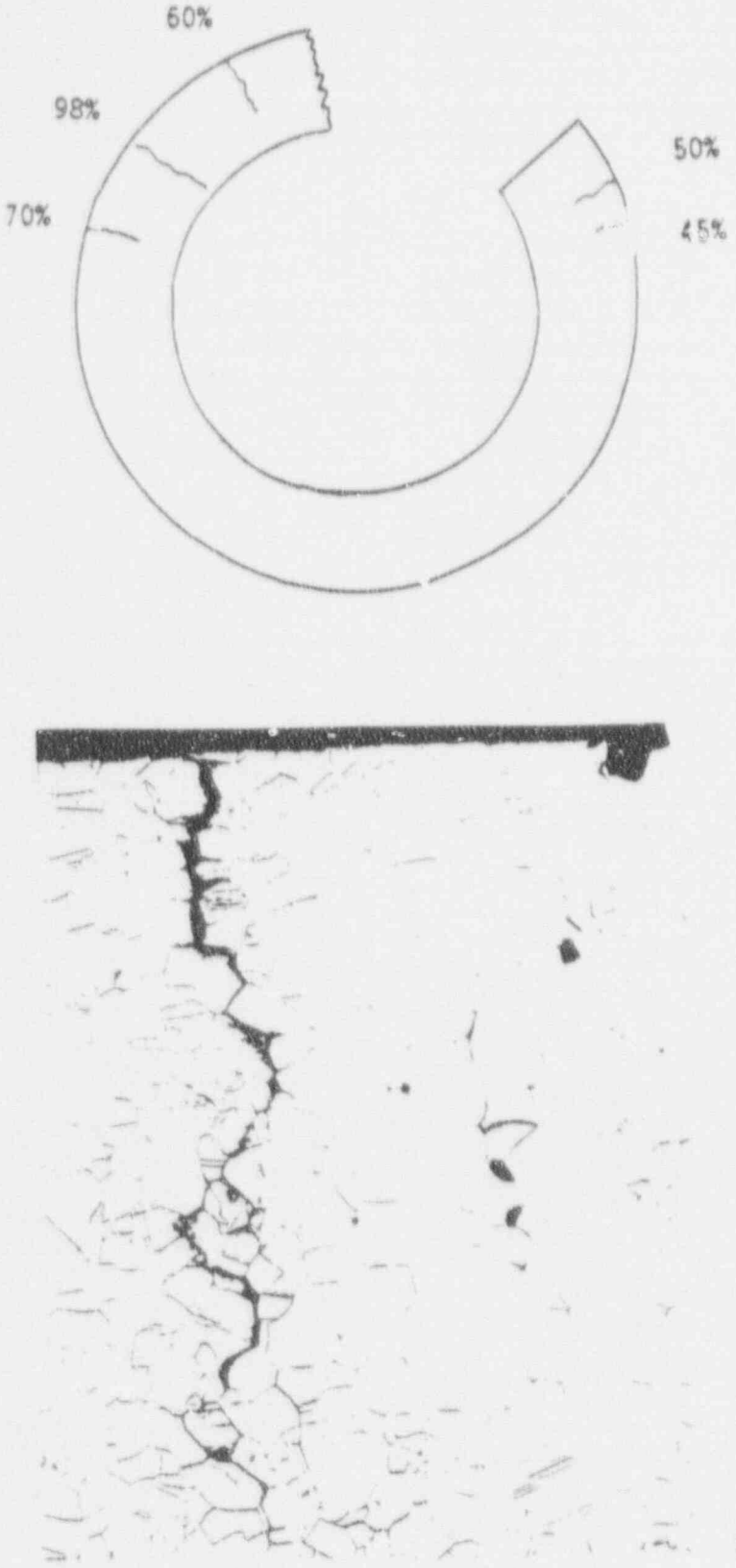

Figure 10-1 Sketch of a metallographic cross section through secondary support plate crevice cracks in Tube 543-4. A typical crack micrograph is also shown.

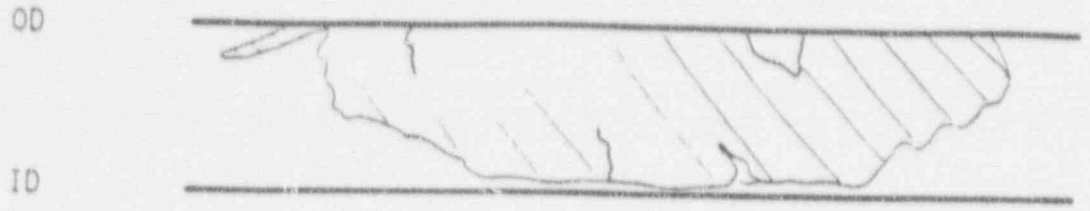

Sketch of Burst Crack

Macrocrack Length = 0.52 inches

Throughwall Length = 0 (98% throughwall)

Number of Microcracks = 6 (all ligaments with intergranular features)

Morphology = IGSCC

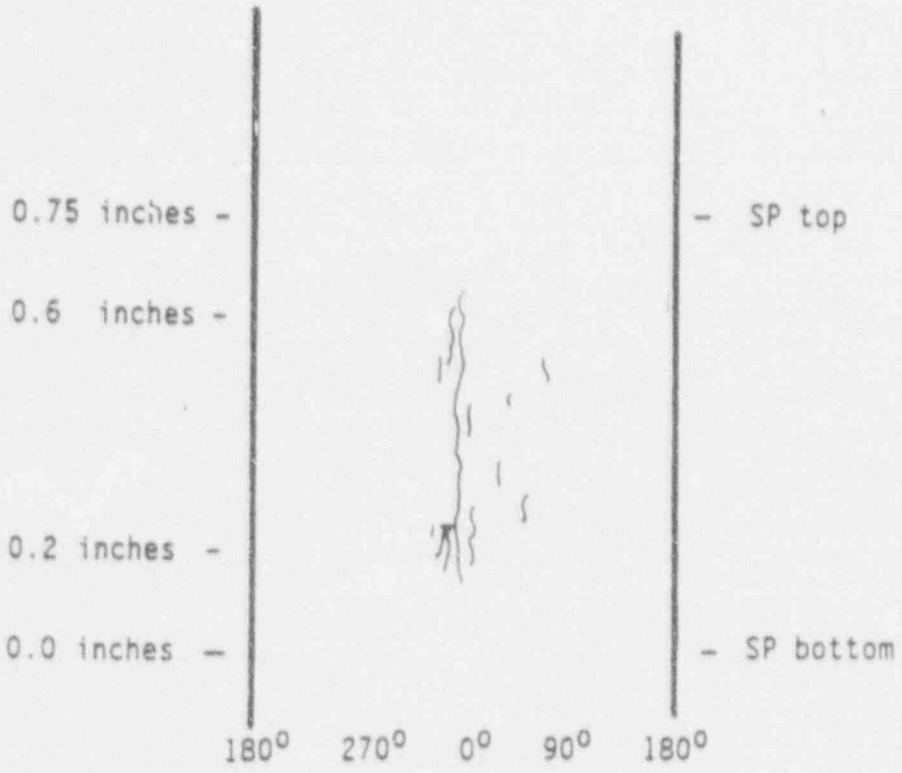

Sketch of Crack Distribution

Figure 10-2 Summary of crack distribution and morphology observed on Tube 543-4.

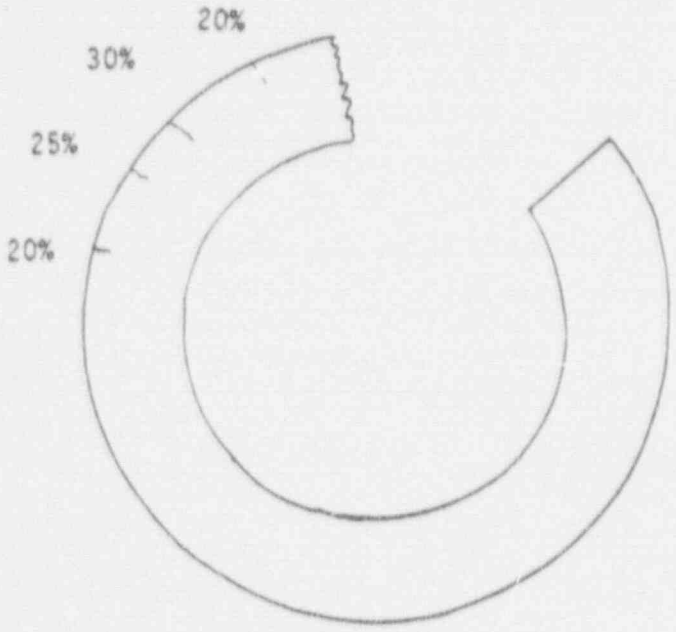

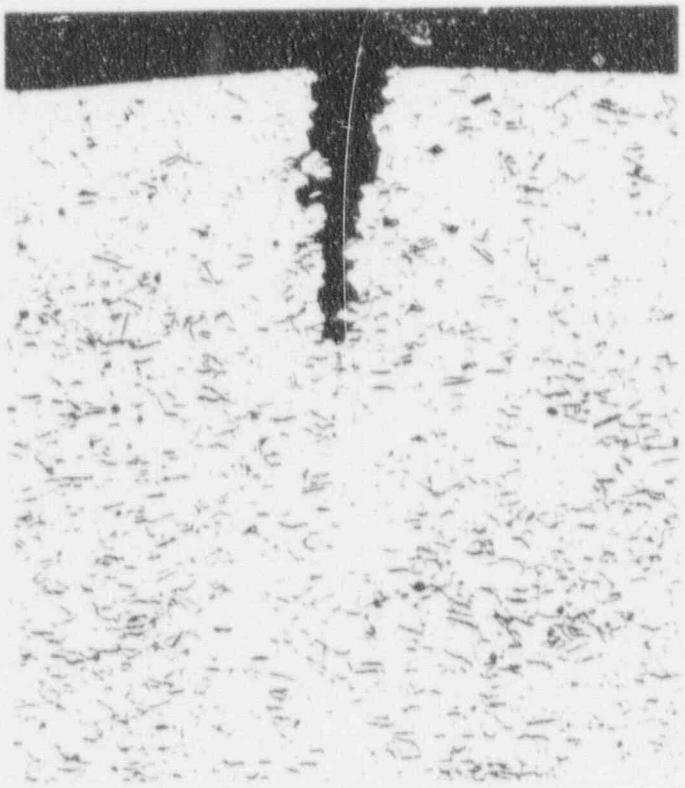

Figure 10-3 Secondary crack distribution in a metallographic cross section of Tube 525 in the support plate crevice region. A micrograph of one of the cracks is also shown.

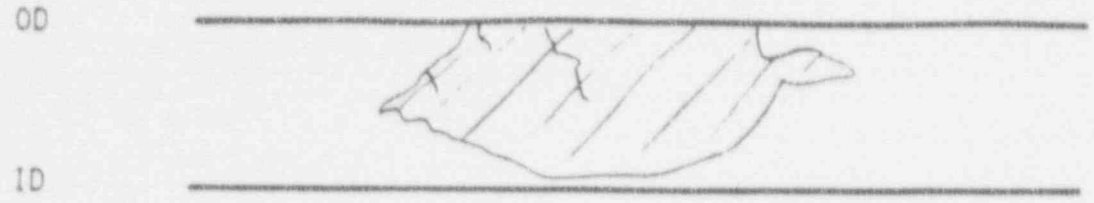

Sketch of Burst Crack

Macrocrack Length = 0.16 inches

Throughwall Length = 0 (95% throughwall)

Number of Microcracks = 3 (all ligaments with intergranular features)

Morphology = IGSCC

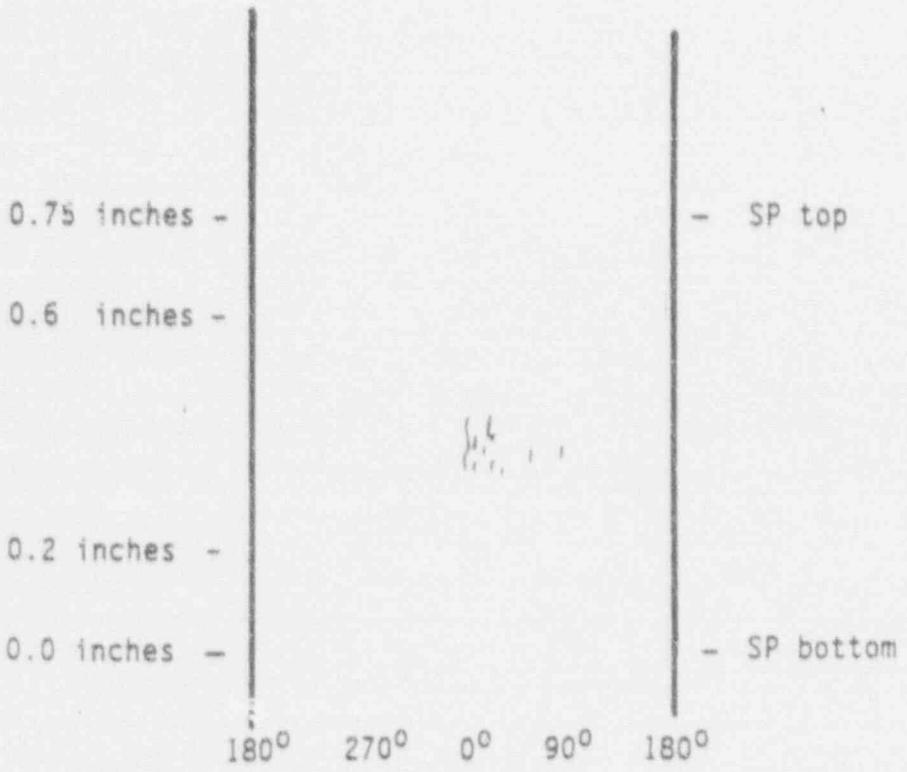

Sketch of Crack Distribution

Figure 10-4 Summary of crack distribution and morphology observed on Tube 525.

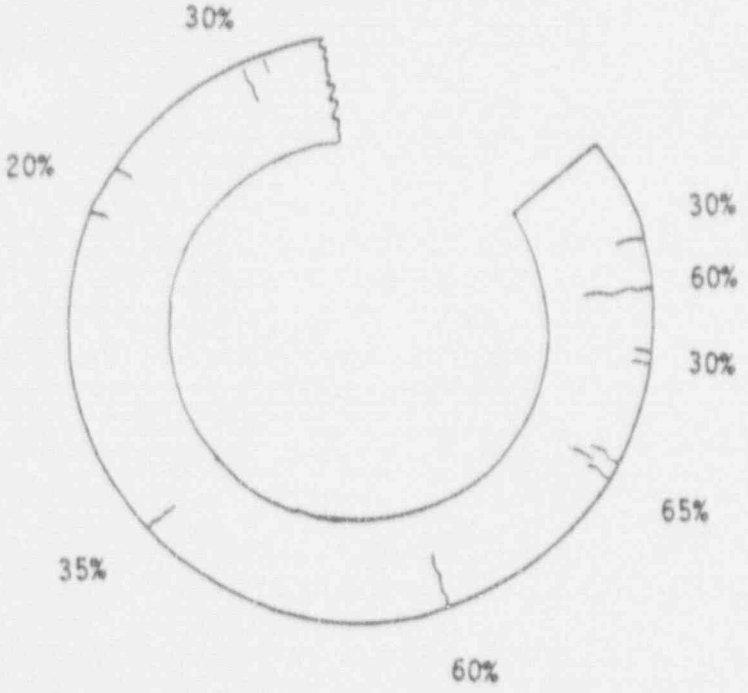

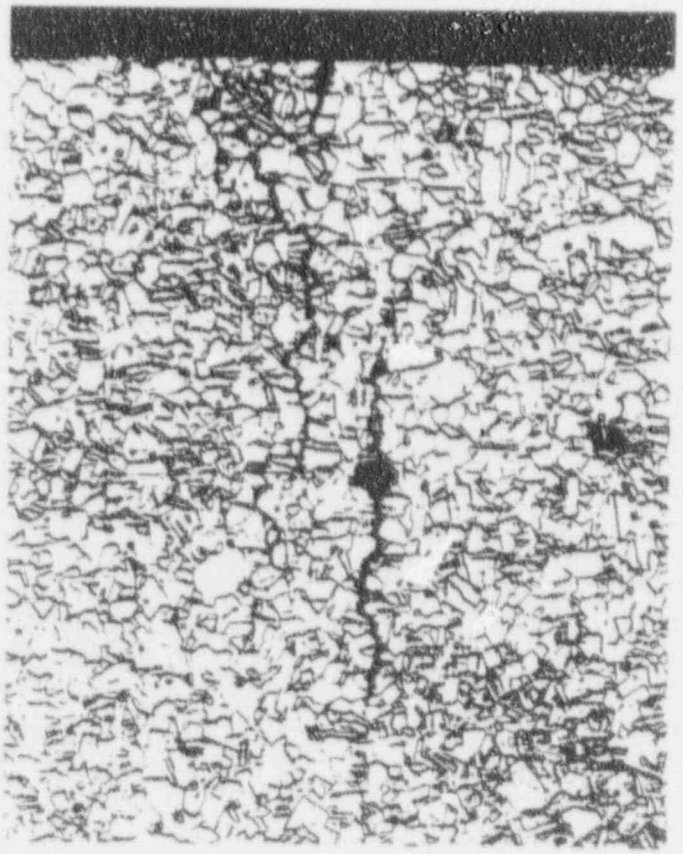

100X

Figure 10-5 Secondary crack distribution and a micrograph of one of these cracks in a metallographic cross section of Tube 533-4.

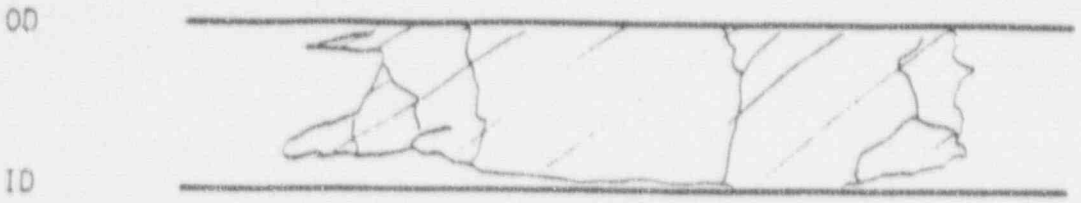

Sketch of Burst Crack

Macrocrack Length = 0.34 inches

Throughwall Length = 0.14 inches

Number of Microcracks = 5 (3 ligaments have ductile features)

Morphology = IGSCC

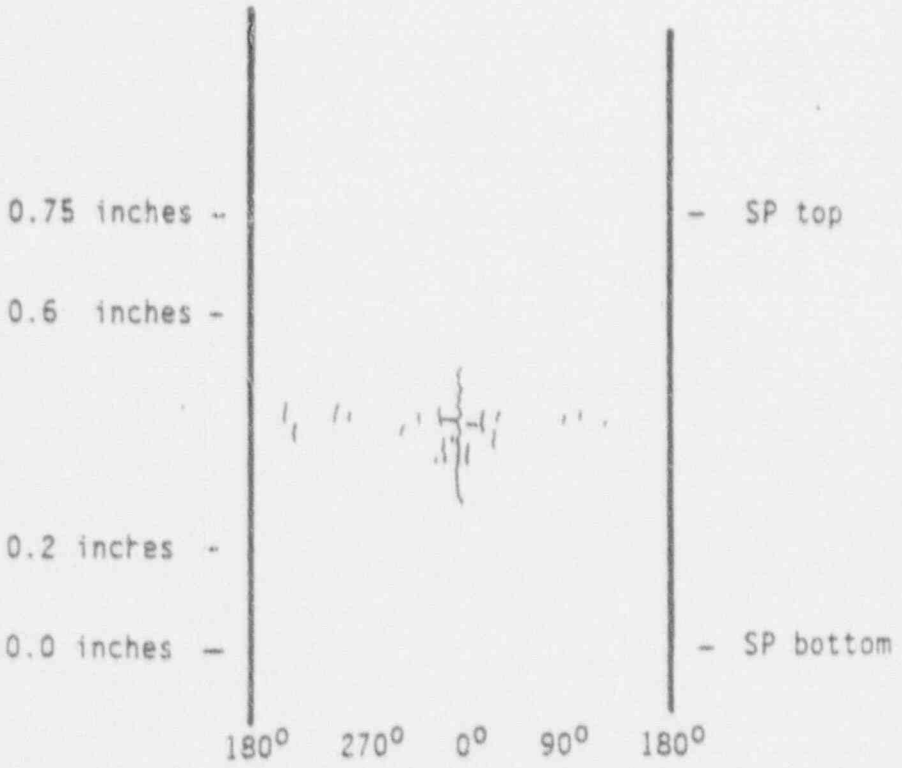

Sketch of Crack Distribution

Figure 10-6 Summary of crack distribution and morphology observed on Tube 533-4.

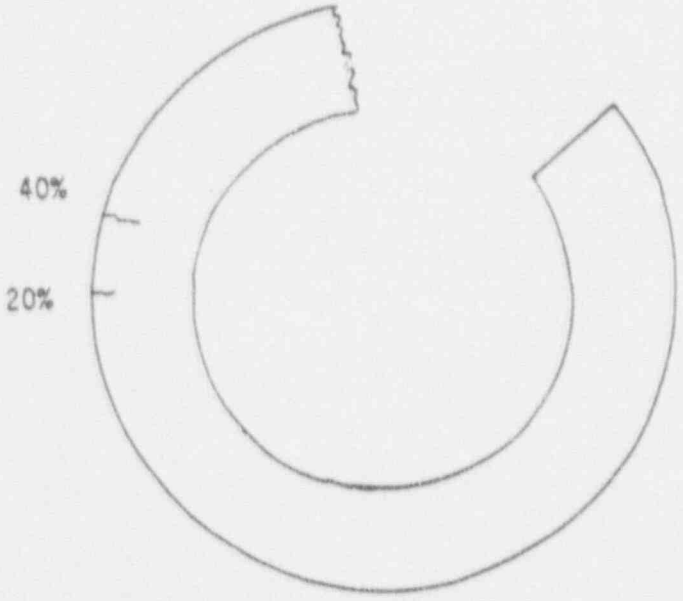

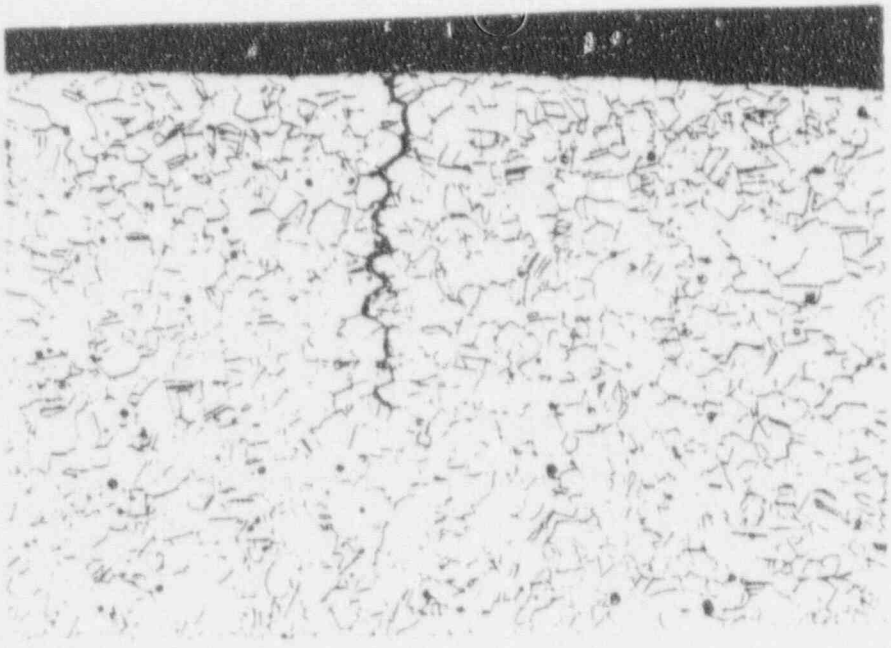

Figure 10-7 Secondary crack distribution and a micrograph of one of these cracks in a metallographic cross section of Tube 536-1.

Sketch of Burst Crack

Macrocrack Length = 0.4 inches

Throughwall Length = 0 (90% throughwall)

Number of Microcracks = 5 (ligaments have mostly ductile features)

Morphology = IGSCC

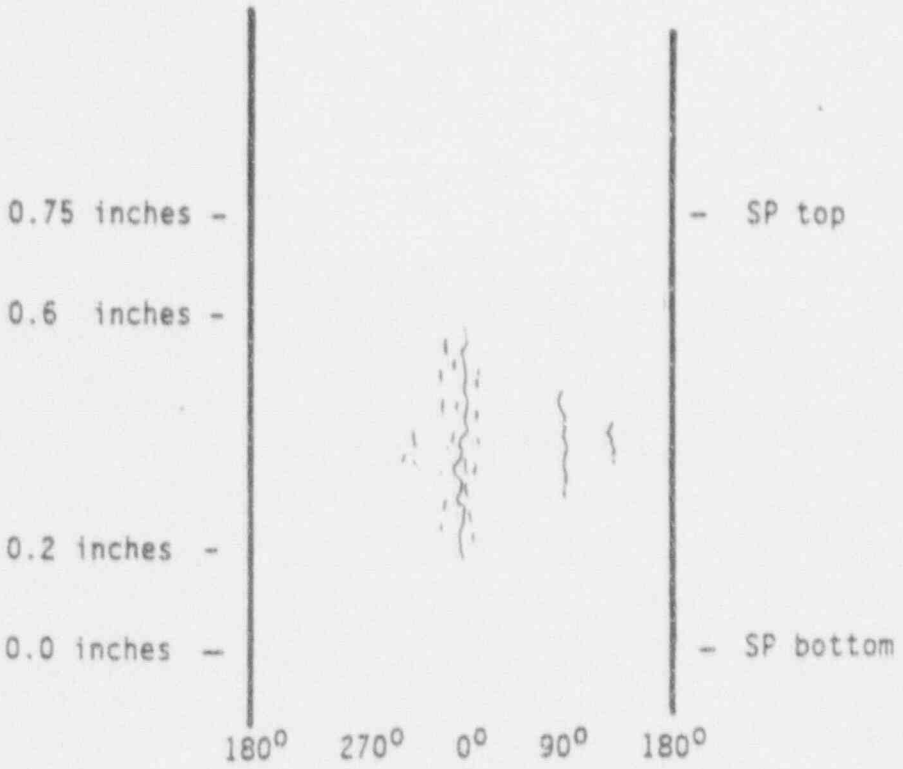

Sketch of Crack Distribution

Figure 10-8 Summary of crack distribution and morphology observed on Tube 536-1.

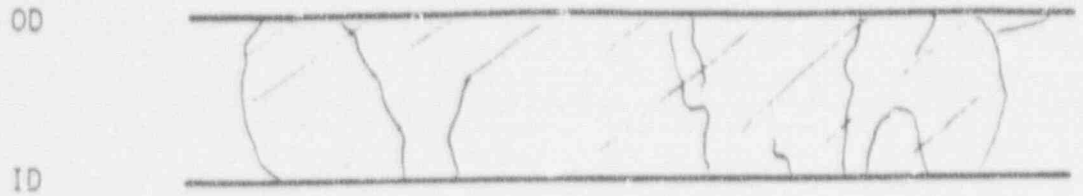

Sketch of Burst Crack

Macrocrack Length = 0.4 inches

Throughwall Length = 0.32 inches

Number of Microcracks = 6 (ligaments have mostly intergranular features with some ductile features)

Morphology = IGSCC

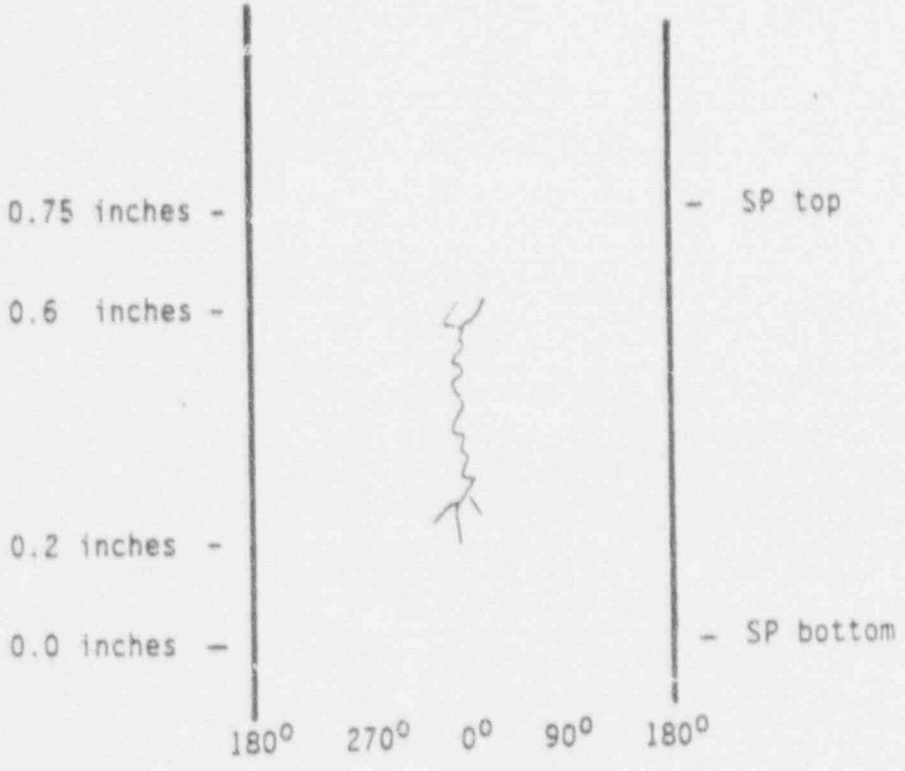

Sketch of Crack Distribution

Figure 10-9 Summary of crack distribution and morphology observed on Tube 558-1.

Sketch of Burst Crack

Macrocrack Length = 0.44 inches

Throughwall Length = 0.35 inches

Number of Microcracks = 1 to 4

Morphology = IGSCC

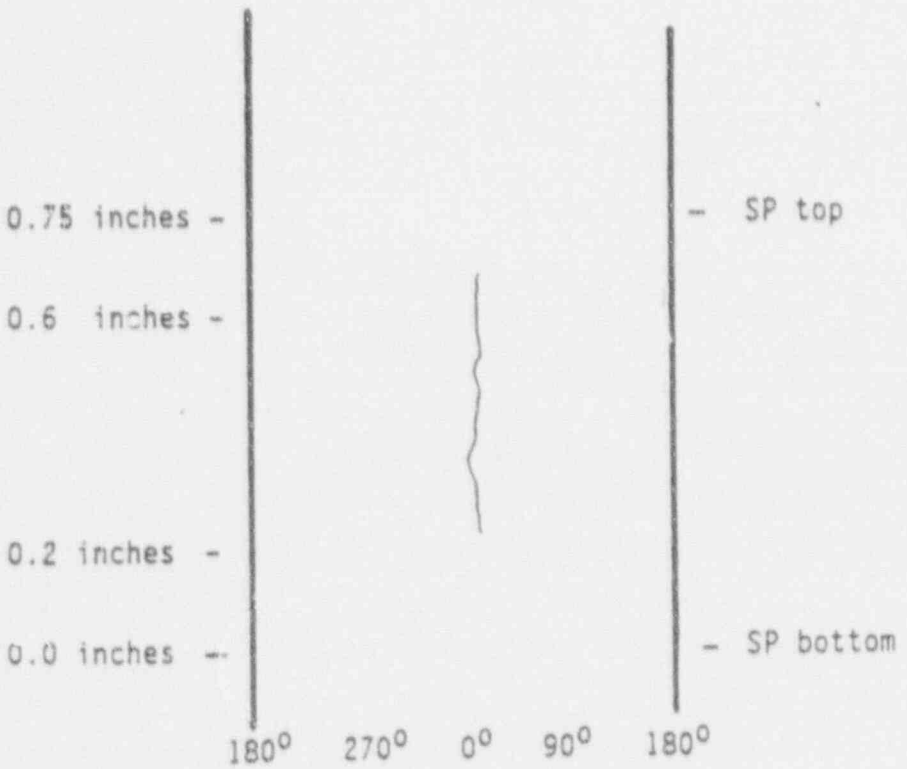

Sketch of Crack Distribution

Figure 10-10 Summary of crack distribution and morphology observed on Tube 571-1.

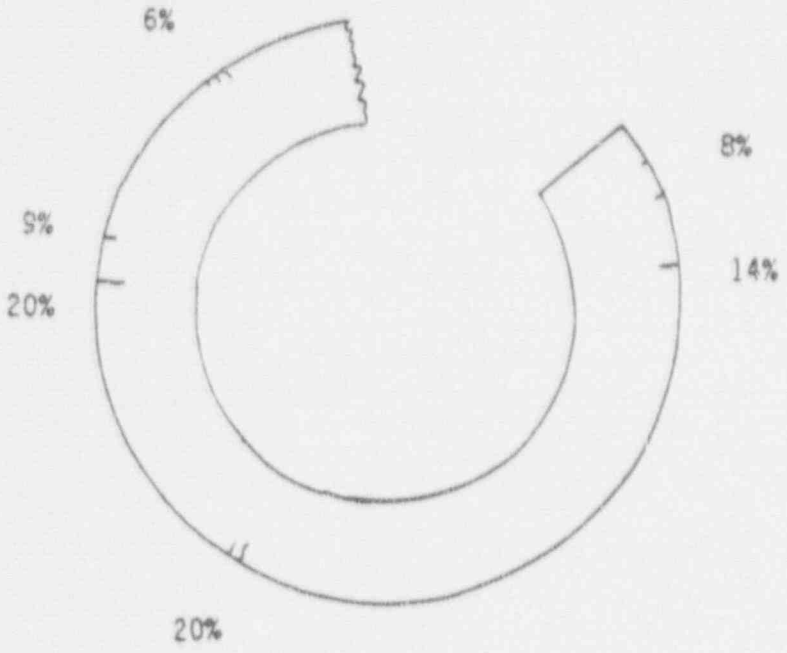

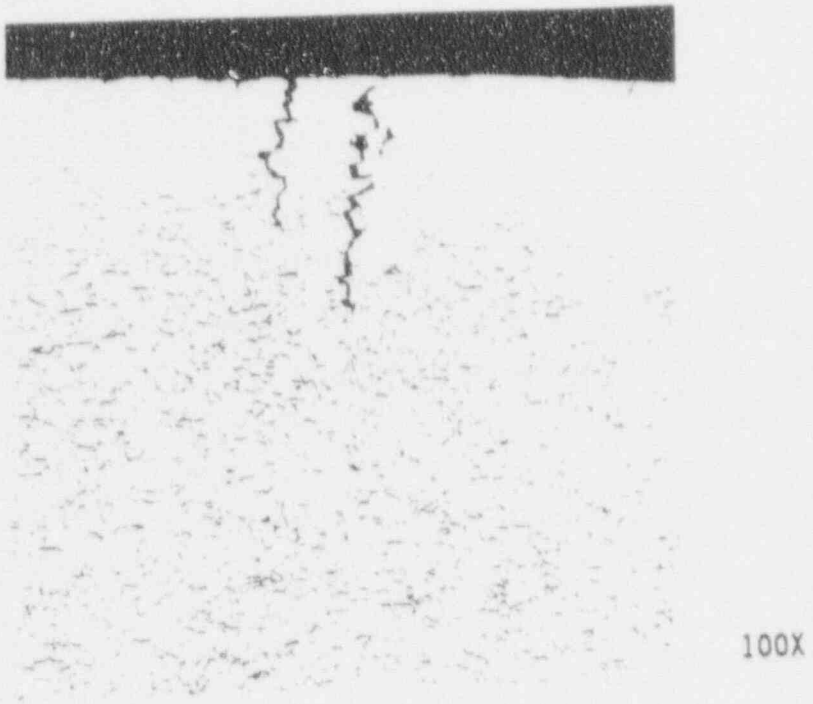

Figure 10-11 Secondary crack distribution and a micrograph of one of these cracks in a metallographic cross section of Tube 533-3 within the Teflon support plate region.

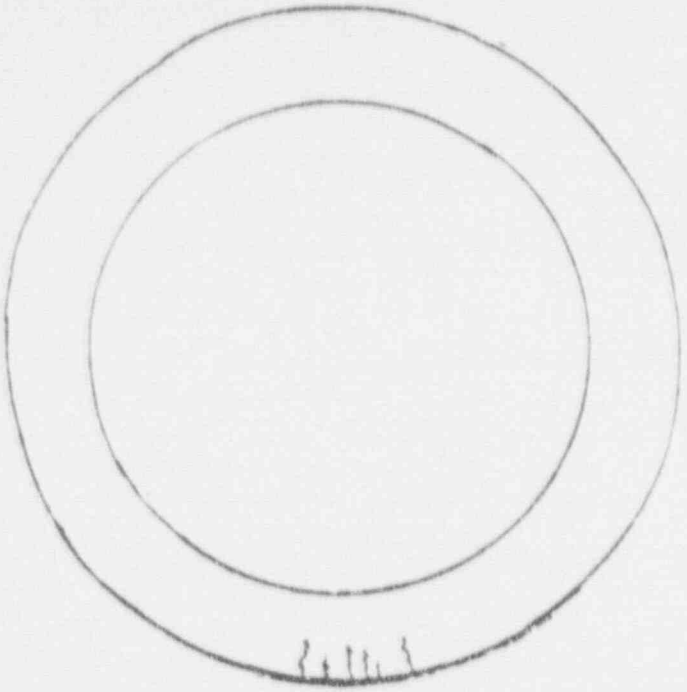

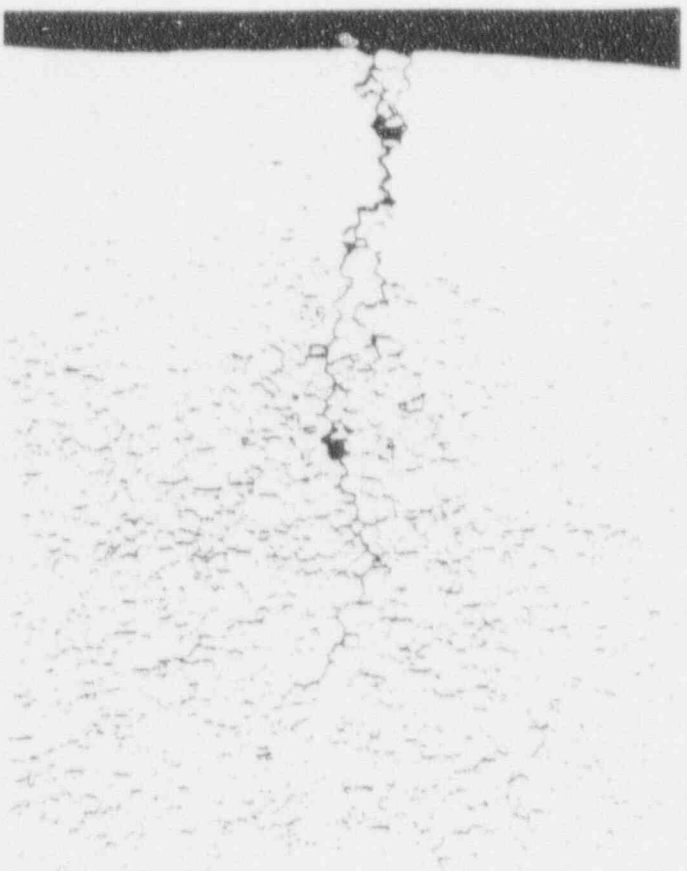

Figure 10-12 Crack distribution and a micrograph of one of these cracks in a metallographic cross section of Tube 533-3 within the steel collar region.

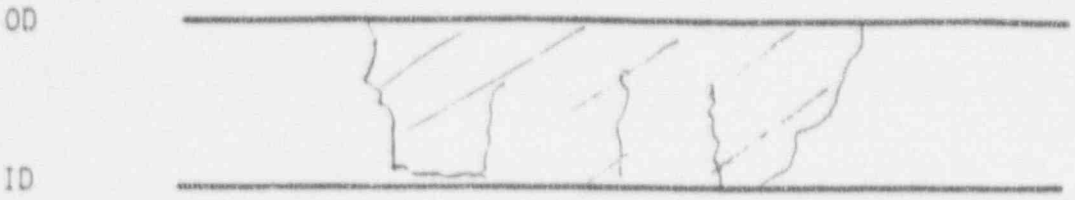

Sketch of Crack

Macrocrack Length = 0.27 inches

Throughwall Length = 0.17 inches

Number of Microcracks = 4 (2 ligaments with intergranular features; 1 with ductile features)

Morphology = IGSCC

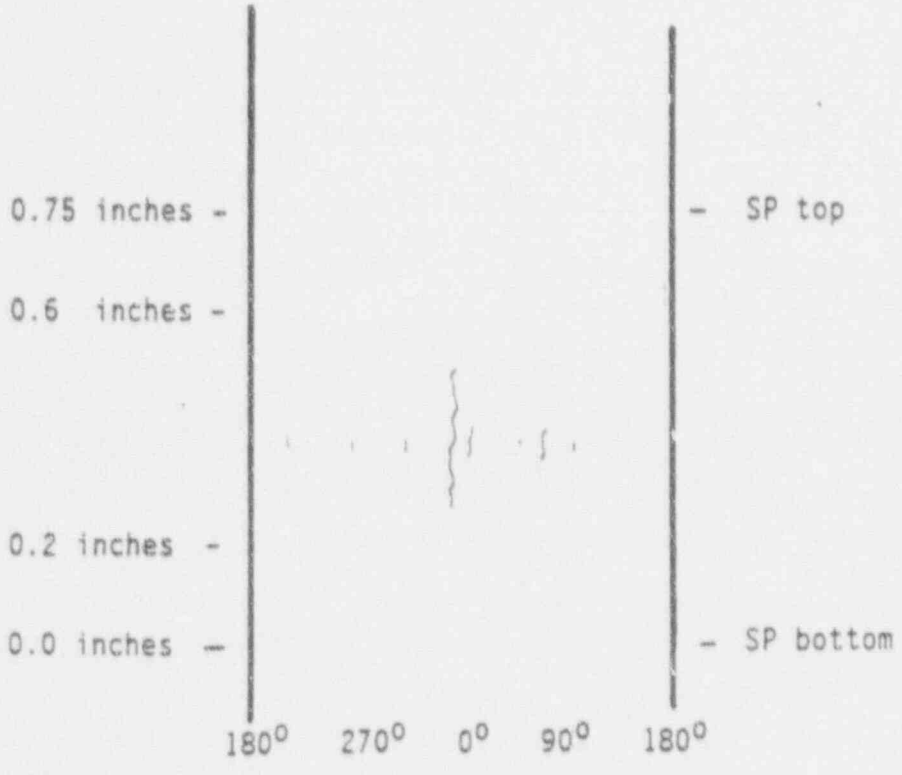

Sketch of Crack Distribution

Figure 10-13 Summary of crack distribution and morphology observed on Tube 533-3 at the Teflon intersection.

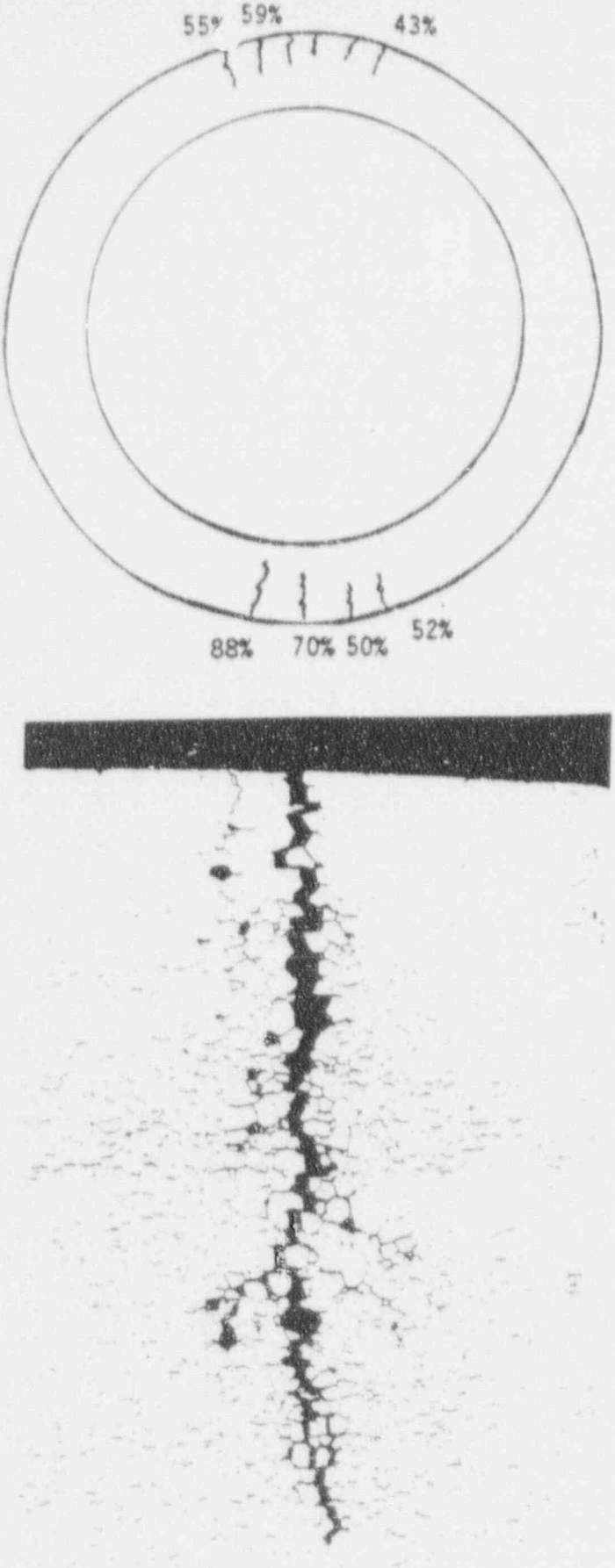

Figure 10-14 Crack distribution and a micrograph of one of these cracks in a metallographic cross section of Tube SL-FH-11 in Plane A.

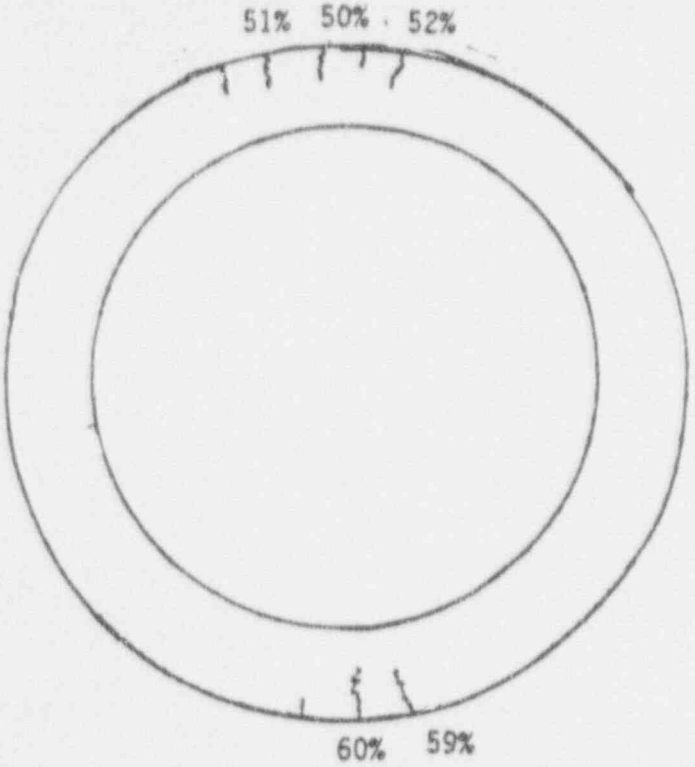

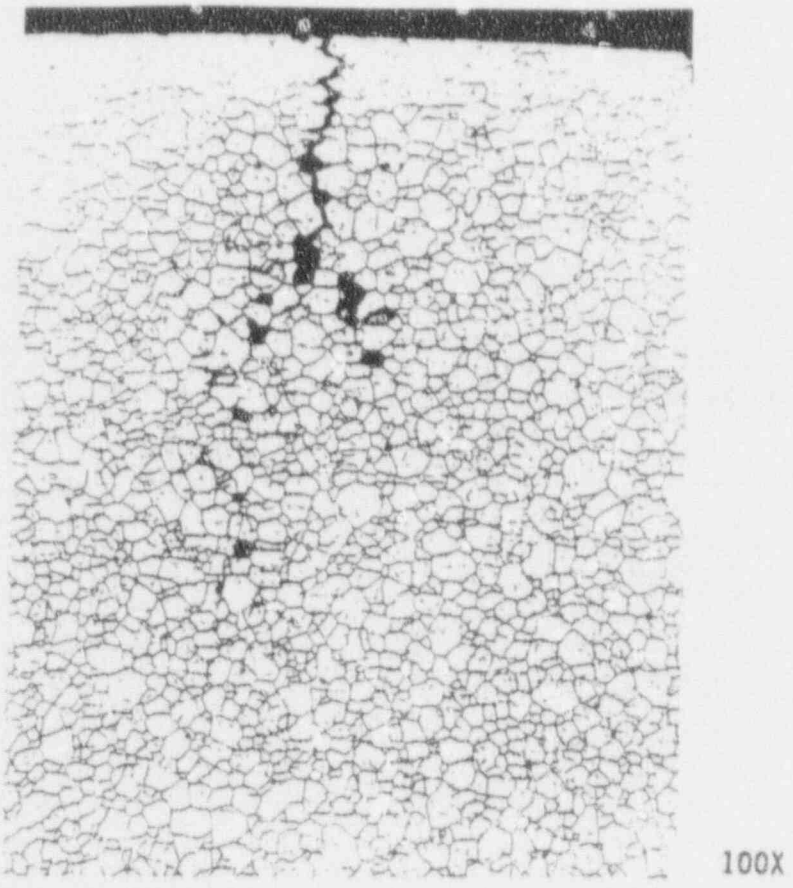

Figure 10-15 Crack distribution and a micrograph of one of these cracks in a metallographic cross section of Tube SL-FH-11 in Plane B.

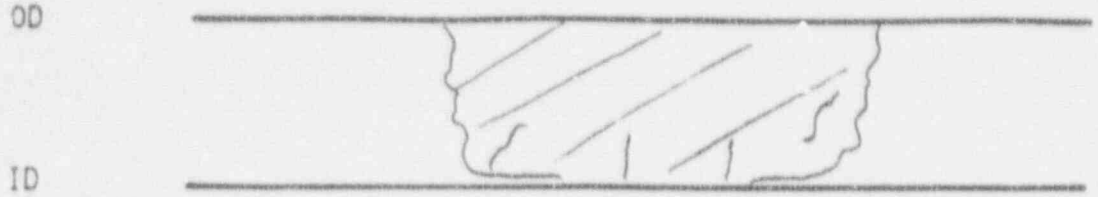

Sketch of Crack

Macrocrack Length = 0.37 inches

Throughwall Length = 0.23 inches

Number of Microcracks = 4 (all ligaments with intergranular features)

Morphology = IGSCC

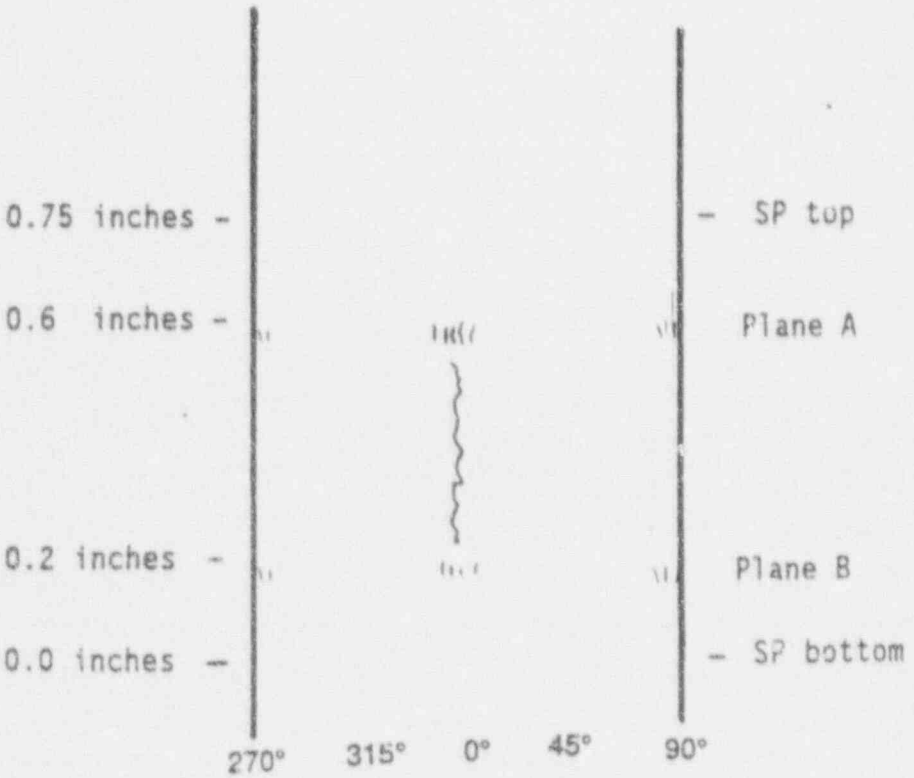

Sketch of Crack Distribution

Figure 10-16 Summary of crack distribution and morphology observed on Tube SL-FH-11.

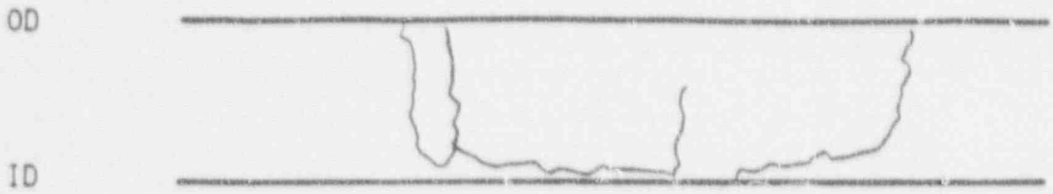

Sketch of Crack

Macrocrack Length = 0.46 inches

Throughwall Length = 0.03 inches

Number of Microcracks = 3 (ligaments have intergranular and ductile features)

Morphology = IGSCC

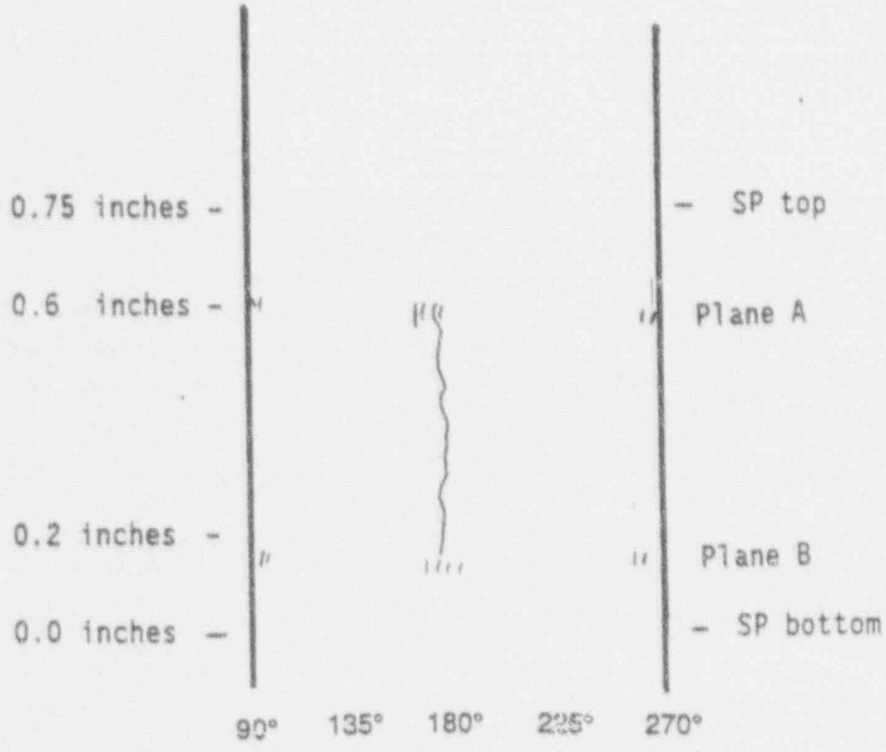

Sketch of Crack Distribution

Figure 10-17 Summary of crack distribution and morphology observed on second crack opened in the laboratory on Tube SL-FH-11.

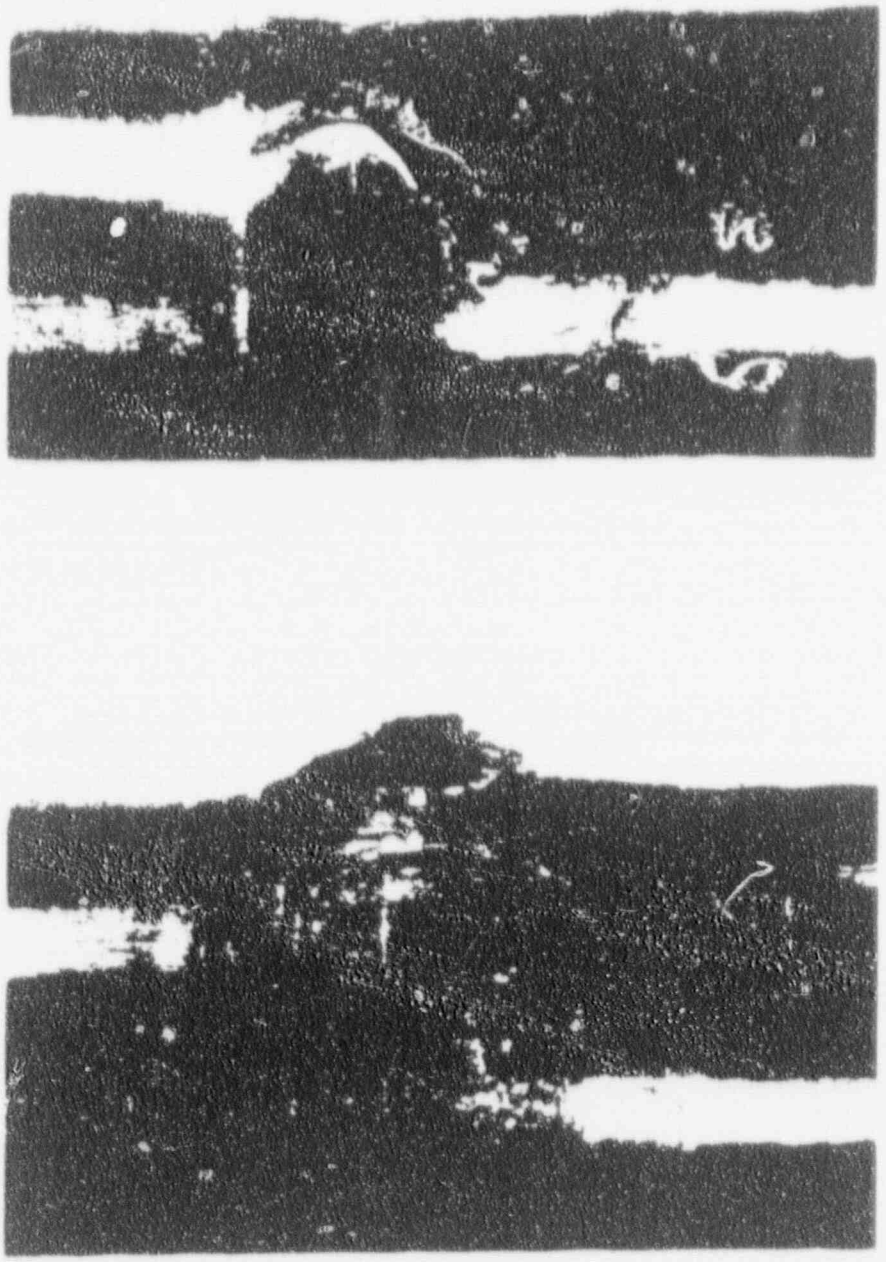

Figure 10-18 Appearance of the major burst crack opening on tube 528-2.

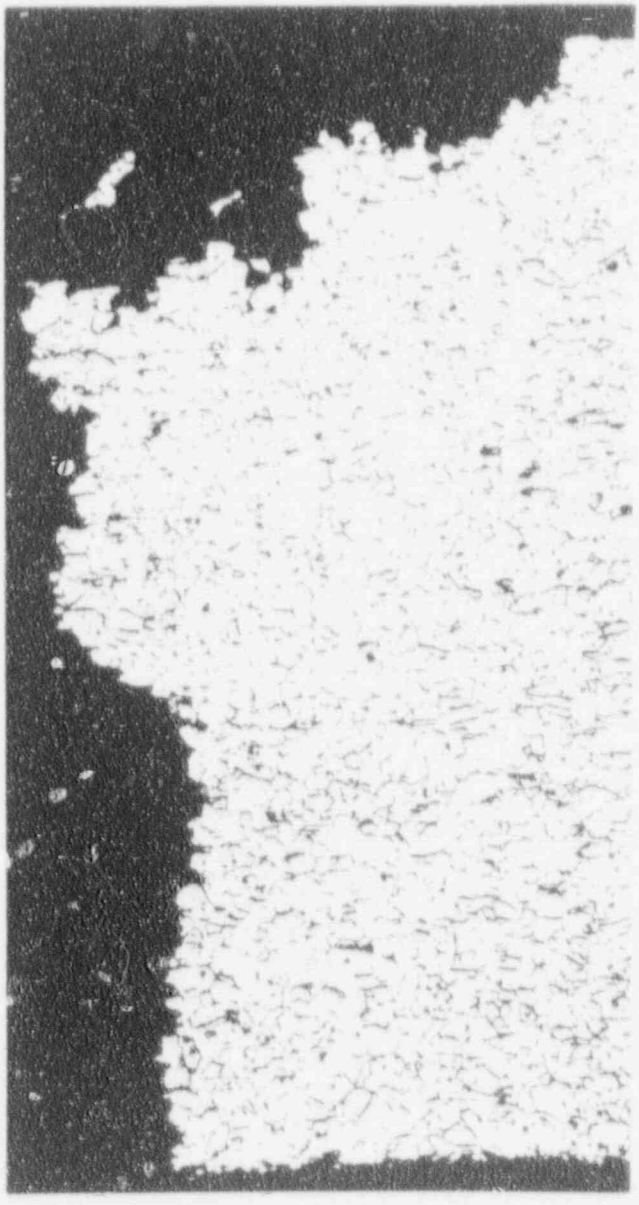

Figure 10-19 Crack morphology of the major burst opening crack (transverse section) showing it to be IGSCC with circumferential extension. Mag. 100X

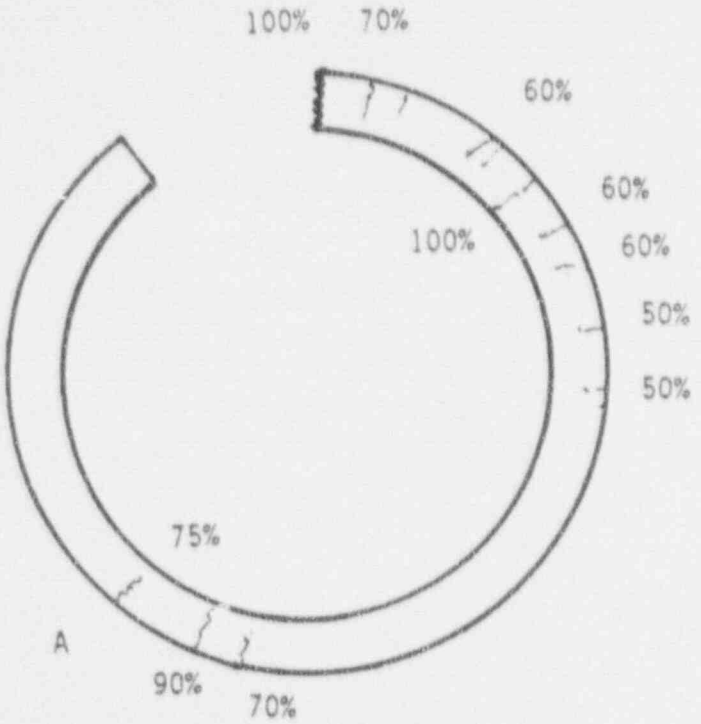

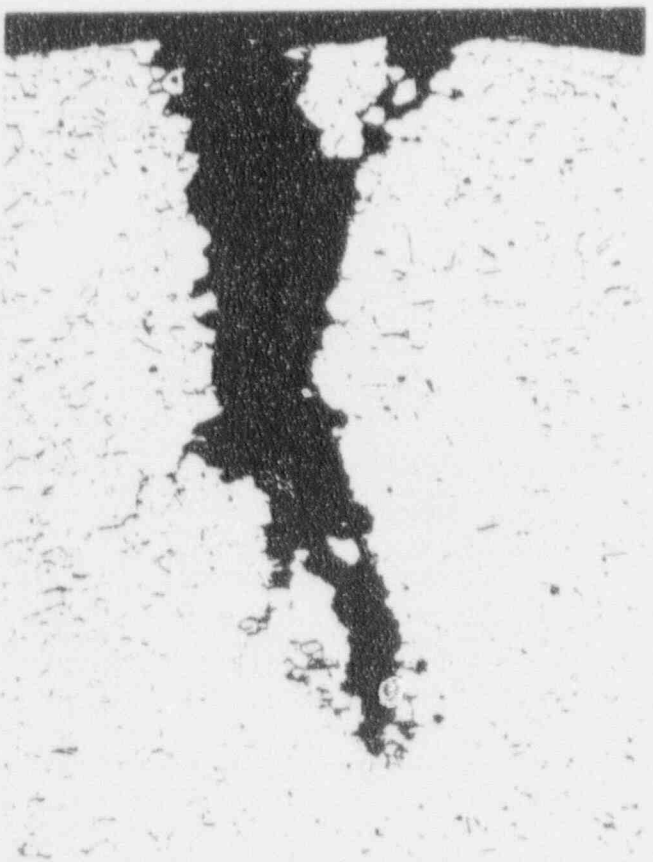

Crack A

Figure 10-20 Crack distribution found by a metallographic cross section through the center of the crevice (top) and a photomicrograph of one of the secondary cracks (bottom) showing IGSCC with negligible IGA aspects. Mag. 100X

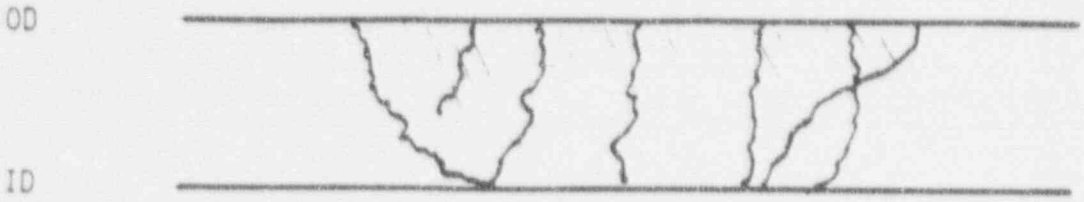

Sketch of Burst Crack

Macrocrack Length = 0.67 inch

Throughwall Length = 0.50 inch

Number of Microcracks = at least 6 (ligaments have intergranular features)

Morphology = IGSCC

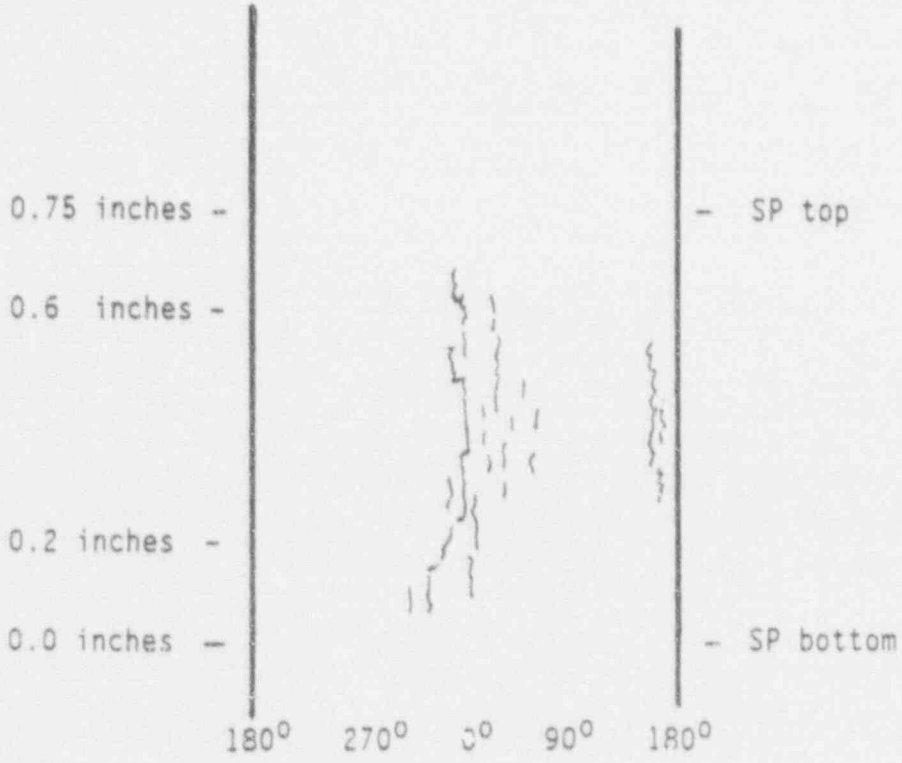

Sketch of Crack Distribution

Figure 10-21 Summary of overall crack distribution and morphology observed on tube 528-2.

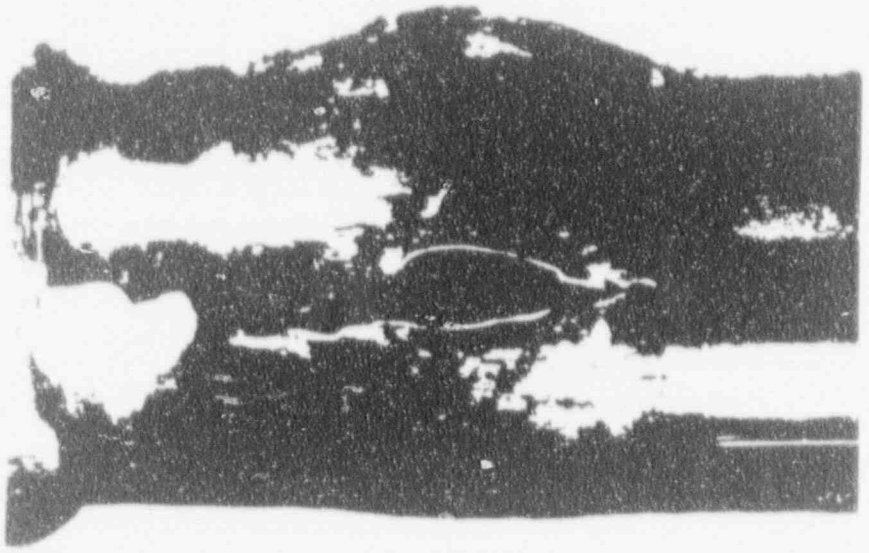

0°

60°

Figure 10-22 Photographs of the longest burst opening and of nearby secondary cracks in tube 532-1 and 0 and 60° locations.

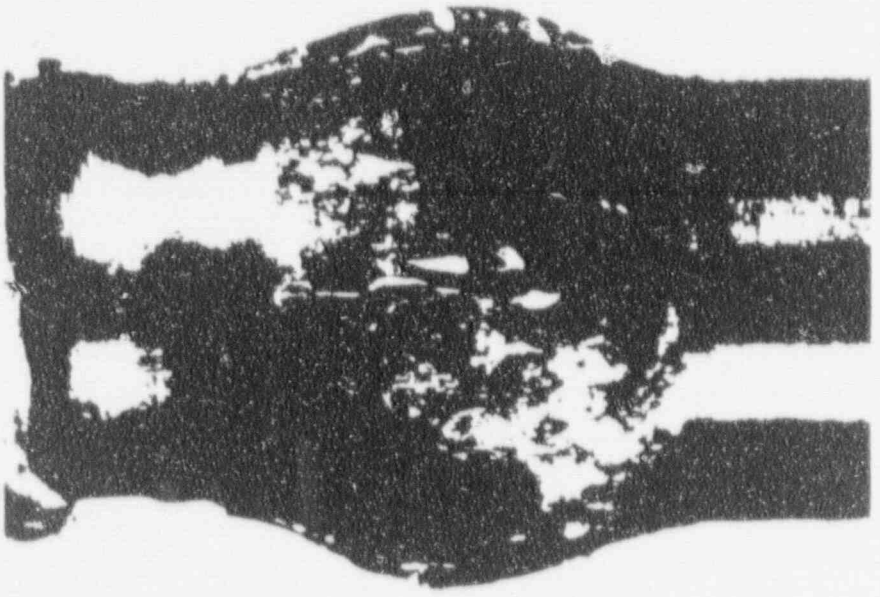

220°

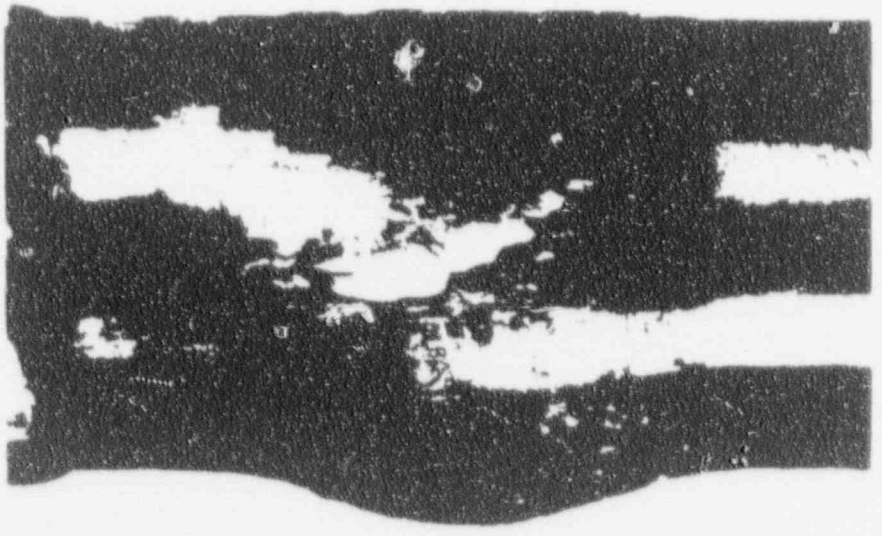

330°

Figure 10-23 Photographs of additional secondary cracks and of a second major burst crack in the crevice region of tube 532-1.

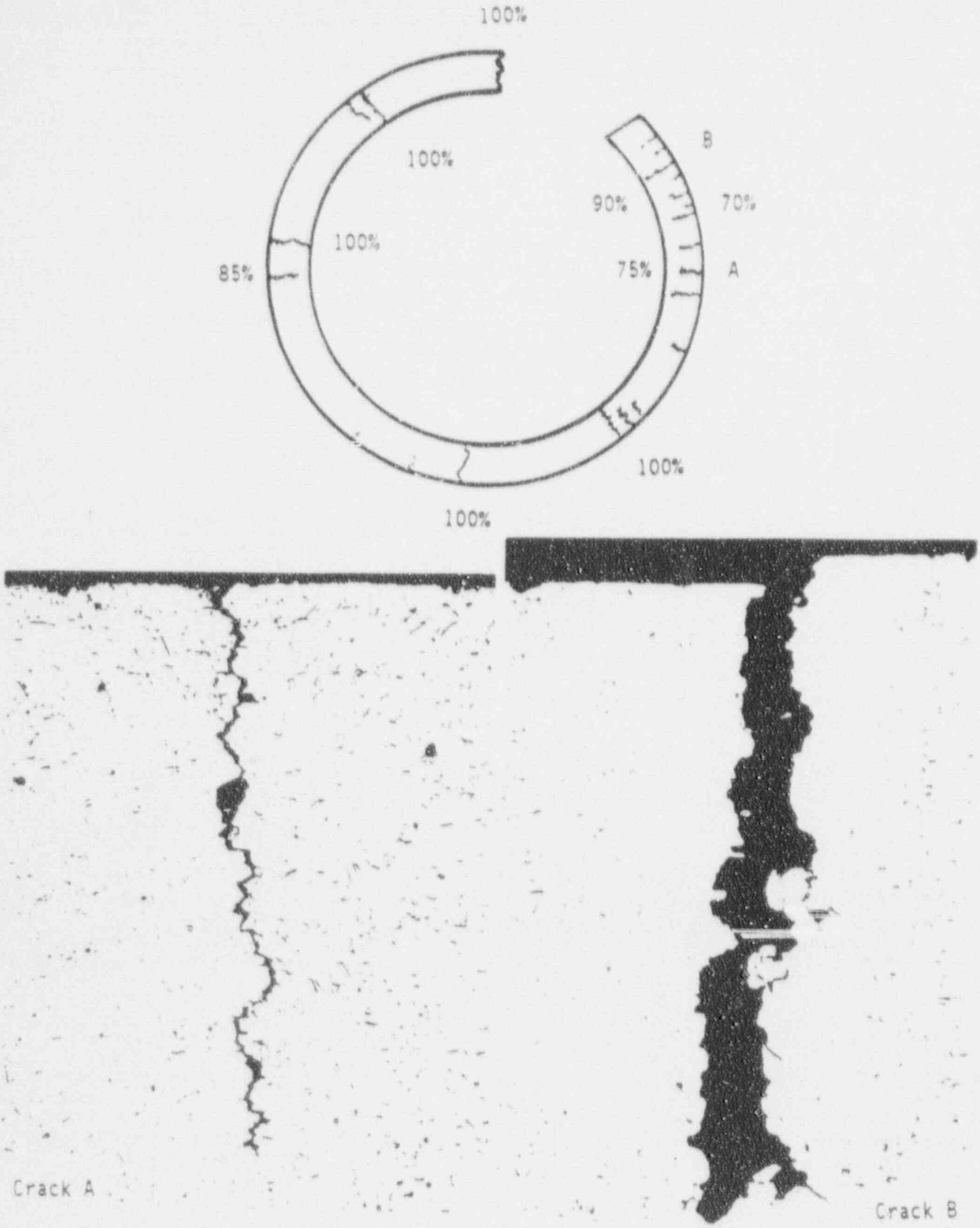

Figure 10-24 Sketch of crack distribution found by a metallographic cross section through the center of the crevice region of tube 532-1 and two photomicrographs of secondary cracks.
Mag. 100X

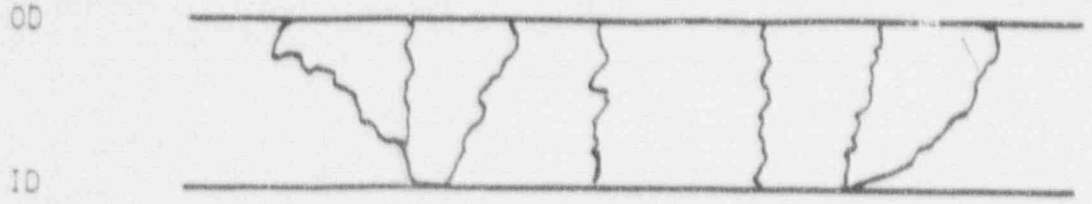

Sketch of Burst Crack

Macrocrack Length = 0.70 inch

Throughwall Length = 0.52 inch

Number of Microcracks = 5 (ligaments have intergranular features)

Morphology = IGSCC

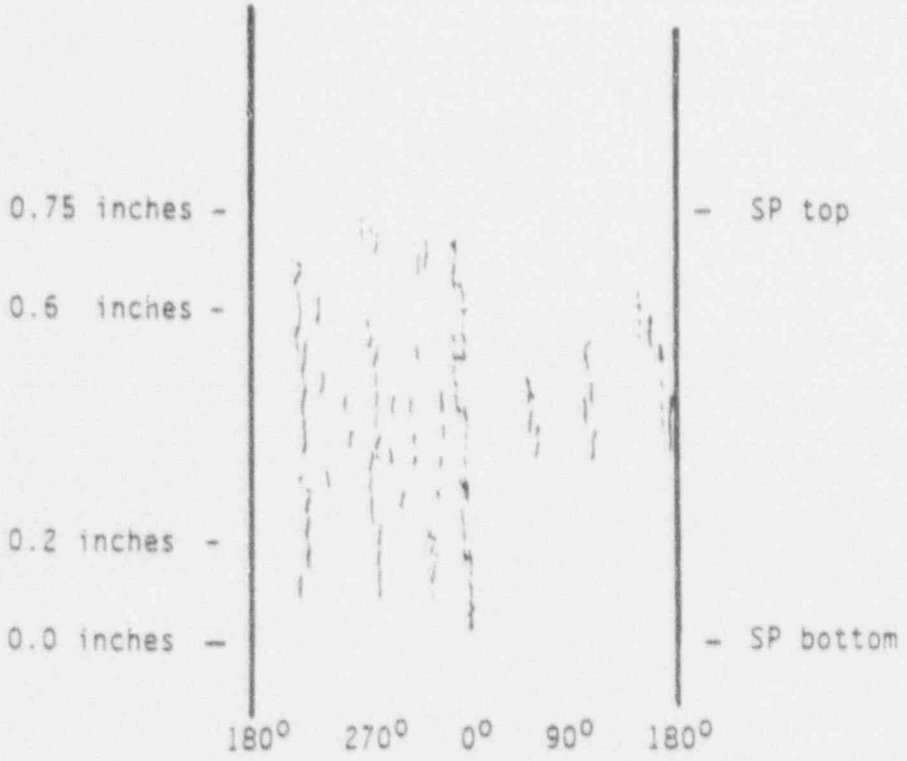

Sketch of Crack Distribution

Figure 10-25 Summary of overall crack distribution and morphology observed on tube 532-1.

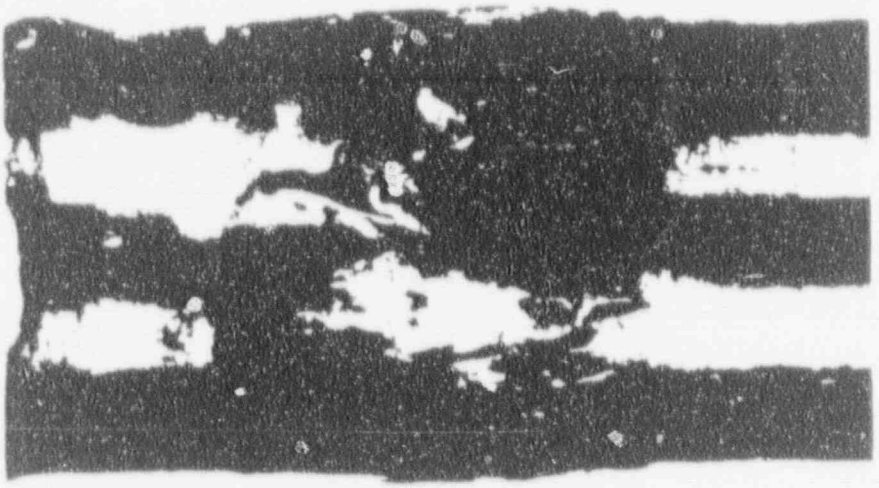

0°

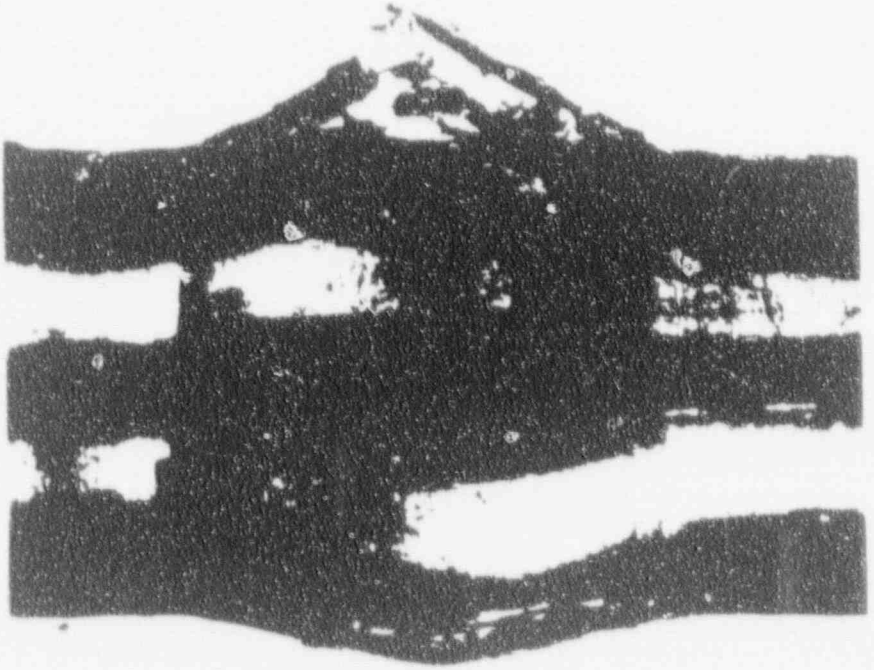

90°

Figure 10-26 Photographs of the major burst opening and secondary cracks within the crevice region of tube 532-2 at 0 and 90°.

180°

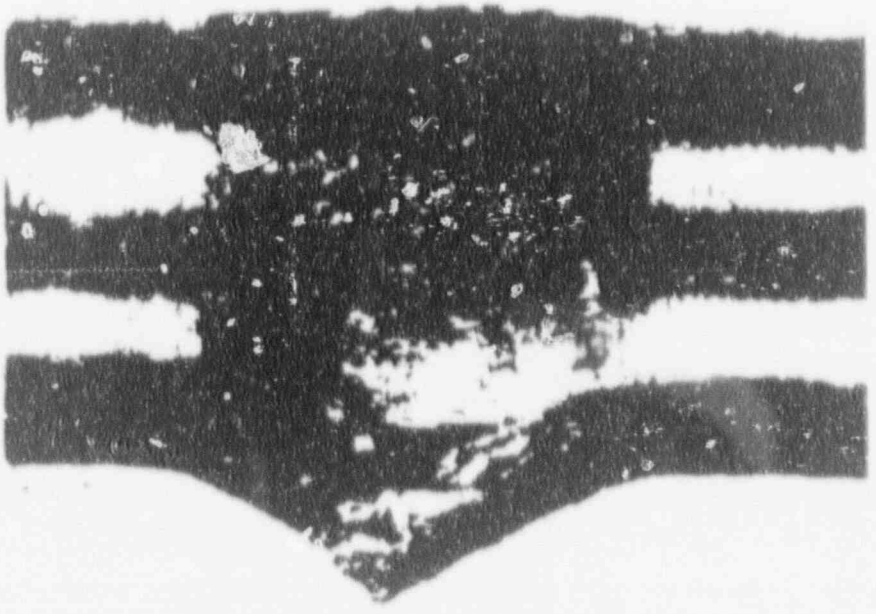

270°

Figure 10-27 Additional photographs of secondary cracks in tube 532-2 at 180 and 270°.

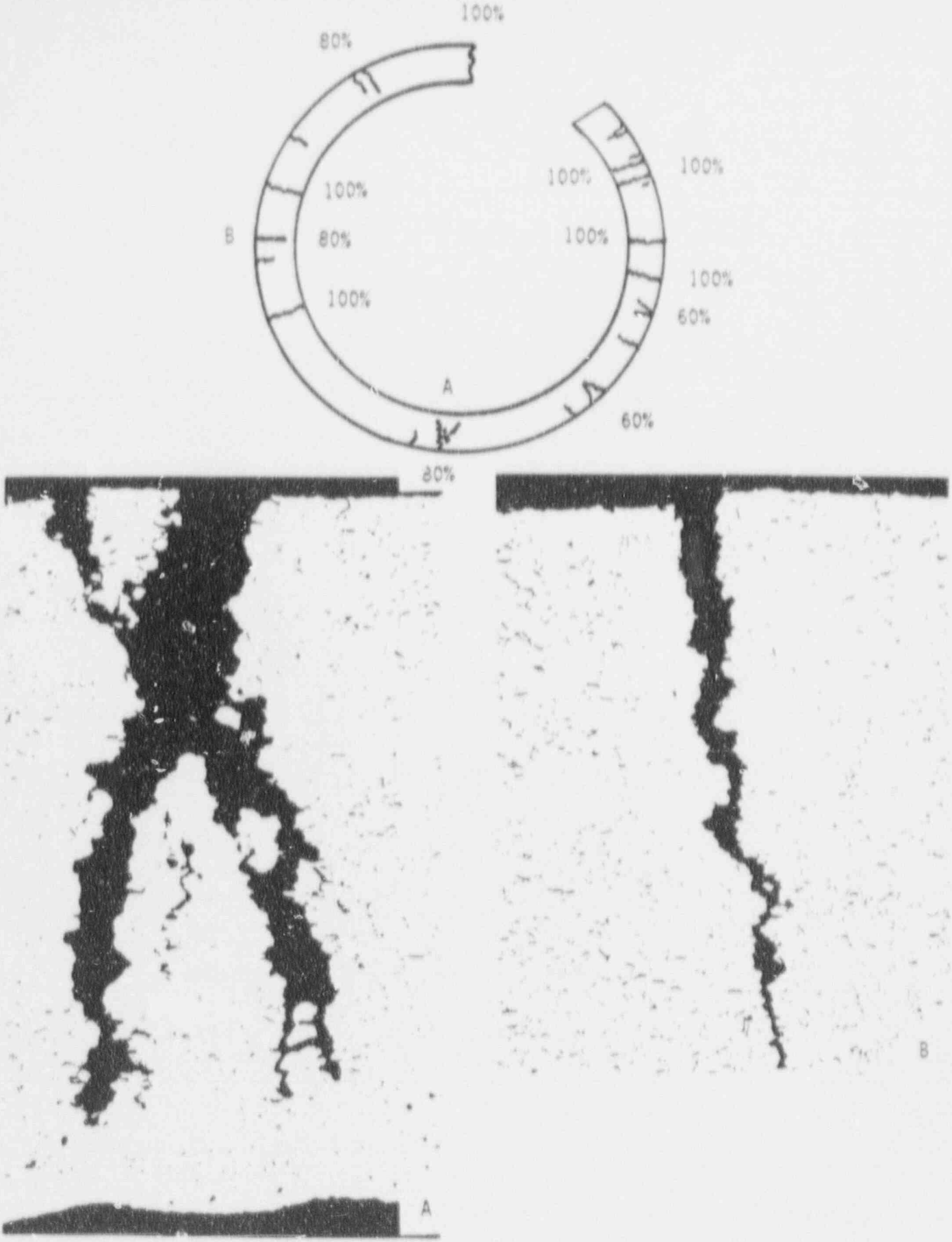

Figure 10-28 Crack distribution as revealed by a metallographic cross section through the center of the crevice of tube 532-2 and photomicrographs of secondary cracks A and B. Mag. 100X

Sketch of Burst Crack

Macrocrack Length = 0.75 inch

Throughwall Length = 0.58 inch (combined through wall length)

Number of Microcracks = at least 6 (ligaments have mostly intergranular features)

Morphology = IGSCC

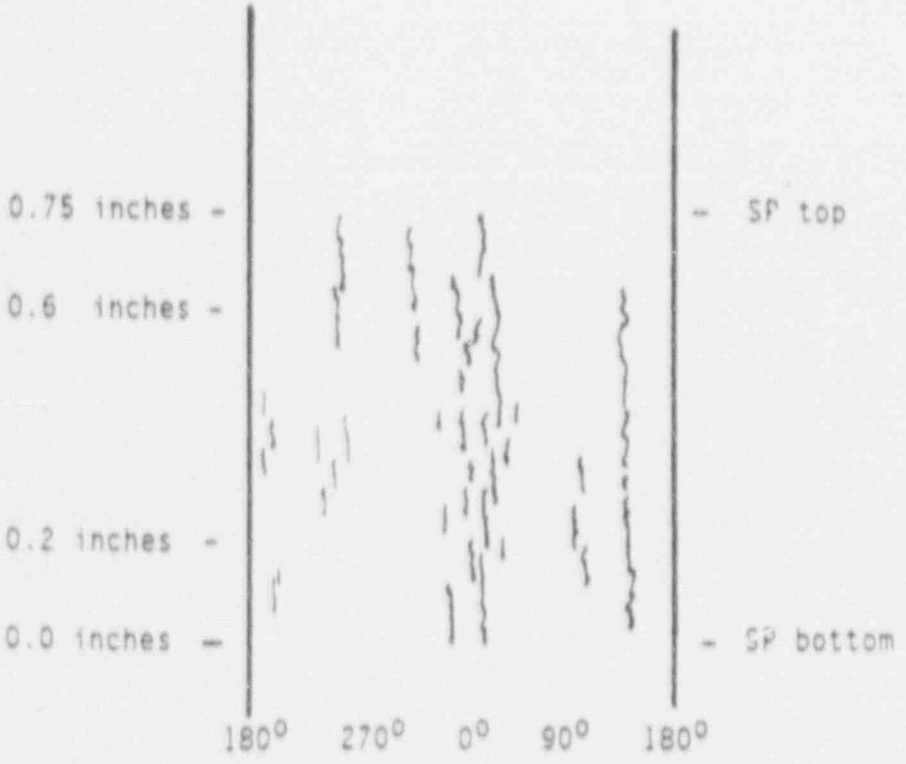

Sketch of Crack Distribution

Figure 10-29 Summary of the burst crack and overall crack distribution in the crevice region of tube 532-2.

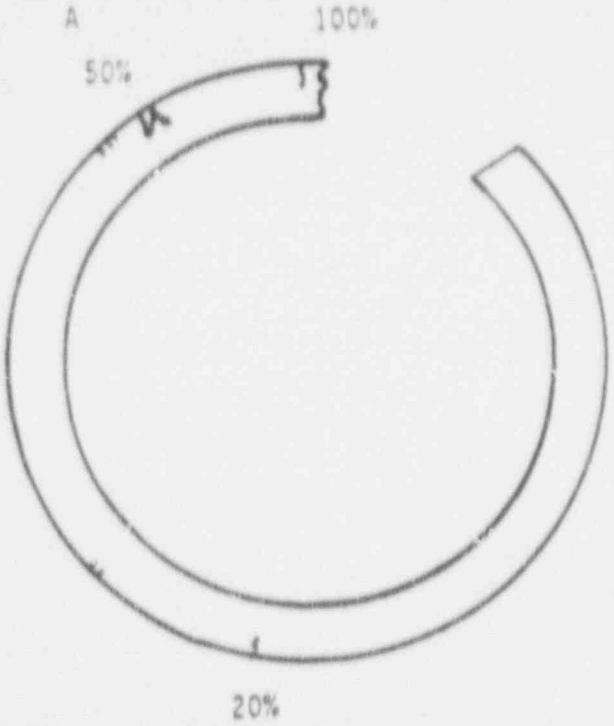

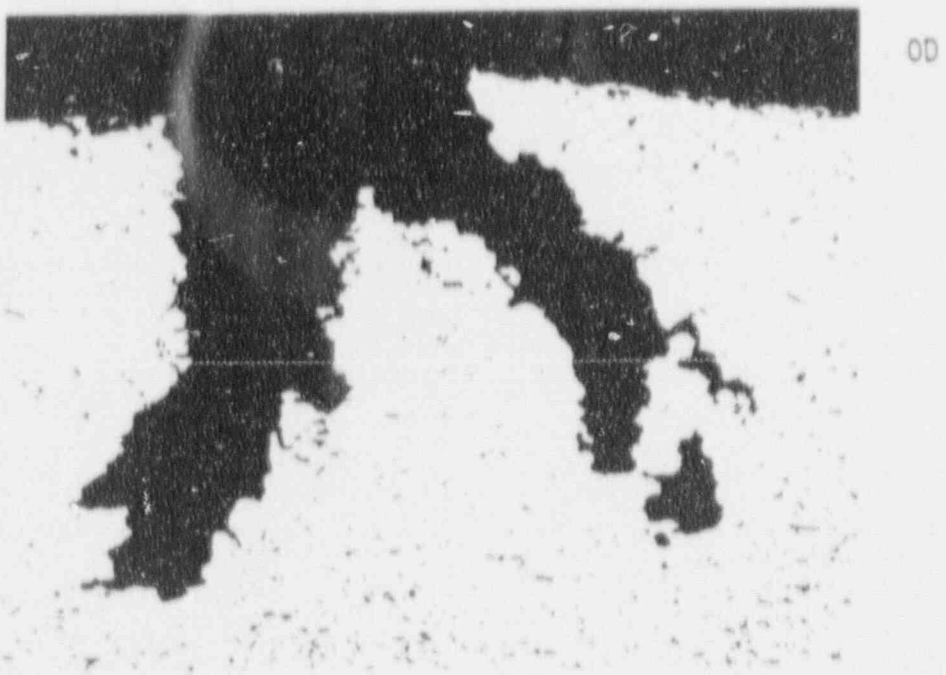

Crack A

Figure 10-30 Sketch of crack distribution in a metallographic cross section of tube 535 through the center of the crevice and a photomicrograph of crack A. Mag. 100X

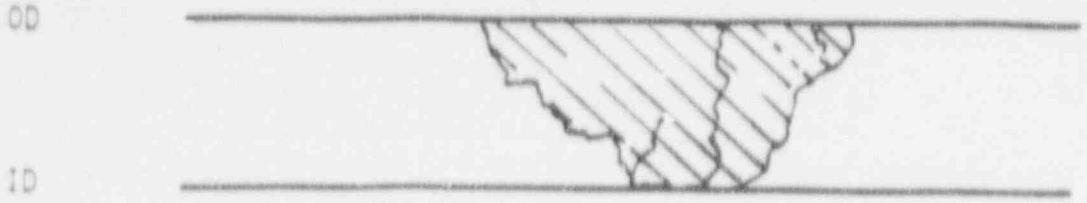

Sketch of Burst Crack

Macrocrack Length = 0.28 inch

Throughwall Length = 0.11 inch

Number of Microcracks = 3(ligaments have intergranular features)

Morphology = ICSCC

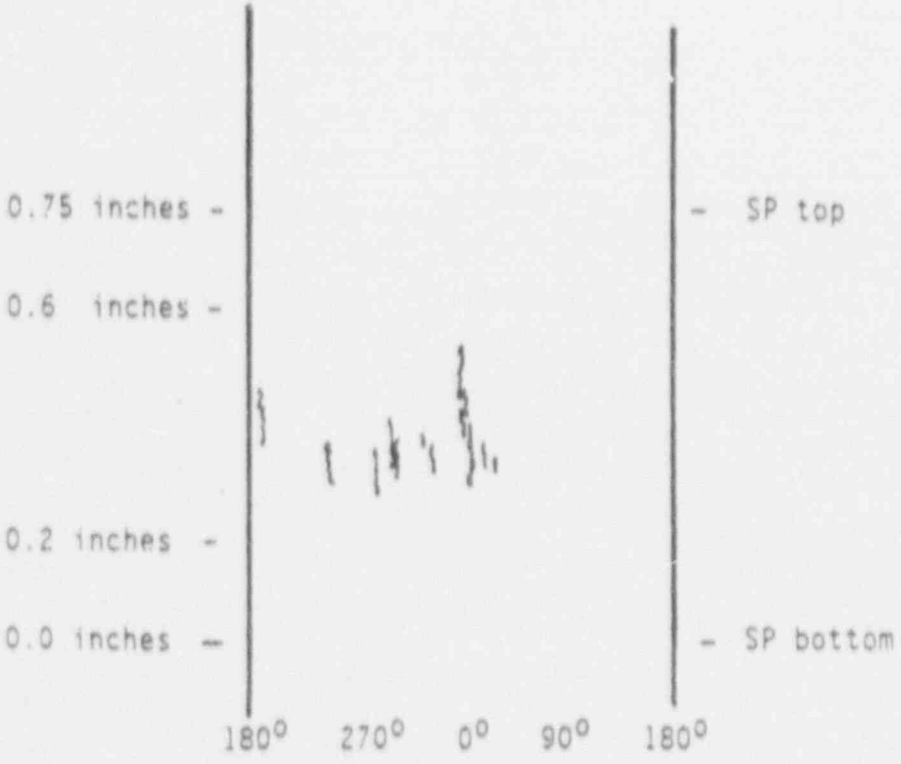

Sketch of Crack Distribution

Figure 10-31 Summary of the burst crack and overall crack distribution in the crevice region of tube 535-1.

Figure 10-32 Photograph of the burst opening and a transverse photomicrograph of the burst fracture in tube 555-3. Mag. 1Cjx

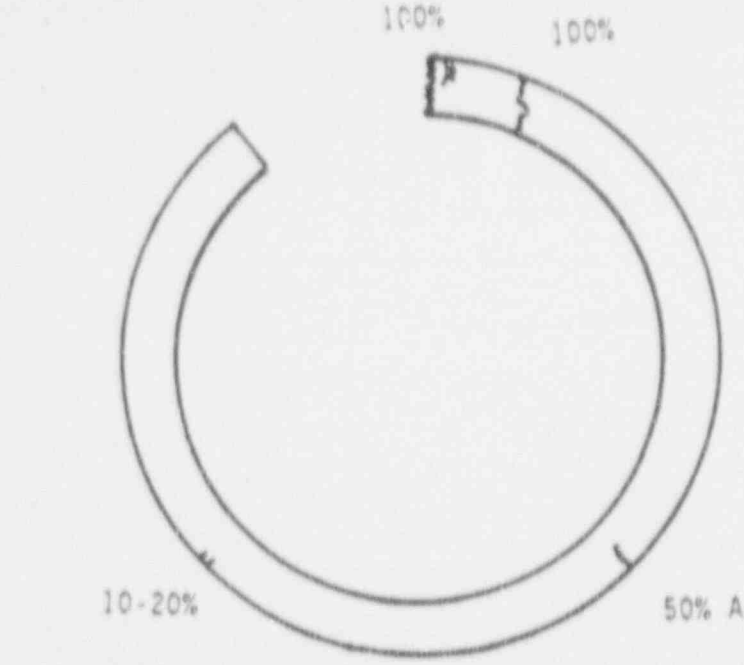

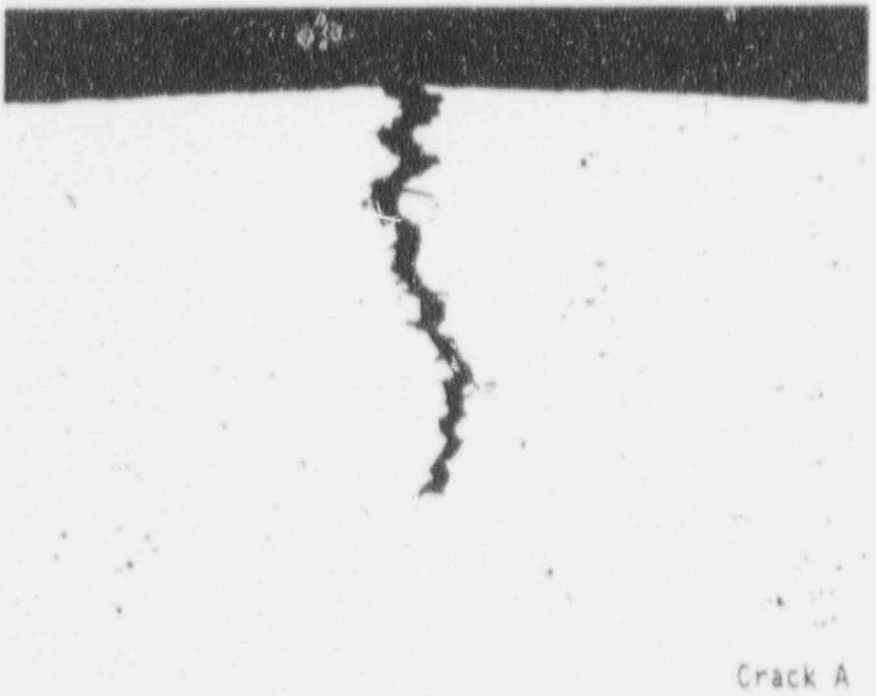

Crack A

Figure 10-33 Sketch of the metallographic cross section through secondary crevice region cracks in tube 555-3. A photomicrograph of Crack A is also shown. Mag. 100X

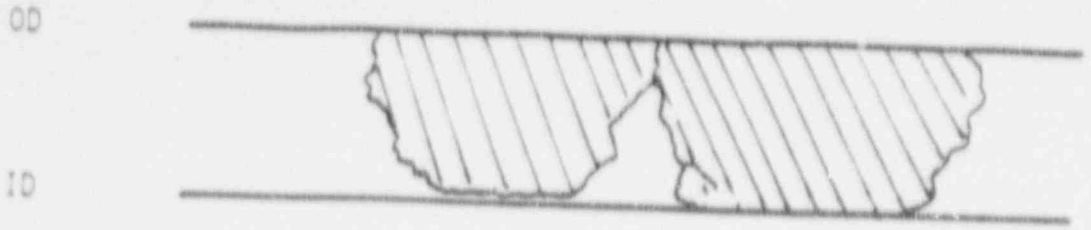

Sketch of Burst Crack

Macrocrack Length = 0.75 inch

Throughwall Length = 0.42 inch

Number of Microcracks = 2 (separated by ductile ligaments)

Morphology = IGSCC

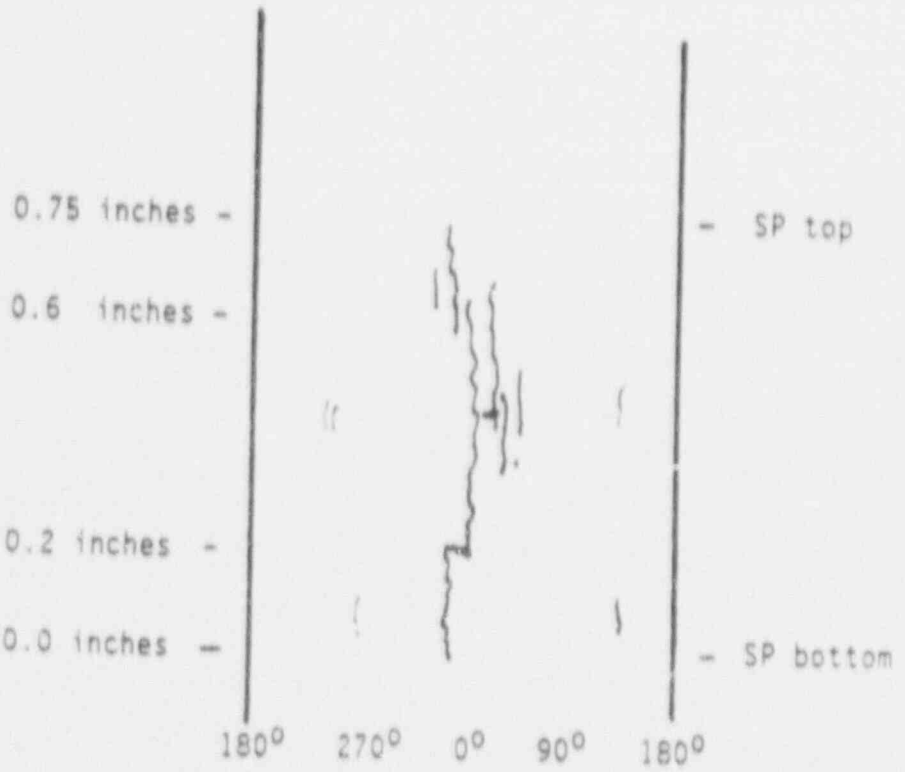

Sketch of Crack Distribution

Figure 10-34 Summary of burst crack observations and the overall crack distribution observed at the crevice region of tube 555-3.

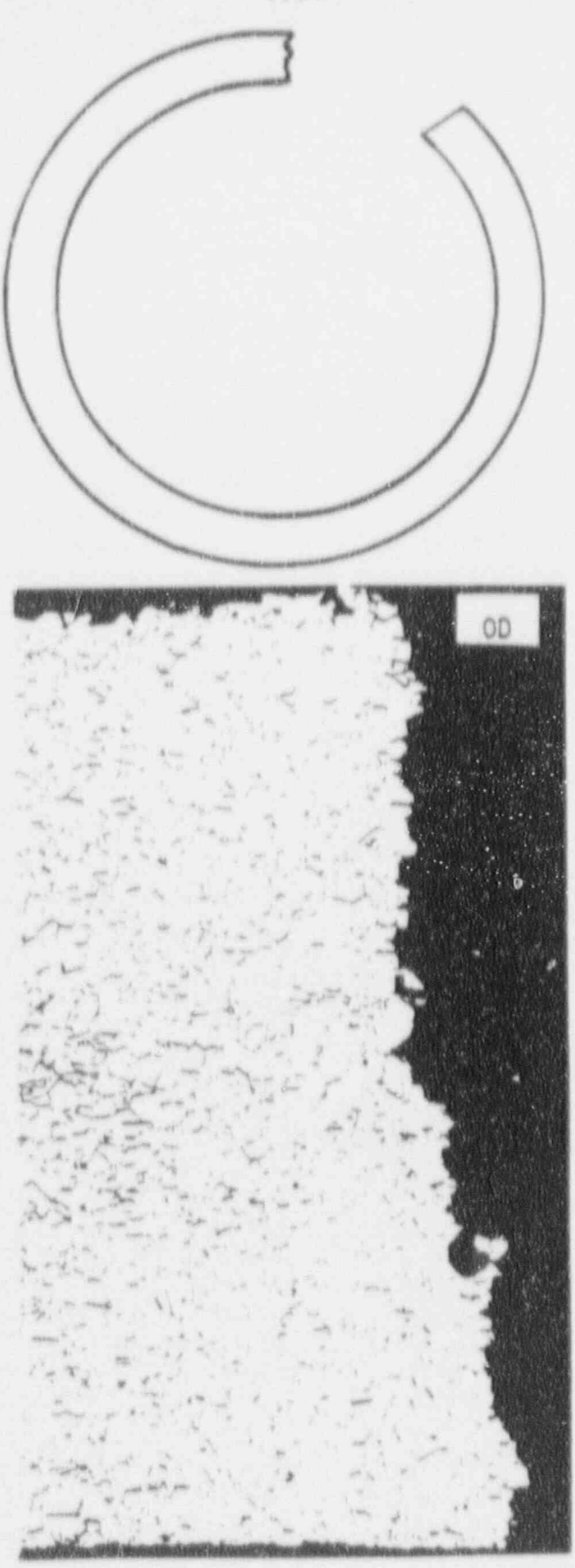

Figure 10-35 Sketch of a metallographic cross section through the center of the crevice region of tube 576-2, showing only the single burst crack, and a photomicrograph of the burst crack.
Mag. 100X

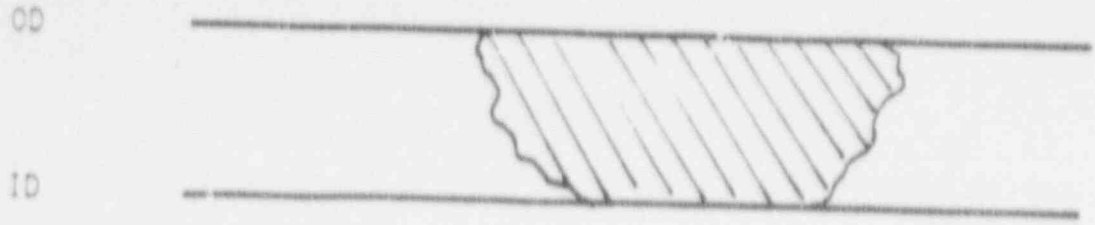

Sketch of Burst Crack

Macrocrack Length = 0.30 inch

Throughwall Length = 0.22 inch

Number of Microcracks = 1 (no ligaments)

Morphology = IGSCC

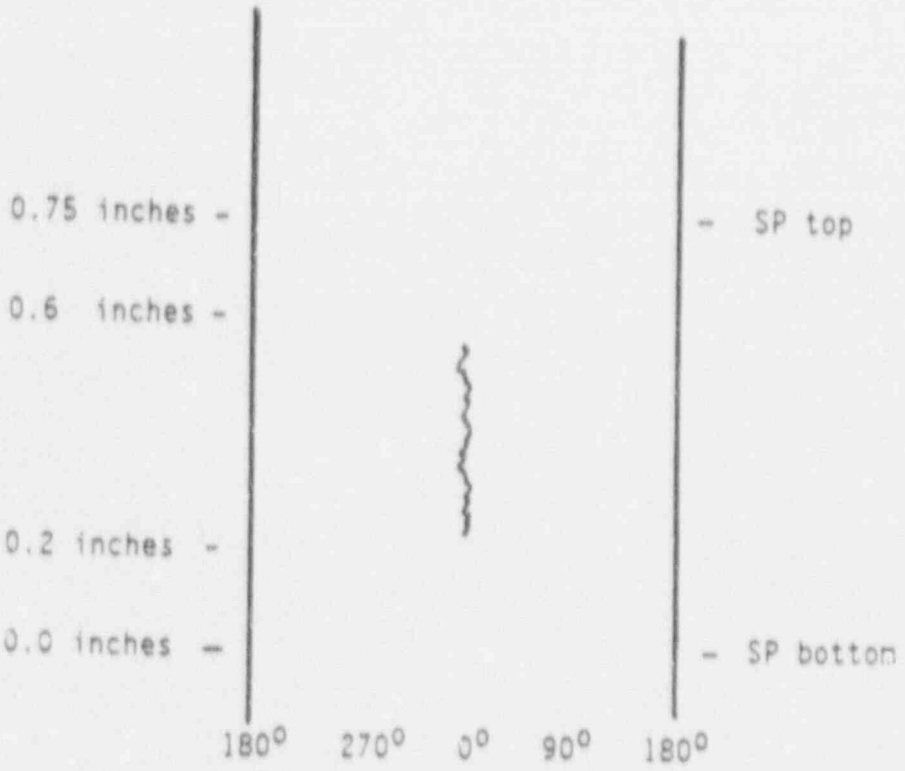

Sketch of Crack Distribution

Figure 10-36 Summary of burst crack observations and the overall crack distribution observed within the crevice region of tube 576-2.

Figure 10-37 Sketch of a metallographic cross section through the center of the crevice region of tube 576-4, showing only the single burst crack, and a photomicrograph of the burst crack.
Mag. 100X

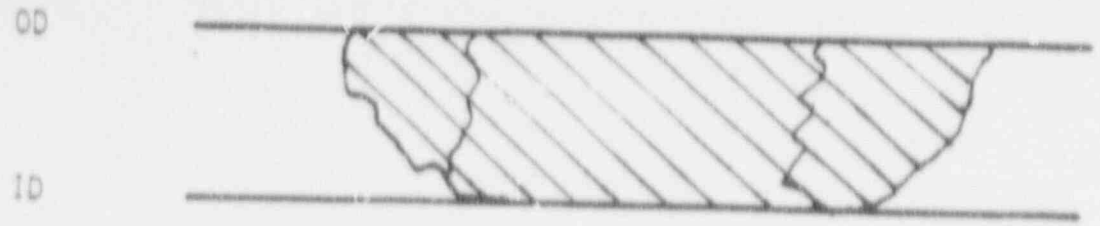

Sketch of Burst Crack

Macrocrack Length = 0.60 inch

Throughwall Length = 0.43 inch

Number of Microcracks = 3 (ligaments have intergranular features)

Morphology = IGSCC with negligible IGA features

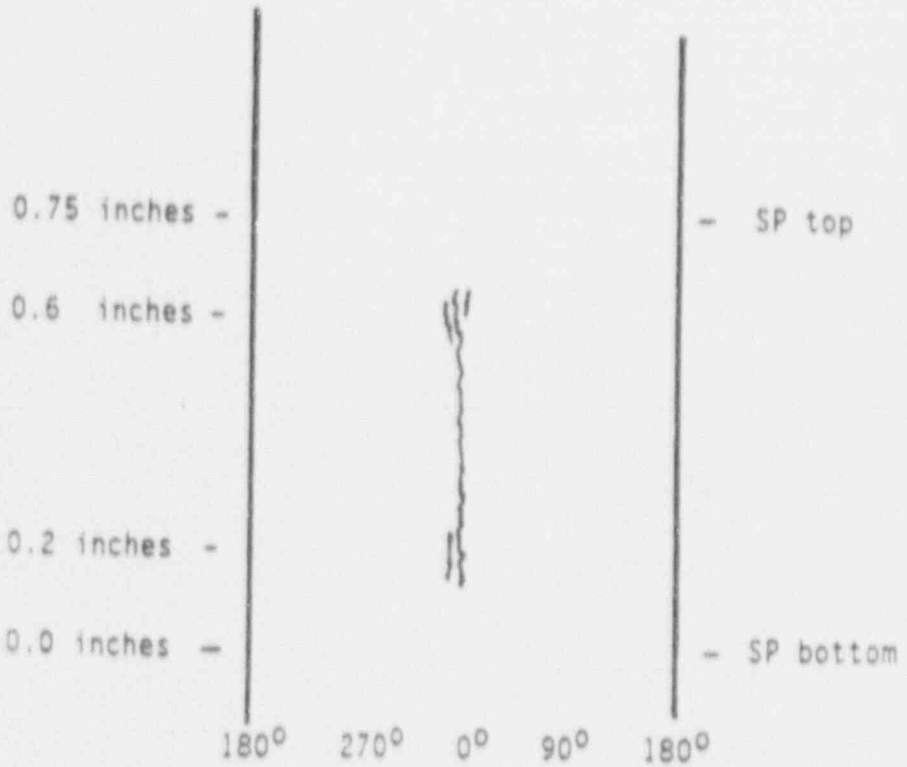

Sketch of Crack Distribution

Figure 10-38 Summary of burst crack observations and the overall crack distribution observed at the crevice region of tube 576-4.

11.0 STEAM LINE BREAK (SLB) AND COMBINED ACCIDENT CONSIDERATIONS

This section gives consideration to the limiting accident conditions and their implications relative to tube plugging criteria applications. If the TSP displacements from normal operation positions are large compared to the crack lengths which can lead to burst during an SLB event, then the benefit of the TSP to prevent tube rupture could be lost. Assuming uniform through wall cracks (not typical of ODSCC) approaching the TSP thickness, displacement of the TSP during the SLB event exceeding approximately 0.75 inch would expose sufficient length of the crack with the possibility that burst margins would not be met. TSP displacements were evaluated using non-linear, dynamic time history analyses to assess the potential for crack exposure, assuming an open crevice.

A combined accident condition for LOCA + SSE (loss of coolant accident + safe shutdown earth quake)is evaluated to identify potentially deformed tubes, if any, at specific locations in the S/G which will be excluded from the proposed plugging criteria. The allowable leakage during an SLB event are developed for the Kewaunee plant based upon radiological analyses associated with the determination of acceptable primary to secondary side leakage during accident conditions. An example calculation of a probabilistic analysis of potential end of cycle SLB leakage is presented for Kewaunee based on the 1991 inspection results for comparison to the allowable value.

11.1 Tube Support Plate Displacement Under SLB Loads

The potential for TSP displacement under SLB loading conditions has been evaluated for open crevices, for small gaps and for corroded TSP conditions of incipient denting which lead to contact forces between the tube and the hard magnetite in the crevices. These evaluations were performed to assess the potential for uncovering of the ODSCC under SLB conditions.

Analyses for TSP displacements with crevice gaps in an SLB event were performed using finite element, dynamic time history analysis methods. Conservative analysis assumptions, such as no friction, which ignores the TSP to wedge to wrapper contact forces, lead to overestimates of the TSP displacements. Given these assumptions, analyses for open, as manufactured crevices, indicate potential displacements yielding plastic deformation of some TSPs. For these results, it could not be assured that the TSPs would envelope the ODSCC at the times of increasing primary to secondary pressure differentials in an SLB event. The incipient denting and dented conditions at TSP intersections prevent TSP displacement under SLB conditions. TSP displacement analyses for varying crevice gaps show that even if the TSP corrosion resulted in up to [ ]^{a} mil gaps at the most limiting plate, the TSP displacements would not uncover the ODSCC.

With corroded TSP conditions, the maximum SLB loads on the TSPs would be less than the forces resulting from tube to TSP contact pressures. To support this conclusion, pull tests were performed to determine the force required to pull the tube from incipient denting and dented crevice conditions. The results show that the ODSCC at TSPs would continue to be enveloped by the TSPs even under accident conditions if even minor crevice packing is present. Since crevice packing has not been demonstrated for the Kewaunee S/Gs, the plugging criteria are conservatively based upon free span ODSCC under accident conditions.

11.2 Combined Accident Considerations

This section deals with combined accident condition loadings in terms of tube deformation and the effects on tube burst pressure. The most limiting accident conditions relative to these concerns are seismic (SSE) plus loss of coolant accident (LOCA) for tube deformation, and SSE plus steamline/feedline break (SLB/FLB) for tube burst. Details of the analysis methods used in calculating tube stresses and tube support plate loads for these loading conditions are also provided.

11.2.1 SSE Analysis

Seismic (SSE) loads are developed as a result of the motion of the ground during an earthquake. A seismic analysis specific to Series 51 steam generators has been completed. Response spectra that umbrella a number of plants with Series 51 steam generators, including the Kewaunee plant, have been used to obtain tube support plate (TSP) loads and the displacement time history response of the tube bundle. A nonlinear time-history analysis is used to account for the effects of radial gaps between the secondary shell and the TSPs, and between the wrapper and shell.

The seismic excitation defined for the steam generators is in the form of acceleration response spectra at the steam generator supports. In order to perform the non-linear time history analysis, it is necessary to convert the response spectrum input into acceleration time history input. Acceleration time histories for the nonlinear analysis are synthesized from El Centro Earthquake motions, using a frequency suppression/raising technique, such that each resulting spectrum closely envelopes the corresponding specified spectrum. The three orthogonal components of the earthquake are then applied simultaneously at each support to perform the analysis.

The seismic analysis is performed using the WECAN computer program. The mathematical model consists of three-dimensional lumped mass, beam, and pipe elements as well as general matrix input to represent the piping and support stiffnesses. In the nonlinear analysis, the TSP/shell, and wrapper/shell interactions are represented by a concentric spring-gap dynamic element, using impact damping to account for energy dissipation at these locations.

The mathematical model which is used is shown in Figure 11-1. The tube bundle straight leg region on both the hot and cold leg sides of the bundle is modeled by two equivalent beams. The U-bend region, however, is modeled as five equivalent tubes of different bend radii, each equivalent tube representing a group of steam generator tubes. In addition, a single tube representing the outermost tube row is also modeled. Continuity between the straight leg and U-bend tubes, as well as between the U-bend tubes themselves, is accomplished through appropriate nodal couplings. Note that the five equivalent tube groups are extended down two support plates before the single tube representation begins. This allows dissipation of tube response differences due to the variation in U-bend stiffnesses.

For reasons that will be discussed later, tube deformation calculations are performed for three TSP groupings, TSP 1, TSP 2-6, and TSP 7. The highest seismically induced TSP forces are 82 kips for TSP 1, 102 kips for TSP 2-6, and 78 kips for TSP 7.

11.2.2 LOCA Analysis

LOCA loads are developed as a result of transient flow, and temperature and pressure fluctuations

following a postulated main coolant pipe break. For the 51 series S/Gs in another plant, LOCA loads are developed for five different pipe break locations. These include three primary pipe breaks and two minor pipe breaks. The primary pipe break locations include the steam generator inlet and outlet lines, and the reactor coolant pump outlet line, while the minor pipe breaks include the pressurizer surge line and the accumulator line.

Prior qualification of the Kewaunee steam generators for leak before break requirements for the primary piping results in the limiting LOCA event being either the accumulator line break or the pressurizer surge line break. Bounding LOCA loads calculations for Kewaunee for the accumulator or pressurizer surge line are not available, however. Therefore, as a conservative approximation, the LOCA loads for the prior primary piping breaks are used to bound the Kewaunee smaller pipe breaks. As the results presented later in this section will show, the large pipe breaks are several times larger than the smaller pipe breaks, and thus, it is judged that these loads form a conservative basis for the small pipe breaks for Kewaunee.

As a result of a LOCA event, the steam generator tubing is subjected to the following loads:

1) Primary fluid rarefaction wave loads.

2) Steam generator shaking loads due to the coolant loop motion.

3) External hydrostatic pressure loads as the primary side blows down to atmospheric pressure.

4) Bending stresses resulting from bow of the tubesheet due to the secondary-to-primary pressure differential.

5) Bending of the tube due to differential thermal expansion between the tubesheet and first tube support plate following the drop in primary fluid temperature.

6) Axially induced loads resulting from differential thermal expansion between the tubes and tie rods/spacers due to the tube being tight in the first TSP, and the reduction in primary fluid temperature. (Based on available data, the majority of intersections are considered to be tight. Because the majority of the intersections are tight, the TSP will respond with the tubes, and the resulting loads on the tubes are judged to be small for this loading.)

Loading mechanisms 3) through 5) above are not an issue since they are a non-cyclic loading condition and will not result in crack growth, and/or result in a compressive membrane loading on the tube that is beneficial in terms of negating cyclic bending stresses that could result in crack growth.

11.2.2.1 LOCA Rarefaction Wave Analysis

The principal tube loading during a LOCA is caused by the rarefaction wave in the primary fluid. This wave initiates at the postulated break location and travels around the tube U-bends. A differential pressure is created across the two legs of the tube which causes an in-plane horizontal motion of the U-bend. This differential pressure, in turn, induces significant lateral loads on the tubes.

The pressure-time histories to be input in the structural analysis are obtained from transient thermal-hydraulic (T/H) analyses using the MULTIFLEX computer code. A break opening time of 1.0 msec to full flow area (that is, instantaneous double-ended rupture) is assumed to obtain conservative hydraulic loads. A plot of the tube model for a typical T/H model for determining LOCA pressure time histories for the tubes is shown in Figure 11-2. Pressure time histories are determined for three tube radii, identified as the minimum, medium, and maximum radius tubes. For the structural evaluation, the pressures of concern occur at the hot and cold leg U-bend tangent points. Plots of the hot-to-cold leg pressure drops for the limiting major and minor pipe breaks, the steam generator inlet break and the accumulator line break, are provided in Figures 11-3 and 11-4, respectively, for each of the three tubes considered. These results show that significantly higher pressure drops occur for the primary pipe break than for the minor pipe break.

For the rarefaction wave induced loadings, the predominant motion of the U-bends is in the plane of the U-bend. Thus, the individual tube motions are not coupled by the anti-vibration bars. Also, only the U-bend region is subjected to high bending loads. Therefore, the structural analysis is performed using single tube models limited to the U-bend and the straight leg region over the top two TSPs. The LOCA rarefaction pressure wave imposes a time varying loading condition on the tubes. The tubes are evaluated using the time history analysis capability of the WECAN computer program. The structural tube model consists of three-dimensional beam elements. The mass inertia is input as effective material density and includes the weight of the tube as well as the weight of the primary fluid inside the tube, and the hydrodynamic mass effects of the secondary fluid. The geometry of the three tube models used for the LOCA analysis are shown in Figure 11-5, with the node numbers identified.

To account for the varying nature of the tube/TSP interface with increasing tube deflection, three sets of boundary conditions are considered. For the first case, the tube is assumed to be laterally supported at the top TSP, but is free to rotate. This is designated as the "continuous" condition, in reference to the fact that the finite element model for this case models the tube down to the second TSP location. As the tube is loaded, it moves laterally and rotates within the TSP. After a finite amount of rotation, the tube will become wedged within the TSP and will no longer be able to rotate. The second set of boundary conditions, therefore, considers the tube to be fixed at the top TSP location, and is referred to as the "fixed" case. Continued tube loading causes the tube to yield in bending at the top TSP and eventually a plastic hinge develops. This represents the third set of boundary conditions, and is referred to as the "pinned" case.

Using the pressure time histories from the T/H analyses, lateral loads are calculated for each tube length at each time point and the dynamic response of the tube is calculated. The analysis shows the continuous set of boundary conditions to give the largest TSP loads for the minimum and medium tubes. For the maximum radius tube, the fixed condition is found to be most representative due to its increased flexibility and higher tube rotations at the top TSP. Each of the dynamic solutions results in a force time history acting on the TSP. These time histories show that the peak responses do not occur at the same time during the transient. For the Kewaunee analysis, however, it is assumed that the maximum reaction forces occur simultaneously. Using the results for these three tubes, a TSP load corresponding to the overall bundle is then calculated.

Summaries of the resulting TSP forces for the Inlet break and the Accumulator line break are shown in Table 11-1. Based on the plots shown, a bi-linear representation is assumed for the peak amplitudes as a function of tube radius. Summaries of the overall TSP forces are provided

in Tables 11-2 and 11-3 for the top TSP for the Inlet and Accumulator line breaks, respectively. Note that for tube rows 1-6, the peak response is assumed to be constant and equal to the Row 6 response. Shown in Figure 11-6 is the distribution of TSP load for the Inlet break for the top TSP. A summary of the resulting TSP loads for each of the breaks for the top TSP and for the TSP below the top TSP is provided in Table 11-4.

11.2.2.2 LOCA Shaking Loads

Concurrent with the rarefaction wave loading during a LOCA, the tube bundle is subjected to additional bending loads due to the shaking of the steam generator caused by the break hydraulics and reactor coolant loop motion. However, the resulting tube stresses from this motion are small compared to those due to the rarefaction wave induced motion.

To obtain the LOCA induced hydraulic forcing functions, a dynamic blowdown analysis is performed to obtain the system hydraulic forcing functions assuming an instantaneous (1.0 msec break opening time) double-ended guillotine break. The hydraulic forcing functions are then applied, along with the displacement time-history of the reactor pressure vessel (obtained from a separate reactor vessel blowdown analysis), to a system structural model, which includes the steam generator, the reactor coolant pump and the primary piping. This analysis yields the time history displacements of the steam generator at its upper lateral and lower support nodes. These time-history displacements formulate the forcing functions for obtaining the tube stresses due to LOCA shaking of the steam generator.

Past experience has shown that LOCA shaking loads are small when compared to LOCA rarefaction loads. For this analysis, these loads are obtained from the results of a prior analysis for a Model D steam generator. To evaluate the steam generator response to LOCA shaking loads, the WECAN computer code is used along with the seismic analysis model discussed previously. The steam generator support elements are removed, however, because the LOCA system model accounts for their influence on the steam generator response.

Input to the WECAN model is in the form of acceleration time histories at the tube/tubesheet interface. These accelerations are obtained by differentiation of the system model displacement time histories at this location. Acceleration time histories for all six degrees of freedom are used. The resulting LOCA shaking loads used for the this analysis are 17.1 kips for TSP 1-6 and 15.5 kips for TSP 7 for the large break LOCA, and 7.75 kips for all TSP for the minor breaks. The small break loads are scaled from the large break loads based on a comparison of support displacements from system analyses for the two types of breaks.

11.2.3 Combined Plate Loads

In calculating a combined TSP load, the LOCA rarefaction and LOCA shaking loads are combined directly, while the LOCA and SSE loads are combined using the square root of the sum of the squares. The overall TSP load is transferred to the steam generator shell through wedge groups located at discrete locations around the plate circumference.

For the Series 51 steam generators, there are six wedge groups located every 60° around the plate circumference (see Figure 11-7). The distribution of load among wedge groups is approximated as a cosine function among those groups reacting the load, which corresponds to half the wedge groups. Except for the bottom TSP, the wedge groups for each of the TSPs are located at the same angular location as for the top TSP. Thus, if TSP deformation occurs at the

lower plates, the same tubes are affected as for the top TSP. For the top TSP, however, the wedge groups have a 10 inch width, compared to a 6 inch width for the other plates. This larger wedge group width distributes the load over a larger portion of the plate, resulting in less plate and tube deformation for a given load level. For the bottom TSP, the wedge group width is 6 inches, and the wedge groups are rotated 36° relative to the other TSPs. The distribution of load among the various wedge groups for the LOCA load, which can only act in the plane of the U-bend, is shown in Figure 11-8 for TSP 2-7. Although, the wedges are rotated for TSP 1, the rotations are such that the same load factors result. For seismic loads, which can have a random orientation, the maximum wedge load is 2/3 of the maximum TSP load.

Summaries of the resulting TSP and wedge loads for the Inlet and Accumulator line breaks are provided in Tables 11-5 and 11-6, respectively.

11.2.4 Tube Deformation

[

]a

11.2.5 Effect on Burst Pressure (SSE + FLB/SLB)

Since the tube support plates provide lateral support to tube deformation that may occur during postulated accident conditions, tube bending stress is induced at the TSP intersections. This bending stress is distributed around the circumference of the tube cross section, tension on one side and compression on the other side, and is oriented in the axial (along the tube axis) direction. Axial cracks distributed around the circumference will therefore either experience tension stress that tends to close the crack or compressive stress that tends to open the crack. The compressive stress has the potential then to reduce the burst capability of the cracked tube due to the crack opening.

[

]a

11.3 Allowable Leak Rate for Accident Conditions

A calculation has been completed to determine the maximum permissible steam generator primary-to-secondary leak rate during a steam line break for the Kewaunee steam generators. Based on a 30 rem thyroid dose at the site boundary, a leak rate of 260 gpm is determined to be the upper limit for allowable primary to secondary leakage in both loops. The S/G in the intact loop is assumed to have primary to secondary leakage of 150 gpd, which is the maximum value defined by the proposed technical specification. Although the leakage in either loop may be distributed among all regions of the tube bundle, the calculation was performed conservatively assuming that all the leakage is at TSP locations (above the mixture level).

Thirty rem was selected as the thyroid dose acceptance criteria based on the guidance of Standard Review Plan (NUREG-0800) Section 15.1.5, Appendix A. Only the release of iodine and the resulting thyroid dose was considered in the leak rate determination. Whole-body doses due to noble gas immersion have been determined, in other evaluations, to be considerably less limiting than the corresponding thyroid doses.

The salient assumptions used in the evaluation are those presented in Kewaunee USAR Section 14.2.5, with the exception of the iodine partition coefficient assumed for the steam generator in the faulted loop (1.0 versus 0.1). The assumptions follow:

- Initial primary coolant iodine activity - 1% fuel defects
  (approximately 2.39 µCi/gm of dose equivalent I-131)
- Initial secondary coolant activity - 1.0 µCi/cc of dose equivalent I-131 (Tech. Spec. LCO)
- Steam released to the environment (0 to 2 hours)
  - from S/G in intact loop = 290,000 lb (plus primary-secondary leakage)
  - from faulted loop = 99,000 lb + primary-secondary leakage
    (the entire initial S/G water mass, does not include feedwater)
- Iodine partition coefficients:
  - S/Gs in intact loop - 1.0 for primary to secondary leakage (since leakage is assumed to be above the mixture level) and 0.1 for steam release
  - S/G in faulted loop - 1.0 due to dry S/G (USAR assumes 0.1)
- Atmospheric dispersion factor - 2.23E-4 sec/cu m
- Thyroid dose conversion factor for I-131 - 1.48E6 rem/Ci (TID-14844)

The radioactivity released to the environment due to a main steam line break can be separated into two distinct releases: the release of the initial iodine activity contained in the secondary coolant and the release of primary coolant iodine activity that is transferred by tube leakage.

Based on the assumptions stated previously, the release of the activity initially contained in the secondary coolant (2 S/Gs) results in a site boundary thyroid dose of approximately 6.6 rem. This is independent of the leak location.

Relative to activity release due to primary-to-secondary leakage, the dose contribution from the faulted loop S/G or from the intact loop S/G, regardless of the leak location, is approximately 0.09 rem/gpm.

Because of the S/G tube uncovery issue that is currently under investigation, treatment of the leakage is different depending on its location. Following a reactor trip, the mixture level in the S/G can drop below the apex of the tube bundle. For the S/G in the non-faulted loop, leakage that occurs in the tubesheet region is assumed to mix with the secondary coolant (partition coefficient associated with steaming is 0.1), while the leakage that occurs at a support plate is conservatively assumed to transfer directly to the environment without mixing or partitioning since the leakage site is assumed to be above the mixture level. Although less than 4 feet of the bundle is expected to be above the mixture level, any leakage at a support plate is conservatively assumed to be uncovered for the duration of the accident recovery. The S/G in the faulted loop is assumed to steam dry (no mixture level). Hence leakage to this S/G is assumed to transfer directly to the environment regardless of the location of the leak.

The accidents that are affected by primary to secondary leakage are those that include, in the activity release and offsite dose calculation, modeling of leakage and secondary steam release to the environment. The accidents addressed in the Kewaunee USAR that result in a secondary steam release include:

- Excess Heat Removal Due to Feedwater System Malfunction, USAR 14.1.6
- Loss of Reactor Coolant Flow (locked rotor), USAR 14.1.8
- Loss of External Electrical Load, USAR 14.1.9
- Loss of AC Power, USAR 14.1.12
- Steam Generator Tube Rupture, USAR 14.2.4
- Rupture of Steam Pipe, USAR 14.2.5
- RCC Assembly Ejection, USAR 14.2.6

Of these events, only the tube rupture and steam line break include an offsite dose analysis (RCCA ejection states that doses will be within the 10 CFR 100 guideline, but no explicit analysis is presented).

The reason that the steam line break is generally limiting is because of the assumption that leakage to the faulted steam generator is assumed to be released directly to the environment, i.e., no mixing with the secondary coolant or partitioning of activity is assumed, since the steam generator in the faulted loop is subject to dryout. Depending on the elevation of the degradation (at the tubesheet region versus at a TSP), for other accidents in which there is a secondary side steam release there is justification for mixing and iodine partitioning in the steam generators following the potential initial uncovery of the top of the tube bundle after the reactor trip. These factors, along with a smaller primary to secondary pressure differential, significantly reduce the release of iodine to the environment for accidents other than steam line break.

As noted above, mixing and iodine partitioning is dependent upon the elevation of the degradation. For the non-SLB accidents in which there is a secondary side steam release, there is justification for mixing and partitioning if the primary to secondary leakage is at the tubesheet

region (below S/G water level). If the degradation is at a TSP, such that the reactor coolant leakage could directly get into the steam space, the release path (for radioactivity) is assumed to be direct to the environment, just as it is for the faulted S/G following an SLB.

Following the implementation of the plugging criteria, tubes are not expected to burst during SLB conditions; however, it cannot be assumed that the tubes will not leak. SLB is the bounding accident condition for which the primary to secondary leakage is to be limited so as to maintain radiological consequences within acceptable levels. Thus the potential leakage during an SLB should be kept below the maximum allowable value determined above.

11.4 SLB Leakage Determination

A number of tube intersections with voltage signals that satisfy the proposed criteria will remain in service until inspected and reevaluated at the next refueling outage. Some of these would have the potential for leakage under SLB conditions as leak rate testing has demonstrated some potential for leakage under SLB pressures in tubes with voltage signals less than 3.5 volts. Therefore, leak rate during SLB conditions is to be evaluated for the tubes remaining in service at each outage. The methodology used in the evaluation is a probabilistic approach based on the leak rate versus voltage correlation and the population of voltage signals at TSP intersections left in service. Uncertainties in voltage signal, growth allowance and leak rate versus voltage are accounted for using Monte Carlo techniques. Thus, an end of cycle voltage population is assessed (accounting for uncertainties) for its potential for leakage during a postulated SLB.

A current distribution of number of indications versus voltage signal will be obtained at each outage similar to those presented in Section 5 for each steam generator in Kewaunee. Also, the most recent change in voltage (voltage growth rate) between the last two inspections will be obtained. The current voltage distribution (cut off at the voltage plugging limit) is then combined with the voltage growth rate using Monte Carlo techniques to establish an end of cycle (EOC) voltage distribution. Uncertainty in the voltage signals for the current inspection is accounted for in a statistical manner via the Monte Carlo simulations. Finally, the EOC voltage distribution is evaluated for leak rate using Monte Carlo techniques and the leak rate versus voltage relationship given in Section 9.7 and in Figure 9-3.

The method described above has been applied to the Kewaunee voltage distribution from the 1991 inspection for each steam generator. The methodology utilizes the following data for Kewaunee.

Current Voltage Distribution of Indications

The 1991 inspection results shown in Figure 5-3 with a voltage cutoff of 3.5 volts defines the distribution of indications returned to service assuming application of the current plugging criteria.

Eddy Current Uncertainty

Section 8.8 defines the eddy current uncertainty distribution for the voltage amplitudes as 10% (one standard deviation) with limits of ± 15%. This uncertainty is applied statistically (by Monte Carlo simulation) to the above distribution of indications.

Growth Rate

As developed in Section 5.3, an average growth rate of 40% is applied. Figure 5-15 shows the growth rate distribution from the last Kewaunee operating cycle. The distribution is provided as a cumulative distribution function for percentage voltage growth. The Figure 5-15 growth rates are given as growth over the last cycle and are multiplied by the ratio of the planned EFPY for the next cycle to the EFPY for the prior cycle. This growth rate distribution is randomly sampled for the Monte Carlo analysis and added to the current distribution along with sampling for eddy current uncertainties to obtain the projected end of cycle distribution. Equal operating cycle lengths for prior and projected cycles are assumed for the Kewaunee analysis results given below.

SLB Leak Rate

The linear regression fit of Figure 9-3 is used to obtain a leak rate for a projected voltage. A Monte Carlo selection is made at each voltage within the prediction interval described by the statistical parameters developed in Section 9.7, and summed over the total distribution of indications to obtain the projected total leakage at SLB conditions for each steam generator.

A maximum expected leak rate for a postulated SLB was determined to be 0.1 gpm for Kewaunee compared to the 260 gpm allowable. Therefore, the cutoff value of 3.5 volts conservatively limits the potential for leakage during SLB and no further restriction would be required.

Table 11.1

Summary of TSP Forces - Top TSP
Dynamic Time History Analysis
LOCA Rarefaction Pressure Wave Loading

[ ] a

Table 11.2

Summary of Total TSP Force - Top TSP
LOCA Rarefaction Pressure Wave Loading
Steam Generator Inlet Break

[ ] a

Table 11.3

Summary of Total TSP Force - Top TSP
LCCA Rarefaction Pressure Wave Loading
Accumulator Line Break

[ ]a

Table 11.4

Summary of TSP Forces

LOCA Rarefaction Pressure Wave Loading

[ ] a

Table 11.5

Summary of Wedge Loads
Combined LOCA + SSE Loading
Steam Generator Inlet Break

[ ] a

Table 11.6

Summary of Wedge Loads
Combined LOCA + SSE Loading
Accumulator Line Break

[ ] a

Table 11.7

Summary of Calculations to Determine Area Under Force/Deflection Curve

Crush Test No. 2

[a,b]

Table 11.8

Summary of Number of Deformed Tubes as a Function of Load

[ ] a,b

Table 11.9

Summary of Number of Deformed Tubes at Wedge Locations

TSP 1

[ ] a

Table 11.10

Summary of Number of Deformed Tubes at Wedge Locations

TSP 2-6

[redacted] a

Table 11.11

Summary of Number of Deformed Tubes at Wedge Locations

TSP 7

[ ] a

Table 11.12

Applicability of Test Results to Wedge Locations

[ ] a,b

Table 11.13

Combined Bending and Internal Pressure Burst Tests

on Tubes With Through Wall Slots

[ ] a,b

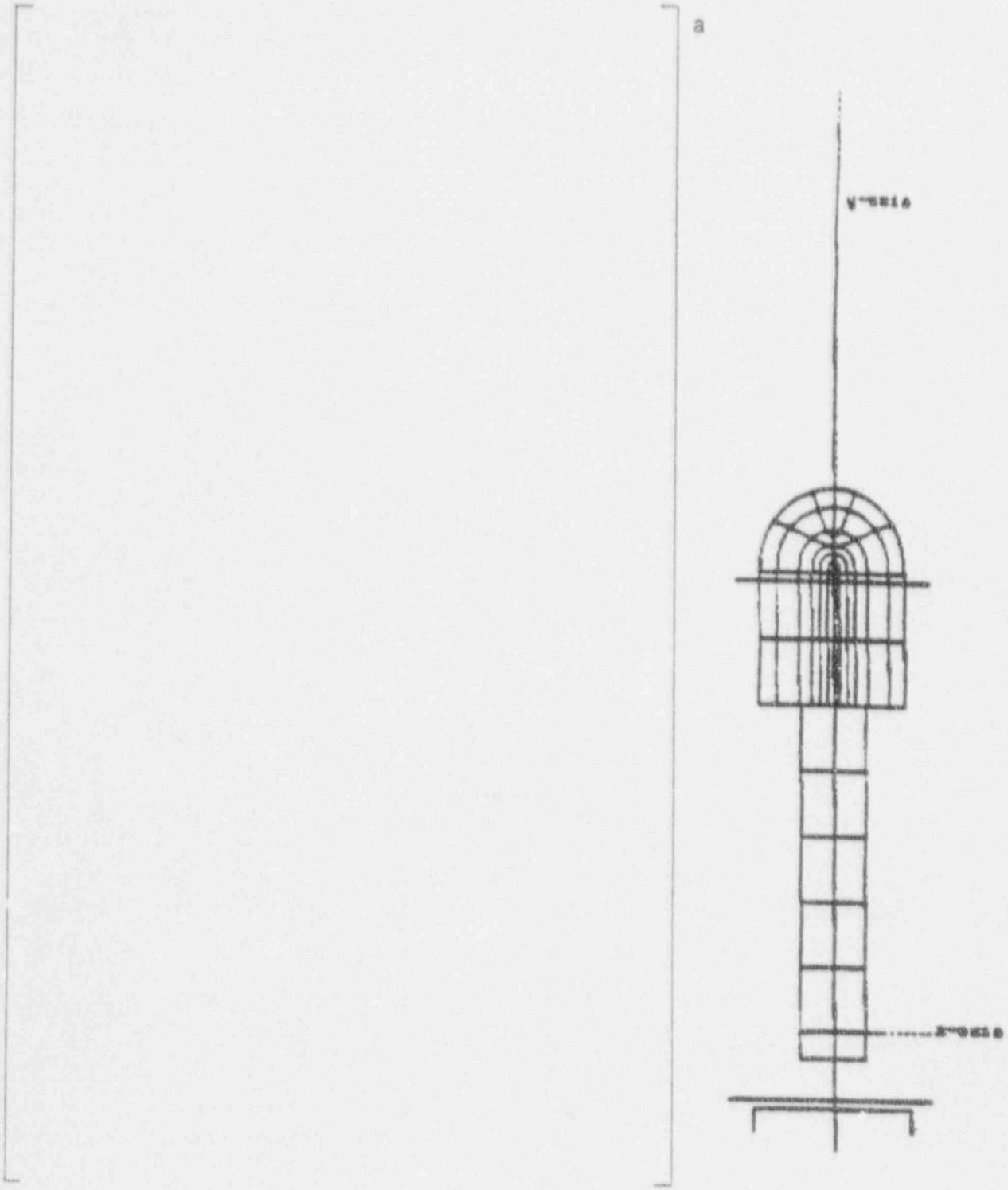

Figure 11-1. Series 51 Seismic Finite Element Model Geometry

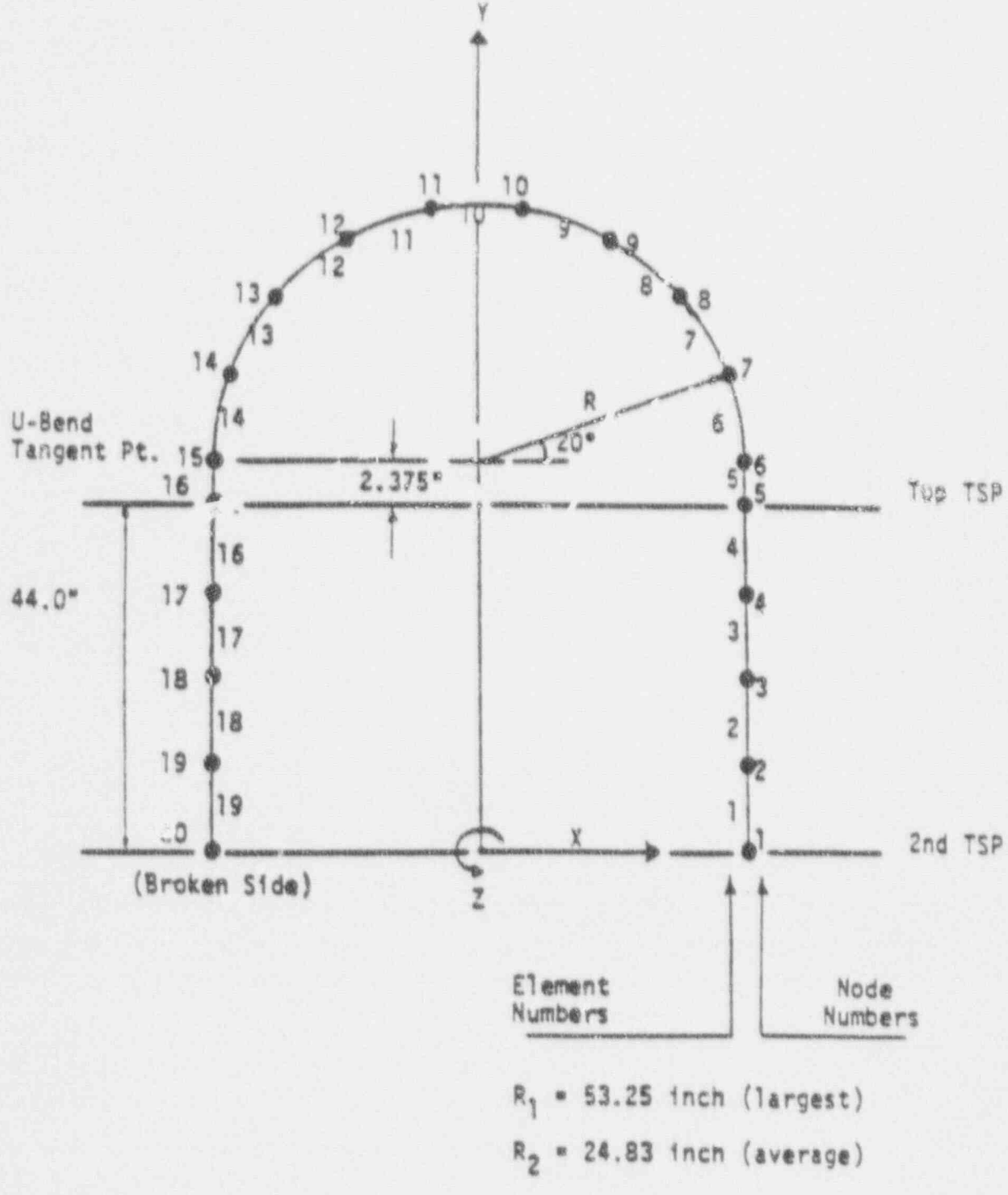

Figure 11-2. T/H Tube Model for LOCA Rarefaction Wave Analysis

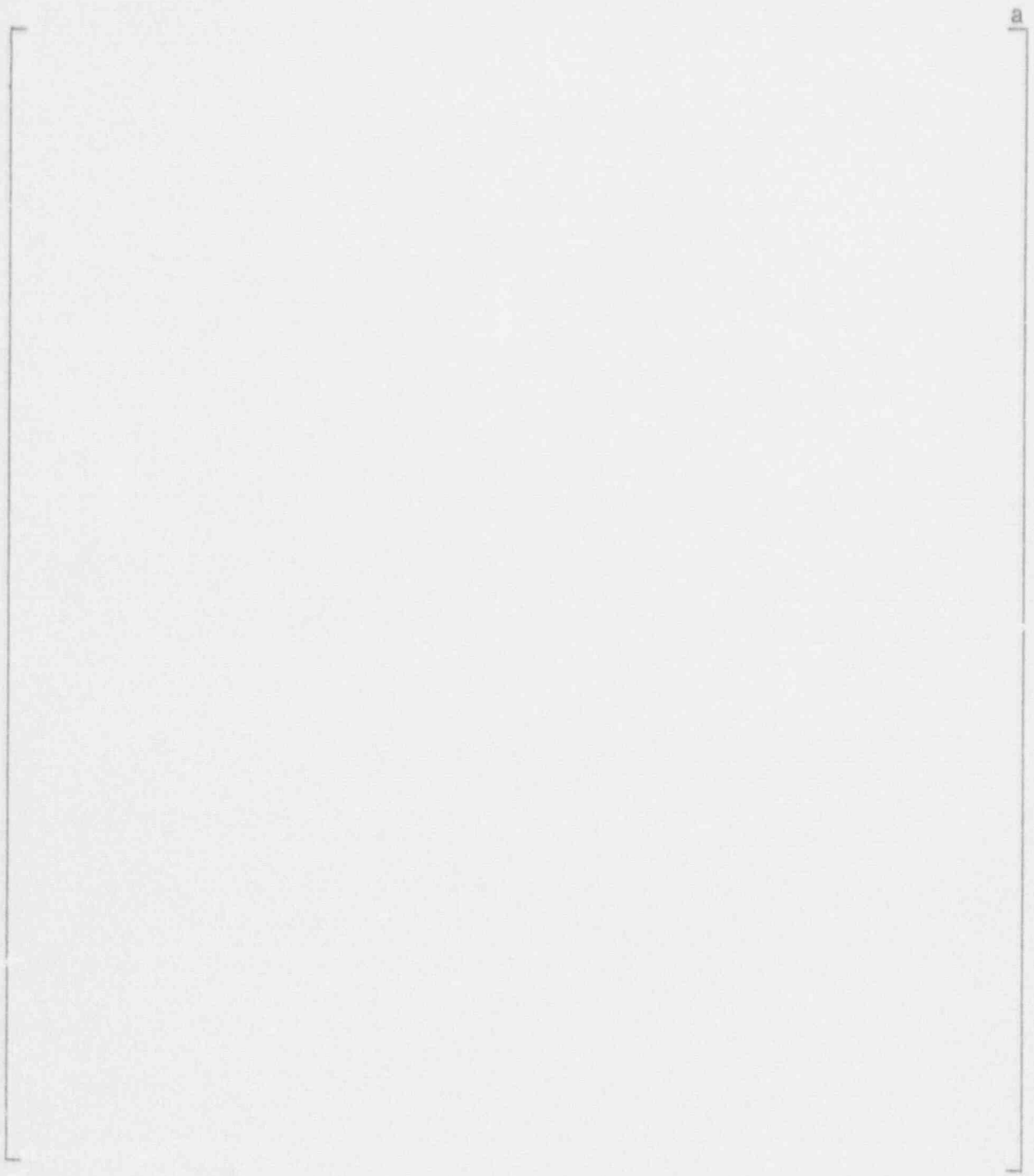

Figure 11-3. LOCA Pressure Differentials for S/G Inlet Break

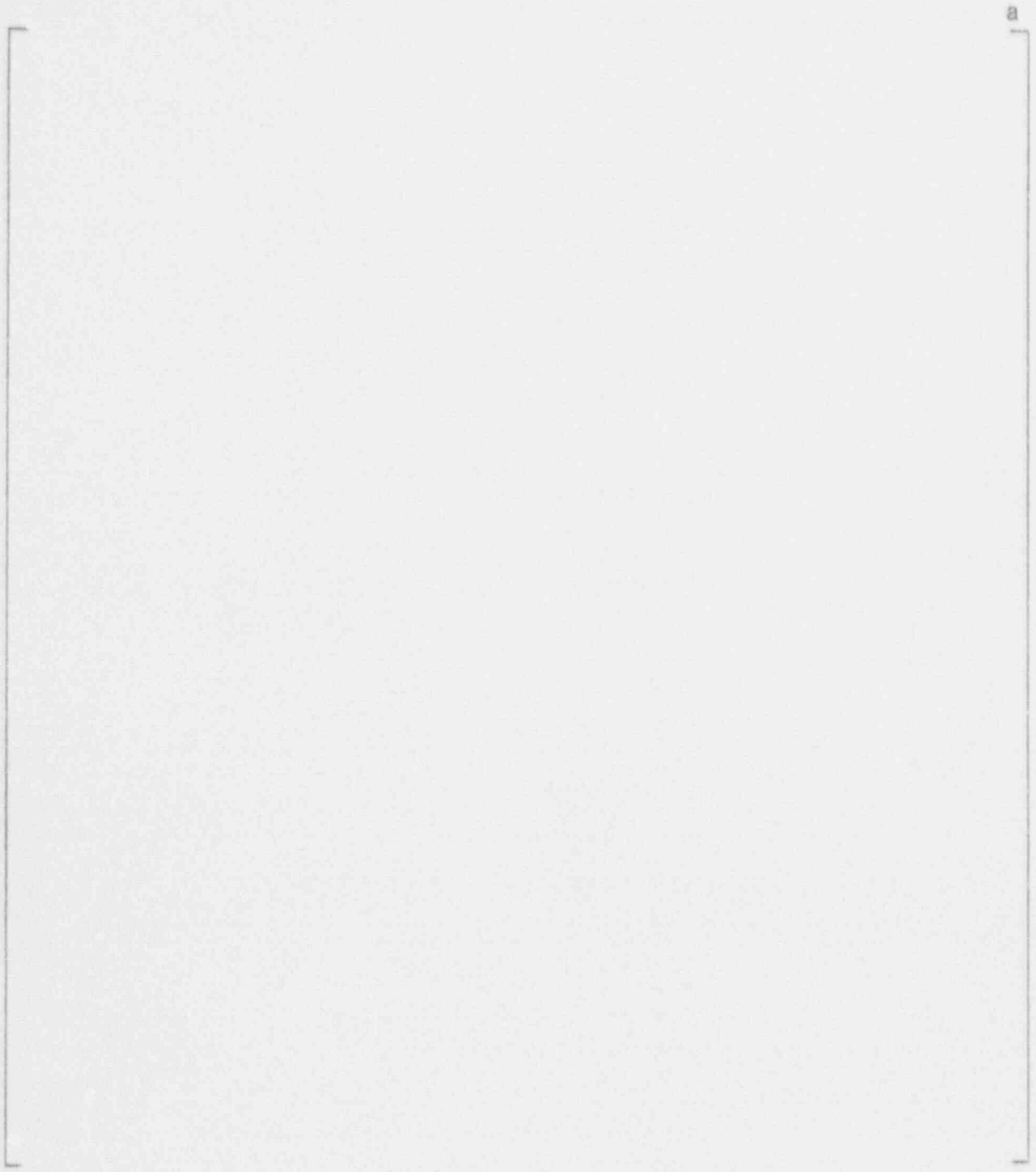

Figure 11-4. LOCA Pressure Differentials for Accumulator Line Break

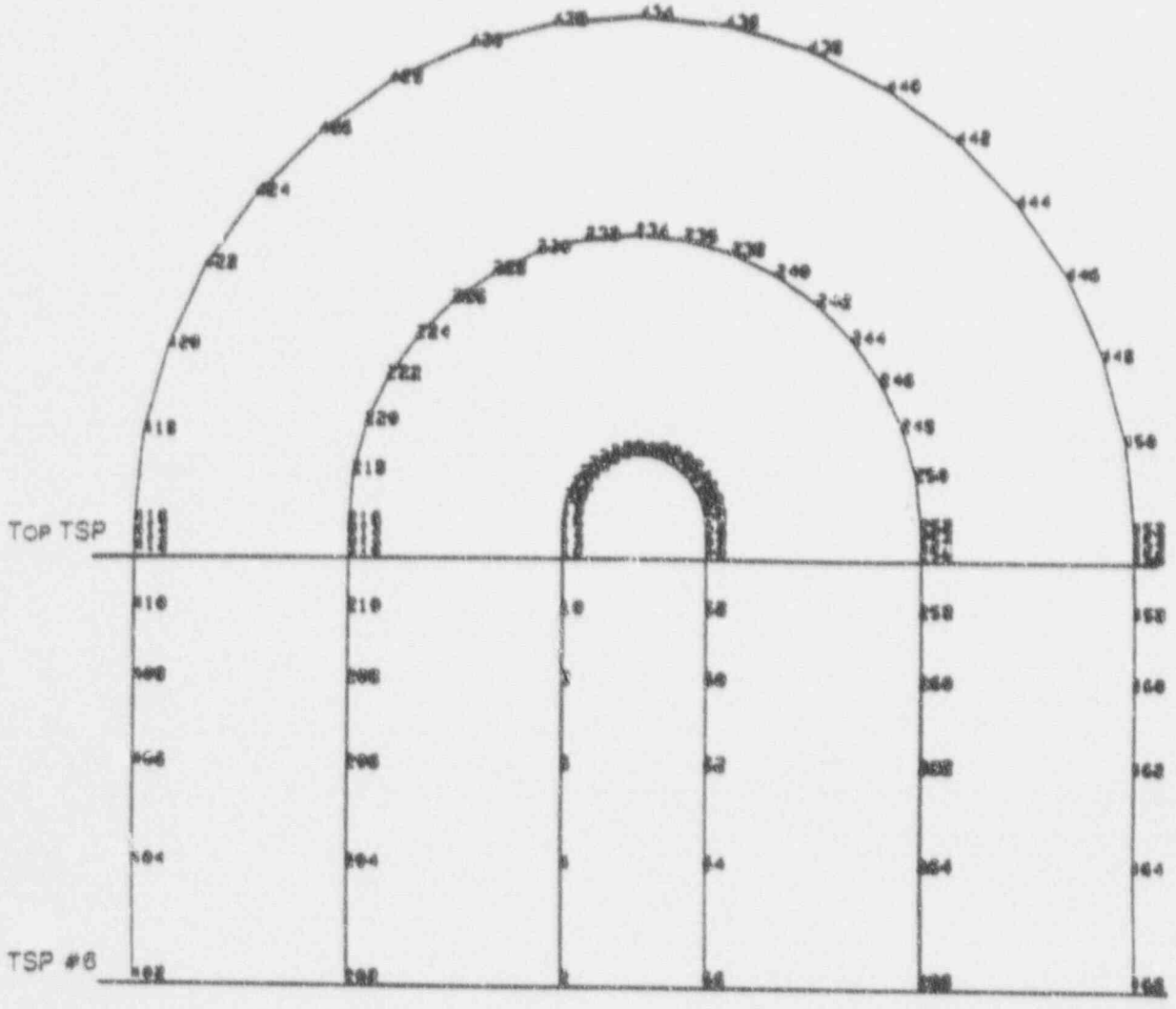

Figure 11-5. Finite Element Model for Structural LOCA Time History Analysis

Figure 11-6. LOCA Rarefaction Force Distribution for S/G Inlet Break

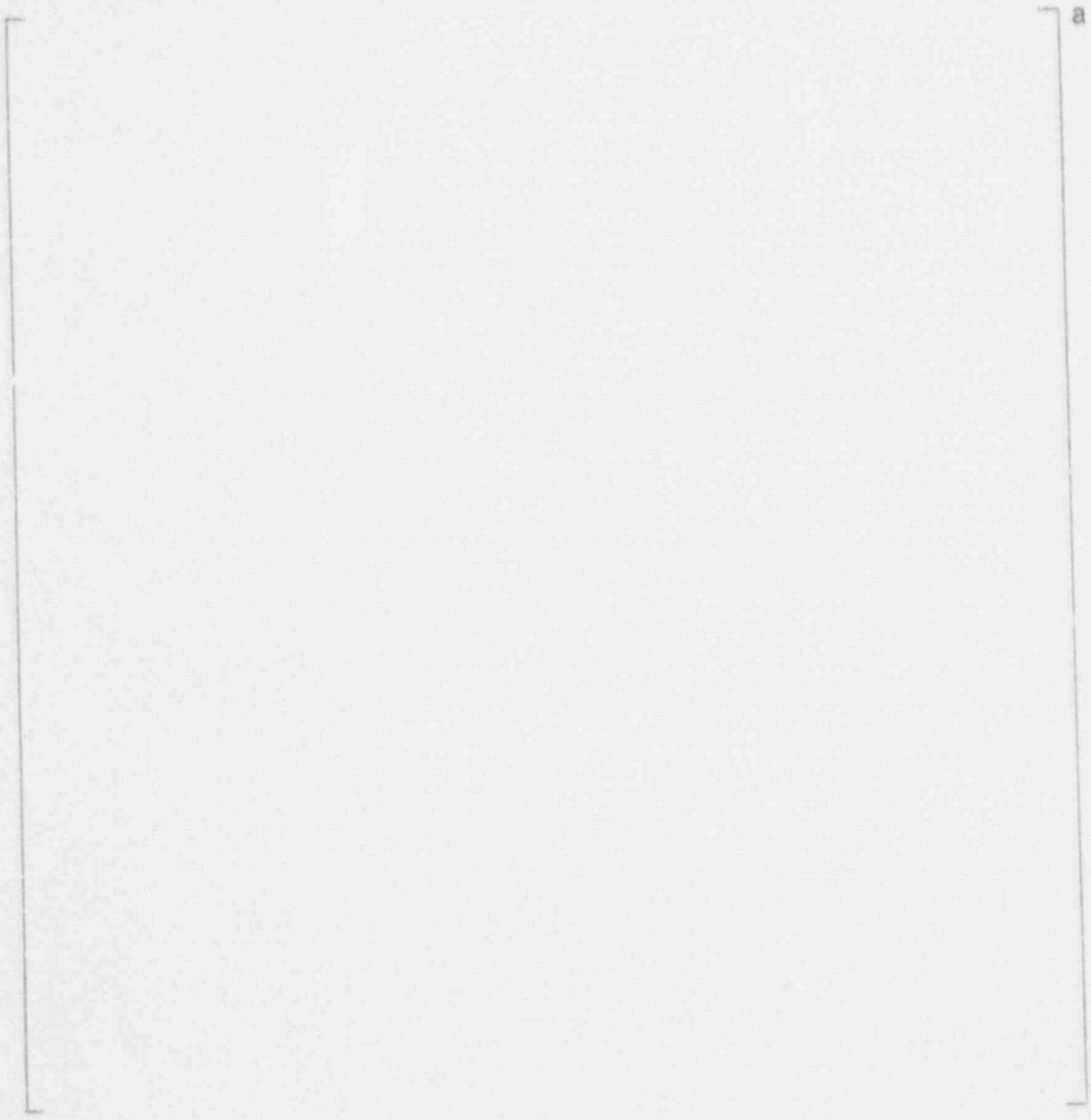

Fifgure 11 -7. Wedge Group Orientation Looking Down on TSP

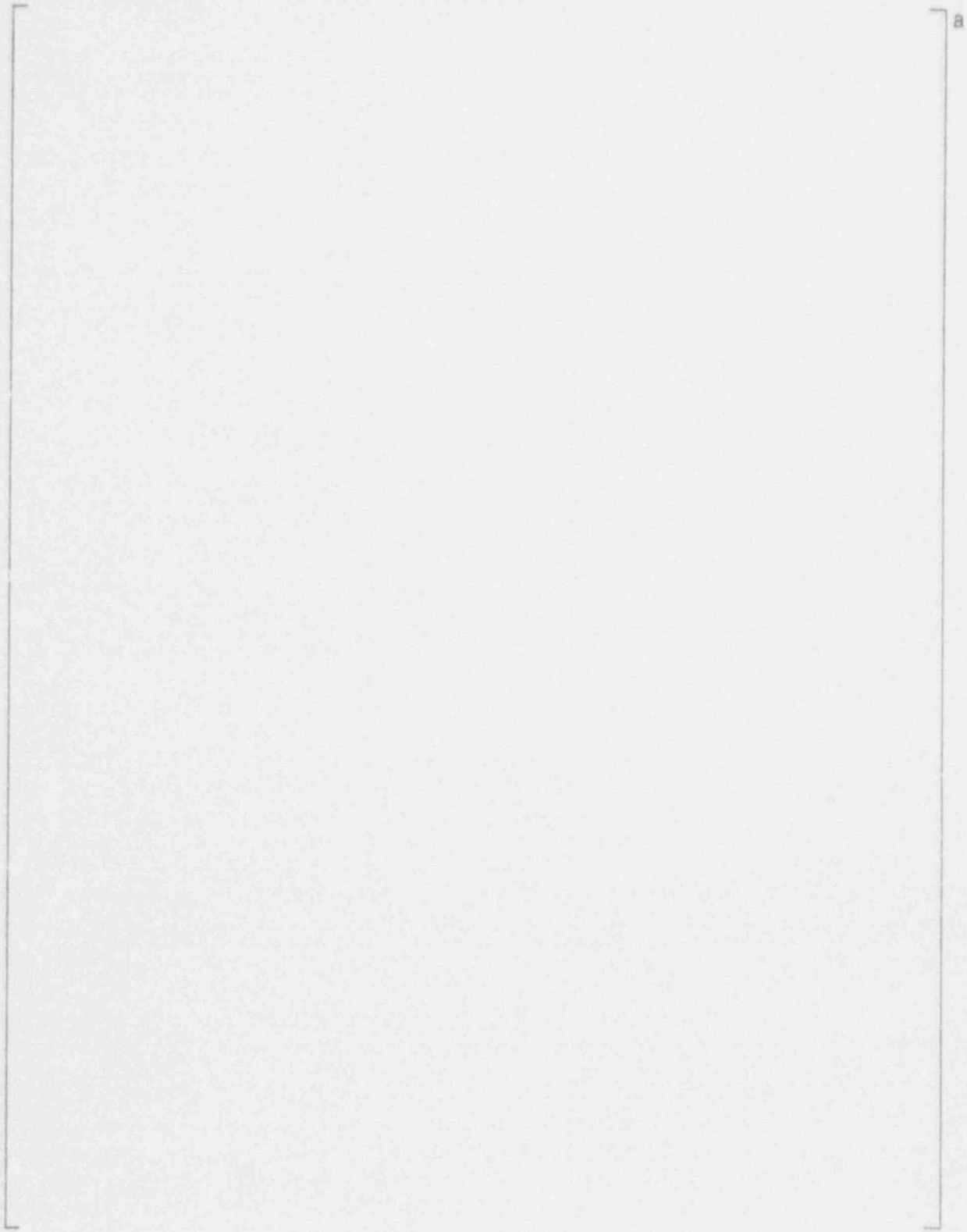

Figure 11-8. Summary of Wedge Load Distribution for TSP 2-7

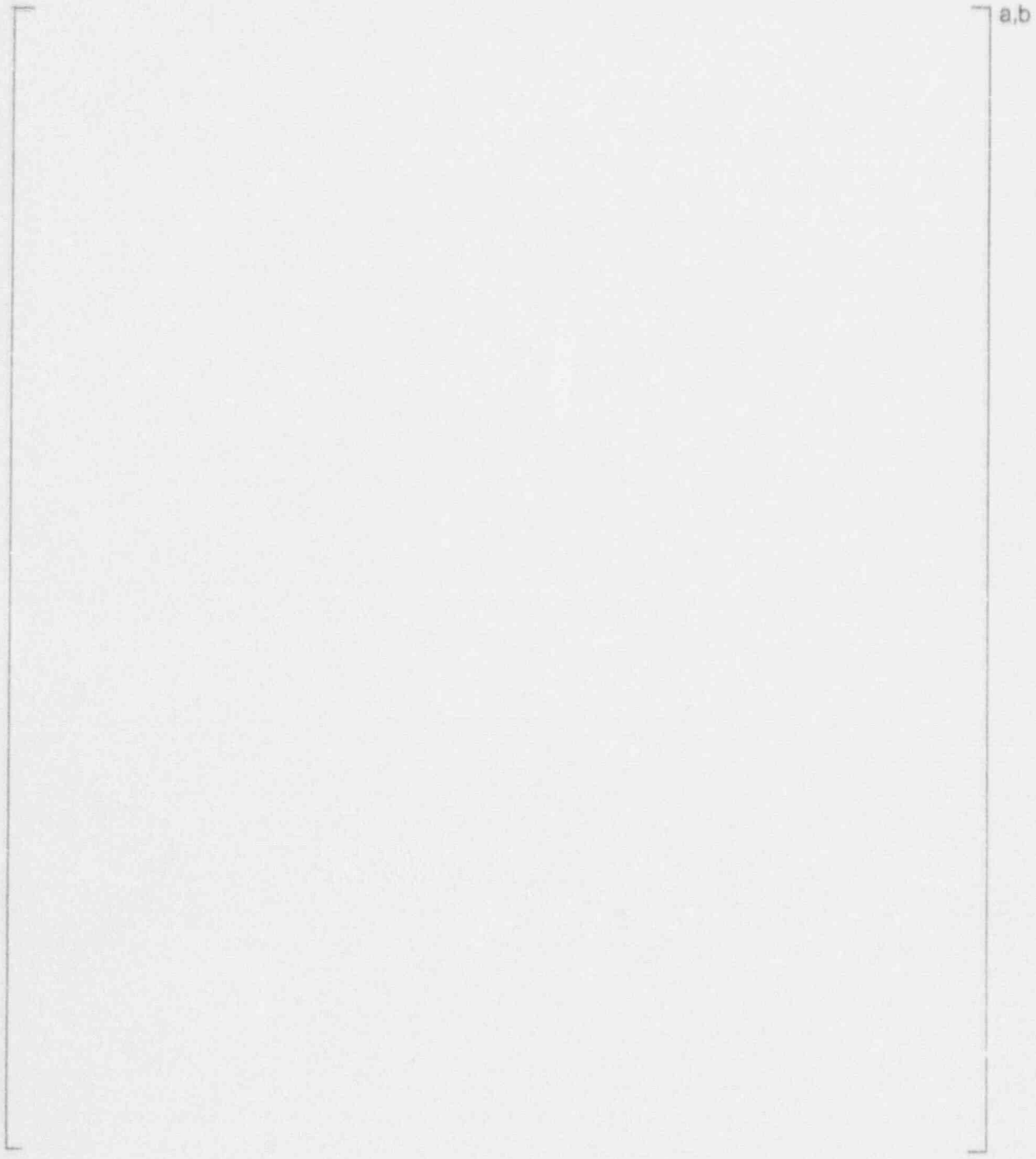

Figure 11-9. Crush Test Results - Force vs Deflection

Figure 11-10. Crush Test Results - Number o. Deformed Tubes vs Force

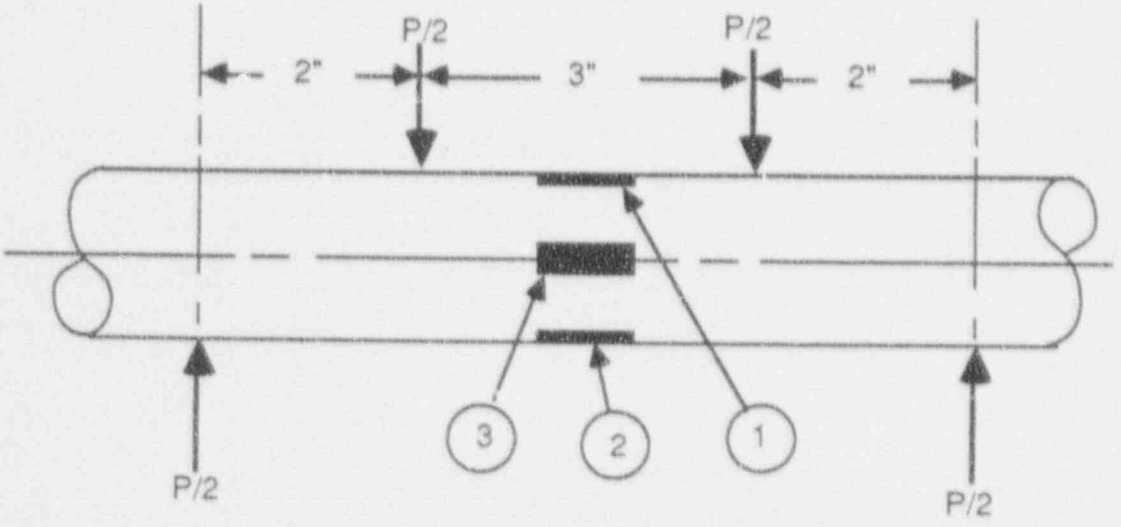

Figure 11-11. Externally Applied Bending Load and Locations of Through Wall Slots

12.0 TUBE PLUGGING CRITERIA FOR ODSCC AT TSPS

This section integrates the results obtained from the prior sections to develop the technical basis for tube plugging criteria for ODSCC at TSPs.

12.1 General Approach to Plugging Criteria

The general approach taken to develop the tube plugging criteria for the Kewaunee S/Gs includes:

1) Specifying conservative burst correlations based on free span ODSCC under design basis accident conditions to demonstrate structural integrity.

2) Conservatively assuming open crevice conditions to maximize leakage potential.

3) Satisfying the R.G. 1.121 structural guidelines for tube burst margins by establishing a conservative structural limit on voltage amplitude that assures 3 times normal operating pressure differential for tube burst capability.

4) Satisfying the USAR requirements for allowable leakage under accident conditions by demonstrating that the dose rate associated with potential leakage from tubes remaining in service is a small fraction of 10 CFR 100 limits.

5) Including considerations for crack growth and NDE uncertainties in both the structural assessment and leakage analysis.

6) Specifying a requirement to perform 100% BC inspection for all hot leg TSP intersections and all cold leg intersections down to the lowest cold leg TSP where ODSCC indications have been identified.

12.2 Test and Field Data Summary

The model boiler test data supporting the plugging criteria were discussed in Sections 8 and 9. To clarify the application of the laboratory data, the laboratory burst pressure and leak rate data used for the criteria development are given in Table 12-1. For 7 of the first 13 specimens of Table 12-1, leak rates were measured twice. After the initial measurements at normal operating conditions for these specimens, the generally tight model boiler TSP simulants were removed for supplemental testing. The subsequent eddy current measurements generally showed increased values and preceded the SLB leak rate and burst measurements and thus are the appropriate values for the burst and leakage correlations. Only the second test results are included in the data base of Table 12-1.

Field data supporting the criteria are given in Table 6.2 for pulled tube burst pressure/leak rate data, Table 6.3 for occurrences of operating leakage, Figure 6-1 for pulled tube bobbin coil voltage and depth and Figure 6-4 for typical field inspection data for tubes without operating leakage. The field data of Tables 6.2/6.3 and Figure 6-1 are combined in Figure 12-1 with the model boiler data of Table 12-1 to show an integrated data base. Also shown in Figure 12-1 are

the data points with leakage under SLB conditions. Only the data of Tables 6.2 and 12.1 are used in the voltage versus burst pressure and SLB leak rate correlations. The voltage/burst correlation is given in Section 9.6. The SLB leakage correlation and analysis model are developed in Sections 9.7 and 11.4. These data together with the Kewaunee growth rates given in Section 5.3 and the NDE uncertainties developed in Section 8.8 define the data base used to develop the Kewaunee tube plugging criteria for ODSCC at TSPs.

The actual in-service leakage from ODSCC at TSP intersections has been very limited on a world wide level. No leakage from ODSCC has been reported for U.S. plants with nondented tubes. This experience is consistent with a depth-based repair policy, even if deeper defects cannot be precluded and may exist. Other countries following a policy similar to that currently used in the United States have reported only one leakage event. This event occurred at a Spanish plant and resulted from a pluggable indication that was missed during the previous outage.

In European countries with no repair criteria to prevent through-wall defects at TSP intersections, reported leakage events are low. In Belgium, no leakage has been observed at Plant K-1 (where all 3 steam generators are known to have been affected by ODSCC for a number of years). A 1990 leakage event reported for plant E-4 cannot be quantitatively correlated with the two detected leakers at the TSP level because of three leaking tubes attributed to primary water stress corrosion cracking (PWSCC) in the expansion zones (EZ) of roll transitions. In France, 11 units with ODSCC at TSP intersections have been operating for a significant period (more than five years for at least two units) without detectable leakage.

This insignificant in-service leakage from TSP ODSCC, even when no criteria are set to prevent through-wall defects, is likely to result from a combination of the following factors:

- Crack morphology is such that wall penetration is not readily achieved (relatively long cracks are prevented from leaking by a thin ligament on the ID side and, even after penetration, the ID length remains substantially less than the OD length). Also, unbroken ligaments between the crack faces often tend to restrict the leakage path.

- The small opening areas of through-wall cracks can get clogged easily by circulating corrosion products, impurities, or precipitates.

- The crevice chemistry may block the leak path, either by corrosion product accumulation (leading to "packed crevices"), or by tube denting from the corroded TSP.

While this experience indicates that leakage from TSP-ODSCC is not an operational concern, consideration is given in Section 12.5 to tube leak-before-break (LBB) to deal with possible unanticipated leaks or cracks that might grow at a greater than expected rate and thus challenge the adequacy of the structural repair limit. Using the LBB methodology to reduce the probability of tube break to a negligible level also addresses the issue of a single large leaker (outside the predicated range) during postulated faulted loads.

12.3 Tube Plugging Criterion for Margins Against Tube Burst

The tube plugging criteria are developed to preclude free span tube burst if it is postulated that TSP displacement would occur under accident conditions. The plugging limits to provide R.G. 1.121 tube burst margins are developed in this section.

12.3.1 Voltage Limit for Structural Requirement

Tube burst test results are given for pulled tubes in Table 6.2 and for model boiler specimens in Tables 9.1 and 12.1. The combined field and laboratory burst test results are evaluated in Section 9.6 to develop a correlation between bobbin coil voltage and burst pressure. This correlation was adjusted to account for operating versus test temperatures and for minimum material properties to obtain a reference, burst pressure correlation at the lower 95% confidence level. The results given in Section 9.6 show that a bobbin voltage amplitude of [ ][a] volts satisfies the R.G. 1.121 guidelines that burst pressure capability exceeds 3 times the normal operating pressure differential across the tube. Thus the structural requirement for the tube plugging criteria is a limit of [ ][a] volts for the bobbin coil amplitude.

12.3.2 Allowance for NDE Uncertainty

The allowance for NDE uncertainties was developed in Section 8.8 as a 10% uncertainty. The 10% is applied at the voltage limit requiring tube plugging. To support this uncertainty, voltage calibration standards normalized to the reference laboratory standard are utilized for Kewaunee S/G inspections applying the plugging criteria of this report.

A probe wear standard may be used to maintain probe centering capability within the 10% uncertainty limit as described in Sections 8.4 and 8.8. Preliminary field experience has indicated some difficulties in applying the wear standard within the physical constraints of the channel head with the associated limited vertical height where bending of probe leads can influence probe centering. Pending further field experience with the probe wear standard, the NDE uncertainty has been set to 15% for the EC data acquisition guidelines and conservatively increased to 20% for development of the plugging limits in Section 12.3.4.

12.3.3 Allowance for Crack Growth

Voltage growth rates for the Kewaunee S/Gs are developed in Section 5.3 and compared with other plant data in Figure 6-12. Growth rates are defined in terms of percent growth per cycle and are applied at the voltage amplitude requiring tube plugging. The Kewaunee percent growth rates from historical data are shown to decrease with increasing BOC (beginning of cycle) amplitude while data from a European plant indicates percent growth may be essentially independent of amplitude. It is thus conservative to assume percentage growth is independent of BOC amplitude and to use overall average growth from Kewaunee operating experience for the growth rate allowance in the plugging limits.

Table 5.1 summarizes voltage growth rates. For additional margin, the growth rates obtained by setting negative changes in measured voltages between cycles to zero is applied to obtain plugging limits. This process conservatively ignores negative fluctuations in voltage growth while keeping positive fluctuations in the average growth rate calculation. Overall, the more random positive and negative fluctuations would be expected to average out to approximately zero in the average growth.

It is seen from Table 5.1 that zeroing negative growth tends to increase implied growth rates by 5 to 13%. Kewaunee growth rates have decreased since 1987 with an average value over the last 4 cycles of 13.4%. Growth rate over the last operating cycle was 5%.

To provide margin for variations in future cycles, an average growth allowance of 40% per cycle

is conservatively applied to establish tube plugging limits. Average growth rates are considered to provide an adequate allowance for growth in satisfying R.G. 1.121 structural guidelines for burst pressure capability of three times normal operating pressure differential. Per R.G. 1.121, an allowance for NDE uncertainties is included in developing the tube plugging limit from the structural requirement for tube burst as shown below in Section 12.3.4. Allowances for growth uncertainties are addressed by demonstrating large margins against burst at SLB conditions as described in Section 12.4.

12.3.4 Tube Plugging Criterion

The structural voltage limit must be reduced by the allowances for crack growth and NDE uncertainty to obtain the voltage limit for tube plugging or repair consistent with R.G. 1.121 guidelines for margins against tube rupture. This can be expressed as:

$$V_{RL} + V_{NDE} + V_{CG} = VSL \qquad (12\text{-}1)$$

where: V_{RL} = voltage limit for tube repair or plugging,
V_{NDE} = NDE voltage measurement uncertainty,
V_{CG} = voltage growth rate per cycle, and
V_{SL} = voltage structural limit from the burst pressure versus BC voltage correlation.

The NDE voltage uncertainty and voltage growth rate terms are provided as a percentage of measured BC voltage (% V_{NDE} and %V_{CG}). Using V_{RL} as the maximum measured BC voltage to be left in service, V_{NDE} and V_{CG} are:

$$V_{NDE} = V_{RL} \times \%V_{NDE}/100, \text{ and}$$

$$V_{CG} = V_{RL} \times \%V_{CG}/100.$$

Using these expressions for V_{NDE} and V_{CG}, Eq. (12-1) can be rewritten as:

$$V_{RL} = V_{SL}/(1 + \%V_{NDE}/100 + \%V_{CG}/100). \qquad (12\text{-}2)$$

Values for V_{SL}, %V_{NDE} and %V_{CG} are given in Sections 12.3.1 to 12.3.3 above and are V_{SL} = [ ][a] volts, %V_{NDE} = 20 and %V_{CG} = 40. Substituting these values into Eq. 12-2 gives

$$V_{RL} = V_{SL}/1.60 = 3.5 \text{ volts} \qquad (12\text{-}3)$$

An alternate summary of the development of the tube plugging or repair voltage limit is given in Table 12-2. The criterion for tube plugging is that the measured bobbin coil voltage exceed 3.5 volts. This criterion is applied independent of the bobbin coil indicated crack depth.

For the smaller diameter (680 mil) probe used for the EC testing of a few tubes at Kewaunee, an NDE uncertainty (%VNDE) of 20% may be used as discussed in Section 8.9. The voltage growth rate (%VCG) of 40% is independent of the probe diameter and hence is applicable to the 680 mil diameter probe indications. Thus the calculations of Table 12.2 are valid for the smaller

diameter probe. The bobbin coil voltage plugging criterion of 3.5 volts is applicable to both the 720 mil and the 680 mil diameter probes used in Kewaunee inspections. Use of the 680 mil diameter probe will be limited to small radius (of U-bend) tubes which do not permit passage of a 720 mil probe.

12.4 SLB Leakage Evaluation

This section describes both margins against tube burst at SLB conditions and analysis requirements for demonstrating acceptable SLB leakage. In Section 11.3 it was shown that the bounding accident condition for primary to secondary leakage is the SLB event and that the allowable SLB leak limit is 260 gpm.

12.4.1 Margins Against Burst at SLB Conditions

Margins against burst at SLB conditions are demonstrated by considering the throughwall crack length required for tube burst and by a statistical estimate considering cracks left in service, growth and the voltage burst correlation.

Burst pressure versus axial crack length data from multiple sources are shown in Figure 12-2 as taken from EPRI Report NP-6864-L. The methods to perform the burst tests for the upper figure curves differ in the techniques for applying the required pressure for tube burst. In testing of tubes with through-wall slits [

]^{a,c}. However, recent tests in Belgium have demonstrated that for axial cracks, foil reinforcement of seals leads to the same burst pressures as in tests with very high capacity pumps and no seal whatsoever. This is illustrated in Figure 12-2. The Westinghouse and British curves do not use any seal reinforcement and lie below the Belgian burst curve. The burst data without any sealant system falls along the burst curves where seal reinforcement was used. Therefore it is appropriate to remove the conservatism of the Westinghouse axial crack burst curve and use the Belgian burst curve. The Belgian burst curve for 7/8 inch diameter tubing is shown in the upper plot of Figure 12-2. It is seen that a throughwall crack length of 0.84 inch is required for burst at SLB conditions. The TSP height is 0.75 inch so that even a uniformly throughwall crack equal to the length of the TSP, which is extremely unlikely, would not burst under accident conditions.

The probability of tube burst at SLB conditions for a tube left in service at the plugging limit can be estimated by the product of the probability of the maximum projected EOC (end of cycle) indication times the probability of tube burst at the maximum projected indication voltage. Conservative estimates for Kewaunee are given in Table 12-3. It is assumed that an indication at the tube plugging limit has the maximum NDE uncertainty with a conservative probability of 0.1 as described in the footnote of Table 12-3. The growth per cycle is taken as the growth found in the last inspection (Figure 5-15) at 99% cumulative probability. From Figure 5-14, it is seen that the large growth rates apply to small voltage indications and could have an even lower probability of occurring at a voltage corresponding to the plugging limit. Thus the assigned

growth per cycle is also extremely conservative.

The maximum EOC indications and associated probabilities are obtained as the plugging limit values multiplied by the NDE uncertainty and growth factors. From Table 12-3, it is seen that the maximum EOC indications are less than the lower 95% confidence bound on tube burst at SLB conditions. The conservatively estimated probability for burst at SLB of a tube left in service at the plugging limit is ~5×10^{-7}/cycle. Even assuming 2000 indications per S/G were left in service at the plugging limit would conservatively result in a 10^{-3}/cycle probability of burst at SLB even without including the low probability of an SLB event occurring.

Based on the above deterministic crack length assessment and estimated probabilities, it can be concluded that burst at SLB would not occur for the plugging limits of this report.

12.4.2 SLB Leakage Analysis

The SLB leakage limit of 260 gpm per S/G was developed in Section 11.3. It is required that an SLB leakage analysis be performed following each inspection to demonstrate that the potential SLB leakage for tubes left in service is less than the 260 gpm limit.

Laboratory measurements on cracked tubes indicate no significant leakage for tubes with through wall crack lengths up to about 0.2 inch at normal operating conditions and about 0.15 inch for SLB conditions. Typical examples with SLB leakage <1 gpd include Plant A Tubes R4 C73 (0.18"TW), and R21 C22 (0.15"TW) and Model Boiler Specimens 509-3 (0.16"TW) and 535-1 (0.11"TW). With OD to ID crack length ratios > 2 found for ODSCC, tubes with through wall cracks and measurable leakage even in the laboratory can be expected to have significant voltage amplitudes. Thus a threshold voltage value can be expected for measurable leakage.

For normal operating conditions, the data of Figure 12.1 show: a 6.5 volt model boiler specimen with operating leakage; a field leaker at 7.7 volts; no reported field leakage below this 7.7 volt leaker including a substantial number of field indications below about 4 volts; and no measurable leakage for the Plant A-2 pulled tube at 2.8 volts. Thus a reasonable judgment is that the voltage amplitude for the leakage threshold at operating conditions is between 2.8 and 6.5 volts. Furthermore, there is significant likelihood that the voltage threshold for operating plant leakage detectability would exceed 6 volts.

For SLB conditions Plant A-2 tube R4 C73 at 2.8 volts had a very small leak rate of 0.17 l/hr while pulled tubes at 2.31 and 1.44 volts, but not through wall penetration, had no leakage. The lowest voltage found for a pulled tube with a through wall crack (0.01 inch long) was 1.9 volts (3/4 inch diameter tube) and this tube had no detectable leakage in the laboratory. These data indicate that a threshold voltage of about 2.8 volts would result for through wall cracks long enough to leak at SLB conditions.

This no leakage threshold would apply for leakage analysis at EOC conditions. To estimate a BOC voltage threshold for negligible EOC leakage, the procedure of Section 12.3 to adjust for NDE uncertainties and growth can be applied. Thus the 2.8 volt threshold would be reduced by a factor of 1.6 to obtain ~ 1.7 volts as a BOC threshold for negligible SLB leakage. Based on available data, a bobbin coil leak rate threshold of 1.5 volts is used for Kewaunee applications. As discussed in the SLB leakage model discussion of Section 11.4, the leakage threshold of 1.5 volts is not applied when the probabilistic SLB leakage model is used. The 1.5 volt threshold is used as one consideration to establish a 1.5 voltage limit above which RPC inspections are

required as noted in Section 12.6 below.

The probabilistic SLB leakage model of Section 11.4 combines an outage distribution of voltage indications left in service, NDE uncertainties, the cumulative probability distribution of voltage growth over the operating cycle and the leak rate for all indications left in service. The SLB leak rate versus voltage correlation will be periodically updated as additional data becomes available to improve the estimated SLB leak rate.

If it is found that the potential SLB leakage for degraded intersections planned to be left in service exceeds 260 gpm, then additional tubes would be plugged to reduce SLB leakage potential to below 260 gpm. As also noted in Section 11.4 applying the current leakage model to the distribution of indications found at the last Kewaunee outages would yield a maximum of 0.1 gpm per S/G at SLB conditions which is well below the 260 gpm limit per S/G.

12.5 Operating Leakage Limit

R.G. 1.121 acceptance criteria for establishing operating leakage limits are based on leak before break (LBB) consideration such that plant shutdown is initiated if the leakage associated with the longest permissible crack is exceeded. The longest permissible crack is the length that provides a factor of safety of 3 against bursting at normal operating pressure differential. As noted above, a voltage amplitude of [ ]^{a} volts for typical ODSCC cracks corresponds to meeting this tube burst requirement at the lower 95% confidence level on the burst correlation. Alternate crack morphologies could correspond to [ ]^{a} volts so that a unique crack length is not defined by the burst pressure to voltage correlation. Consequently, typical burst pressure versus through wall crack length correlations are used below to define the "longest permissible crack" for evaluating operating leakage limits.

The CRACKFLO leakage model has been developed for single axial cracks and compared with leak rate test results from pulled tube and laboratory specimens. Fatigue crack and SCC leakage data have been used to compare predicted and measured leak rates as shown in Figure 12.3. Generally good agreement is obtained between calculation and measurement with the spread of the data being somewhat greater for SCC cracks than for fatigue cracks. Figure 12.4 shows normal operation leak rates including uncertainties as a function of crack length.

The through wall crack lengths resulting in tube burst at 3 times normal operating pressure differentials (4590 psi) and SLB conditions (2650 psi) are about [ ]^{a}, respectively, as shown in Figure 12-2. Nominal leakage at normal operating conditions for these crack lengths would range from about [

]^{a} would cause undue restrictions on plant operation and result in unnecessary plant outages, radiation exposure and cost of repair. In addition, it is not feasible to ensure LBB for all tubes by reducing the leak rate limit. Crevice deposits, presence of small ligaments and irregular fracture faces can, in some cases, reduce leak rates such that LBB cannot be ensured for all tubes by lowering leak rate limits.

An operating leak rate of 150 gpd (~0.1 gpm) will be implemented in conjunction with application of the tube plugging criteria. As shown in Figure 12-4, this leakage limit provides for detection of [

]^{a} Thus, the 150 gpd limit provides for plant shutdown prior to reaching critical crack

lengths for SLB conditions at leak rates less than a lower 2σ confidence level and for 3 times normal operating pressure differentials at less than nominal leak rates.

The tube plugging limits coupled with 100% inspection at affected TSP locations provide the principal protection against tube rupture. The 150 gpd leakage limit provides further protection against tube rupture. In addition, the 150 gpd limit provides the capability for detecting a rogue crack that might grow at much greater than expected rates and thus provides additional protection against exceeding SLB leakage limits.

12.6 Supplemental Requirements for Implementation of the Plugging Criteria

Upon implementation of the tube plugging criterion and associated limits on operating SLB leakage, additional requirements as noted in this section are to be implemented.

A 100% bobbin coil inspection is required for all hot leg TSP intersections and for cold leg intersections down to at least the lowest TSP with ODSCC indications. This requirement provides confidence that all ODSCC indications which could contribute to SLB leakage are identified for the leak rate evaluation. If <100% inspection is performed below cold leg TSP intersections with previously identified ODSCC indications, and indications at TSPs are identified, the inspection must be extended to 100% of the affected TSP or the 50% depth limit for tube plugging must be applied for all indications.

An RPC inspection is required to establish that the principal indications can be characterized as ODSCC. For Kewaunee, the RPC inspection will be performed for all ODSCC indications left in service that exceed a 1.5 volt bobbin coil amplitude. The RPC results are to be evaluated to establish that the principal indications can be characterized as ODSCC. As discussed in Section 8.1, bobbin coil indications <1.5 volt for degradation other than ODSCC are not expected to impact tube integrity, for potential tube degradation at Kewaunee. Thus, characterization of the type of degradation above 1.5 volts by RPC is adequate to determine appropriate plugging limits. If indications other than ODSCC are identified, these indications should be evaluated against a 50% depth requirement for tube plugging. The >1.5 volt bobbin coil amplitude for RPC inspection also provides a threshold value below which SLB leakage is expected to be negligible as noted in Section 12.4. Once an indication at a TSP is confirmed to be ODSCC, reconfirmation by RPC inspection at alternate refueling outages is acceptable.

Branching of cracks in the circumferential direction is acceptable within the tube plugging criterion. Circumferential branching has been found in pulled tubes and model boiler specimens. Examples are summarized in Table 12-4. These data are included in the voltage/burst correlation. The branching includes some IGA effects as well as SCC. At the higher voltages (>20 volts) summarized in Table 12-4, the effects of branching and tearing of ligaments between axial microcracks can be seen in the orientation of the burst crack opening. Even for these tubes, the burst pressures are comparable to burst pressures for indications without circumferential branching. The burst tests tend to indicate that at very high voltage levels (model boiler specimens 543-1, 543-2 with voltages >100 volts), the branching effects may result in reduced burst capability compared to uniquely axial cracks. Thus voltage levels much higher than the plugging limits of this report are required before the circumferential branching effects influence tube integrity for ODSCC at TSPs. Thus no special inspection techniques are required to inspect for indications with circumferential branching.

Circumferential cracks at TSPs have only been found in one Westinghouse plant that has significantly more and larger dents than found in the Kewaunee S/Gs. No circumferential cracks have been found at the TSPs in Kewaunee S/Gs and none are expected based on operating experience in other plants. The RPC inspections required for indications >1.5 volt are adequate to continue to monitor for potential occurrence of circumferential cracks. RPC resolution is considered adequate to define separation between circumferential and axial cracks. It is not necessary to resolve potential circumferential cracks between closely spaced axial cracks since circumferential cracking is not anticipated at Kewaunee. Any initial identification of circumferential cracks by RPC should be based upon a well defined circumferential indication as contrasted to inadequate RPC resolution. If a well defined circumferential indication should be identified at the TSPs in the Kewaunee S/Gs, guidelines for RPC interpretation would be reviewed at that outage and consideration given to supplemental UT inspection for resolution of the degradation mode. Tubes with identified circumferential indications would be plugged or repaired.

12.7 Summary of Tube Plugging Criteria

As developed in the sections above, the plugging criteria for ODSCC at TSPs can be summarized as follows:

Tube Plugging Criterion

Tubes with bobbin coil indications exceeding 3.5 volts will be plugged or repaired. This limit is applicable to ODSCC indications at TSPs from both the 720 mil and the 680 mil diameter probes.

SLB Leakage Criterion

Predicted end of cycle SLB leak rates from tubes left in service must be less than 260 gpm for each S/G, including considerations for NDE uncertainties and ODSCC growth rates.

Inspection Requirements

A 100% bobbin coil inspection shall be performed for all hot leg TSP intersections and all cold leg intersections down to the lowest cold leg TSP with ODSCC indications.

All tubes with bobbin coil indications>1.5 volts at TSP intersections shall be inspected using RPC probes. The RPC results shall be evaluated to support ODSCC as the dominant degradation mechanism. Indications at TSPs confirmed to be ODSCC shall be reinspected by RPC at alternate refueling outages (once in two outages) for reconfirmation as ODSCC.

Operating Leakage Limits

Plant shutdown will be implemented if normal operating leakage exceeds 150 gpd per S/G.

Exclusions from Tube Plugging Criterion

Tubes with RPC indications not attributable to ODSCC and circumferential indications shall be evaluated for tube plugging based on a 50% depth limit.

Table 12.1

Model Boiler Specimens: Test Data Summary

No.	Model Boiler Spec. #	Bobbin Coil Volts	Bobbin Coil % Depth	RPC Volts	RPC # Cracks	Leak Rate (l/hr) N. Op. ΔP	Leak Rate (l/hr) SLB ΔP	Burst Press. - psi	Destructive Exam. Length - inch Max.	Destructive Exam. Length - inch Thruwall
[redacted]										

---

* For specimens without throughwall penetration, maximum depth of penetration is listed.

** Destructive examination and review of RPC data shows that only 1 crack has a significant response that contributes to the bobbin signal.

*** Tube not burst tested due to physical limitation of specimen.

Table 12.2

Tube Plugging Limits to Satisfy Structural Requirements

Item	Volts	Basis
Maximum Voltage Limit to Satisfy Tube Burst Structural Requirement	[ ][a]	Section 9.6, Figure 9-2, Burst Pressure vs. Voltage Correlation at 95% confidence level.
Allowance for NDE Uncertainty	-0.7 (20%)(1)	Section 8.8 shows development of 10% uncertainty. Increased to 15% for EC data acquisition guidelines pending field experience with probe wear and conservatively increased to 20% to establish tube plugging limits.
Allowance for Crack Growth Between Inspections	-1.4 (40%)(1)	Section 5.3, Table 5.1 shows average growth/cycle of 13%. Allowance increased to 40% of Tube Plugging Limit to provide conservative margin for variations in future cycles.
Tube Plugging Voltage Limit	3.5	

o Acceptable Limit to Meet Structural Requirement

Note 1. Voltage percentage allowances for NDE and growth/cycle applied to Tube Plugging Voltage Limit of 3.5 volts.

Table 12.3

Estimated Probability of Tube Burst at SLB Conditions

	Value	Probability
Indication at Plugging Limit	3.5 V	1.0
Maximum NDE Uncertainty	15%	<0.1(1)
Growth/Cycle at 99% Cumulative Probability Based on Last Operating Cycle	80%	0.01
Maximum EOC Indication(2)	7.0 V	$<1x10^{-3}$
Tube Burst Voltage at Lower 99.95% Limit	7.9 V	$5x10^{-4}$
Estimated Probability Tube Burst at SLB Conditions		$<5X10^{-7}$/cycle

Notes:

1. From Figure 8-19, even assuming a worn probe (0.02" wear) the 15% uncertainty corresponds to >1.5 standard deviations or <10% probability.

2. Obtained as product of indication voltage, NDE uncertainty and growth.

Table 12.4

Examples of Circumferential Branching for ODSCC at TSPs

Plant:Tube	B.C. Voltage	Burst Pressure Pulled Tubes	Destructive Exam Figures	Circumferential Branching Description
			Pulled Tubes	
A-2:R38C46	[	] g	4-11 to 4-13	Numerous microcracks of axial and circumferential orientation
A-2:R31C46			4-1 to 4-2	Minor circumferential branching
B-1:R4C61			4-3 to 4-4	Short circumferential cracks with IGA patches
			Model Boiler Specimens	
528-2			10-18 to 10-21	Burst opening includes circumferentially oriented ligaments
532-1			10-22 to 10-25	Burst opening includes minor circumferential orientation
532-2			10-26 to 10-29	Irregular burst opening involving tearing of interconnecting ligaments
535-1			10-30 to 10-31	Example of minor branching within tube wall
555-3			10-32 to 10-34	Burst involves irregular pattern with turn connecting ledges between cracks

Figure 12-1. Field and Model Boiler Data Base Including Leakage Under SLB Conditions

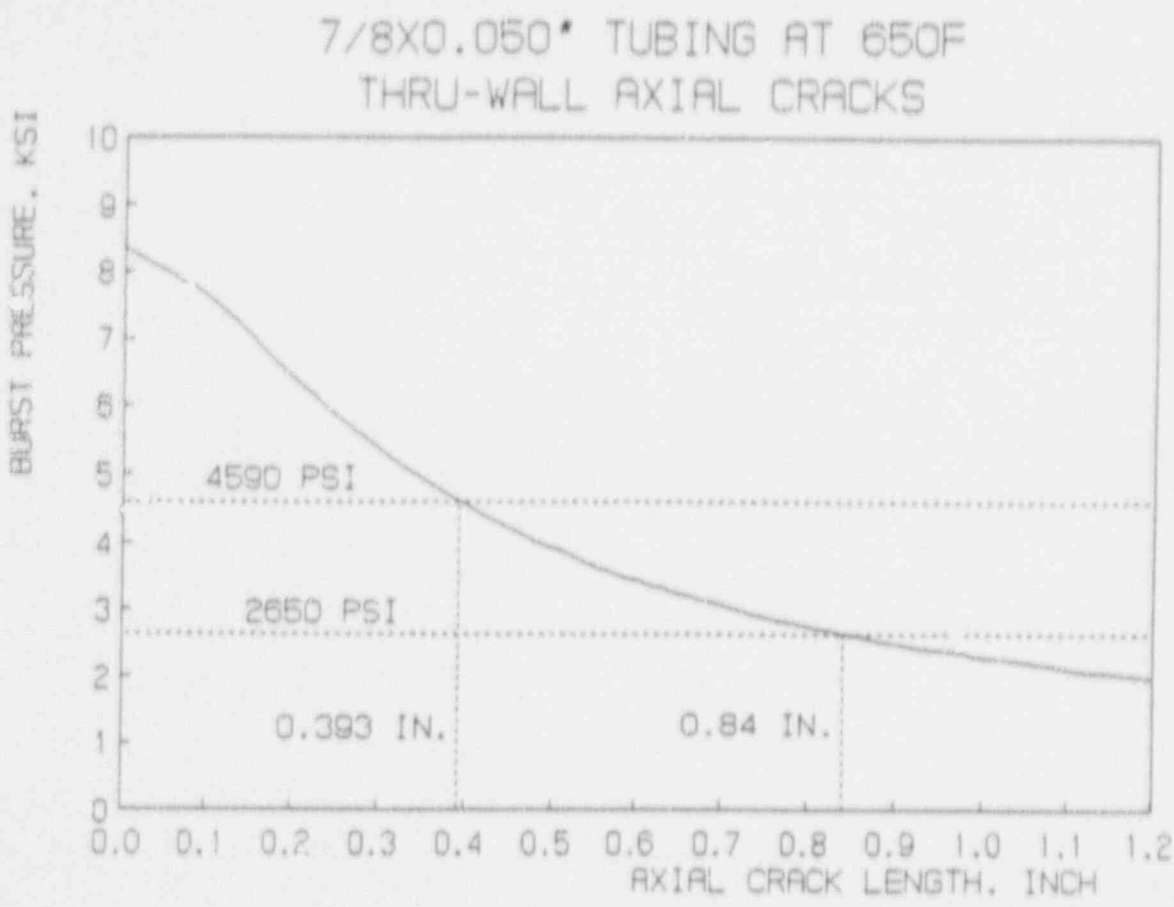

[[b,c

Figure 12-2. Burst Pressure vs. Crack Length

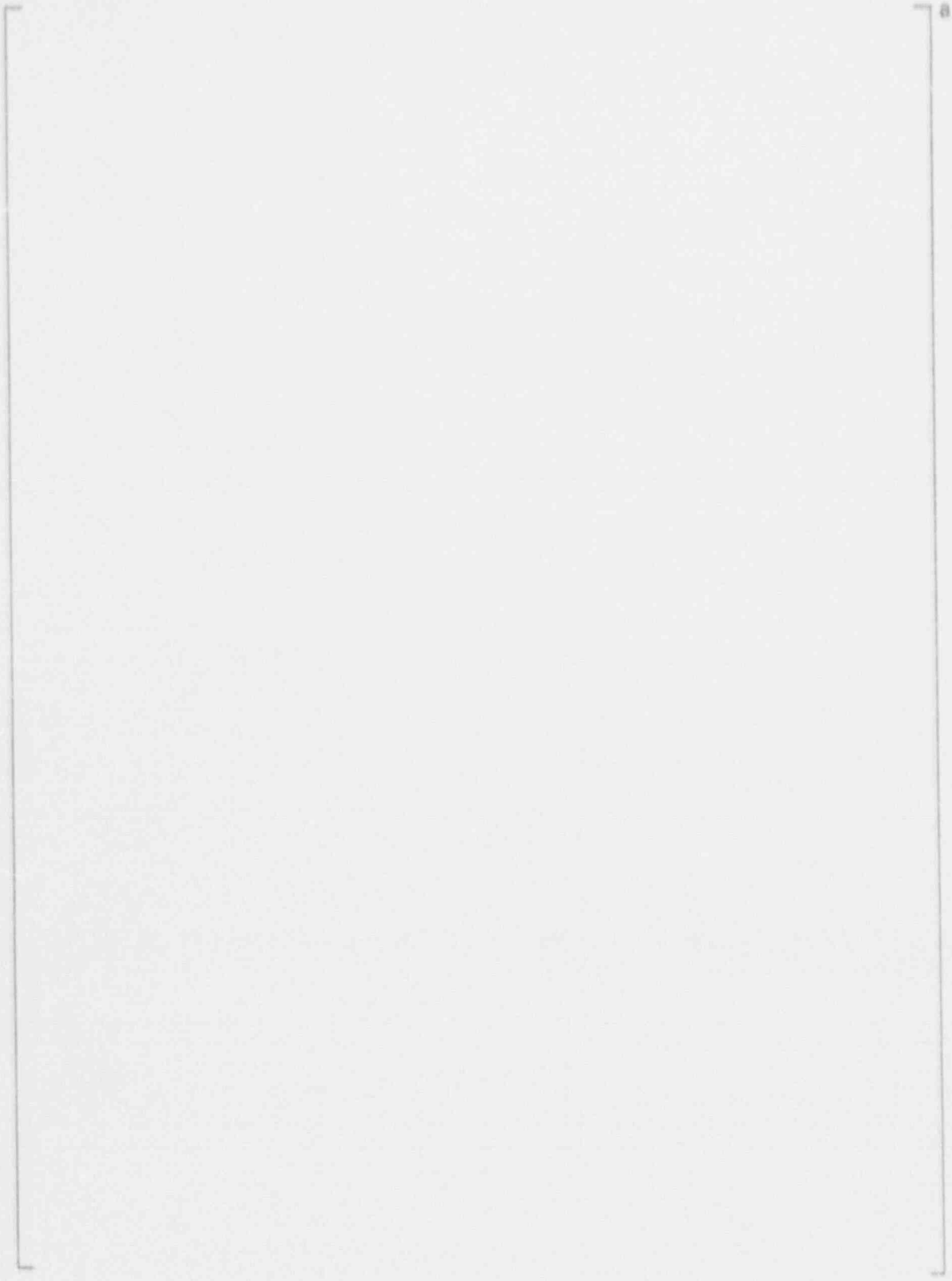

Figure 12-3. Comparison Between Predicted and Measured Leak Rates

Figure 12-4. Normal Operating Condition Leak Rate vs. Axial Crack Length